Preventing Wide Area Blackouts in Transmission Systems: A New Approach for Intentional Controlled Islanding using Power Flow Tracing

SEAN WILLIAM NORRIS

Preventing Wide Area Blackouts in Transmission Systems: A New Approach for Intentional Controlled Islanding using Power Flow Tracing

Seán Norris

School of Engineering and Computing Sciences

Durham University

A Thesis submitted with the requirements for the degree of Doctor of Philosophy

2014

I. Abstract

A novel method to reduce the impact of wide area blackouts in transmission networks is presented. Millions of customers are affected each year due to blackouts. Splitting a transmission system into smaller islands could significantly reduce the effect of these blackouts. Large blackouts are typically a result of cascading faults which propagate throughout a network where Intentional Controlled Islanding (ICI) has the advantage of containing faults to smaller regions and stop them cascading further.

Existing methodologies for ICI are typically calculated offline and will form pre-determined islands which can often lead to excessive splits. This thesis developed an ICI approach based on real time information which will calculate an islanding solution quickly in order to provide a 'just-in-time' strategy. The advantage of this method is that the island solution is designed based on the current operating point, but well also be designed for the particular disturbance location and hence will avoid unnecessary islanding. The new method will use a power flow tracing technique to find a boundary around a disturbance which forms the island that will be cut. The tracing method required only power flow information and so, can be computed quite quickly.

The action of islanding itself can be a significant disturbance, therefore any islanding solution should aim to add as little stress as possible to the system. While methods which minimise the power imbalance and total power disrupted due to splitting are well documented, there has been little study into the effect islanding would have on voltage. There a new approach to consider the effects that islanding will have on the voltage stability of the system is developed.

The ICI method is based on forming an island specific to a disturbance. If the location of a source is known along with information that a blackout is imminent, the methodology will find the best island in which to contain that disturbance. This is a slightly different approach to existing methods which will form islands independent of disturbance location knowledge. An area of influence is found around a node using power flow tracing, which consists of the strongly connected elements to the disturbance. Therefore, low power flows can be disconnected. This area of influence forms the island that will be disconnected, leaving the rest of the system intact. Hence minimising the number of islands formed. Finally the methodology is compared to the existing methods to show that the new tool developed in this thesis can find better solutions and that a new way of thinking about power system ICI can be put forward.

II. Table of Contents

III. List of Figures

IV. List of Tables

V. Declaration

I hereby declare that this thesis is a record of work undertaken by myself, that it has not been the subject of any previous application for a degree, and that all sources of information have been duly acknowledged.

This thesis was part of a joint project with partners from Durham University, University of Edinburgh and University of Southampton. This work in this thesis developed a novel approach which is independent from partners work. The methodology is an individual contribution. The results from the methodology are compared with the work carried out by partners. Where project partners' results are used for comparison, they are clearly referenced and acknowledged. Project partners' results are used in Chapter 11 in a comparative study. All other work in this thesis is the individuals own work.

Signed: _____

VI. Statement of Copyright

VII. Acknowledgements

I would like to sincerely thank my doctoral supervisor Janusz Bialek for his guidance, support and positivity throughout my years in Durham. He has helped me develop as a researcher, taught me to challenge anything and most importantly, that we are "always learning". I would also like to thank him for the great number of opportunities he exposed me to outside of the PhD studies and the many 'life lessons' he was able to teach me.

I would also like to thank a number of the academic staff in Durham, Chris Dent for his continued input and support throughout the PhD, and for the experience of the Castle dinners which I will never forget. To Paddy McNabb, from whom I have learnt a great deal, I am grateful for your support and guidance. I also wish to thank Song Guo, whom I worked closely with on different projects and have also learnt a great deal from.

I would also like to thank out project partners in the University of Edinburgh and the University of Southampton whom I worked closely with over the course of the PhD, especially Ruben Garcia-Sanchez, Zhenzhi Lin and Hongbo Shao, Max Fennelly, Ken McKinnon and Paul Trodden.

To all my colleagues and friends who made my time in Durham so pleasant, Peter Wyllie, Katie Ridley, Donatella Zappala, Mustafa Elsherif, Terry Ho and Padraig and Lorna, I am eternally grateful.

I would especially like to thank my family for their support and love, my mother and my father for always looking out for me and my sister Ciara, for always reminding me that I was still a student. I would like also like to thank Ray and Maria Maynard, Lauren and Angela for their kindness and making me feel welcome.

Finally I would like to especially thank Carly, for everything, for her support, kindness, patience and comfort.

VIII. Dedication

I would like to dedicate this thesis to my Grandfather, Willie Conroy who passed away during my Study. It was through him that I developed my passion for Engineering where I was first introduced to the mechanical and electrical world when I was younger. I learnt a great deal from my time with him and I continue to build upon the knowledge that he bestowed upon me. I am extremely thankful for the times we had together and I hope I can continue learning with the same passion he had for learning, solving problems and facing challenges

IX. List of Publications

Conference papers

1. Guo, S., Norris, S., Wilson, D. and Bialek, J., *"Increasing the available transmission capacity by using a dynamic transient stability limit",* ISGT Europe 2011, Manchester, 5-7th December 2011
2. *Norris, S. ; Guo, S. ; Bialek, J., "Tracing of power flows applied to islanding",* IEEE Power and Energy Society General Meeting, San Diego, California, 2012
3. *Norris, S ; Shao, H ; Bialek, J., "Considering voltage stress in preventive islanding", IEEE* Powertech 2013, Grenoble, 2013
4. *Shao, H; Norris, S; Lin, Z; Bialek, J,." Determination of when to island by analysing dynamic characteristics in cascading outages",* IEEE Powertech 2013, Grenoble, 2013

Journal Papers

1. *Guo, S., Norris, S., Bialek, J., "Adaptive Parameter Estimation of Power System Dynamic Model Using Modal Information", IEEE Transaction on power systems. (Accepted*
2. *Sanchez-Garcia, R., Fennelly, M., Norris, S., Niblo, G., Wright, N., Bialek, J. and Brodski, J., "Hierarchical Spectral Clustering of Power Grids", IEEE Transaction on power systems. (Accepted)*

Working Group

1. Vaiman, M., Hines, P., Jiang, J., Norris, S., Papic, M., Pitto, A., Wang, Y., Zweigle, G., "*Mitigation and prevention of cascading outages: Methodologies and practical applications*", Prepared by the Task Force on Understanding, Prediction, Mitigation and Restoration of Cascading Failures of the IEEE Computing & Analytical Methods (CAMS) Subcommittee, IEEE Power and Energy Society General Meeting (PES), 2013, 21-25 July 2013

1 Introduction

1.1 Background

The risk to modern power systems has increased despite major advances in technology. Along with growing demand, modern power systems are changing due to economic and environmental pressures. As electricity systems moved to market based structures, the demand for cheaper electricity has grown. This has led to major increases in cross-border trading where it is often cheaper to import power than invest in new power stations. The Italian blackout in 2003 was a prime example where Italy was importing 25% of required power from the rest of the UCTE area. This was typically supplied from the cheap nuclear generation in France. The deficit in Italy is largely due to its ban on nuclear generation, which is now being seen again in other countries in the wake of Fukushima in 2011. Germany is facing major problems with energy deficits caused by the shutting down of their nuclear units. The results from these kinds of decisions will typically mean importing power from neighbouring countries. Therefore, the interconnectors which were originally designed for greater frequency stability are now becoming vital sources of power. As the imported power is often cheaper than building new power stations, it is a trend that is increasing but cannot last as Europe cannot rely completely on the nuclear power from France.

However, this is not the only pressure facing power systems. Major targets have been set for renewable generation across the world. Many of these targets range from 20% [1] with a push to see 50% in the future. This means the ageing power plants will be replaced with newer carbon friendly technologies, most likely wind generation as wave and tidal technologies are still in development stages. While this brings about great benefits for carbon reduction, it puts added pressure on the systems for control and stability. Many of the power systems across the world are an old design, and were designed to carry power from large power stations to major loads. There were normally strong reasons behind the locations of power stations, such as near a coal mine, port etc. with large transmission corridors linking them to loads. However, the newer generation such as wind farms are rarely located in the same places and have specific sites also, i.e. where it is windy. Therefore the new technology is being connected into an old grid design but will require major grid reinforcement. Another issue with these technologies is that they provide no inertia to the system. While steam turbines associated with nuclear and coal plants have very large rotors, this large rotating mass adds inertia to a system. Wind farms are connected through a series of power convertors which decouple them from the grid and

therefore offer no inertia. While it can be artificially created, it is still not as large as the plants they are replacing. Therefore, in a system with 50% renewables, the system inertia will be greatly reduced. This will mean that for any disturbances in the system, frequency can change much faster. Also, the weaker coupling between machines means that the system is likely to experience very different dynamic behaviour which will be much more difficult to control.

With the future power system being put under extra pressure, it is important to understand how vulnerable the current power systems are. Any vulnerability in the current systems is likely to be exacerbated unless appropriate action is taken. The largest blackout in the history of power systems occurred in 2012 in India which affected 620 million people. In 2011, a Blackout in Brazil affected 55 million people while in 2010, Chile lost 15 million customers. In 2003, three major blackouts occurred. The United States with 55 million people affected, Italy with 56 million people affected and finally, 5 million in Scandinavia. A Europe-wide blackout was narrowly avoided in 2006 but 15 million customers were still affected due to un-intentional islanding.

Taking the Indian Blackout as an example, the major contribution to the blackout was the high imports on the interconnectors. One of the difficulties power exporters face is with importers keeping to the contractual levels. Before this blackout, many of the interconnectors were severely overloaded as areas were importing more power than the agreed levels. In fact, the Italian blackout was caused by much the same reason. Therefore, the cause of many blackouts is often a lack of proper communication between neighbouring operators. The 2006 European event was another example where a planned outage was not communicated properly to the neighbouring operators. Events such as the Brazilian and Scandinavian blackout were examples of hidden failures in the system which are often not highlighted until the critical moments. Scandinavia lost a major generator but was then followed by a mechanical busbar fault which took out a key high-voltage corridor. While for the Brazilian blackout it was found that in a severe storm the isolators were not adequate to cope with the high level of rainfall.

It is clear that modern power systems are vulnerable and as more pressure is placed on them, events such as these are likely to become more frequent. Many of these systems have had the benefit of technological advances such as Special Protection Schemes (SPS) or System Integrity Protection Schemes (SIPS) which were designed to prevent such events. Conventional protection systems and controls have seen major development to add robustness to power system. However, in some cases the protection systems themselves can be major contributors to blackouts such as the US blackout in 2003. As systems become increasingly complex it is much

more difficult to rely on the old protection designs which are often fitted and forgotten about. Then when new systems are added, conflicts can arise between the old protection settings which can lead to problems such as those seen in San Diego in 2011. This event highlighted the need for proper co-ordination between existing systems in order to provide the desired protection.

Therefore, even the systems in place to protect the power system can fail, and can be due to poor design or co-ordination with the existing protection systems. There are a multitude of reasons behind blackouts, and while each blackout event is different, they can normally be reduced down to a number of key facts; lack of communication between operators, poor coordination of protection systems and hidden failures. The latter is very difficult to design for. With the evolution of the power systems to reach new targets, it is important to develop new techniques which can act to protect against blackouts.

Given how the situational awareness within power systems has increased significantly in recent years through new measurement technologies, Wide area measurement schemes etc., new solutions based on this increased situation awareness should be developed and exploited to enhance future security.

1.2 Research Objectives

There is clearly a need for new methods of blackout prevention as the current methods have been shown to be inadequate. System Integrity Protection Schemes (SIPS) are widely used in power systems to deal with major contingencies. However, SIPS are designed for specific problems as a solution to that problem. These are designed during the planning stages and are generally not adaptive to new problems/disturbances. The existing protection has been shown to be inadequate. As each blackout event is different, there is a need for adaptive prevention methods which can be applied to prevent blackouts in any system. In this thesis the problem of creating an adaptive blackout prevention tool will be developed. All of the blackouts mentioned are the result of cascading failures in a network. The key to preventing the blackouts therefore lies is preventing the cascades. This work will set out to solve that problem.

The method chosen to prevent cascades is power system Intentional Controlled Islanding (ICI) or separation. The basic principle lies in the fact that through ICI, the area available for a disturbance to cascade through is minimised. By separating the network into a series of islands, the disturbance is confined to one island and the remaining islands remain isolated from the disturbance. However, there are a number of associated problems which ICI brings.

The first of these problems is how to create a suitable island. There are a number of methods that have previously been developed for intentional islanding such as slow coherency methods and a variety of graph theory methods. The shortcoming of such methods is that they take a generalised approach to the disturbance and so create many islands in the hope that one island will confine the disturbance. By splitting the system up into many smaller islands, the system becomes more vulnerable as each small island has less inertia, may have generation imbalances and can be difficult to resynchronise. These are major problems which need to be solved; how to create an ICI solution which would not further jeopardise the security of the system.

The best solution would be to create only two islands. One which contains the disturbance, and any cascades. The other island will be the remaining part of the network. In order to minimise the area that a cascade can spread through, this disturbance island should be as small as possible. With increased penetration of measurements, disturbance location is now possible. The problem therefore comes down to finding the area in which to contain that disturbance. Any solution that is created needs to be extremely fast if it is to be used in conjunction with real time measurements. This adds further complexity to the problem, to identify an area for an island in real time using information obtainable from the power system.

In order to create a good ICI solution, all forms of stability should be considered. Therefore, frequency, voltage and rotor angle stability are all major components to be addressed. There are many well-known methods for evaluating the various forms of stability, however many are reliant on time domain simulations. For real time ICI assessment, time domain simulations would take too long, therefore an additional problem is added by this constraint on time.

Therefore, the aim is to provide a new solution to blackout prevention, one which overcomes the shortfalls of previous islanding techniques and one which will consider all forms of stability to provide a fast solution which enhances system security and stability.

1.3 Contribution to Knowledge

The contribution to knowledge within this thesis comes from the approaches used to solve the above problems. A novel method to identify the islands was developed which aims to form two islands, one which contains the disturbance and the second which is the remaining network. Previous methods look to find the natural splits in the network through various criteria, however this approach looks to start at a disturbance node and create a boundary about that node. Power flow tracing is used for this purpose. The application of power flow tracing allows power flow contributions between all nodes in a system to be found. This expresses how dependent one

bus is on another in terms of real power. An algorithm was created which uses the power flow tracing information to find a boundary by creating a set of nodes to form the disturbance island. Starting from the disturbance node, if a neighbouring node is highly dependent upon that node, then they are strongly connected. Their dependency can be based on both receiving and sending real power. All the nodes that are then found to be strongly connected will remain connected and will form the disturbance, or 'sick' island. All nodes which were weakly connected will be disconnected and will form the healthy island. Therefore, only two islands are created and there is no unnecessary risk or reduction of security posed to any customers in the healthy network. Another advantage to this method is that it relies on power flow information only, which can be easily obtained from measurements or state estimators. The power flow tracing method is also an extremely fast method and so is very applicable to real time use.

The methodology was then adapted to include stability considerations. As the tracing method uses the dependency of real power between buses as its measure of a strong connection, the weakly connected nodes will have a low dependency, which translates as a low power flow between them. This is very useful when considering frequency stability which is highly reliant on the balance between generation and load. By creating an island, lines with weak power flows are being cut. Therefore, the imbalances between generation and load are being inherently minimised. This is a useful addition as it is automatic in the tracing algorithm and does not require any further complexity.

For rotor angle and voltage stability, it is difficult to assess these properly without running full time domain simulations (TDs). Therefore, an approximation method was used to assess the rotor angle stability. The aim was to minimise the shock that a generator would experience as a result of tripping the lines and forming islands. This is directly related to the changes in power that would be required by each generator. If a generator experiences a large change in the required electrical power it may be sufficient to cause the generator to lose synchronism with the rest of the island and cause instability. It is the transient stability that is of interest here. This work therefore minimises the shock that the generators would experience by minimising the changes in real power. For each of the lines that are cut in the system, their absolute sum of the real power will give an indication to the total change in real power. This is used as a method to quickly assess the effect on transient stability. It can also be shown than when forming islands using this criteria, similar boundaries to those found using slow coherency can be achieved. Therefore, this is a fast approximation that can take transient stability into account and has been shown to prevent islands from going unstable.

Finally, voltage stability is considered. However, as voltage stability requires full time domain simulations to assess the various control and load dynamics it is difficult to assess in real time. While there are a number of existing static stability assessment tools such as modal analysis and reactive power distribution factors, these were not suitable. For ICI, a number of lines are tripped which is a large system perturbation. Previous methods relied on linearization of the power flow equations and therefore were only suitable for very small changes about the operating point. It was shown that ICI could not be considered as a small perturbation. A new method was then developed. This required a new definition of the problem whereby the methodology aims to minimise voltage stress on the system. Voltage stress will be defined as the instantaneous or transient voltage change as a result of tripping a line or series of lines.

A method was developed by which to evaluate the potential change in voltage stress by computing the local imbalances in reactive power that may exist in the moments just after islanding. It was shown that there is a very strong correlation between local imbalances in reactive power and the instantaneous change in voltage. The analysis of the post-split reactive power profile can provide an approximation into the potential effects on voltage stress. It is therefore the aim that by minimising the voltage stress that the possibility of voltage collapse will inherently be minimised.

The voltage stress method relies on the reactive power flow information only to create a reactive power profile. Therefore, it is faster than Time Domain simulations (TDs) and can be computed using load flow solutions only. It can provide an approximation into the possible effects on voltage much faster than running a time domain simulation. While a time domain solution would provide much more accurate result, the accuracy must be sacrificed for speed in this approximation. It was shown that by minimising the voltage stress using this method that the voltage changes could be minimised and the risk of voltage collapse could be minimised.

Therefore, a novel way of considering ICI using on power flow tracing to create a minimal number of islands was developed. The methodology was then further adapted to consider the effects on voltage when the time to run TDs is limited. The results showed that it is possible to create islands based on this concept while minimising the impacts on the power system stability.

2 Blackouts and Prevention Methods

2.1 Introduction

The purpose of this chapter is to show the motivation behind developing new methods for blackout prevention. It is easy to assume that power systems are reliable and faults are rare. However, this chapter will show that systems are not impervious to faults and major events which can leave millions of people without power. For the purpose of this review, only the most recent and largest events are considered in order to highlight the scale of the problem, despite the advanced protection and security measures.

Modern power systems are designed to operate with maximum reliability and security of supply where there is a vast quantity of fault protection schemes implemented across the world's electrical networks. However, many systems are now having demands placed on them that were never originally designed for. One example of this is the cross-border trading of electricity that is becoming more and more common among TSOs (Transmission system operators). In [1], increased liberalisation of the electricity market is investigated as the reason for the increase in cross border trades which are usually not properly accounted for when assessing system security. As the world's consumption of electricity increases, there is an increased demand put on the transmission and distribution systems in order to cope. The traditional way of operating a transmission system is no longer sustainable. This method used to have one operator responsible for their own control area, where as now, country's grid are interconnected and there are numerous operators involved in power transmission, exportation and importation of power. There has not been a new effective control scheme put in place to deal with these new demands. It is very much still operating on the traditional methods of communication and information exchange which can lead to further problems when something goes wrong.

This interconnected system has many advantages, such as better frequency stability and less susceptibility to voltage swings. However, with such a system, a serious fault, or series of faults, can lead to a cascading blackout and a fault can then interfere with the entire interconnected grid and cause a wide area blackout. Without the necessary changes it means that the risk of future blackouts will increase, or the alternative is to run the interconnected system very conservatively maintaining large security margins at a high cost to the consumer. A number of blackouts will now be described which were all recent events, and it can be seen that there were common factors between each event that led to the blackout.

2.2 Blackout Case Studies

2.2.1 India 2012

The largest event in the history of power systems occurred on the Indian system in 2012 with the loss of over 650 million customers. The inter-regional power transmission corridors were weakened due to multiple existing outages which were a mix of forced and planned outages [2]. No explanation of the forced outages was available at the time of publishing. This left only one main AC circuit available between the West region (WR) - North region (NR). Excessive demand by utilities in NR with unscheduled interchange contributed to high loading on the tie line. There was also inadequate response by load dispatchers in NR and under drawl and excess generation in WR. As the interface was weak, the line tripped due to zone 3 relays from load encroachment[1]. When the two areas separated, the NR loads were not met through the WR-ER-NR route, which caused a power swing. The centre of the swing was in the NR-ER interface and the corresponding lines tripped isolating the NR system from the rest of the grid. The NR system collapsed due to under frequency and further power swings.

However, there was a second event which followed shortly after, the difference being that the power swing was observed on the ER-WR interface and lines tripped in ER for which a small section was isolated. This led to power swing in the NR-ER interface and resulted in further separation of the NR system. All three regions then collapsed due to multiple tripping attributed to internal power swings, under frequency and over voltage in different places.

2.2.2 Chile 2011

This blackout affected 9 million people where the cause was equipment failure at a substation from a short circuit in a 220 kV capacitor bank. There was a subsequent malfunction in the protection to prevent cascading failures which then eventually led to the disconnection of customers. Four power companies were charged for improper maintenance of the equipment since it represented a real threat to the power system security and also for problems in applying the procedures for restoration of supply. It highlighted the necessity for companies to maintain correct maintenance and procedure and would serve as a lesson for future events.

1 Load encroachment, which means the apparent impedance entering the protective zone due to the changing of the transmission network structure and the shifting of power flows under steady-state operating conditions.

2.2.3 California 2011

This was an 11 minute disturbance which led to cascading outages and left 2.7 million customers without power [3]. It was initiated with the loss of a single 500 kV line, but this was not the sole cause. If the system was N-1 secure it should withstand this loss, in fact this line had tripped on multiple occasions without causing cascading outages. However, on this occasion, the system was not N-1 secure. With this major transmission corridor broken, the power flows instantaneously redistributed throughout the system, increasing flows on lower voltage systems to the North. As it was during hours of peak demand and there was lower than peak generation levels in San Diego and Mexico, the instantaneous redistribution of power flows caused sizeable voltage deviations and equipment overloads to the north of the Southwest Power Link. There was significant overloading on three 230/92 kV transformers. These factors then had a ripple effect as transformers, transmission lines and generating units tripped off, initiating automatic load shedding throughout the region in a relatively short time span. Seconds before the blackout, one path carried all flows into San Diego area as well as parts of Arizona and Mexico. The excessive loading on this path initiated an intertie separation scheme which led to the loss of nuclear units and eventually a complete blackout of San Diego and the corresponding control area. During the event's 11 minutes, the reliability coordinator issued no directives, and only limited mitigation actions were taken by TSO of the affected areas.

2.2.4 Brazil 2009

In 2009, Brazil suffered a large blackout, affecting 60 million people where the root cause was a short circuit due to badly weathered isolators which led to the loss of an important 750 kV corridor [4]. Heavy rain and strong winds led to the short circuit that left 40% of the Brazilian network disconnected while Paraguay suffered a compete outage. A series of phase to ground faults tripped the lines in quick succession which left SW Brazil isolated from the grid. 5.6 GW was then tripped at the Itaipu dam due to load rejection. Additional line trips led to nearly 3 GW of further load rejection. The DC link connecting the 60Hz and 50Hz sections was then automatically disconnected which led to total disconnection of transmission system and directly connected generation, a total of 24 GW of interruption. Equipment was not rated for severe environmental conditions; In this case, insufficient isolator insulation from rainfall with Brazil's standard of 1mm/min being less than international standards of 5mm/min.

2.2.5 US/Canada blackout 14th August 2003

In 2003, a major event occurred on the US-Canadian system where 62GW were lost and 50 million people were affected [5]. The events directly involved six control areas which started in Northern Ohio controlled by First Energy (FE). Figure 2-1 shows the distribution of power in the

area as well as the control areas in the region. Northern Ohio was supplied directly from the south and indirectly from the west via PJM. Michigan was supplied from the south and Ontario was supplied from the east and the west.

The loads that Northern Ohio was supplying were moderately high, with the voltages low, but consistent with historical values. FE was importing 2.5GW into its service territory which caused the system to consume high levels of reactive power. Heavy power transfers usually see high consumption of reactive power. Transmission losses caused by reactive power flows are observed in the form of heating and therefore, there is less headroom for real power generation and transmission before the thermal limits are reached. In Cleveland, two active and reactive power production anchors were shut down but there was a loss of another unit, shown in Figure 2-2 and this further depleted critical voltage support for the Cleveland-Arkon area. This however was not a critical fault, and the system was still able to operate safely. It did mean that FE had to import an additional 540MW to make up for the loss of the unit which made voltage management more challenging in Northern Ohio.

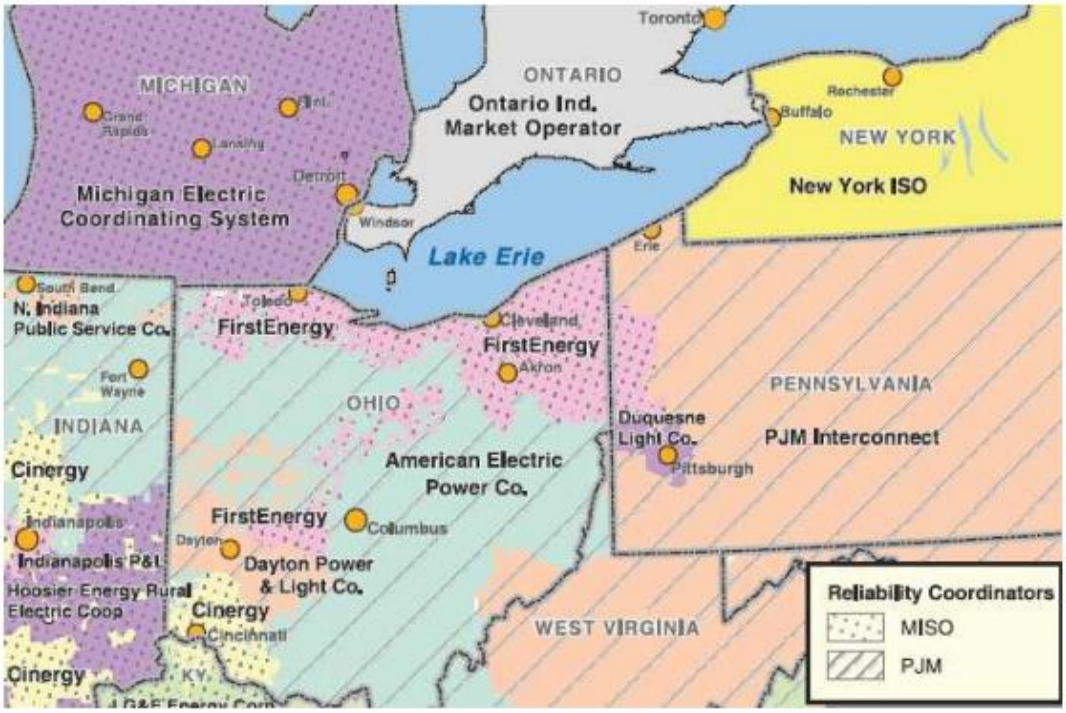

Figure 2-1 Reliability Coordinators and Control Areas in Ohio and Surrounding States

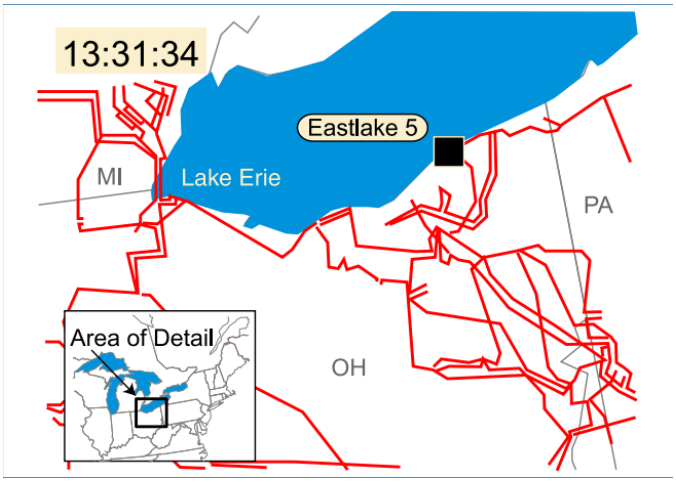

Figure 2-2 Eastlake 5

Dayton Power & Light's (DPL) Stuart-Atlanta 345 kV line then tripped due to a tree flashover, but this line had no direct electrical effect on FE's system. The Midwest Independent System Operator (MISO) is the reliability co-ordinator in FE's area in Northern Ohio and there was a problem with their primary system condition evaluation tools, its state estimator. The state estimator was unable to assess system conditions for most of the period when these faults occurred. PJM was the reliability coordinator for the DPL line, but the tripping of the line had effects on other MISO lines. Without an effective state estimator, MISO was then unable to perform contingency analysis within its reliability zone. It could not determine what would happen with the loss of the anchor and the effect of the tripped line, and that other transmission lines would overload if FE lost major transmission line. The full sequence of events can be found in [5] where it can be seen how the cascades occurred throughout the network and eventually left a large area with a blackout.

2.2.6 Scandinavian Blackout on 23rd September 2003

On the 23rd of September, there were a series of major disturbances on the Nordic power system which resulted in a blackout event in Southern Sweden and Eastern Denmark [6]. About 5 million people were affected and there were 4850 MWs of power lost in the event. There were a number of transmission links and power stations down for maintenance on the day, but these were planned events, and so the system was operating reliably. Eastern Denmark was producing 2250 MW and 400 MW of this was exported to Sweden through the interconnector. The total capacity that was ready to go into operation was 3300 MW, so there was plenty reserve generation available. One of the Nuclear power plants at Oskarshamn began to have problems with the valve in the water feeder circuit and the production from the unit had to be decreased

and soon it stopped altogether with a loss of about 1200 MW of production. However, this was then followed by a double busbar fault due to mechanical failure in an isolator at a 400kV substation in the South Sweden transmission grid. The busbar fault caused four 400 kV lines to be disconnected, two of which were a major connection between south and central Sweden, and the other two connected units 3 and 4 at Ringhals Nuclear station. These units were then disconnected from the grid which resulted in a further loss of 1800 MW of production. This then led to large fluctuations in frequency and voltage and created severe low voltage conditions in many areas. Protection systems then began to trip a number of lines separating areas further until the system was left in a blackout.

2.2.7 Italian Blackout 28 September 2003

This blackout occurred at 3 am when Italy was importing 6651 MW from France, Switzerland, Austria and Slovenia and 6951 MW including the HVDC link with Greece [7]. This import was 24% of Italy's demand. Much of Italy's power is imported due to their energy deficit since banning nuclear power in 1987. This means that there are quite often very large flows in the transmission networks of France, Switzerland, Austria and Slovenia that the TSO's know little about. An example of this was, on the night of the blackout, Italy was importing about 300 MW more than the agreed level. At the time, the Swiss transmission grid was highly stressed and operating close to (N-1) security criterion. [8]

The system can be seen from Figure 2-3 with the line of separation that resulted from the disconnection of the lines. It also shows the order and location of the lines that were tripped that led to the blackout.

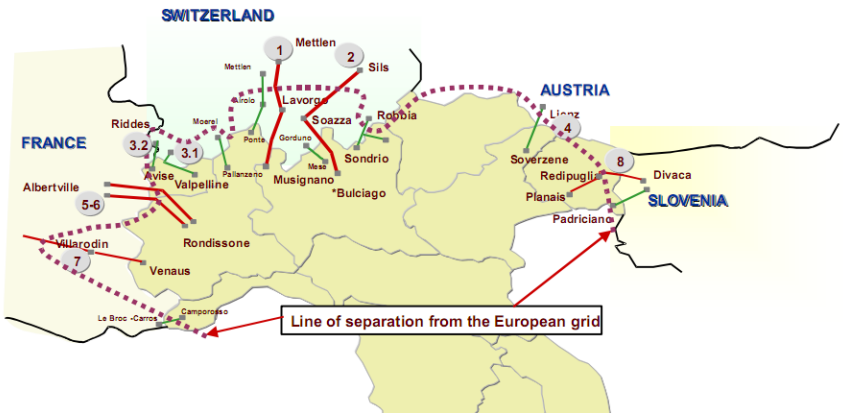

Figure 2-3 Separation from rest of UCTE

Initially, a line tripped due to a tree flashover which then put added pressure on remaining lines. As Italy was importing a large amount of power, these lines were carrying more than the agreed

limits and Italy was asked to reduce the demand. However, this reduction took time due to the lack of proper communications. During this time voltage oscillations began to occur between north of Italy and the rest of the UCTE area. As remaining lines tripped due to the overloading, Italy was left disconnected. However, due to the voltage swings; there were also very low voltage conditions in the North of Italy. This led to the disconnection of generators and therefore further generation was lost and faults cascaded throughout the system leaving Italy in darkness.

2.2.8 System Disturbance on UCTE system, November 4th 2006

This event did not result in a Europe-wide blackout, but resulted in the disconnection of 15 million consumers [9]. The event was not directly caused by a fault but by human error and it resulted in the UCTE region to split up into 3 areas with different frequencies as seen in Figure 2-4. On the 18th September, Meyerwerft shipyard requested a disconnection of the double circuit 380 kV Conneforde-Diele line from E.ON Netz so that a ship could travel safely underneath. The request was for 1:00 on November 5th 2006.

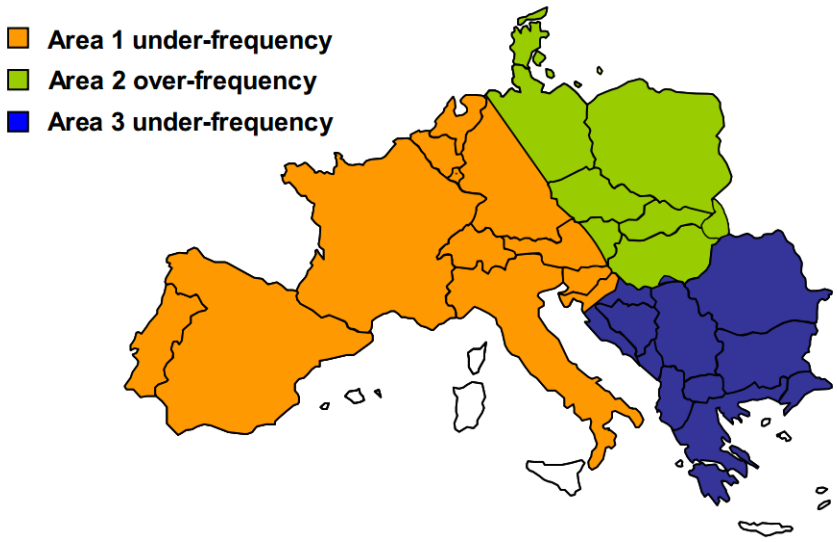

Figure 2-4 Schematic map of UCTE area split into three areas

A full analysis on the impact of disconnecting this line and found that there was no violation of the (N-1) criterion and so provisionally approved the request on the 27th October. An agreement was also made between EON Netz and TenneT to reduce cross border transmission capacity from EON Netz to TenneT by 350 MW for November 5th between 00:00 and 06:00.

However, on November 3rd, the shipyard requested an advance on the disconnection to 22:00 on November 4th and this was provisionally agreed by EON Netz based on an analysis which showed no (N-1) violation. Critically, RWE TSO and TenneT were not informed about this and no

analysis was carried out by the other TSOs for the planned outage. The late request from the shipyard made it impossible to reduce the exchange program between Germany and the Netherlands in the same way as was set up for the original 1:00 scheduled time. It was only at 19:00 on 4th November, 3 hours prior to switching off of line, did EON Netz inform TenneT and RWO TSO about the new time for the event. Based on an empirical evaluation of the grid situation, the N-1 criterion would be met after switching off the line. The numerical analysis was not completed properly, and the evaluation was in fact incorrect. The grid was not secure. When the line tripped, there were a number of factors not considered such as very high wind production in north Germany along with incorrect relay settings in interconnectors. Also, operator actions to reduce current on lines in fact led to larger currents. It then progressed into a series of cascading line trips throughout the UCTE area, and eventually divided the UCTE grid into three unbalanced areas affecting millions of customers.

2.2.9 Common reasons for the blackouts

[1] investigates some of the common reasons behind blackouts. While the blackouts in 2003 caused a number of utilities to take steps to ensure secure operation, the wide area event in 2006 had been caused by the same underlying reason which is a lack of adequate inter-TSO coordination such as real time information exchange. Another key issue to be noted is that all of the blackouts occurred at the boundaries between systems in the interconnected network when transmission failures interfered with the bulk cross border trades. Looking at all the blackouts, one common fault with the system is that new demands are placed on an old network design which is fundamentally an outdated system. The way that the grid is now operated has not seen the same evolution that the use of the grid has seen.

2.2.10 Lessons Learnt

The main issues in all blackouts can be reduced down to the following [10]:

- A lack of coordination and information between TSOs in emergency conditions
- Lack of information and awareness of DG in the networks for the TSOs
- Not enough operators trained to deal with emergency conditions
- Poor coordination between TSO's defence plans
- Market liberisation means little knowledge of actual power flows (India and Italy)
- Improper maintenance
- Lack of urgency in dealing with conditions

2.3 Prevention Methods

Special Protection schemes are designed to detect and alleviate conditions which would otherwise cause unusual stress on a power system, however they perform a function other than or beyond the tripping of elements directly required to clear a fault. This is what distinguishes them from normal protection schemes. Special protection systems can be defined as a set of pre-planned coordinated measures intended to ensure that the power system is protected against extreme contingencies. In general a SIPS would involve one or more of the following actions [11]

1. Generator adjustment
    - Including generator tripping, manual or automatic – to balance gen/demand, alleviate constraints etc.
2. Demand rejection
    - Reduction, tripping of demand
3. Transmission switching
    - Often automatic – reconfiguration of the transmission networks to eliminate excessive flows or voltage problems following generation/demand changes or topology changes
4. Reactive power adjustment
    - Capacitive or inductive to satisfy voltage constraints

Special protection systems share a number of common traits such as being designed to control power system stability in cases where the uncontrolled response is likely to be more damaging that the controlled response. They are devised by off-line analysis as opposed to real time control, many of the schemes can be armed or disarmed as the operators see fit. All the schemes provide a particular type of remedial action which is designed to alleviate a certain observed system condition, or to take pre-determined action when a certain event occurs. This is an important distinction between SIPS and conventional protection.

2.3.1 SIPS Design

As SIPS are designed for certain events, there is a logical procedure in their designs. Detailed information on the design and implementation can be found in [12]. The procedure can be summarised from [13] as follows. The first step is to understand how the system responds to certain disturbances, where some are more serious than others and can depend on location, duration and complexity. Some disturbances may be so severe that the devices normally used

for protection are inadequate in which cases SIPS may be required. The first stage is to define the critical conditions; those which are expected to have devastating effects on the system and identification requires many stability studies for different operating conditions and disturbances. When the disturbances of interest are found it is also possible to devise the possible corrective actions using simulation. When the disturbances have been identified, the recognition triggers are defined which are relays of various types used to detect the SIPS response. The final stage of the design is the operator control and relaying the information to the operator to decide whether to arm or disarm the system according to a predefined set of rules.

2.3.2 SIPS/SPS/RAS

To deal with the large number of complex disturbances in modern power systems, SIPS, SPS or Remedial Action Schemes (RAS) have been employed in systems across the world and are the subject of continuous research. [10] outlines the SIPS used on the WECC, ERCOT systems and also on the Italian network. In the WECC system alone there are over 190 SIPS and have become widely accepted where a guide has been created for developing new SIPS. The main forms of SIPS are generator tripping, switching and load shedding. The Italian case has a specially designed defence plan where one line of defence is against cascading failures and subsequent network separation through fast tripping of critical generators, load shedding and blocking of tap changers.

In North Wales there was an arrangement of 2 hydro units and 2 nuclear units which were connected through an 80km 400kV double circuit and a parallel low voltage path. There were a number of potential problems surrounding this arrangement and so a special protection scheme was developed to counteract the problems. There were a number of different scenarios which were considered, such as different parts of the 400 kV network tripping and the scheme would be dependent on which section was lost. The main line of defence was to use intertripping which would automatically trip either generator or remaining lines if a section of the 400 kV network tripped. In one section of the 400 kV network, tripping could lead to overloading of the lower voltage lines and instability. In these instances, intertripping would trip the lower voltage paths and allow the generators to serve local load only. However, in another part of the 400 kV network, tripping could lead to pole slips in the hydro plants and hence intertripping was designed to disconnect these generators.

In France, a special protection scheme was designed around load shedding and system separation in the event of severe disturbances. This is evidence of previous attempts at system

ICI as a method of special protection. There were 4 stages of load shedding at 4 different frequency levels. This dealt with frequency drops in the system, however, a system separation scheme was developed to counteract a problem with voltage beats which was a symptom of loss of synchronism caused by generators operating at different speeds. The sectioning points were located at the boundaries of groups of generators which were found to swing together. Equipment was designed to count the beats at these points. While this system has a number of successful operations, each of the relays in this system operated autonomously and hence tripping was staggered and in some cases islanding regions which were out of synchronism was not sufficient to prevent the disturbance from spreading and worsened the situation.

A new system was then created based on voltage phase angles which would send data to a central point where orders could be sent to particular relays to shed load/separate areas. This was a much more reliable system as it avoided the staggering of trips with the older system.

In Canada, a scheme was developed in the 1980's due to delay in the building of a new 500 kV circuit. New large nuclear stations were built but without the new 500 kV circuit they could not operate a full capacity while maintaining normal security levels. The station would therefore be limited to half its capacity at a cost of $1 Billion. However, a scheme which would reject a number of units in the area automatically upon detection of a fault could allow the units to increase capacity reducing the cost to $175 million. This was an example of an SIPS to offset the delays in building new infrastructure. A similar scheme was also developed in order to increase the transmission export capacity of the Canadian system.

A SIPS based on on-line transient stability assessment was developed in Japan which would assess the stability at five-minute intervals used telemetered data from the system. If a potential instability was detected generator rejection would be implemented.

There are numerous SIPS in use in the worlds power systems, where many are still being developed and new methods are always being proposed. The hydro-Quebec SIPS is described in [14] where the present plan is outlined as generation rejection and/or remote load shedding which is used against multiple line outages or bypassing of series compensated capacitor banks in key locations. There is also an under-frequency load shedding scheme, shunt reactor switching, under-voltage load shedding and network separation. Many of the tools are those which have been mentioned previously. The work goes onto describe what would change for the future network and that new defence plans were required again using the same range of tools.

The design of an SIPS scheme to maintain high security at high import levels is proposed in [15] which was based around selective load shedding which was found to maintain high security under various transfer levels and a series of double contingency conditions. A SIPS to prevent blackouts on the Thailand power system was presented in [16] where it was used as a cheaper and faster alternative to network reinforcement and again consisted of generator tripping and load shedding along with clever use of FACTs devices.

In [17] generator tripping is used to minimise the consequences of double outages in a particular section of the Brazilian network. The former SIPS would trip generation in the area in jeopardy; however it was shown that tripping fewer units much further away was able to offer greater stability and hence could offer increased cost savings. As the power systems across the world become more heavily loaded, a number of countries are turning to SIPS as a more economical way of increasing transmission capacity, such as Chile [18]. It would be designed with the system congestions in mind in order to free congestion for cheaper power transmission.

Therefore, SIPS are an invaluable part of power systems. They have a variety of applications from preventing blackouts to providing a cheaper alternative to network building. As SIPS are designed with a specific problem in mind, they are rarely adaptive. This becomes an issue as the network begins to change as conflicts can arise from increased complexity due to the large number of SIPS employed, where it is stated in [19] that the reliability of SIPS becomes more difficult to ensure. Indeed, this has called for better methods of modelling SIPS in simulations to ensure that current SIPS are modelled correctly when designing new systems. [20]

2.3.3 Load Shedding

One of the most widely used forms of SIPS is load shedding especially as a tool against blackouts. Load shedding is where loads are tripped in order to protect the system. It is typically applied when frequency is falling, but is also used in low voltage situation. While there are many different ways to optimise the load shedding scheme, there are typically two main types. Under-frequency load shedding and Rate Of Change Of Frequency (ROCOF) load shedding.

With under-frequency load shedding, when frequency drops below a set point, the frequency relays trip to disconnect parts of the load according to pre-defined steps thus preventing a further decay in frequency [21]. These schemes are based on a timed stepwise approach, are usually predefined, and not adaptive. It is designed to trip different levels of load at set frequency values throughout the system. The fact that it cannot be adjusted to cope with the

disturbance at hand is however a disadvantage of the scheme. In some cases too much load, or not enough load is shed. This makes it easier to implement but difficult to rely on.

Rate of change of frequency methods (ROCOF)

ROCOF relays utilise the gradient of the frequency decline to shed load. The relay settings are a function of df/dt [22]. High frequency settings are used for large values of df/dt, while lower frequency settings are used for small values of df/dt. I.e. for a small gradient in frequency decline, the load can be shed at a lower frequency value. This means that if a large imbalance is present between load and generation, the UFLS relays can be quickly initiated and shed more load faster than the conventional stepwise system [23].

An advantage to the ROCOF method is that the magnitude of the disturbance can be found by measuring the rate of change of frequency at the start of a disturbance. This allows the amount of load to be shed to be dictated by the size of the disturbance. In conventional stepwise systems, there is no knowledge of the size of the disturbance which can lead to over shedding, or under shedding. An adaptive method with would take the size of the disturbance into account was developed in [24]. A two-step method was used where in the first stage, the frequency and the rate of frequency change were estimated by a non-recursive Newton-type algorithm. The using a simple expression of the generator swing equation, in the second stage, the magnitude of the disturbance is determined. The system inertia plays an important role in the rate of change of frequency, where a higher system inertia equals a lower rate of change of frequency which can be seen in [25]. However, when the inertia changes in a system, the rates of change may differ from the designed values and so can lead to problems with spurious tripping.

2.4 Conventional Protection Systems

2.4.1 Overcurrent relays

Over-current relays are one of the most abundant types of protection in power systems and operate using a time – current characteristic based on I^2t. This means that for larger fault currents the breaker must act sooner. The characteristic can be seen using a series of curves and each relay will act according to that curve. Relays closer to the fault that experience higher current will trip sooner and should they fail, the next breaker should trip soon after according to the characteristic. There are a variety of these relays such as time delay overcurrent relays, instantaneous relays and directional relays which are used when the direction of flow is important. The time delayed relays have set areas in which to protect while the instantaneous relays cannot act in such a manner and are independent of other relays. Another form of

overcurrent relay is the Inverse Definite Mean Time (IDMT) relay. It has a characteristic which minimises the time delay where the operating time is inverse with the fault current magnitude.

2.4.2 Distance Protection

Transmission lines are usually protected using distance relays which respond to the impedance between the relay location and the fault location. The impedance of a length of transmission line is fairly constant where these relays respond to the distance to a fault on the transmission line. The relays can also be created based on the admittance or the reactance, up to the fault location which can be desirable in some instances.

Distance protection usually operates based on a number of zones with varying levels of reach into the network shown in Figure 2-5. The first zone is usually an under-reach zone whereby it will protect the zone between 85-90% of the line length and does not interfere with the protection at the other terminal. Over-reaching protection is then applied as a back-up in case there is any relay failure of the zone 1 relays further along the line. The second zone then extends beyond the next terminal along the next line, typically 120-150%. However, this has a time delay which is added in order for it to allow zone 1 relays to act and not interfere with their protection.

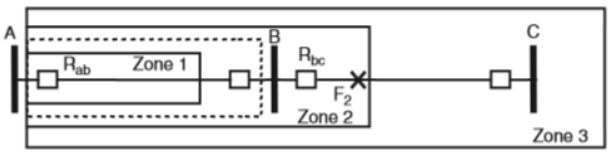

Figure 2-5 Distance Relay Zones [26]

There is a final zone of protection which is of particular interest to the background in this thesis. The third zone of protection usually extends from 120% to 180% of the next line section but must be coordinated in time and distance with the second zone of the neighbouring circuit. It usually has an operating time of 1s, longer than zone 1 and 2 actions.

Zone 3 was originally used as a backup for zones 1 and 2 of an adjacent line in the event of a relay or breaker failure which prevented clearing the fault locally. However, setting the reach is a complex problem as the zone 3 characteristic must provide protection against faults but should not operate for normal system conditions such as heavy loads or stability swings. Load encroachment can quite often be a problem where increased loading on the lines causes the relay to enter into the trip area and operate such as in Figure 2-6

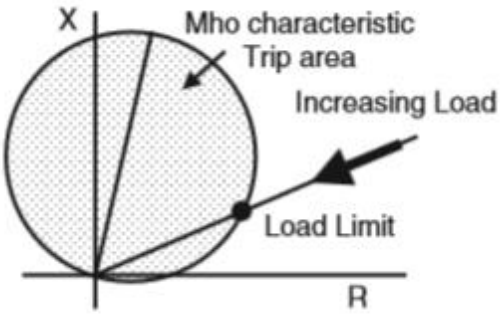

Figure 2-6 load encroachment [26]

2.4.3 New methods for Distance protection

While the principles for distance protection design have remained the same, there are new developments in the way they are operated and set. The development of adaptive distance relays [27] has opened up new opportunities for employing distance protection. A distance protection scheme which was designed to protect parallel circuits using a correction factor based on the information of the surrounding system was proposed in [28] and was used in the impedance calculation. A method to increase the zone-2 coverage without overreach problems was proposed in [29]. A method in [30] could adjust the distance relay zone-reach using available signals to achieve an optimal distance protection performance. In [31] an adaptive method was proposed based on wide area information where an adaptive setting algorithm for the current and phase overcurrent relays were proposed based on fault indicators to determine the fault and update the settings. An adaptive zone -3 setting is proposed in [32] where the technique is based on modelling a fault by considering single-level contingencies and a series of short circuit studies.

One of the fundamental issues with Zone-3 relays in particular is their maloperation which has been a contributing factor to many blackouts. This maloperation is typically due to an increase of the load level to the limit that the relay interprets the system voltage and current relation as if it is a fault even though it is not, e.g. load encroachment. Other causes for the maloperation of zone 3 are power swings and voltage instability which have also the same effect on the impedance measured by the relay as load encroachment.

In order to counteract this problem, work has been done to block zone-3 relays from acting in certain conditions. One such proposal was given in [33] where the decision to block the relay was based on a comparison between the actual measured value of the power flow with the pre-determined value, where the decision to block the relay would hold when the estimated and the measured value of power are identical. However, the authors of [34] state that the

estimation of the line power flow is not always guaranteed to be right due to loop-flows and could possibly cause problems. It proposes a method capable of blocking the relay operation during load encroachment. The method is based on a "Difference-like Impedance-Algorithm" which uses the value of the fault resistance to differentiate between load encroachment and real faults. Phasor measurement units are used for this and the detection of load encroachment adds a necessary enhancement for the zone 3 relays. [35] uses phasor measurements to block zone 3 operation during power swings. A method based on synchronized sampling based fault location is proposed to correct distance relay maloperation during power swings and out-of-step events. Fault location techniques are used to precisely determine the location of a fault on a transmission line and can be used to verify if a fault is indeed present on a line and then take breaker action. It is based on an algorithm which uses raw sample of voltage and current data synchronously taken from both ends of transmission line.

Therefore, new methods of setting and operating the basic distance protection are always being developed. Due to their contribution to a number of recent blackouts, research in this area is an important addition.

2.4.4 Generator Tripping

Generators require a great deal of protection in order to protect the many aspects of their operation. The abnormal conditions can be summarised into the following, winding faults, overload, over-speed, abnormal voltages and frequencies. For generators it is also important to consider underexcitation, motoring and start up. The actual protection of these elements is not overly complex and can be done with standard protection such as overcurrent relays or mechanical sensors. It should be emphasised that these types of protection are not the only reason for a generator to be tripped, these are only to protect the generator itself. Damage to a generator can be very costly to repair and they therefore have certain limits by which they operate. Some of the problems with low frequency will be explained later however it can be summarised that many of the generator's ancillaries, pumps, fans etc. require constant frequency and voltage levels in order to maintain constant feeds to generators. If pumps slow down, the generator can slow down, further decreasing the frequency. Generators can also be tripped using intertripping where a generator is tripped in order to protect another aspect of the power system.

2.4.5 Intertripping

Intertripping is a method by which generators or lines are tripped due to a trip elsewhere in the system and is hardwired into the system. It is a form of special protection where the loss of a

line can cause further stability/overloading and in order to combat these, a generator or line is automatically tripped elsewhere to relieve the overload/risk of instability. These methods are not based on relay measurements but are designed to operate based on a relay trip elsewhere in the system.

2.4.6 Out-of-step relaying

Out of step relays are designed to trip during power swings. As a fault causes the apparent impedance to come into the zones for distance relays, a stability swing will do the same thing. Therefore it is important to be able to distinguish between the two. The difference is in the speed at which they occur. A fault trajectory will move into the zone instantaneously while a stability swing is much more gradual. In order to set the relays, numerous stability swings are simulated using a transient stability program and the stable swings should not encroach into the tripping zone. Any unstable swings are therefore set so that they will enter the tripping zone and hence will be tripped detecting the out-of-step condition. In some cases is it desirable to block out-of-step tripping where tripping could separate the system into greatly unbalanced islands with large generation/load imbalance. Such a situation can arise if two systems are interconnected by a few lines and there is one remaining line holding the systems together. Blocking is also useful when there is no fault on the protected line but only a transient penetration of the trip zone due to the oscillatory condition. Therefore, there can be benefits to tripping and blocking. Deciding whether to trip or block is usually the result of stability studies to investigate whether it is safer to trip or block a swing condition [13].

2.5 Problems with Load Shedding

As the main method of emergency control before a blackout, the problems with current load shedding methods are discussed here in order to provide further evidence for the need to look at new emergency control methods such as ICI.

While load shedding is fairly developed in many power systems, load shedding has not always prevented a number of major blackouts such as the Italian and U.S. cases in 2003. Load shedding has some drawbacks in its design which prevent it from working in all situations, and it can be seen that in the Italian blackout, load shedding functioned as designed, but the collapse occurred as load shedding could not alleviate the problems.

2.5.1 Italy 2003

One of the fundamental flaws in this blackout was the lack of coordination between load shedding and generation trip settings. This meant that generation was tripping along with load

being shed, as in Figure 2-7. Load was being shed to reduce the generation-load imbalance but generation was also being tripped off and as a result, load shedding could not reduce the gap. Generation should not trip until 47.5 Hz, but it was found that a large proportion of generation was lost at around 49 Hz. According to the UCTE report, the load shedding in Italy had performed properly, yet there was still a system blackout. The load shedding had performed according to the designs, but the design was meant for a drop in frequency only, and in the blackout of 2003, it was much more complicated than just a generation/load imbalance. In 1993, a similar event took place in Italy where a major line was lost, however, there was no blackout. Instead the country successfully islanded itself from Europe. This was because no other stability problems arose. It was manageable and load shedding could stabilise the system. In 2003, there was a large angle and voltage instability in the system which was what made it so difficult to manage. The voltage instability meant that the voltage began to fall and then generation began to trip as ancillaries require good quality voltage levels. 21 out of 50 large thermal units were lost before the 47.5 Hz threshold was reached, mainly due to voltage collapse which was caused by dynamic interactions between the UCTE main grid and the Italian grid during the disconnection phase. Also, only about 85% of 1300 frequency relays functioned normally to disconnect load automatically.

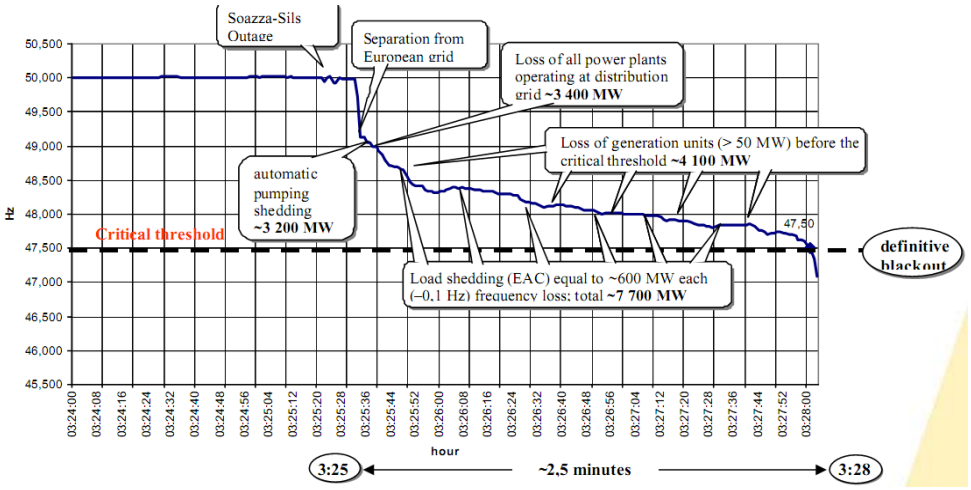

Figure 2-7 frequency behaviour in Italy in the transitory period [7]

2.5.2 Blackout in U.S. 2003

When load shedding does take place, it does not always drop enough load relative to local generation to rebalance and arrest the frequency decline. Hence, more power has to flow on the lines to carry power into generation deficient areas. This can lead to lines overloading leading to a cascade. In the U.S. Case, a similar sequence of events took place to the Italian blackout, and it resulted in at least 265 power plants tripping. Much of the generation again

tripped at the same time as load shedding was being carried out. Due to the delays in relays, much of the generation did not trip at the trigger point, but a few seconds after. So many generation plants tripped to protect themselves from being damaged but many tripped too early, or unnecessarily. Others were not coordinated with load shedding so that rendered it less effective. According to the U.S. report '*It must be emphasized that the entire northeast system was experiencing large scale, dynamic oscillations in this period. Even if the UFLS and generation had been perfectly balanced at any moment in time, these oscillations would have made stabilization difficult and unlikely*.' Based on this, conventional load shedding cannot act fast enough. In a transient disturbance, there is the issue that load shedding is designed with a delay to prevent false tripping, but this delay is too long for transient cases. If the delay was shorter, then it could be prone to false tripping etc.. Figure 2-8 illustrates some of the oscillations that were present in the system. It is these types of oscillations that can make UFLS (underfrequency load shedding) and UVLS (undervoltage load shedding) difficult to carry out. These large power swings made it difficult for load to be shed, and it reduced the amount of load that could be shed as there were high rates of change of voltage at the load buses.

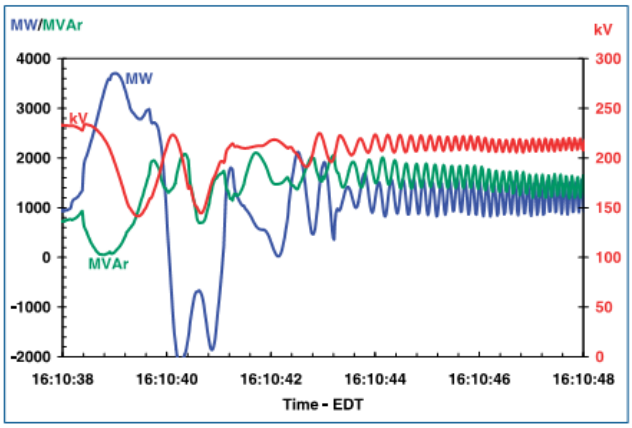

Figure 2-8 Active and Reactive Power and Voltage from Ontario into Detroit

2.5.3 Load Shedding and Location

As was seen in the U.S. blackout, the issue with frequency load shedding is that is has no bias for location which is inherent in the signal that it uses. Frequency is a global signal and load shedding that relies on frequency can only balance load on a system wide basis as it has no knowledge of where to shed load, or how much at a given location, (based on current UFLS schemes). UFLS allows the generation/demand gap to be reduced, but only on a system level. For example, the loss of a generator in London could lead to load shedding in Scotland. However, this only creates a redistribution of power flows. In an already overloaded or stressed system, this redistribution can put excess load on lines, causing those to trip and this can cascade

throughout the system. The problem with load shedding is that it needs to shed load local to the loss of generation. This will mean that generation demand balance is restored both globally and locally and it will prevent large redistribution of power flows owing to a system cascade. The complexity comes down to the signal required. Frequency is used to find the generation demand imbalance, but frequency cannot be broken into local areas, it only provides the global information. Only local load shedding can help to reduce these high power flows, which is difficult due to the lack of an appropriate signal.

2.5.4 Key Problems

The main problems with load shedding can be listed as follows which are summarised from the described case studies.

- Lack of coordination with generators
- Not relative to local generation
- Not fast enough for transient instability
- Can do very little to help manage dynamic oscillations
- Load shedding is hardwired, and so cannot be adjusted dynamically
- No signal available for local load shedding to prevent cascades
- Typical UFLS can lead to line trips

2.6 Summary

This chapter outlines a large number of serious events on power systems. The greatest problem with the majority of the cases is lack of coordination between the various operators, which is a very real problem. While technology is always advancing, there is still the fundamental issue of lack of coordination. As power systems become more dynamic with increased renewable and smaller distributed generators, the problem is only going to get worse. With less inertia, there is less time to act and current standards will not be able to cope. A simple example is from the Italian case where a phone call was required to request the load to be reduced. If less time is available for corrective actions, there needs to be rigid protocols and structures in place for interconnected systems. Another issue is that many of the problems are hidden from the day to day running, and only become apparent in extreme events. Such problems are difficult to account for, and therefore there is always some doubt with power system security.

Therefore, there are a range of issues which can put modern power systems at risk. As the Indian blackout has shown, the problem is growing ever bigger. New methods to avoid blackouts should be a welcome intervention in order to reduce the risk to generators, operators,

customers, governments and worldwide economies, all of which are greatly affected by the occurrence of a blackout. While there has been great innovation in the area of protection, the events presented in this chapter highlight the necessity for further approaches that can be used as a last resort if all existing methods fail.

The second part of this chapter described the main defence against blackouts, SIPS. It described what they consist of and how they are designed. A brief overview of existing conventional protection was then given, with detailed description on zone-3 distance relays. These relays have been major contributors in a number of blackouts due to poor operation. The main form of SIPS is load shedding and this was described along with many of its problems and examples of its performance in one blackout case. Clearly there is a strong case for a new adaptive methodology.

3 Review of Islanding Methods

3.1 Islanding Introduction

Power system islanding as a method of network protection is not a new concept, however it has gathered increased momentum in recent years. This is largely due to the large blackouts that have affected many of the world's modern power systems. This is despite advanced protection schemes and modern control measures. ICI concepts can be found dating back to 1940 in [36]. The networks of 1940 were much simpler than the networks of today where islanding consisted of tripping the very weak interconnecting lines between load areas. The Detroit network had five load areas with weak interconnections between them. If a fault was detected, using voltmeters, one of the load areas would be separated from the rest of the network and would continue to run in a self-sufficient manner. This was very simplified where the boundaries were already clearly defined. There are more examples of ICI from the 1960's where [37] looks a developing a relay specifically for simultaneous opening of lines to separate systems. This was said to be advantageous compared with the accumulation of near out-of-step conditions that successive line trips can cause.

The work in [38] references two further papers from the 1960's in [39, 40]. It states that with these schemes, a power system can be automatically divided into electrically isolated systems during emergency conditions. However, according to the authors in [38], these methods lack flexibility as they require certain restrictions in system operation or have very poor performing load shedding and generator tripping actions after separation. Therefore, there were only limited benefits to these schemes. However according to [41], ICI schemes were becoming a useful part of system operation. Such a scheme existed on the French system [42], where the separation was initiated by low frequencies or severe oscillatory conditions and also high power flows. Again, according to [41], [43] describes the South African electric system where a section of network isolated on fault could be further split to separate generation and matching demand in that section. This made restoration easier which would take place 3-4 seconds after the separation actions. The information of [42, 43] comes from [41] as they cannot be accessed directly.

Much of the work with network splitting is computationally heavy; therefore there was a limit to what could be done without powerful computers. As computing power increased and became more freely available in research, much more work could be developed on network splitting with increased complexity. [44, 45] introduced a method of partitioning power networks based on a

sparse eigenvalue based approach. While the method is not used for ICI, it is used for partitioning a power system into areas for corrective control. It was based on the concept of electrical distances among buses. It used a simplified version of the admittance matrix where it used clustering to group buses together based on their electrical distance. In [45] buses that are electrically interdependent are put into a cluster, while buses of different clusters are electrically distant from each other.

While computerised methods for emergency islanding operation were not yet developed, it was not unusual to island the system in emergency conditions based on operator experience. When operating in emergency conditions, controllers will behave differently and [46] looks at the implementation of automatic generator controllers for use during emergency conditions, particularly in islanding and restoration. Typically, Automatic Generator Controller, (AGC) would be suspended during emergency conditions, including islanding. However, it was realised that there were benefits to using AGCs during these times. Many utilities were designing protection schemes to create viable islands rather than blacking out portions of the network. The guideline was 'a successful island is a much better condition than a blackout'. Therefore, there was a push to design appropriate control measures which showed that there was an interest in islanding schemes as a method of emergency control.

As there was now a strong case behind islanding, new methods for islanding began development. [47] looked at the different types of disturbances and the methods available for protection, including islanding protection. The islanding method searched for situations where the generation compared to loading is at the biggest and the smallest. The island area is selected to have a 10% surplus, where the load is divided into two under frequency activated steps.

As the research into ICI began to grow, there were a number of main streams for optimal islanding solutions, these were graph theory based methods, minimal cutset enumeration methods and slow coherency methods. Much of the subsequent work can be described under these headings.

3.2 Slow Coherency based ICI methods

In a multi-machine power system after a disturbance, some generators have the tendency to swing together. This forms the basic observation of the coherent area identification. There are two main methods to determine the coherent generators. The first of these is to apply a disturbance and observe the swing curves of the generators. The second of these is to evaluate coherency properties, which are independent of disturbances. Slow coherency can be used to

identify the weak connections in a power system. It is for this reason that slow coherency was considered for ICI. According to [48], when a disturbance occurs, separation in the transient time scale is required. Otherwise, fast dynamics could propagate the disturbance very quickly. In this time scale, slow dynamics will remain constant on the tie lines. Once fast dynamics are detected on the tie lies, they are being propagated through the weak connections. Slow coherency is physical evidence of a weak connection, which is a network characteristic. There usually exists groups of strongly interacting units with weak connections between groups. But even very weak connections will become strong connections with significant interactions after a short period of time. The slow coherency work aims to disconnect weak connections before slow interaction becomes significant, or before the fast dynamics propagate.

Slow coherency is used in [49] to theoretically identify these weak connections. The method has the advantage that slow coherency among groups of generators does not vary significantly by the change of initial condition and disturbance. It also describes inherently the oscillation feature of large scale power systems, the fast oscillations within a group of machines and the slow oscillations between the groups via weak tie lines. [49] presents a slow coherency based method for network partitioning which groups generators and loads simultaneously into several coherent areas using slow Eigen vectors. The primary use of the grouping was however in network reduction and not islanding.

A new method is examined in [50] for simpler identification of coherent groups. Computationally practical coherency indices are developed which do not require significant computer storage. A study in [51] looks at extending the normal form techniques to investigate the mechanism of the system separation. Using this technique, the system trajectory at the vicinity of a relevant Unstable Equilibrium point (UEP) can be studied. The effective unstable modes and the associated nonlinear modal characteristics play a significant role in system separation. The technique was used to explain some of the complicated system separation phenomena. Time domain simulations compares well to the results of the normal form methods. Using normal forms algorithm was developed in [51-53] to find the natural grouping formed by machines due to nonlinear interaction. The normal forms algorithm was used in [53] to analyse a specific aspect of the Manitoba hydro system. Following the major loss of a HVDC system, severe under frequency was observed in the system due to the large deficits. One solution was to develop a separation scheme. The method of normal forms was used following the loss of the HVDC to investigate whether it could predict a natural grouping formed by the machines. The groupings would then provide a basis for developing an islanding scheme.

Slow coherency is used to find ICI cutsets in [48, 54]. When the grouping information has been found, an ICI program is developed based on graph theory techniques. The method finds cycles which it shrinks to single nodes and then provides an exhaustive search-based list of all the possible cutsets with the generation imbalance information. Slow coherency is used in [55] for generator grouping, but the problem is converted to a minimal cutset search to construct the islands with minimal net flow. Net flow is the power flow in the tripping lines which can be used to indicate the imbalance within the islands.

An automatic islanding program is developed in [48] using a C++ program to identify from the grouping information the exact locations in the network where islands can be formed. The program reduces the original system down based on a number of steps to create a manageable search area between two areas. A brute force search is then conducted on the network between these two areas to determine the cutsets to form the islands. The optimal cutsets are then found which consider the topological requirement and the minimum generation load imbalance requirement. The technique was applied to then 2003 US blackout in [56]. While the US-Canadian task force recommended a load shedding method to prevent the blackout, the authors applied a load shedding only method to the scenario and also applied the islanding method with load shedding in the load rich islands. It was found that the islanding method outperformed the load shedding method in reducing the transmission line flows but both methods had similar effects on voltage and relative angle behaviour.

[57] [58] proposes a technique for partitioning a large power system into a number of coherent areas for application to dynamic vulnerability assessment. The coherency concept is combined with a fuzzy clustering algorithm grouping of buses. The clusters are found by selecting representative buses from the data set in such a way that the total fuzzy dissimilarity within each cluster is minimized. This is not used as an islanding technique, but dividing a network into zones for the purposes of PMU placements. Such a method is useful for identifying the key areas for PMU placement in order to use PMUs for islanding purposes. For use in islanding, an on-line approach to determine the optimal separating points is proposed in [59]. It uses the coherency of generators during a disturbance which is determined from the simulation. When a transient stability disturbance is detected, a simulation is started until rotor angles between the leading generators and lagging one reaches 180 degrees. The generators are classified into a leading group and lagging group. The lines are tripped between the groups, separating the system. The separation points are adjusted to make both islands nearly balanced. Coherent groups are identified using PMUs in [60] for use with a k-means technique for splitting using the Matlab

Bioinformatics toolbox. The toolbox is used for real time clustering of the generators which swing together, enabling faster splitting of the system. However, for this method, a PMU is required on each generator bus. Configuration of the system islanding is based on predetermination of the coherent generator groups. It is based on two steps, to find the coherent generators, and then to find where to split the system taking load and generation balance into account.

According to slow coherency grouping, generators with similar oscillation modes will separate into different optimal groups, and [61] aggregates these generator groups together with corresponding buses to form virtual coherent nodes. A Laplace partitioning strategy is used where a weight index is proposed to measure the 'distance' of two adjacent nodes. A heuristic neighbourhood search partitioning strategy is used to search the possible cutsets while reducing generation-load imbalance. The partitioning is based on a K-way partitioning where the Laplace partitioning matrix has been extended to consider network topology and the directions of power flow. Then around each of the coherent generator groups, the other nodes can be collapsed into several large virtual nodes to obtain the best cutset.

3.3 Graph theory methods

This section is primarily focused on graph theory techniques where the primary function was to reduce the system complexity. A power system lends itself nicely to graph theory operations where buses and lines can be converted into a directed graph with vertices and edges. The islanding problem is then transferred into the graph domain where graph partitioning techniques can be applied. A simulated annealing program is developed in [62] to partition a graph. It is based on assigning every node to an arbitrary sub-network. Then, for every node, a trial reassignment of this node to a randomly selected sub-network is made. If this trial reassignment has reduced the cost function, it is accepted. While this process can find a satisfactory solution, it is a very time consuming process. This method was improved in [63] which combined the characteristics of the simulated annealing and a neural network. This method has a rapid convergence of the neural network and preserves the solution of the simulated annealing.

Ordinary Binary Decision diagrams (OBDDS) are used as a splitting technique in [64] [65] [66] [67]. The aim is to determine proper splitting points to separate the network ensuring generation/load balance and satisfying the transmission capacity constraints. However, such a problem is NP-hard and complex due to the combinatorial explosion of the search space. The

OBDD based programs can perform searching of the whole search space, and will always detect a solution if one exists. It has systematic ways to explore structural information which can avoid the combinatorial explosion issues making the solutions of large system feasible. [65-67] look at increasing the amount of off-line work for increased efficiency. [65, 66] considers only the steady-state constraints while [67] also considers the transient stability in the formulation. The graph is simplified in order to make these techniques faster. The complexity of the partitioning problem is highly dependent upon the size of the network, especially the number of edges which is also equal to the number of decision variables in system splitting. In [66] the graphs are simplified using the reduction of irrelevant nodes and edges and then combining nodes by area. The combinations are based on grouping nodes together based on their voltage levels.

[68] builds upon the method in [66] by improving efficiency for larger networks. It identifies that many of the previous methods could not ensure the stability of every island as the focus was on steady-state constraints to enable fast decision making. Stability was assumed to be kept with corrective control. The new method does not assume stability is kept and uses parallel processors to consider simultaneously real time searching along with the offline strategies. Using the real time strategies it finds which strategies will lead to unstable islands which are then excluded. Only feasible islands are then found, and splitting strategies can be computed in real time when using arbitrarily assumed asynchronous groups of generators.

A Minimal Cutset Enumeration Algorithm is used in [69] for islanding. A source node S and a sink node L are chosen in a graph G. Removal of the edges connected to S stops S from arriving at L. If one of these edges is not removed, S has a path and can get to L since the rest of the graph is connected. These edges form the minimal cutset of G. The paper looks at generalizing a source node S into a source node set SS. A minimal cutset is then composed of all the edges emitting from the source node set SS.

[70] looks at the islanding problem using the computational efficiency property of binary Particle Swarm Optimization (PSO) to counter the combinatorial explosion problem. The cost function used is based on the balance between real power generation and load, the relative importance of customers, the capacities of distribution and transmission systems and the possibility of region to be impacted. Finding the optimal solution is not key however as it is deemed that finding an efficient solution in real time is better than finding the optimal solution in an unacceptable time. The method does not consider the dynamic response behaviour, but given a suitable measure, the algorithm could include it in the optimisation solution. Angle

Modulated PSO (AMPSO) is more computationally efficient than Binary PSO and was used by [71] to find a number of efficient islanding solutions. It is used to optimize a fitness function which is defined according to generation/load balance, importance of loads and desired number of islands. However as this provides only static stability solutions it was further adapted in [72] to include a dynamic element using the slow coherency grouping technique to group generators. The AMPSO is then used to optimize a fitness function which is defined according to generation/load balance and similarity to the desired generator grouping. The resulting islanding algorithms provide good static and dynamic stability.

The combinatorial explosion problem is one of the key limiting factors to many of these methods. A network preparation method is used in [73] to reduce the system scale to an acceptable level. By analysing the physical connection and electric distance of nodes, load condition of lines and topological characteristics of original power networks, a simplified system is created. It is a much smaller scale than the original, yet retains most of its static and dynamic characteristics and is reduced using redundant bus elimination, area partition and bus aggregation. When this reduction is complete, a further stage called OMDD Graph Simplification is performed. The result is the simplest undirected graph without any multi-edge and one-degree vertex that can be obtained which is the layer that the strategy searching is performed on.

However, according to [74], most of the previous methods demonstrated on reduced size systems are sub-optimal within some limits. To overcome this, the slow coherency method is combined with a new graph theory method to determine the island boundary. One new element that is added is an edge index based on the voltage level on the line. As previous work did not consider this, the partitioning solutions was considered sub optimal. The graph is then simplified according to the voltage levels of the different components. A k-way graph partitioning problem was adopted to compute the best islanding point. It was found to be computationally heavy for real systems so a multilevel k-way partition algorithm was used which would split the graph into smaller islands, perform the searches before projecting the solutions back onto the original graph.

A method for islanding by combining both the dynamic and static characteristics is introduced in [75] using a Krylov projection method and a new optimization algorithm to minimize load shedding. The method is able to reduce the large initial search space for islanding strategies, especially when considering the dynamic characteristics. The method limits search space to only

the boundary networks of coherent machines. A spanning tree search algorithm is used to find all combinations of stable islands. The method works quite fast and is suggested for real time calculation. The first step is to calculate the interarea modes of the system as well as clustering the network machines and buses in different coherency groups as primary islanding strategy. The second step of the splitting strategy is a minimum spanning tree based breadth first search algorithm is used to balance and minimise the net flow between the islands tie lines.

A power flow tracing method is applied to ICI in [76] to determine the domain of each generator. An initial splitting boundary based on grouping information of generators on the graph model is found. The initial splitting boundary is then refined to find the final splitting boundary. The method is based on two principles: 1, coherent groups of generators should be determined and should be in the same island. 2, the reduction of generation load imbalance in each island reduces the amount of load shedding to be done. Power flow tracing is used to determine how much active power a load node receives from a particular generator node, and a load node can be designated to the generator node. The generator node and its designated load nodes form the domain of that generator node. The initial splitting boundary is a coarse one. After the system loses stability, according to grouping information, the initial splitting boundary search is executed on the graph model with domains of various generator nodes determined with all nodes in some domain. The edges whose incident nodes are in two different domains are found and if the generator nodes in the two domains are asynchronous, this forms the initial splitting boundary. The initial boundary may provide islands with unacceptable imbalance and assuming a reasonable splitting boundary is located between asynchronous generators, the reasonable splitting boundary must be near the initial splitting boundary. Consequently, the reasonable splitting boundary can be found from the initial. A neighbourhood of a load node v is the union of the islands in which at least one of the load nodes is adjacent to v. Such nodes can then be moved into their neighbouring areas. By moving the node which can minimise the imbalance the most, the system is recalculated as well as the neighbourhood nodes. This is repeated until the unbalance degree can no longer be reduced. It is a very fast method, for the 118 bus system, for two cases, the solution was achieved in less than 10ms. However, it was stressed that the post-split conditions could be unstable and would rely heavily on corrective control. This was verified in [77] where the method was tested to make the generation load imbalance is small as possible.

[78] presents a new simplification algorithm to reduce the complexity of the system. Generators belonging to the same slowly coherent group are collapsed into a dummy node, and a graph

partition library is used to split the graph into a given number of parts. Some extra islands formed by the partition library are merged into their adjacent large islands and the original cutset of the actual power system is recovered from the highly simplified graph. The authors were able to show that, under fault conditions without any corrective action, their system would result in uncontrolled islanding and some generators would lose synchronism while splitting the system into two pre-designed islands prevented this loss of synchronism. This method was tested on the WECC system [79] using 4 extreme contingencies under two different operating conditions using time domain simulations. It was found that with controlled islanding, frequency and voltage stayed within an acceptable operating range, less load shedding was required and the system was not sensitive to the choice of cuts. This suggests the same cuts can be made for a range of contingencies.

[80] uses a graph partitioning method to investigate secondary voltage control. The method divides a system into regions to prevent the propagation of disturbances and to minimize interaction between these regions. The network is divided into regions that are designed to have minimum interaction and therefore any disturbances in a particular region will not strongly propagate to the other regions. The regions can be reconfigured and updated in accordance with variations in grid structure. In this paper, disturbances are defined as increases of active and reactive power to the loads.

3.4 Spectral Partitioning methods

The latest research using graph theory techniques is based around spectral partitioning which is widely used in image processing, data mining and the machine learning communities. It is considered superior to traditional clustering algorithms in terms of having deterministic solutions and its equivalence to graph min-cut problems. For the purposes of this review, the spectral methods are described with their use in ICI. A spectral partitioning ICI strategy is proposed in [81]. The underlying principle is that Graph Eigenvalue analysis provides some insight into the intrinsic structure of the power system. Spectral graph theory is used to identify transmission lines that lead to the creation of islands and in comparison to other methods; it requires fairly low computational effort. The spectrum of a graph is the set of eigenvalues associated with the various matrices representing the graph. In a graph with n vertices, there are n eigenvalues. The spectra from the different matrices contain the information about the graph connectivity, sizing and degree of the nodes. The analysis of the graph eigenvalues and eigenvectors provides and important insight into understanding the graphs in a power system. The spectral method computes a separator from the eigenvector components. The different

constraints in the partitioning problem allow breaking up the graph. A partitioning can then be achieved by progressive bi-sectioning of the graph. A term called the Fiedler vector is obtained from the second eigenvalue and the corresponding eigenvector of a Laplacian matrix. The properties of the vector then reveal the connectivity properties of a graph and the Eigen pair is closely related to the vertex and edge connectivity. The theory behind the efficiency of using the Fiedler vector can be found by looking at the Cheeger inequality [82]. The spectrum of the Laplacian matrix is therefore used to study the islands or sub-graphs through the second eigenvector. It also requires low computational effort and the computation time has a linear relationship with the number of edges. The method is applied in [81] for the 68 bus system with successful separation, however it only splits the system into islands, without proper emphasis on the dynamic or static problems outlined in other work. The authors addressed this issue [83] by adopting a two stage approach. The first stage splits the islands using the graph theory method described above while the second stage aims to balance the islands using UFLS.

As these methods did not consider any dynamic assessment, [84, 85] introduced a two-step spectral clustering method where the first step looks at the dynamic component, and the second step looks to evaluate the static components. In the first step, the machine nodes (generator and dynamic loads) will be grouped by normalised spectral clustering with dynamic models to satisfy the dynamic constraint. In the second step, all the nodes will be grouped by constrained spectral clustering with power flow data to satisfy the static constraint and get the minimal cut solution. The aim is to find a partition of the graph such that edges between different groups have a very low index and the edges within a group have a high index, they can then define a cost function to the graph bisection. To achieve reliable ICI operation, generators in each island should be synchronous approximately where the slow coherency method is adopted to find the weakest connection between machine groups. Using a classical undamped electromechanical model, a linearized second order dynamic model of m-machine power system is used. The reduced admittance matrix is used to form a Laplacian, so a dynamic graph can be created. The entries of the graph affinity matrix denote the partial derivative of the active power between machine vertices with respect to the rotor angle. Using a generalized eigenproblem with normal spectral clustering algorithm, a solution of the optimization problem can be found and the solution is a spectral graph view of slow coherency. The static component is based on the power flow data and a second graph is constructed. The entries of this graph affinity matrix denote the absolute value of active power between two buses. By neglecting network loss, this matrix is symmetric and non-negative. It is then possible to get the Laplacian matrix of the graph. To

incorporate the dynamic graph into the optimization, the machine grouping result can be used as prior knowledge to form Must-Link constraints and Cannot-Link constraints. Then the constrained spectral clustering can be used to solve the problem. One method is to modify the edge indices of the graph. If two nodes belong to the same class, the index is increased, if the two nodes belong to different classes, the edge index is decreased. However, the approach used here is to use a projection matrix to modify the subspace. The simulation results and further analysis indicated that the spectral clustering based method is particularly efficient for large scale power systems. Since one, or more, of the created islands might reach an unstable operating point, and therefore cause a blackout, [86] proposed a methodology which includes at least one blackstart unit within each island and assures sufficient generation capability to match the load consumption with each island. By assuring blackstart capability and sufficient generation capability, parallel power system restoration is planned in case of any eventuality.

A grid based service for intentional islanding has been developed and demonstrated in [87]. A number of PCs were aggregated together to set up a grid environment. The authors then use a graph partitioning network based on the Laplacian matrix and the Fiedler eigenvalue and eigenvector. The grid service works with the assumption that the number of partitions are given, and then is has to minimise the power imbalance among the newly formed islands along with minimising the number of lines to be cut.

3.5 Islanding experience and actions

Islanding methods do not have to rely on computer simulations in order to detect or find an islanding boundary. There are many solutions for islanding through intelligent relay design that will island a system when a certain action, or sequence of events take place. Such methods are usually developed if there is an underlying problem in a system where a system is frequently prone to split, or collapse at weak points. [88] looks at designing equipment to separate the power system when an out-of-step is detected between generators. It uses a prediction algorithm to predict when the phase angle between generators exceeds a threshold and continues to increase. It is at this point that the system would be separated to prevent the entire power system from collapsing. [89] discusses power system separation, but not as a protection scheme, as uncontrolled islanding where elements cascade and lead to the separation. It then discusses the actions that need to take place in order to stabilise the system, mainly looking at the imbalance. It is stated that adaptive load shedding is preferable before system separation. The dynamics on the Spanish and Portuguese system are investigated in [90] using long term time domain simulations. As these systems were susceptible to separation from the rest of

Europe, it was important to have good stability studies for system planning and operation. The main goal was to evaluate the performance of two main simulation programs for long term stability and analyse the influence of some important control and protection elements. It was found that elements that affect longer term stability were not standard in transient stability analysis, such as load frequency control and power plant dynamics. It was found that very different system behaviour can be obtained depending on whether or not all relevant dynamics are considered or not and therefore accurate models are necessary for proper evaluation of the system.

There are frequent faults and blackouts on the Bangladesh Power development board grid and restoration can take almost a full day for all generators to be brought back on line. [91] developed an easy-to-implement and affordable method for ICI. The viability of post fault splitting at pre-specified buses and lines is studied, determining the criteria on which the decision for islanding is taken to avoid a blackout. The island boundaries are pre-specified on the basis of geographical proximity of the synchronous generators. The machines in the same geographical section oscillate coherently when a fault occurs in the system. Depending on the location and severity of the fault, the system can be divided into 2-5 completely separate islands. These are formed by 5 geographical sections. The decision to island is based on real time monitoring of the MW flows on the lines between these sections. There are set threshold values computed where the lines are tripped if the thresholds are exceeded for two successive sampling instances. The threshold value was set through studies of previous blackouts. Alongside the ICI, there was additional generator/load shedding at various locations to maintain stability of the machines in the islands. The amounts and locations are to be obtained from transient stability studies. A short term splitting strategy to relieve overloaded sections of a network is proposed in [92]. This preserves the carrying capacity of transmission lines. The main strategy utilised to prevent blackouts is fast and slow under frequency load shedding. However there was a strong case for system separation with a power deficient part to prevent blackouts. The main criteria for the optimal splitting point are dictated by two main criteria, the least number of users disconnected, and the most favourable conditions for automatic synchronization.

An optimization technique for determining the settings of various emergency power system controls is developed in [93]. The aim is to produce a comprehensive defence plan against events such as cascading blackouts. The goal of the technique is to find a new equilibrium point following a severe contingency. The proposed technique considered generator tripping, load

shedding and ICI as the main emergency control actions. Genetic algorithms are used due to their success at solving nonlinear combinatorial optimization problems. This is used to find the optimal combination of generators and loads to be tripped as the best solution for the network to regain a new equilibrium point whilst maintaining supply to as many customers as possible. If a successful solution cannot be found from this, then system ICI can also be applied. The optimization technique uses transient stability evaluation algorithms, based on time domain simulation, to assess the fitness of the potential solutions. A Genetic Algorithm is used to find an optimal islanding scheme to geographically restrict the extent of the fault. The authors claim that the algorithm is robust and produced a superior defence plan when compared to the present defence plan when tested on the Libyan network. It was tested on a historical blackout and worked effectively.

On the Chinese system, when an out-of-step problem is detected it is typically separated from the main grid as a last resort preventing widespread blackouts. In some instances there can be large generation deficit which can cause low voltage and high frequency at the beginning of the islands forming. This frequency can be high enough to initiate generators over speed protection which can cause cascades. In these situations, under-voltage load shedding measures cannot work quickly enough due to its time delay. Therefore [94] proposes a new measure to keep the island stable. The main concept is that a certain proportion of the load is shed when system splitting is operated, the quantity can be set according to the generation deficit. After that point, other load shedding measures can act for the other conditions. This is said to improve the voltage profile, increase the generators output power and limit island frequency change. If there are no power oscillations, the frequency will decrease due to a generation deficiency, however, if power oscillation or out of step has occurred before ICI, the generator voltage in the disturbed area will also oscillate. Hence, the power output of the generators oscillates as well. As generators' mechanical power changes very slowly, in some area with large generation deficit, in an oscillation period, the time when the generators' power input is larger than their output is longer than half a period. That means the generators will accelerate. Then the system is split to two or more islands, the generators are subjected to severe disturbance again. It is for these instances that the method aims to reduce the problems. The proposed method will shed load at the time of splitting so that the deficit at the time of splitting is reduced and this is calculated and applied. It was found that it will work to keep an island stable.

[95] describes two wide-area protection schemes for controlled islanding of the Uruguayan electrical power system. The first scheme relies on a local signal available for distance protection

relays, while the second scheme is based both on local and remote synchrophasor measurements. Both schemes are compared in terms of load shedding required. The first scheme is based on conventional power swing blocking and out of step tripping functions included in distance protection relays. The controlled islanding was performed by measuring locally, the rate of change of impedance at both ends of the 150 kV lines. This strategy acts at 4 pre-selected 150kV locations to make a North-South separation. The second scheme utilises a novel algorithm based on synchrophasors called predictive out-of-step tripping. The detection of unstable oscillations is based on voltage phasors that are measured at both ends of the 500 kV lines. Both schemes performed better than the current scheme while the Power Swing Blocking-Out of Step Tripping (PSB-OST) reduced load shedding by 18% and the OOST reduced it by 30%. While the Out Of Step tripping (OOST) appears better, the PSB-OST method was far simpler and it has the advantage that is can be implemented with the current protection.

The power flow tracing method is used in [96] to create a distribution factor matrix (DFM) for islanding. The elements of the DFM indicate the distribution in power transfers between the generators and loads. In each island, power should be roughly balanced. This distribution information is used to group generators and loads and can provide the principle islands for islanding. For large interconnected systems a genetic algorithm was used to improve the feasible searching strategies. The GA searches for a solution to a problem by working with a population of individuals each of which represents a possible solution. At each generator, a new set of between approximations is created by selecting individuals according to their fitness in the problem domain.

A study of islanding in the Uruguayan power system is presented in [97]. The system is highly dependent on two 300 kV transmission lines connecting the largest generators and the Argentinian interconnector, both in the North, to the large loads in the South. There have been occasions where these lines have tripped leading to widespread blackouts. The paper investigates controlled separation of the Uruguayan network into two stable islands using PSB and OST tripping protection functions. The investigation is based on transient stability studies, using comprehensive models. The study compared the amount of load shedding required to achieve similar transient performance with and without controlled islanding. It was able to show through extensive simulations, that with islanding, a 20% saving on load curtailment could be made.

An auto load shedding and islanding scheme is developed in [98]. The paper develops the sequences and conditions needed in order to use the different load shedding schemes and islanding strategies. The method relies on a series of steps of load shedding based on the rate of change of frequency. If the frequency continues to fall after a number of steps, the grid is separated into a number of parts; however, these parts are determined by relays that are already in place and programmed offline. The scheme is then tested on a number of blackout scenarios. The authors claim that when a system is radial in nature, it is easier to identify the buses where the system can be disintegrated by carefully inspecting the mismatches between loads and generation of different zones. As the power system that it is designed for and tested on is radial, this is the method that is used.

3.6 When to Island?

The focus of this thesis is on the *'where to island'* problem, as is much of the work described thus far. However, there is still the issue of knowing *'when to island'*. There have been a number of techniques employed to answer this questions which are briefly described here.

Decision trees (DT), from [99], can be used to control globally the conventional protective schemes to enable/disable devices such as relays. DTs for the system are generated in the form of offline pre-calculated logical paths. They serve as a statistical alternative to the deterministic system models. If a large number of contingencies are analysed, and DTs generated offline, these trees can be quickly accessed in real time for prediction. Using sensory data (WAMS), the condition of an evolving system can be traced on the branches of a DT and a rapid response may be initiated. Here, generator angles and velocities are used as the inputs. It was found from simulations that transient stability behaviour was best characterized by generator angles and velocities, which were also found to be sufficient to understand the degree to which a stable machine is disturbed. The output is the decision whether the system is potentially stable or unstable. The DT itself does not island the system. Strategically located relays are armed by the DT, to trip independently in response to local sensory signals. The relay locations correspond to weak links connecting groups of coherent machines. A disturbance takes time to reach the cut set of lines so the DT must arm the relays within this time window. Decision trees need to be trained; in this case of the 179 bus system, three phase bolted faults of different clearing angles were simulated for all buses of the power system. When the simulation was complete, they were classified as stable or unstable. The globally trained DT gave a good indication of overall stability but did not respond satisfactorily to events in a sensitive portion of the network. DTs focused on a particular area/bus may better complement the response of such a globally trained

unbiased tree. It is unbiased as all buses are tested with the same fault. However, as the operating point changes, a new set of DTs may be required for robust security analysis. The rate of refreshing DTs would depend on the sensitivity of the DTs to changing operating points.

[100] presents a technique to predict and quickly analyse effective defence mechanisms following the outage of critical lines. System studies can provide details of lines that are at or near capacity, lightly loaded lines and under/over voltages. Potential line outages that may lead to a cascading event are also analysed through contingency analysis. This can then be used to define the weaker areas of the network, where a list of weak nodes is prepared and probable island ties are devised. Predicting the initiating disturbance is difficult as it requires regular and systematic system analysis. To overcome this, a set of contingencies were pre-selected as in [101]. These were then used at the initiating disturbances for cascading outages. The authors state that defining island boundaries just prior to an impending disturbance is not possible, since the disturbance cannot be predicted. Instead, some boundaries are loosely defined based on monitoring line flows and calculating the line outage distribution factors. The lines that are near capacity tend to trip during disturbances. These lines are then closely observed while conducting load flow studies and contingency analysis.

[102] presents the problem of when to initiate controlled islanding accounting for power marketing objectives using a multi objective Pareto optimization. The paper examines the trade-off between controlled islanding and the retention of the large AC system interconnection. Previous work did not consider the power market viability and the role of the system operator was not included. The term Pareto optimization in this context refers to the constrained optimization of multi-objectives. The *where to island* aspect is based on slow coherency grouping. The main objectives of the optimization are to maintain as large an operational stability margin as possible and retain all interties between purchasing and selling entities in power marketing transactions, especially high value trades. The transient stability load margin is used as the objective function for transient stability.

[103] develops an efficient simulator to estimate the sequence of automatic events that follow a contingency leading to islanding and cascading outages. It is natural islanding that is being investigated, or how a system will form into islands through cascading tripping rather than intentional islanding. The simulator first identifies the islands that a network will split into through the null space of the network susceptance matrix. Each island is then tested for a surplus or deficit of primary frequency regulation, followed by any necessary corrective load shedding

or generator tripping. Then each islands load flow is solved and tested for possible line overloads and corresponding line tripping. The overall contingency analysis reruns until all loads are shed or the islands can operate at some reduced load level within their operational bounds. Traditionally the study of cascading events required time domain simulators which meant large computational burden and it could take minutes to hours to solve. This is an alternative which models more efficiently the sequence of automatic events that follow the occurrence of a set of triggering contingencies. The proposed simulator computes the quasi-steady state reached by the system whenever a load, generator or line is disconnected. The fundamental assumption of this paper is that every stage of the system remains stable and converges to a new steady state. The advantage of this simulator is the vast reduction in computation time. It is recognised that this method will overlook the possibly important transient behaviour between the states, and does not consider the protection that may be initiated by such transients. The results are therefore fast, but possibly overly optimistic.

Another decision tree assisted scheme using phasor measurements is presented in [104]. The timing to form pre-defined islands is determined in real time by proposing an event-triggered controlled separation scheme using decision trees (DT). For any critical contingency that may lead to transient instability, a DT is trained specially to predict the impending loss of synchronism. Using phasor measurements, instability assessment results can be obtained within only a few cycles after the initial disturbance and an islanding strategy can then be armed to form the islands.

An ICI scheme must be inherently predictive in nature, as well as reliable, according to [105]. This algorithm monitors the synchronous stability of the system at a global level using a Prony analysis. It is coupled with detection of local out-of-step conditions to decide when to island the system. The actual island boundaries are formed using the slow coherency grouping methods already described. There are a number of frequency domain decomposition methods that can be used to detect unstable oscillatory modes as in [106]. One such method, called Prony analysis can be used to identify the system dynamics after a disturbance is detected. It is useful, for a multi-machine system, to examine a portion of the network to be islanded separately from the rest of the network. In the portion to be islanded, the dynamics of the machines resemble those of a single machine, while those in the rest of the network resemble those of an infinite bus. The method of calculating candidate modes of separation from the coherency between machines (possible system instability) is demonstrated. The Prony method gives good results for a linear system identification problem. However, it was recommended that further attention to prony

analyses in transient stability assessment should be done. The method is based on R-Rdot relays and using this method to arm them. The relays would already be located in strategic locations in the network.

Real time controlled islanding based on the correlation coefficients of generators is presented in [107]. Online measurement of the generators rotor angle oscillations are used to produce correlation coefficients between all pairs of generators, from which coherent groups of generators are identified. Splitting indices between coherent groups are evaluated from these coefficients. Following a disturbance, in the case of splitting coherent groups towards ICI, the values of the splitting indices start to increase detecting tendency of coherent groups towards splitting state. The work focuses on when to split based on network degradation due to dynamic instability of generators and formation of asynchronous coherent groups of generators. The increase rate and sign change of the indices are used as an alarm for tendency of coherent groups to separate from each other and propelling the network into splitting state.

3.7 Summary

A number of different approaches and methods have been investigated for the purposes of ICI. Many of the techniques are based on graph theoretic approaches and by converting the network into a graph, there are a number of graph partitioning algorithms that can be applied. These methods can include graph simplification in order to perform faster searching through various methods. While graph simplification is useful for speed, some of the detail will be lost which some authors have identified as being an issue.

To consider the dynamics, the typical approach is based on slow coherency where it is believed that the weak connections between generators are the best points to split a network. There are numerous ways of detecting slow coherency which have been covered and there are also a number of ways to use it in ICI. As slow coherency is rarely used on its own to island, it is combined with some objective function such as minimal power imbalance.

One of the issues with many of these techniques is the generalised approach that is taken. Very few methods are disturbance dependent, and as a result, the number of islands formed may be excessive for the type of disturbance that is observed. While there are methods that can perform ICI without using graph theory techniques to form the islands, these are usually case-specific solutions. They can also be classed as special protection systems described earlier. In these cases, there is a frequent problem with the network where the ICI solution is already known, it

is just a case of splitting along this boundary. Such methods then rely on predictive relay operation that will arm the strategically positioned relays in the system.

Spectral clustering techniques are some of the newer methods being applied due to their computational efficiency. They rely on eigenanalysis of the graph and can spit the system into two, or more islands depending on the chosen index. There have been a number of advances to these methods such as two step approaches to consider dynamics and also black start restoration.

The final part of this review looked briefly on the *when to island* work that has been developed. Much of this work relies on offline training using decision trees and so are not truly adaptive. This is still an on-going topic of research, as much of the previous developments can be computationally heavy, or require offline analysis which then needs to be updated for every new operating point.

4 Power System Stability

4.1 Introduction

The purpose of this section is to outline the typical areas of stability within a power system and to give a brief overview of the effects and outcomes of each type of stability. As much of this thesis is aiming to split a network without causing instability, it is useful to see what principles are involved with each type of instability. Power system stability can be divided into three main areas, Rotor angle stability, Frequency stability and Voltage stability as seen in Figure 4-1. They can be further divided into different types of stability depending on the size of the disturbance and also defined by their time periods of interest.

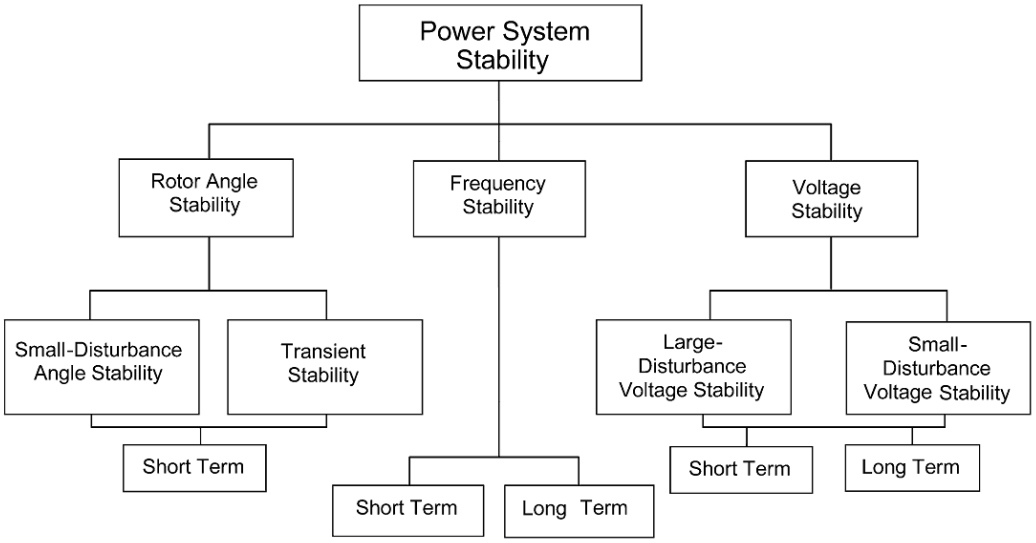

Figure 4-1 Classification of power system stability [108]

4.2 Frequency Stability

4.2.1 Introduction

Frequency stability generally deals with large disturbances such as the sudden connection of a large load, or sudden loss of generation by protection equipment. These types of faults generally introduce a long term imbalance in the power produced by generators and consumed by loads. The effects of the imbalance are initially reduced by using the kinetic energy of the rotating rotors of turbines, generators and motors after which point the system frequency will change. If the frequency drop is prolonged, and continues to fall, the system can experience a frequency collapse, such as that shown in Figure 2-7. In this case, the lowest operating frequency was 47.5

Hz. Should the system drop below this point, protection systems will start to trip generators, and generally the system will blackout like Italy in 2003.

However, in understanding frequency stability and the facts surrounding its behaviour, there are a number of issues including control and operational procedures that govern it. The following description briefly describes some of the main control features in a power system to maintain frequency.

4.2.2 Governor controls

When the load in the system is suddenly increased, the electrical load at the generator will increase and will exceed the mechanical power input. The power deficiency is initially supplied by kinetic energy stored in the rotating system. The reduction in the kinetic energy causes the turbine speed to drop and hence the generator frequency also falls. This change in speed is then sensed by the turbine governor which will adjust the turbine input valve to change the mechanical power output to bring the speed to a new steady state. However, governor action takes time to change the generators speed due to the large inertia.

4.2.3 Prime mover model

The prime mover is the term used to describe the source of mechanical power and could be a hydraulic turbine in a river, a steam turbine where steam is produced from burning coal, gas or nuclear fuel, or a gas turbine. The most common are steam turbines where the model of the turbine relates the changes in mechanical power out to changes in steam valve position. There are a wide range of characteristics depending on the types of turbines. Depending on the mix of generation in system, a very different frequency response could be observed, where turbines such as hydro plant can change their output very quickly. Steam turbines in coal plants take much longer to change due to the requirement to generate more steam and also overcome the large rotor inertia. For hydro turbines, the mechanical input power can be generated quite readily by allowing more water through. Wind turbines also have a very quick response as the speed is related to the pitch angle which can be adjusted quite quickly. However, such devices are decoupled from the grid due to power converters, and hence provide no inertia. However, advances are being made to create artificial inertia, though this is still very small compared to conventional generation.

4.2.4 Automatic Generator Control

The way the frequency changes in a system is also heavily dependent upon the operation of the AGC. As a system is made up of a number of generators and loads, the total power will vary throughout a day. However, these variations are well understood and operators can rely on daily

load curves to anticipate the loading throughout the day. These changes are dealt with using unit commitment where a daily schedule is drawn up for which generators will be used for generating or reserve, or simply shut down. This is typically done once per day while economic dispatch is used for the shorter intervals to determine the actual output of the generators on a 30 minute basis. It is the changes outside of these intervals that are covered by AGCs where the load changes would be smaller, but faster. The purpose of the AGC is to

- Maintain frequency at the required value
- Maintain power interchanges with neighbouring control areas at their required values
- Maintain power allocation among the units in accordance with area dispatching needs

The frequency of a system is dependent upon the power as the rotational speed of the generators is proportional to frequency.

4.2.5 Necessity for Frequency Limits

There are a number of reasons for maintaining frequency within set limits [109]:

1. Speed of AC motors are directly related to the frequency. While many of these machines are not really affected by frequency variation of even 50+/- 1.5 Hz, there are certain applications where speed consistency must be of a high order.

2. If the nominal frequency is 50 Hz and turbines are run at speeds corresponding to less than 47.5 Hz or more than 52.5 Hz, the blades of the turbine can be badly damaged. Therefore strict limits on frequency should be adhered to as stalling of a generator will further aggravate the problem if the system is operating at low frequency.

3. Running power transformers in under-frequency operation is not desirable. In order to maintain constant voltage, if the frequency drops the flux in the core increases. As transformers are designed corresponding to the 'knee-point' on the B-H curve, a small increase in B can drive the transformer into the saturation region. As a result the magnetising current can exceed the normal full load current, where a sustained under frequency condition can damage the transformer winding due to overheating.

4. If the frequency and voltage fall in a system, load shedding is usually initiated which means loss of revenue to the suppliers as there is less demand.

5. One of the main reasons for maintaining nominal frequency is for the thermal power plants safe operation. The operation of a thermal plant relies on the consistent operation of two types of fans. An ID fan (Induced Draft Fan) draws out flue gas from

the furnace of boiler and handles hot air/dust. The FD fan (Forced Draft Fan) supplies the necessary air into the furnace for combustion of fuel and it handles air at normal temperature. At reduced frequency, the blast from these fans is reduced and as a result the generation also decreases and becomes a cumulative action and can lead to the complete shutdown of a plant if corrective actions are not taken.

4.2.6 Definition of Frequency Stability

The *IEEE/CIGRE Joint Task Force on Stability Terms and Definitions* defines frequency stability as the ability of a power system to provide a steady frequency following a severe system disturbance which results in a significant imbalance between the generation and the load. [110] It is dependent upon the system's ability to restore equilibrium between the generation and load with the minimum unintentional load being shed. Frequency instability can occur from sustained frequency swings that can lead to generators and loads tripping. A severe system disturbance will generally result in large excursion of frequency, power flows, voltage and other system variables. These excursions will usually invoke the actions of processes, controls and protection that are not typically modelled in transient stability or voltage stability analysis as they may typically be slow such as boiler dynamics, or in the cases of protection may only be triggered in severe conditions.

The times of the processes and actions that are activated can range from fractions of a second for devices such as under-frequency load shedding and generator controls and protection to several minutes for prime mover energy supply systems and load voltage regulators. Hence, as seen in Figure 4-1, frequency stability can be short term, or long term. An example of short term instability can be found in [111] where a formation of an under-generated island with insufficient load shedding meant that frequency decays rapidly causing a blackout in the island within a few seconds. For longer term instability, they are usually more complex such as steam turbine over-speed controls or boiler protection and controls which can range in the time of tens of seconds to several minutes.

During a frequency excursion, the voltage magnitudes can vary significantly, especially in islanding conditions with under-frequency load shedding that unloads the system. The changes in voltage magnitude can be higher percentages than the frequency changes, and these too can affect the load/generation imbalance. A high voltage can cause undesirable generator tripping by poorly designed or coordinated loss of excitation systems or volts/Hertz relays. For an overloaded system, if the voltage is too low it can negatively affect the operation of impedance relays.

4.3 Voltage Stability

4.3.1 Reactive power and voltage control

The sources of reactive power in a system are generators, capacitors and reactors. A generator's reactive power is controlled by field excitation. Other methods of improving the voltage profile of the transmission network include transformer load-tap changers switched capacitors, step-voltage regulators and static VAR control equipment. To maintain generator voltage and reactive power output, generators are fitted with excitation systems to change the currents being fed to the rotors on generators, and hence the reactive power that the machine produces. In older machines, excitation was provided through slip rings and brushes by means of a DC generator mounted on the same shaft as the rotor of the synchronous machine. In modern excitation systems, ac generators with rotating rectifiers, known as brushless excitation, are more common. The primary means of generator reactive power control is the generator excitation control using an automatic voltage regulator (AVR). The role of the AVR is to hold terminal voltage magnitude of a synchronous generator at a specified level.

An increase in the reactive power load of a generator is accompanied by a drop in terminal voltage magnitude. The voltage magnitude is sensed through a potential transformer on one phase. The voltage is rectified and compared to a dc set point signal. The amplified error signal controls the exciter field that increases the exciter terminal voltage. This increases the field current in the generator which results in an increase in the generated emf. The reactive power generation is increased to a new equilibrium, raising the terminal voltage to the desired value.

Section 4.2 shows how the real power demand affects the frequency but here; a change in the reactive power mainly affects the voltage magnitude. Generally, the interaction between voltage and frequency controls is weak enough to consider them separately in analysis

4.3.2 Definition of Voltage Stability

Voltage stability is defined in [110] as the ability of a power system to maintain steady voltages at all buses in the system after being subjected to a disturbance from a given initial operating condition. A progressive fall, or rise, in voltages can bring about instability, which can result in loss of load in an area, tripping of lines and other elements due to protective relays which can cause cascading outages. Such a fall in voltage can be seen in Figure 4-2.

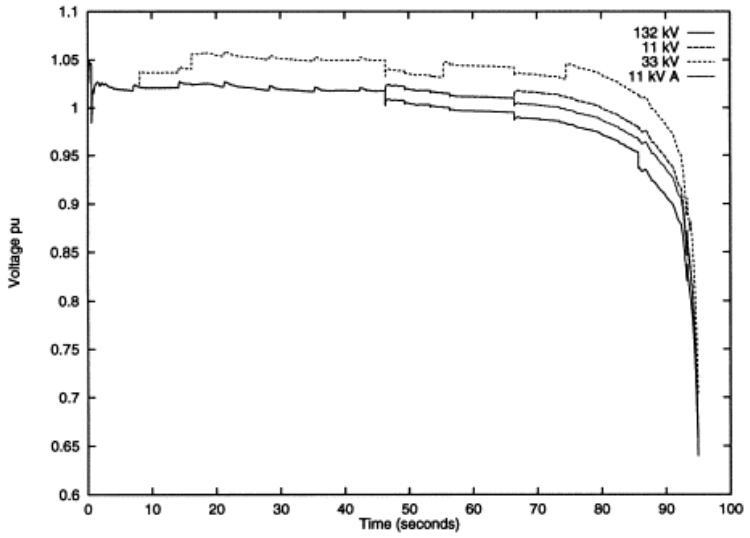

Figure 4-2 Voltage collapse [112]

A progressive drop in voltage can also be associated with rotor angle instability. Consider the loss of synchronism of machines as the rotor angles between two groups of machines approaches 180°. This can cause a rapid drop in voltages at intermediate points in the network close to the electrical centre. This would typically be taken care of with protection to separate the two groups where the voltage levels would then recover. However, if the system is not separated, the voltages near the electrical centre will rapidly oscillate between high and low values due to the 'pole slips' between the two groups of machines.

Another term that is frequently used when discussing voltage instability is voltage collapse. Voltage collapse is the process by which the sequence of events corresponding to voltage instability lead to a blackout or abnormally low voltages in a significant part of a network. The main force behind a voltage instability is usually the loads. In response to a disturbance, the power consumed by the loads tends to be restored by the action of motor slip adjustment, distribution voltage regulators and tap changing transformers. However, restored loads increase the stress on the high voltage network by increasing the reactive power consumption which then causes further voltage reduction.

One of the major contributors to voltage instability is the voltage drop that occurs when active and reactive power flow through inductive reactances of the transmission network. This limits the transmission capability of the network for power transfer and voltage support. These can be further limited when some generators reach their field or armature imit. Therefore, voltage stability is at risk when a disturbance increases the reactive power demand beyond the sustainable capacity of the available reactive power resources.

The most common form of instability is in the form of progressive voltage drops. However, the risk of overvoltages cannot be neglected, and has been seen in [113]. The overvoltages are caused by the capacitive nature of the network as well as by underexcitation limiters preventing generators from absorbing the extra reactive power. In these cases, the instability is associated with the in-ability of the combined generation and transmission systems to operate below a certain load level.

From Figure 4-1 there are two main categories of voltage stability, namely *Large-disturbance voltage stability* and *Small-disturbance voltage stability.* Large-disturbance voltage stability refers to the system's ability to maintain stability following a large disturbance such as system faults, loss of generation or circuit contingencies. To evaluate the long term voltage stability, it is necessary to examine the non-linear response of the power system over a period of time sufficient to capture the performance and interactions of devices such as motors, under load transformer tap changers and generator field current limiters. The study period can be a few seconds to tens of minutes. Small-disturbance voltage stability on the other hand refers to the system's ability to maintain steady voltages when subjected to small perturbations such as incremental changes in load. This type of stability is more closely related to the load characteristics and the continuous controls. It is useful in evaluating how the system voltages will respond to small system changes, and is based on linearization of the system equations. These linearized equations allow for the computation of valuable sensitivity information in identifying factors influencing stability. However, they cannot account for the non-linear effects such as tap changer controls. A typical approach is to use a combination of the linear and non-linear analyses to provide a full evaluation.

As with the frequency stability, there exists both short-term (Transient) and long-term voltage stability which are summarised in Figure 4-3. Short-term stability involves the dynamic behaviour of fast acting load components such as induction motors, electronically controlled loads and HVDC converters. The study period will typically be several seconds and the full analysis requires the solution of the system differential equations, making it similar to the rotor angle stability analysis. Dynamic load models are often required to properly account for the dynamic load component. Long term instability involves slower acting equipment such as tap-changing transformers, thermostatically controlled loads and generators current limiters.

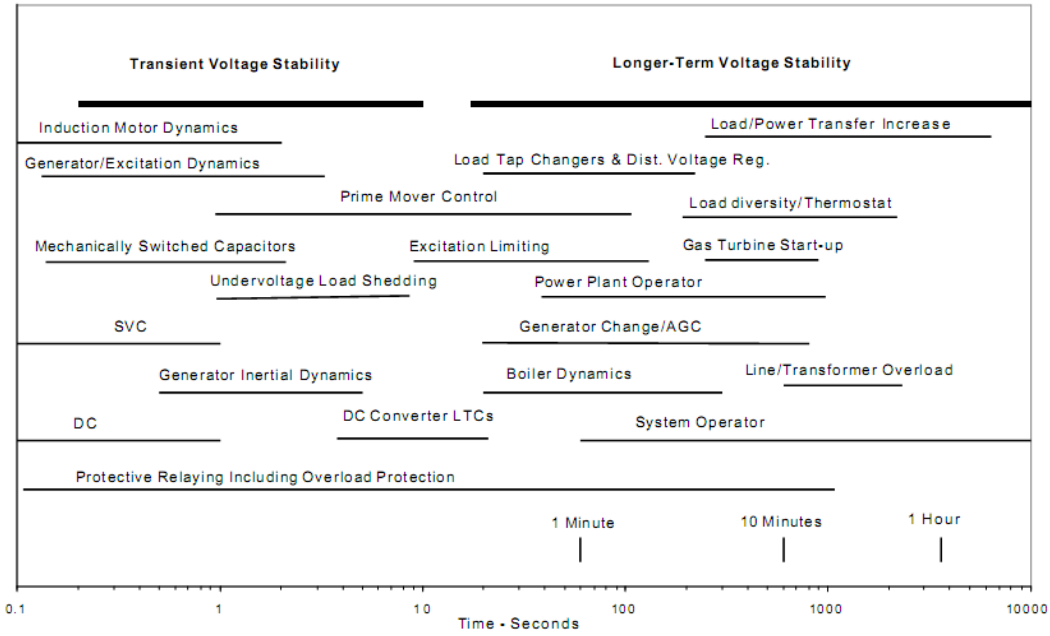

Figure 4-3 Types of voltage instability [114]

The study period can be as high as several minutes and longer term simulations are required to study the system dynamic performance [115]. Stability is usually determined by the resulting outage of equipment rather than the severity of the initial disturbance. Instability is due to the loss of long term equilibrium. An example being loads trying to restore their power beyond the capability of the transmission network and connected generation or the lack of attraction towards a stable post-disturbance equilibrium point which could be caused from remedial actions that are taken too late. In many cases, static analysis [116-119] can be used to estimate the stability margins, identify factors influencing stability and screen a wide range of system conditions and a large number of scenarios. For detailed studies that would require the timing of the control actions, a Quasi-steady-state time domain simulation would be required which is a combination of a static and dynamic approach to analyse different aspects at different time periods [120].

4.3.3 Evaluating Voltage Stability

From the various study times required for voltage stability, there are a number of techniques available for assessing voltage stability. These can be divided into two main categories, static methods and dynamic methods. There are also two main areas in which voltage is assessed. The first is a loadability limit and the second is contingency analysis. The loadability limit of a power system is related to the ability of the network to transmit the required power and the ability of the active and reactive power sources to produce the required power. Contingency analysis studies the system's ability to maintain stability after a series of contingencies.

Static methods

Static methods consist of using *snapshots* of system conditions at various times. At these snapshots, the time derivatives of the state variables are assumed to be zero and these variables take on values corresponding to that specific time frame. Therefore, the overall system equations reduce to purely algebraic terms which allow the use of static analysis techniques [121]. In order to test the loadability limit using static methods a series of load flows are required. For each successive load flow the system is stressed further due to increased load or generator increments. This type of study can include voltage control devices, however these can lead to convergence problems as there are too many adjustments with each iteration. The load is incrementally increased until the load flow diverges which indicates the loadability limit of that system. Standard load flows will stop just before the stability limit, therefore a continuation power flow is used. This allows the load flow to go beyond the stability limit which is necessary to produce the P-V characteristic as shown in Figure 4-4. The loading parameter shows the amount by which the load is multiplied by. A similar curve can be created for Q-V.

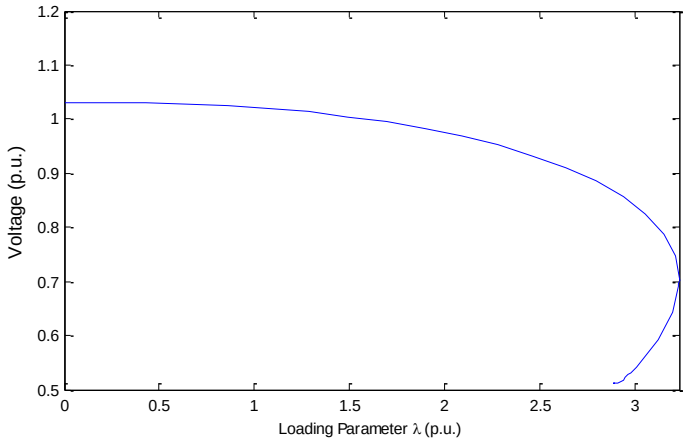

Figure 4-4 Example P-V Curve

To determine how sensitive a bus is to voltage stability, the slope at the nose of the curve is used. [122] However, this must be carried out for each bus individually. This means that a characteristic must be obtained for every bus in the system which must then be analysed in order to obtain the information for that bus. While there are methods by which to speed up the process such as finding the distance between the upper and lower parts of the curve, these would still require individual study for each bus. Another problem with these methods is they provide no insight into the causes of the instability. Also, as the buses must be carefully selected

at which to generate these plots, it may not always be possible to plot the curves due to a divergence in the power flows from a point elsewhere in the system.

By using the static approach, at a snapshot in time, the power flow equations can be linearized around that operating point. It is upon this linearization of the power flow equations that static methods area based. By performing linearization of the power flow equations, the Jacobian matrix can be used as a sensitivity matrix for small perturbations about that operating point.

A method known as V-Q Sensitivity analysis looks at the relationship between the voltage and changes in the reactive power. The information used in the analysis comes from the load-flow Jacobian. The stability is assessed based on the following definition. A system is voltage stable at a given operating condition if for every bus in the system, bus voltage magnitude increases as reactive power injection at the same bus is increased. A system is voltage unstable if, for at least one bus in the system, bus voltage magnitude decreases as the reactive power injection at the same bus is increased. In other words, a system is voltage stable if V-Q sensitivity is positive for every bus and unstable if V-Q sensitivity is negative for at least one bus. Therefore, by monitoring the changes in the load flow Jacobian over the different load levels, or indeed contingencies, one can observe when a bus changes from being stable to unstable by analysing the elements of the matrix.

Modal Analysis is another static method which is based on V-Q sensitivity analysis with eigenvalue analysis. The advantage of this method is that it gives information about the instability and also the mechanism of the instability. The modal analysis is based on a reduced power flow Jacobian to provide the sensitivity between the voltage and reactive power. It will provide a series of eigenvalues, where a negative eigenvalue means the system is unstable, and a small positive eigenvalue means it is close to instability. The method then uses eigenvectors and participation factors to locate which buses or branches in the system are associated with these sensitive eigenvalues. This provides an insight into where instability occurs and how close to instability the system is. If a system is close to instability, then the components which are highly participating to these modes of instability are of interest.

Another method linked to the linearized load flow Jacobian is reactive power distribution factors. While it is not directly a stability tool, it can be used to quantify the change in bus voltages due a line loss. By deriving sensitivities from the load flow Jacobian and injecting power through that matrix, the resultant changes in voltage can be found. It is a useful tool for assessing the direct effects on voltage due to a line trip.

These are the main static stability methods in use. A wider range of static analysis methods for voltage stability can be found in [108].

Dynamic methods

The static methods described can be used in different scenarios; long term planning with loadability limits and it is widely used for contingency analysis because of its speed. However, for increased accuracy, dynamic modelling is required to account for load models which vary with voltage and the effects of the various control in the system. Dynamic methods are all based on time domain simulation which can account for all the various dynamics. Depending on the length of the simulation, both long term and short term stability can be assessed. For loadability studies, loading can be gradually changed and will allow the controllers to react to that change. This information cannot be obtained from static methods.

Dynamic methods are also much better for contingency analysis as they can give very detailed analysis after the fault has occurred. Advantages include finding the location of voltage problems; assessing the protection behaviour which may act for temporary voltage dips and investigating the effects of controllers before severe problems.

However, in order to gain all this detail, huge computation power would be required and would takes tens of minutes to complete. There are methods by which static and dynamic methods can be used together such as contingency ranking where only the severe contingencies are assessed using dynamic methods.

Therefore, there are a number of techniques available for voltage stability assessment. There have been a number of on-line assessment tools which are based on mixes of static and dynamic methods, however many still take in the order of minutes. The problem with these methods, such as [123] is that they rely on decision trees. These must be trained offline and hence will only work if the measured condition has been one which was trained for.

4.4 Rotor Angle Stability

Rotor angle stability refers to the ability of synchronous machines in an interconnected power system to remain in synchronism after a disturbance. It is dependent upon the ability to maintain or restore the equilibrium between electromagnetic torque and the mechanical torque of each synchronous machine in the system. The instability that occurs would be in the form of increasing angular swings of some generators leading to a loss of synchronism with other

generators as shown in Figure 4-5 where the generator shown in blue is going unstable and oscillating against the machines shown in red.

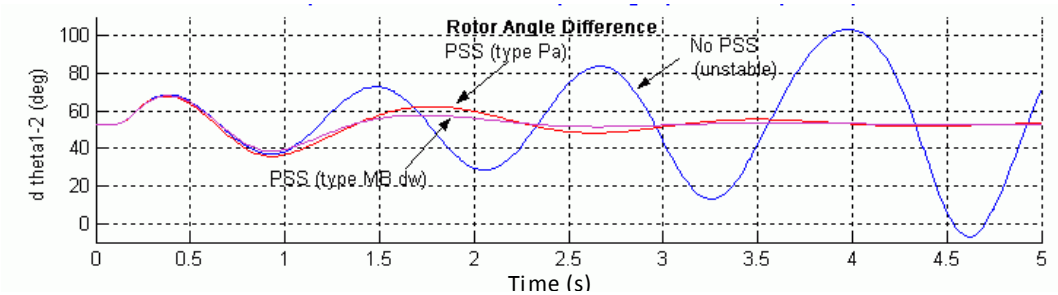

Figure 4-5 Rotor angle stability [124]

The study of the rotor angle stability problem is based on the electromechanical oscillations that are inherent in the power system. One of the fundamental principles in the problem is the way that machines vary their power outputs as the rotor angle changes. For steady state conditions, there is equilibrium between the input mechanical torque and the output electromagnetic torque of each generator and the speed will therefore remain constant. However, when the system is perturbed, the equilibrium is upset and results in an acceleration or deceleration of the rotors according to the laws of motion of a rotating body. If one generator temporarily runs faster than another, the angular position of its rotor relative to that of the slower machine will advance. The resulting angular difference transfers part of the load from the slow machine to the fast machine, depending on the power-angle relationship. This tends to reduce the speed difference and hence the angular separation. This power-angle relationship is highly non-linear, and beyond a certain limit, an increase in angular separation is accompanied by a decrease in power transfer such that angular separation increases further. The instability will occur if the system cannot absorb the kinetic energy corresponding to these rotor speed differences. For any given situation, the stability of the system depends on whether or not the deviations in angular positions of the rotors result in sufficient restoring torques [121]. Loss of synchronism can occur between one machine and the rest of the system, or between groups of machines, with synchronism maintained in each group after separation.

The change in the electromagnetic torque of a synchronous machine following a perturbation can be separated in to two components

- *Synchronizing Torque component*, in phase with the rotor angle deviation
- *Damping torque component*, in phase with the speed deviation

Both of these components are necessary for system stability to exist. A lack of sufficient synchronizing torque results in aperiodic or non-oscillatory instability while a lack of damping

torque results in oscillatory instability. Indeed it can be shown in [125] that there is a link to voltage and the synchronising torque. Lower voltages at a generators terminals can be related to reduced synchronizing torque, and therefore lower stability. It is therefore important to maintain high voltage levels for rotor angle stability. Rotor angle stability can be separated into two categories.

Small-disturbance (or small signal) stability

This type of stability deals with a power systems ability to maintain synchronism under small disturbances, where the disturbances are sufficiently small so that linearized system equations can be used for the analysis. The stability depends on the initial operating state of the system and instability can arise in two forms, i) an increase in rotor angle through a non-oscillatory or aperiodic mode due to lack of synchronizing torque, or ii) through increasing amplitude of the rotor oscillations due to a lack of sufficient damping torque. In modern power systems, it is usually the insufficient damping of oscillations that causes trouble as opposed to the aperiodic instability which has largely been eliminated.

Small signal stability problems can be either local or global in nature, where local problems are usually associated with rotor angle oscillations of a single power plant against the rest of the system. These are called local plant mode oscillations and the damping of these oscillations depends on the strength of the transmission system as seen by the power plant and the associated generator controls. The global problems are caused by interactions among large groups of generators and have widespread effects. They involve oscillations of a group of generators in one area swinging against a group of generators in another area; hence they are called interarea mode oscillations. These are more complex and significantly differ from those of local modes of oscillations. The load characteristics can have a major effect on the stability of interarea modes. The time period of interest for small signal stability is typically between 10-20 seconds following a disturbance.

Large-disturbance rotor angle stability

Large-disturbance rotor angle stability, also referred to as transient stability, deals with the ability of a power system to maintain synchronism for severe disturbances, such as a short circuit on a transmission line. The resulting system response involves large excursion of generator rotor angles and is influenced by the nonlinear power-angle relationship. Transient stability depends on both the initial operating state of the system and the severity of the disturbance. Any

instability is usually in the form of aperiodic angular separation due to insufficient synchronizing torque, manifesting as first swing instability. In large power systems, transient instability may not always occur as first swing instability associated with a single mode and it could actually be the result of superposition of a slow interarea swing mode and a local plant swing mode causing a large excursion of rotor angle beyond the first swing. It can also be the result of nonlinear effects affecting a single mode causing instability beyond the first swing. For transient stability, the timeframe of interest is usually between 3-5 seconds following the disturbance and may extend to 10-20 seconds for very large systems with dominant interarea swings. Both these types of stability are classified as short term as seen from Figure 4-1. The rotor angle stability is part of a parallel project, and hence is not discussed in detail in this thesis.

4.5 Summary

This chapter introduces the three main types of instability of concern in power systems. While the topic of power system stability is a large area, this chapter aims to give a brief description of each type, and what the common causes and effects of each type are. The descriptions in this chapter should help give a further background to the events shown in chapter 2.

It has been shown that frequency stability is typically related to generation and load imbalance. There are a number of factors which can influence it, such as generator control. It has also been described why it is important to keep frequency levels high as there are a number of devices that rely on high quality frequency levels such as motors. Voltage stability was also addressed and the main form of control was explained from automatic voltage regulators. It was shown that a progressive drop in voltage can lead to a voltage collapse, and the causes behind such a collapse were discussed. A brief overview of the methods used to study voltage stability was then given. The static and dynamic methods were outlined along with the types of stability that are studied.

Finally rotor angle stability was introduced and the main influences that govern generator synchronism were explained. Rotor angle stability is important as the loss of synchronism of a machine will generally cause it to disconnect and lead to a generation load imbalance, which can cause frequency collapse. Therefore, there is a connection between all types of stability which should be considered.

5 Methodology

This chapter will introduce the methodology behind the thesis, from the reasoning behind the development of a new method to an overview of the problem solution. The purpose of this chapter is to formalise the conclusions of the previous chapters to build up the grounding and thinking behind the new method that will be explored in this thesis. Chapter 2 has provided strong motivation for this project. It is clear that there is a need to investigate methods that can reduce the risk of blackouts without having to rely on load shedding and existing forms of protections systems. While there are many different forms of protection systems, there is clear evidence that these do fail leading to major events. A new method of protection is therefore proposed that can offer one final line of defence when all the previous protection systems have failed.

5.1 Previously developed Islanding schemes

ICI is one method that can mitigate the effects of cascades and prevent blackouts. Chapter 3 has given a comprehensive review of the developments and advances in ICI schemes. There are methods ranging from slow coherency generator grouping and graph theory methods to intelligent relay designs that will automatically detect severe events and island a system. Indeed it has been shown through the various methods that ICI can prevent blackouts when applied to real events. This thesis presents a method that is comparable with the network searching methods like slow coherency and graph theory methods rather than the fixed relay methods. The fixed position relay methods are system specific and are typically located on lines where there are frequent problems, or where operators have experience of weak connections. The focus is instead on the best islanding solution for a system based on the real time information from that system. The island solution will be dependent upon the operating point of that system, i.e. island boundaries can change depending on the network conditions.

It is of the author's opinion that there is still one issue that has not been addressed properly by previous methods which is dependence of fault location. When looking at the coherency methods, and in fact much of the work covered in chapter 3, the island solution is a generalised solution. It is independent of the fault location and size. While this has been mentioned as an advantage in some of the approaches as it allows the same solution to be applied regardless of the fault and hence reduces computation times as a generalised solution exists. Indeed, the

coherency principle is very much based on the fact that coherency will not be affected by the size or location of the disturbance and was hence chosen as the ideal candidate.

The issue with generalised solutions is that they can lead to unnecessary islanding and can in fact lead to an overall reduction in system security. Taking the slow coherency methods as an example, there are islands created for each of the coherent groups. The slow coherency method forms the foundation for many of the methods presented in chapter 3, and therefore provides a good comparison here. The methods that create multiple islands could be represented by Figure 5-1, where it shows that for a disturbance in the system, it is likely to end up in one of the generalised islands formed.

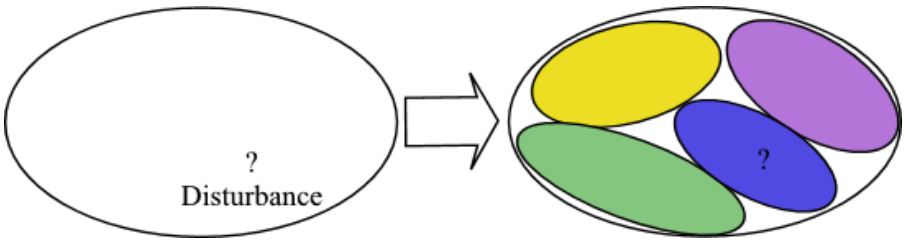

Figure 5-1 Previous Methods

5.1.1 The disadvantages identified

As these methods create a number of islands based on the various grouping methods, it means that a system is split into a number of smaller areas. This has a number of possible drawbacks however. If there are a large number of islands created, then these islands may have very low inertia within them. In fact, it is possible for an island to be created with almost no inertia if created around a wind farm. Creating many smaller islands will always have a lower inertia, and therefore have a higher risk than when left connected to the interconnected networks. In the smaller islands, any changes in load will cause rapid deviations in frequency in comparison to larger systems. This brings about additional concerns for control. Generator control may be too slow to operate properly as it is tuned to a system with higher inertia. Protection systems are also based on larger systems, and cannot guarantee reliable operation if the frequency is more sensitive. An example being load shedding and how much load would be shed? This is the first major problem, a large number of islands create lower inertia systems which are difficult to control and maintain. Indeed, any islanding action will produce smaller islands with lower inertia. However, in creating a larger number of islands, some of the islands may have been created unnecessarily. Consider again Figure 5-1 to contain the disturbance, it is not necessary to have so many islands.

Another issue comes from the overall reduction in system security. A system with a number of lines means there are multiple paths to deliver power throughout the network. Should one of these lines be tripped, there are other lines that can take up the difference and continue to carry power. If an islanding solution consists of many islands, there will typically be a large number of lines to be tripped between these islands. Should a problem occur, there are fewer paths available to deliver power as the lines have been tripped to form the islands. Therefore the remaining lines must carry the power, which will have a higher risk of overloading and tripping themselves. This can quickly lead to a cascading event and cause a blackout itself. Therefore, it is better to keep in as many lines as possible in order to maintain higher levels of security. While the solutions with multiple islands should mean that a disturbance is contained within one of the islands, the reduced security placed on all other islands is deemed an unnecessary risk.

There is also another disadvantage with forming many islands which is linked to reduced security across the whole network. When a system is broken up into many islands, due to the reduced inertia in each of those islands, these islands are put at greater risk of collapse. Therefore, for the customers in all of these islands, there is a higher risk of loss of supply, for example, a small change in load could lead to a large change in frequency. The load shedding scheme that is hardwired into the network could trip all the load and cause that island to collapse from a slight change in load without any fault occurring.

5.2 A new proposal

It is upon this basis that a new methodology is proposed which will aim to minimise the number of islands and therefore reduce the tendency to create unnecessary islands. As a result, it will also reduce the impact on system security and also minimise the number of customers affected by a disturbance. ICI can be divided into two streams, *When to Island?* And *Where to island?.* This thesis will focus on where to island and will be assuming that the disturbance location has already been identified that is likely to lead to a blackout. A novel method in determining ICI boundaries will be explored and will aim to address the concerns raised in this chapter about previous ICI methods.

5.2.1 Existing Control and Protection

Splitting a network into a number of smaller islands is a severe action, hence it is proposed as a last resort solution. However, ICI any system will still be a major shock to the system. One of the major problems is with the existing control and protection schemes in the system. These are typically set and tuned for operation in interconnected operation and when in islanding mode

there is no guarantee that they will behave as expected. Therefore, the aim is to create an ICI scheme which has minimal impact on the network topology. i.e. the ICI actions should aim to create a system which closely resembles the pre-islanded state in terms of flows etc. If the system can transition to an islanded state with minimal effects on loading, generation and flows then the consequences on control and protection can be minimised. There are devices such as rocof relays which will however perform differently and may need to be dis-armed when in islanding mode. Therefore, in order to create an island that is as close to the steady state pre-disturbance island as possible, the ICI solution should be based on the pre-disturbance system. Therefore and solutions that are applied will aim to return the system to its pre-disturbance state.

5.2.2 Outages for which ICI can be used

The methodology has been designed to be disturbance dependent, however, not all outages are solved using islanding. Islanding is ideal for any disturbance which may result in cascading outages which may cascade into a wider area, much further from the origin of the disturbance. The following table outlines a series of outages for which islanding could be used.

Outage	Effects
Line outage	In heavy loaded system, a line outages may result in further line outages and cascades. Line outages can be the precursor to many blackouts. The following types of outages could be remedied by islanding Causes of line outages • Tree Flashover (phase to ground) • Phase to phase fault • Power swings • Relay maloperation • Load encroachment
Sustained electrical fault	If a severe electrical fault (3-phase) is not cleared due to malfunction of protection, islanding would serve as back up, this may involve a substation or transformer fault.
Loss of Reactive power source	As with US, this led to major redistribution of power leading to cascades and a blackout. Islanding to minimise the redistribution of power would be beneficial in these outages.
Power Swings	Power swings caused by oscillations could be remedied by islanding by splitting the two oscillating groups into two islands
Mechanical faults	Where a mechanical fault such as a switch in a substation fails, islanding could be used to ensure affected areas is minimised. This was

	seen in Sweden in 2003 where a mechanical fault in a bus bar led to the loss of a major transmission corridor.
Generator outage	A generator outage is difficult to tackle with islanding as it will mean that one island will be significantly imbalanced. However, the algorithm could be adjusted to create one balanced island while neglecting the poorly balanced island, in favour of complete blackout
Load Outage	Similar to generator outage, however, this would be better tackled using generator tripping.
Hidden faults	These are problems which are unknown to the operators and the problem is only discovered in an emergency condition. This may involve relays that malfunction, or relays that were set incorrectly. Islanding would provide a safety net for these hidden faults.

There are a number of disturbances for which islanding may not be applicable. They would typically include very fast transient problems. If a major fault causes a major first swing instability, it is likely that an online method will not be fast enough. However, the conventional protection should protect against these. Also, events such as lightning would be covered using conventional protection. It is where any event on the power system leads to a cascade that islanding actions are ideal.

5.2.3 ICI Design Criteria

There are a number of criteria that the ICI solution should meet, or at least consider in order to make it a viable emergency control action. The ICI solution must consider the operation of power systems so that it would be possible to implement such a scheme in a network. It will not just find new ways to split networks, or graphs, but will be linked to power system operation and stability throughout the methodology.

The ICI solution will therefore be designed with the aim of meeting the following:

- Provide a disturbance dependant solution
- Minimise the number of formed islands
- Minimise the effect on network security
- Avoid cutting through lines with high power flows
- Minimise the power that is being affected
- Avoid creating islands with large generation/load imbalance
- Avoid creating islands with could be susceptible to voltage collapse

- Create dynamically stable islands
- The algorithm needs to be fast for use in emergency conditions
- Aim to reach the steady state pre-disturbance operating point

These criteria should form the minimum requirements for providing an effective ICI solution; however, they are not all independent of each other and can be combined to simplify the problem.

5.2.4 Outcome for Sick Island

This methodology will aim to cut out the sick part of the network, hence minimising the exposure that the healthy island has to the major disturbance. If the disturbance is sever enough that is will cause the full system to blackout, then when it is confined to a smaller area, the effects of the disturbance are likely to cause the sick island to blackout. Therefore, the sick island is being sacrificed in order to maintain the majority of the system. As this is the last line of defence against a blackout, it is deemed an acceptable action to let the sick island collapse where the only alternative would be to allow the disturbance to cascade into the healthy island and cause a complete blackout.

5.3 The proposed solution

The method that is being proposed is a disturbance dependent approach rather than the generalised solutions, and will be related to the location of the disturbance. While a generalised solution can be applied for any disturbance, the new solutions will require knowledge about the location of the disturbance. With the use of Wide Area Measurement systems (WAMS) becoming more widespread, it is possible to get very accurate information from the power system much faster than previous methods based on SCADA or state estimators. Therefore having accurate information, in real time, about fault types and locations opens up a new area for developing ICI solutions.

In order to minimise the number of formed islands, the ideal solution would form two islands, one island that contains the disturbance, and one island that consists of the remaining system. This would also minimise the effect on network security as the least number of lines will be cut to form fewer islands. The problem that needs to be solved is finding the boundaries of these islands. Starting from the assumed disturbance node, an area of influence is identified around this node, which forms the island to be disconnected from the rest of the system. This means that there is an island created which contains the disturbance, but all other customers are left connected to the interconnected system. Therefore, there is a larger inertia in the remaining

system, there are no unnecessary lines being cut and the customers outside the area of the disturbance are left with a higher level of security. The worst case scenario here would be the loss of one island in which the disturbance is contained, rather than the possibility of losing many islands due to reduced security. This is preferable to a complete blackout.

The island which contains the disturbance is referred to as the 'sick network' while the area outside this island is called the 'healthy network' and can be seen in Figure 5-2. From this figure, the ideal scenario is two islands. The principle shown in Figure 5-2 is very different from the solution presented in Figure 5-1 with a larger number of islands.

The novelty with this new proposal lies in the fact that it is an online approach which will utilise the real time measurements. Using an online methodology, many of the identified disadvantages can be avoided where the standard methods would use a pre-planned approach which is general, and therefore, overly conservative. Using the online approach allows less conservative approaches to be taken and therefore provides a new way to address power system islanding.

The following sections will provide an overview of how the methodology will be developed, with further details and examples contained in the subsequent chapters.

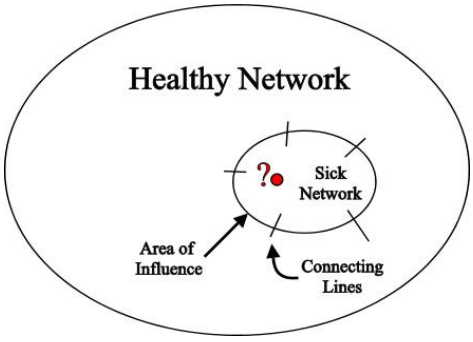

Figure 5-2 The Area of Influence surrounding a sick node that will be islanded

5.3.1 Area of influence

The main part of this thesis is centred on finding the area of influence as this is a novel approach to tackling the ICI problem. If the disturbance location is known, how can a border be drawn around that disturbance? It must separate it from the rest of the network while maintaining good quality of supply within that island as much as possible. In order to find this area of influence, a method known as power flow tracing will be used. The purpose of the tracing is to find all the nodes that are strongly connected to a disturbance node in terms of power flow contributions. I.e. if a node gets 100% of its real power from the adjacent node, then there is a

strong contribution and are strongly connected. The disturbance node is therefore referred to as the seed node for which power is traced to and from this seed node. If the contribution exceeds a threshold value, then the nodes are said to be strongly connected and are placed in the same island to form the sick network. The threshold value will be explained in more detail in the following chapters.

Therefore, the sick island consists of all the nodes that are strongly connected to the seed node, where all nodes outside this island are weakly connected. I.e. there is found to be less contribution in terms of real power between these nodes. The tracing method is also quite useful as it can be designed to meet to first six required criteria. The first three have been explained already, however the next three are inherent in the tracing method. It is preferable to avoid cutting through lines carrying high power as the loss of these lines can cause a large redistribution of power flows, which can also put stress on the generators for dynamic stability. According to the tracing, buses with a high power flow between them will have a strong connection and will be contained within the same island. If two adjacent nodes have a low power flow or contribution between them, then cutting through this line will have less severe impacts on the power distribution. As there is minimal number of islands formed, where the lines are found to have low power flows, the total power (absolute sum of flows on cut lines) is inherently minimised. This is important in terms of the 'shock' that a generator perceives due to a sudden change in power. If the total power being cut is quite high, then some generators could see a very large change in the required power output which will either cause the machine to accelerate, or decelerate. Should the change be severe enough, this acceleration/deceleration may be large enough to push the rotor angle beyond its limit and cause the generator to lose stability.

Another useful advantage of tracing is that is requires information from load flows only, and therefore time domain simulations can be avoided which are time consuming. This is one of the key limitations put on the ICI method that it needs to be fast. Therefore it was decided to extract as much possible information from the load flow information that can be acquired quickly in real time. The area of influence is based on the real power contributions between the buses. However, it is also important to note that because the power flow tracing used here is based on real power only, voltage stability and reactive power would need to be assessed independently.

5.3.2 Frequency stability

The frequency stability of a system is determined by the generation/load imbalance, and also the amount of inertia in the system. If the island has too little generation, the frequency will

decrease where the rate will be dependent upon the total inertia within that island. In order to ensure frequency stability, it is necessary to minimise the imbalance between the load and the generation. The imbalance can be found as the sum of the power on the lines carrying power in and out of the islands. By ensuring that the lines being cut carry low power, the effect on the imbalance can be minimised, and can be easily calculated from the line flow information. The tracing method will aim to find solutions which cut through minimum power flows, hence minimising imbalance. This means that the frequency stability can be considered through the tracing method.

5.3.3 Voltage Stability

While the tracing method for ICI considers many of the required design criteria, it does not consider reactive power or the voltage that is associated with it. As already mentioned, real-time time domain simulations must be avoided due to the long computation times required. Therefore, a method to assess voltage security using power flow information was explored. The issue with voltage stability is that it is highly non-linear in nature, and to be studied properly time domain simulations are necessary. As the prime focus was on speed, it was decided to sacrifice some accuracy and to instead look at developing a method that could give a predictor of voltage stress rather than actual voltage stability itself. With voltage stability, the relationship between real and reactive power with voltage is highly non-linear but is further complicated with controllers in the system that can have a huge effect on the voltage trajectories over time. Chapter 4 described voltage stability and the huge range of factors on which it depends.

There are a number of static methods that have been developed relating voltage stability to power flow equations such as modal analysis, line outage distribution factors and sensitivity studies. However it will be shown later that these methods could not be applied to ICI. Therefore, it was necessary to develop a new method that could predict the post-split voltage stress. The term stress is used, as it is not stability that is measured but stress that is put on the voltage conditions. I.e. a large change in reactive power flows, or change in reactive power injections at a bus. The methods would be looking at the transient voltage drops within a system. If switching a number of lines out of a system resulted in a large transient voltage drop, it could trigger protection or cause damage. However, as voltage collapse is usually the result of successive changes in voltage, the aim is to minimise such voltage changes thereby minimising voltage instability.

To consider the transient voltage changes, a method based on observing the potential change in reactive power injections at buses is developed to provide an indicator of voltage stress. If

there is a large increase in the reactive power injections post-split, a voltage change is usually observed until the reactive power balance can be restored. Therefore, the changes in reactive power can give an indication on which way the voltage changes will tend and give an indication on the size of the voltage changes. When the tracing provides the cutset for island formation, the island is then tested for the voltage stress and assigned a index based on how much the voltage could be stressed by.

5.3.4 Rotor angle stability

Finally, while full dynamic stability assessment is being looked at in another project, it can be related to the tracing methodology by minimising the changes in real power. If the total power is minimised, there is also a smaller disturbance in the electrical power output seen by the generators. This corresponds to less shock on the rotor angle to drive it unstable. While this is only a way to minimise it, it does not guarantee dynamic stability. A generator may already be very close to the limit and only require a very small shock to drive it unstable. This would not be assessed using this method. Also, as there is relationship between voltage and synchronizing torque, it is expected that by minimising the voltage changes, the synchronizing torque can be kept at higher values and so provide additional stability. However, the dynamic stability assessment needs to be fully considered using other methods outside the scope of this thesis.

5.3.5 Block Diagram

The complete block diagram is shown in Figure 5-3 where it can be seen that the focus of this thesis is on the where to island approach which is supplied with information on the fault location and the information on whether or not to island. The step are shown and explained along with the final stage on the recommendation for an island based on the information obtained at each stage. The blocks developed in this thesis are shown in solid blue, while development outside of the thesis are shown by the lighter shades of blue.

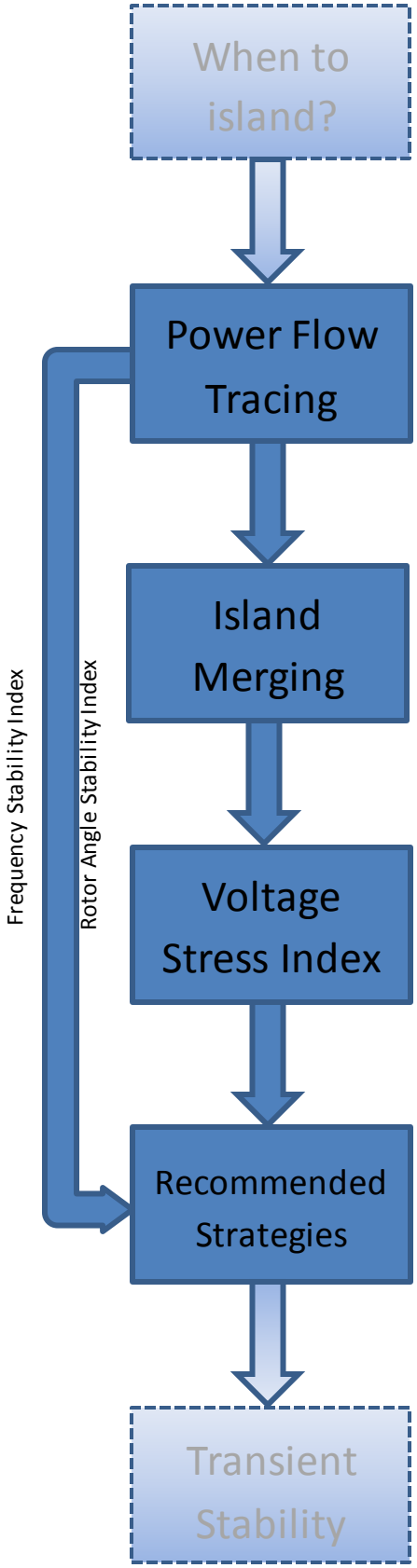

This step determines from real time measurements if a particular disturbance will result in a blackout. It is the subject of a separate project where the results of this project will feed into this thesis. The output of this block will be the disturbance locations along with a yes/no decision to implement ICI. These will be the inputs into this methodology

This block will start from the seed node (location) and find the area of influence around that node. It is based on tracing the real power from the seed node to all strongly connected nodes. The output of this step will be a selection of islands which will be evaluated for stability priority.

The aim of the methodology is to create two islands. In some cases, more than 2 islands will be created where a weakly connected island exists within the sick island. If these islands are small, they will be merged with the closest island. If they are large they may be sustainable and are left unmerged.

As the tracing only considers real power, there is no consideration for reactive power or voltage. This step will assess each of the candidate islands for voltage stress and assign a voltage index to that solution which can later be evaluated for stability.

This step will evaluate the islands using three indices, one each for frequency, voltage and rotor angle stability. The frequency and rotor angle indices are created from the tracing information from cutset power flows. Each candidate solution can be visualised in 3D space showing where the solution lies for each index along with an added constraint on sick island size. A solution can then be recommended based on a selected index, e.g. voltage stability

This step is also outside scope of thesis. This step will take the recommended ICI strategy and evaluate the transient stability fully and determine if the recommended solution will remain stable.

Figure 5-3 Block Diagram of Methodology

5.4 The Recommended solution

The recommended ICI solution will combine all of the developed methods from tracing and the voltage stress analysis tool where the final island will be determined using a number of criteria such as:

- Island Size
- Island imbalance
- Voltage stress index
- Total power cut

There is not usually one unique solution for any one disturbance. The problem then becomes one of finding the best recommendation for the ICI solution. The aim is to minimise the size of the island, however this corresponds to larger imbalances and sometimes larger stress on the voltages. Therefore, a trade off may exist between these criteria. The optimum island should aim to be frequency stable, have a small island size, ideally less than 50% of the network size to ensure that the minimum number of customers is at risk, and also minimise the changes to voltage and reactive power.

5.5 Applying the method

When considering ICI, one of the major issues is what model to use to devise an ICI strategy; the real time model which is cascading or the pre-disturbance system. It has been devised that a hybrid approach be taken as each model has an advantage. The purpose of this methodology is to find an area around a disturbance and island it creating a stable network outside the infected area. If possible, the sick island should also survive. In order to ensure a stable healthy island, the best method it to restore it to the pre-disturbance state. If all the effects of the disturbance can be contained to the sick island, then it should be possible the cut this part out and match the healthy island to the pre-disturbed state. Therefore, the model before the disturbance is used for the ICI solution. If it is done quickly before governors act then there would be little/no change in the generator scheduling and such a solution would be possible. In theory, this will give balanced islands where the flows can be predicted to create a statically stable island.

However, dynamic stability cannot be considered in this way. As soon as the disturbance starts there will be oscillations in the system and generators will start to swing. Therefore, in order to consider the dynamic stability, the real time WAMS measurements will be used. This will come from the current real time model and will accurately reflect the real time oscillatory nature. Therefore, a hybrid approach is required where the pre-disturbance model is used to design the islands and the real time dynamic tool will use the real time measurements to ensure that the

system will maintain stability when these islands are formed. The dynamic assessment part is a parallel project.

5.5.1 Application in real systems

ICI cannot always be applied in real systems due to the limits of the topology. Islanding can be used quite effectively in meshed networks when there are a number of paths for power to flow and reconfiguring the network will still provide a path from source to sink. It is the highly meshed systems where islanding would be applied. However, from the background, many blackouts have occurred in the interconnected power systems, where due to the meshed nature there is a larger area for which a disturbance can cascade. Therefore, the islanding is best applied to these large interconnected systems which are more likely to suffer from cascading outages.

Such systems would include, India, the US and Europe. Smaller systems such as the UK would be difficult to implement islanding within as much of the power flows from north to south, therefore making it difficult to form two balanced islands. Therefore, not all systems would be ideal candidates for islanding.

5.6 Test Systems

In order to do full tests, dynamic systems are required. The number of dynamic tests systems is limited and only two can realistically be used for ICI and these systems should also be well meshed based on the previous comment. The 39 bus system and the 68 bus system. In order to create more options, these systems were modified to give different operating conditions and these are explained in Appendix 1. In total there were 5 test systems created for which the ICI methodology would be tested. These will include different load models, a change in operating point due to a line outage and different levels of stress. The 14 bus system will be used for simple examples and illustrations as it cannot be used to create a number of islands are there are only two real power generators limiting the ICI options.

The test systems contain detailed generator models for the time domain simulations. An overview of the generator models can be found in Appendix 3. The fourth order models are generally regarded as detailed enough for typical stability studies. For use with the current modelling software, the 3rd order model is the minimum requirement for use with exciters. As voltage stability is being assessed the increased detail for voltages make the fourth order models ideal. The information contained in the 4th order model can be found the appendices.

5.7 Summary

A gap in current research has been identified for an ICI method that is disturbance dependent to take advantage of the modern advances in real time measurements. There are a number of advantages to this method that have been discussed, and it is clear that there is a need to consider new types of emergency control actions as blackouts are still occurring despite existing protection systems.

This chapter gave a brief outline of the methodology and how it was designed. The following chapters will explain in more detail how it has been developed and tested, along with the comparisons to some of the voltage stability methods to give an understanding as to why they cannot be used for ICI purposes. The main aim is to form an area of influence around a disturbance node and find the boundaries of this area. By finding a boundary which minimises the total power being cut and also the flows, effects on both frequency stability and rotor angle stability can be minimised. The power flow tracing will aim to find such a boundary. However, as voltage and reactive power are more localised, these need to be evaluated on a bus by bus basis, and evaluating the reactive power flows would not suffice. Therefore a methodology will be developed which looks at finding potential bus injections as a result of splitting that could affect voltage stress. Indeed, it can also be linked to rotor angle stability through the synchronizing torque.

A brief overview of the rationale for pre/post-disturbance models was given. A hybrid approach is being proposed where the pre-disturbance model will be used for the island solutions while the post-disturbance model will be used to verify dynamic stability. The aim of using the pre-disturbance island is to create island solutions which will return the healthy island to the static operating point before the disturbance occurred where safe operation was known. It is the unsafe operation that is then confined to the sick area.

A final ICI decision should then be created on a number of criteria in order to assess all types of stability and find the best island meeting the design criteria. Finally a brief note on the test systems to be used was given which will be used throughout the remainder of this thesis.

6 Power Flow Tracing

6.1 Introduction

Before the electricity markets were decentralised, the electricity supply industry tended to be vertically integrated where power exchanges between utilities were determined by contracts. The companies selling the power to the customers were usually the same companies generating and transmitting the power. Hence, prices were fully controlled by these single operators. However, as the electricity industry became decentralized and generation and transmission were unbundled, these all became businesses in their own right and transmission was seen as a separate business for transporting the electricity from any generator to any area supplier. This led to the creation of National Grid Company in the UK. In the vertically integrated system, there was very little incentive to reduce losses in the network as the additional cost of adding new infrastructure would have been too expensive and also, the cost of the losses could be passed directly to the customer as power was sold directly to them. However, as each aspect of the electricity sector became a separate business, transmission system operators did not want to take on these losses and the typical arrangement in place was to charge the area suppliers through a uniform *pro-rata* charge. As the charge was just being passed along to the area suppliers and not being bore by the transmission system operators, there was again little incentive for area-suppliers to reduce losses. The cost could be directly put onto the end users, and there was no incentive on generators at all. In the UK, transmission losses accounted for 2% of generation which in 1994/1995 cost about £140m [126], therefore the industry regulator urged for proposals to be put forward to deal with the issue as the current arrangement was not encouraging efficiency.

One of the proposals was an electricity tracing method which could be used to charge suppliers and/or generators for the actual amount of losses they contributed to. For example, if a generator was located very far away and there were large losses on their transmission path, they would be penalised for this. This would then incentivise all bodies to generate more efficiently or be penalised. Therefore the power flow tracing algorithm was developed as an economic tool. This tracing methodology was developed in [127] which attempts to trace the flow of electricity in the network from individual generators to individual loads by following the directed graph of flows. It assumes that at any node, the inflows are proportionally distributed among the outflows. The proportional sharing principle on which tracing is based is intuitively reasonable, yet it cannot be proved, nor disproved. It can however be rationalized according to [128] using

cooperative game theory and information theory. It shows that the proportionality assumption results in the optimal cost allocation regardless of the form of the cost function.

The tracing algorithm has been applied to power systems in Northeast China [129] and was also considered as a candidate for the Inter-TSO Compensation in Europe [130]. It is therefore a very practical tool that has been tested and deployed in real power systems. The following sections will explain the method in further detail and show how it can be developed for ICI purposes in this thesis.

6.2 Proportional sharing principle

The tracing method is based on the proportional sharing principle and it divides flows fairly across a system. It is based on the fact that the power flows out of a bus in the same proportion as it comes into the bus. I.e. from Figure 6-1, there is 100 MW flowing into the bus from A and B combined. This 100 MWs then flows out through C and D. To look at this example in terms of contributions, it can be said that 70% of the bus's power comes from B while 30% comes from A. Using the proportional sharing principle then, it is said that the power flowing out of the bus will be of the same proportions. I.e., of the 50 MWs going to D, 70% (50MW x 70% = 35MW) comes from B while 30% (15 MW) comes from A. While the proportional sharing principle applied to power systems can be neither proved, nor disproved, it will be used here to show how much power could be contributed between the buses. Therefore, it will be said that it is possible for 35MW of the power on D to come from B rather than definitively stating this as fact. It divides the flows fairly, which is ideal in economic terms, however, in actual power system operation it may not hold. Therefore, it is used to show possible contributions between buses.

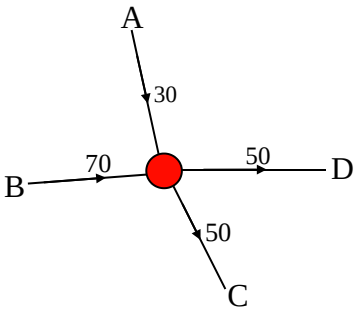

Figure 6-1 tracing example

6.3 Tracing methodology

The electricity tracing method from [127] uses a topological methodology as it deals with how the flows are distributed in a meshed system. The solution of Kirchhoff's current law must be

satisfied for all the nodes in the network. Therefore, it requires only the solution of a load flow which inherently includes Kirchhoff's voltage law in order to obtain the power flows. It is assumed that each MW of power leaving a node is of the same proportion as the inflows into that node based on the fact that the outflows down the line are dependent only on the voltage gradient and impedance of the line. The tracing of power flows can be carried out upstream, from loads to generators, or downstream, from generators to loads. It is therefore possible to trace power from a node both upstream and downstream to any other node in the system. The method behind tracing can now be explained. To simplify considerations transmission losses are neglected so that power flow in any line linking nodes *i* and *j* satisfies $|P_{i-j}| = |P_{j-i}|$.

Tracing can be executed downstream and upstream. First let us consider downstream tracing. Power at a node i is made up of the demand at that node and the outflows to connected lines:

$$P_i = \sum_{j \in \alpha_i^d} P_{i-j} + P_{D_i} \tag{6.1}$$

where P_i is the total power at bus i (i.e. the sum of inflows or outflows), P_{i-j} is the power outflow into node j on line $i-j$, P_{D_i} is the power demand at node i and α_i^d is the set of nodes supplied directly from node *i*.

As $|P_{i-j}| = |P_{j-i}|$, the power P_i can be expressed as

$$P_i = \sum_{j \in \alpha_i^d} (|P_{j-i}|/P_j) P_j + P_{D_i} \tag{6.2}$$

Equation (6.2) defines the power at node i in terms of the demand at node i and all the outflows from i from the directly connected buses as a proportion of the receiving end powers. Taking all the buses into account one gets a matrix equation

$$\boldsymbol{A}_d \boldsymbol{P} = \boldsymbol{P}_D \tag{6.3}$$

where $\boldsymbol{A}_d$ is the $(n \times n)$ downstream distribution matrix (n is the number of buses) defined as

$$[\boldsymbol{A}_d]_{ij} = \begin{cases} 1 & \text{for } i = j \\ -|P_{j-i}|/P_j & \text{for } j \in \alpha_i^d \end{cases} \tag{6.4}$$

$\boldsymbol{P}$ is the vector of total nodal powers and $\boldsymbol{P}_D$ is the vector of nodal demands. Now the nodal power P_i can be extracted as

$$P_i = \sum_{k=1}^{n} \left[\boldsymbol{A}_d^{-1}\right]_{ik} \boldsymbol{P}_{D_k} \tag{6.5}$$

Equation (6.5) shows the contribution to the k^{th} system demand from the i^{th} nodal power as $\left[\boldsymbol{A}_d^{-1}\right]_{ik} P_{D_k}$. In other words $\left[\boldsymbol{A}_d^{-1}\right]_{ik}$ gives the share of the power at bus i that goes to demand node k, and multiplying by P_{D_k} will give this value in MWs.

It is important to appreciate that, as proved in [131], $\left[\boldsymbol{A}_d^{-1}\right]_{ik}$ also shows the share of the nodal power at node *k* that is supplied from node *i* through all possible intermediate paths between the nodes. This interpretation is crucial for understanding how tracing can be used for preventive ICI purposes.

It can be shown in a similar way that tracing can also be executed upstream using

$$\boldsymbol{A}_u \boldsymbol{P} = \boldsymbol{P}_G \tag{6.6}$$

where A_u is the $(n \times n)$ upstream distribution matrix defined as,

$$[\boldsymbol{A}_u]_{il} = \begin{cases} 1 & \text{for } \; i = l \\ -|P_{l-i}|/P_l & \text{for } \; l \in \alpha_i^u \end{cases} \tag{6.7}$$

and $\boldsymbol{P}_G$ is the vector of nodal generation injections and α_i^u is the set of nodes supplying directly node i. Hence matrix $\boldsymbol{A}_u^{-1}$ can be used to trace nodal contributions upstream. In this thesis it will be assumed that the network nodes have been re-ordered according to their order in the acydic directed graph of flows, so that $\boldsymbol{A}_d^{-1}$ is upper triangular while $\boldsymbol{A}_u^{-1}$ is lower triangular [131].

Now it is shown that, for a lossless network, it is enough to use just one of the matrices, either $\boldsymbol{A}_d^{-1}$ or $\boldsymbol{A}_u^{-1}$, to trace flows either upstream or downstream as they are linked by a simple relationship [127]:

$$\frac{\left[A_u^{-1}\right]_{ik}}{\left[A_d^{-1}\right]_{ki}} = \frac{P_i}{P_k} \quad \text{or} \quad \boldsymbol{A}_d^{-1} diag(\boldsymbol{P}) = \left(\boldsymbol{A}_u^{-1} diag(\boldsymbol{P})\right)^T \tag{6.8}$$

Hence examining a row in $\boldsymbol{A}_d^{-1}$ (or a column in $\boldsymbol{A}_u^{-1}$) traces the flows downstream from the node corresponding to the diagonal element while examining a row in $\boldsymbol{A}_u^{-1}$ (or a column in $\boldsymbol{A}_d^{-1}$) traces the flows upstream from the node corresponding to the diagonal element. Therefore in this thesis the application of the methodology will be demonstrated using only $\mathbf{A}_d^{-1}$ and it will be called the tracing matrix T_d .

$$\boldsymbol{T}_d = \boldsymbol{A}_d^{-1} \tag{6.9}$$

If the network nodes have been re-ordered according to their order in the acyclic directed graph of flows, $\boldsymbol{T_d}$ is upper triangular while $\boldsymbol{T_u} = \boldsymbol{A}_u^{-1}$ is lower triangular [131]. The bus reordering is shown in section 6.4

Now let us demonstrate that T_d contains the necessary information about tracing the flows both upstream and downstream of a selected node. A simple example is shown in Figure 6-2 with the corresponding $\boldsymbol{T}_d$ matrix shown in Table 6-1.

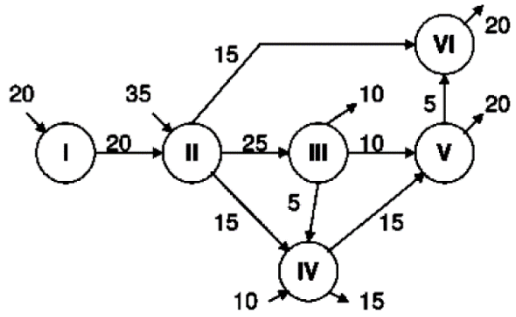

Figure 6-2 Simple 6 bus network for tracing example

Table 6-1 Matrix T_d for system above

1	0.3636	0.3636	0.2424	0.2909	0.3455
0	1	1	0.6667	0.8	0.95
0	0	1	0.1667	0.5	0.125
0	0	0	1	0.6	0.15
0	0	0	0	1	0.25
0	0	0	0	0	1

As discussed above, each column *j* of T_d shows the share of the nodal power at node *j* which is supplied from a node corresponding to a row. This means that investigating a column *j* of T_d corresponds to tracing contributions to node *j* from any nodes upstream from *j*, The diagonal elements of $\boldsymbol{T}_d$ are all one, as all power flowing through a node must come from that node.

Similarly, investigating a row *k* of T_d is equivalent to tracing contributions of node *k* to any nodes, corresponding to columns, which are downstream from node *k*. Those contributions are also expressed as shares of the nodes corresponding to columns. Therefore, instead of using two tracing matrices, one for looking upstream and one for downstream, one matrix can be used where all the upstream and downstream paths from a given node can be traced. Investigating a

column of T_d will correspond to tracing upstream from the diagonal node while investigating a row will correspond to tracing downstream from the diagonal node.

6.4 Bus Reordering

It was mentioned that if buses are re-ordered according to their order in the acyclic directed graph of flows, $\boldsymbol{T_d}$ is upper triangular while $\boldsymbol{T_u} = \boldsymbol{A_u^{-1}}$ is lower triangular [132]. The method for reordering the buses to achieve this triangular structure is now explained.

Consider an example 14 node network found in Appendix 1. It is difficult to visualise from this diagram which direction the power flows, and, visually, would be difficult to trace the power. Similarly, if the tracing matrices were created using this configuration, the upper and lower triangular structure would not be formed. It would be difficult to see which nodes are upstream and downstream. Therefore, the directed graph of flows which are obtained from solving the power flow solution can be created as in Figure 6-3. The matrix is triangular if all the nodes have been re-ordered using their order in the directed graph (digraph) of flows, see [131] [133], as in Figure 6-3. The digraph is then split into a number of levels depending on the flow of the power between the nodes with levels 0 being generators only and the last level being pure loads. All levels in-between can be loads, generators and interconnecting buses. Nodes are then numbered according to the level in which they are located from Figure 6-3, where nodes 1 and 8, found in level 0 are renumbered 1 and 2. The reordering of the buses is shown in Table 6-2.

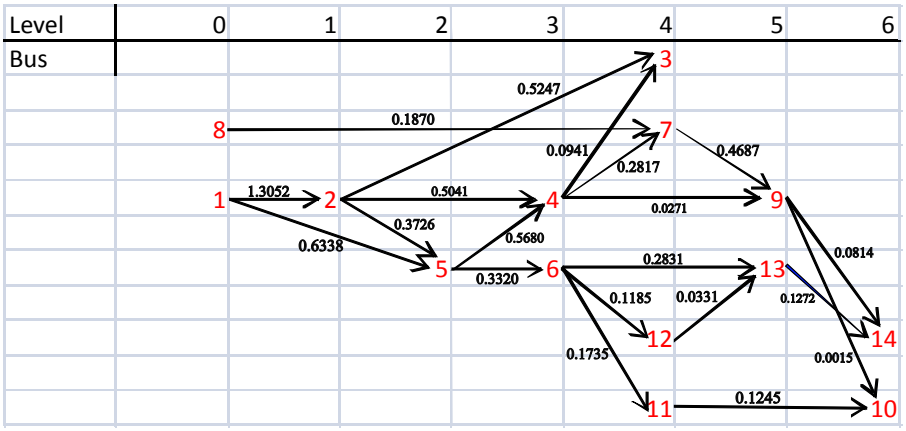

Figure 6-3 Directed graph of flows for the 14 node system.

Table 6-2 Bus Reordering assignment

Original Bus Numbers	Digraph Level	Reordered Bus Assignment
1	0	1
2	1	3
3	4	7
4	3	5
5	2	4
6	3	6
7	4	8
8	0	2
9	5	11
10	6	13
11	4	9
12	4	10
13	5	12
14	6	14

6.5 Application of Tracing to ICI

The methodology chapter introduced an ICI concept which aims to separate the smallest feasible area isolating a disturbance while reducing the effects on voltage and active power. Recall that the aim is to find the area in which to contain this disturbance. The source of the disturbance will be called the seed node (or nodes). If the cause for the disturbance is a generator outage, then the node that the generator is connected to becomes the seed node. If the cause for the disturbance is an outage of line, both nodes beginning and terminating the line become the seed nodes. If the problem area is a collection of nodes, then these all become seed nodes.

This area of influence is the section that will be disconnected, and is referred to as the sick area as shown in Figure 5-2. The problem is then one of finding this area of influence which is carried out using the tracing algorithm. It is not possible to state conclusively that the disturbance affects the surrounding nodes by a certain amount due to the proportional sharing principle, therefore it is used to reflect the possibility for a seed node to infect surrounding nodes based on its connectivity to these nodes. It is therefore important to clarify that the tracing algorithm does not create the definitive island, but rather provides a method by which to reduce the search space. The solutions from the tracing method are then evaluated using suitable measures which will be used to choose the best island. Therefore, the issue with the proportional sharing principle is overcome.

For a generator node, the sick area lies downstream. However for ICI, the seed node does not necessarily need to be a pure source or sink node. Therefore, the sick area is established both downstream and upstream of the seed node. Using the tracing methodology, the nodes that are strongly connected to the seed node, upstream and downstream are identified. It is these nodes

that need to be included in the same island as the seed node where collectively it is called the "sick island".

ICI is carried out by disconnecting the lines that are weakly connecting the sick island to the remaining healthy network. Weakly connected means that the power flow on these lines is relatively low, where it is deemed a small contribution in terms of power between the two nodes. The level of contribution will be defined as a threshold value, where contributions less than a threshold value will be termed weakly connected. The lines connecting the sick and healthy islands will be weakly connected due to the fact that any strongly connected element to the disturbed region becomes part of the sick island. It is important to point out that the term weakly connected here is connected to the chosen threshold value from tracing, and not related to weak connections such as in slow coherency methods. The terms are used to distinguish if a node remains connected to the seed node in the same island, or will be disconnected and left in the healthy island. As the choice of threshold value is not fixed, there is no pre-defined value for a weak connection as with methods like slow coherency. For a chosen threshold value the lines that are found to be these weak connections form the cutset. These are the lines that will be tripped to form the islands.

The matrix T_d, as formed in Table 6-1 using (6.4) and (6.8), shows the proportions of a bus' power that is received, or sent. However, this needs to be modified for ICI purposes. Consider a node which has a very small nodal power, it is of little interest for ICI if all of its power gets to a seed node, as it would be a still a small contribution. Instead, the elements of T_d are converted to MW (p.u.) contributions which will show how much active power is contributed between the nodes. This is much more useful as it provides a quantity for the contribution. A matrix T_d' is formed where $T_d' = T_d diag(P)$ where each column j of T_d is multiplied by its nodal power P_j, i.e. $T_{d_{ij}}' = [T_d]_{ij} P_j$. Each entry $T_{d_{ij}}'$ shows how many MWs of nodal power at j can be supplied from i, both directly and indirectly. The matrix T_d' for the example in Figure 6-2 is shown in Table 6-3 where the proportions shown in Table 6-1 are now presented as p.u. contributions of MWs.

Nodes which are strongly connected to the seed node i are found using matrix T_d', both downstream and upstream from the seed node i, which will form the sick island. Strongly connected means that the value of any contribution downstream from node i, or from any node upstream from node i, is above a threshold value ε. The threshold value will determine the size of the island, however a larger threshold value will minimize the size of the island but can result

in higher power flows being cut. The algorithm for ICI will now be demonstrated using the 6 bus system seen in Figure 6-2.

Table 6-3 Tracing matrix for 6 bus network

0.2	0.2	0.0909	0.0727	0.0727	0.0691
0	0.55	0.25	0.2	0.2	0.19
0	0	0.25	0.05	0.125	0.025
0	0	0	0.3	0.15	0.03
0	0	0	0	0.25	0.05
0	0	0	0	0	0.2

The tracing matrix T_d' is shown in Table 6-3 where all contributions between the buses are shown in p.u. values of real power. This matrix is used to find the area of influence to form the islands. In this example, an arbitrary seed node and threshold value will be chosen for the purposes of illustrating the method. Identifying the complete sick island is performed in a number of iterations; the first being all the nodes that are strongly connected directly to the seed node. This is referred to as the primary island.

1. Select seed node – Node 5
2. Set threshold value – 0.2 p.u.
3. From the tracing matrix, starting at the seed node ($T_{d'_{5,5}}$) – shown in red, move along rows and columns to find value greater than, or equal to the threshold value

0.2	0.2	0.0909	0.0727	0.0727	0.0691
0	0.55	0.25	0.2	0.2	0.19
0	0	0.25	0.05	0.125	0.025
0	0	0	0.3	0.15	0.03
0	0	0	0	0.25	0.05
0	0	0	0	0	0.2

4. Element $T_{d'_{2,5}}$ (shown in green) is equal to the threshold value, therefore it is deemed to have a strong connection to the seed node. This is the only element in row 5 and column 5 that exceeds the threshold value. Node 2 and Node 5 form the primary island shown in Figure 6-4.

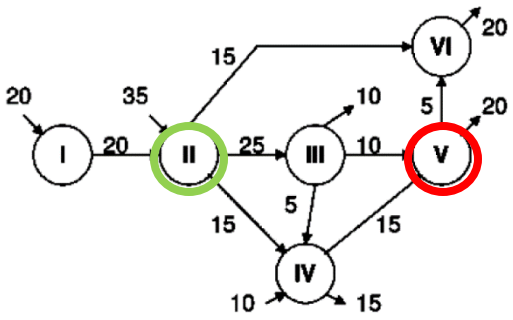

Figure 6-4 Primary island

All nodes in the primary island then become seed nodes themselves where the process is repeated, finding any strongly connected nodes to these new seed nodes. The size of the island increases with every iteration, it is a multilevel approach, where each level has new seed nodes and the tracing algorithm is applied.

1. Node 2, the newly found node, becomes the seed node and is then used to search for strong connections

2. Starting at element $T_{d'_{2,2}}$ (shown in red), search along the row and columns 2 to find any elements that exceed the threshold value

0.2	0.2	0.0909	0.0727	0.0727	0.0691
0	0.55	0.25	0.2	0.2	0.19
0	0	0.25	0.05	0.125	0.025
0	0	0	0.3	0.15	0.03
0	0	0	0	0.25	0.05
0	0	0	0	0	0.2

Now, the contributions between node 2 and nodes 1,3 and 4 all are greater or equal to the threshold value, and become part of the sick area and form the secondary island. The sick island now consists of nodes [1 2 3 4 5] and it can be seen from the T_D' matrix that the contributions to node 6 are all below the threshold value for all nodes. Therefore, this is deemed a weak connection and not included in the sick island. Therefore, all strong connections were formed in two levels and the solution is shown in Figure 6-5.

While this is not a feasible solution due to the networks small size, it is useful to demonstrate the tracing method. The iterations continue until no more nodes are connected to the sick island above the threshold value ε. Hence the lines connecting the islands to the rest of the system are below the threshold value and can be cut. This provides the line cutset that minimizes the power

flows being affected where cutting a line carrying a large power can have negative consequences such as exacerbating cascading trips in the system.

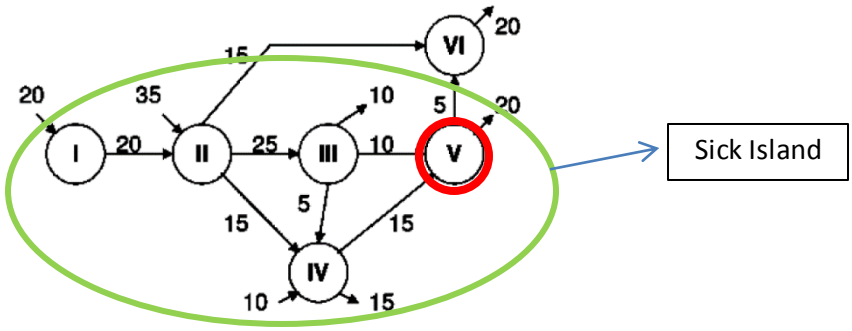

Figure 6-5 Optimal solution - simple network

A specific threshold value is not defined in this section as it is not sufficient to consider only active power in the formation of the island. Instead, a range of threshold values are used where the islands corresponding to each threshold are then tested for additional criteria such as effects on voltages. Therefore, there should be a number of different solutions for any seed node in the system where the 'best' one should be selected subject to further criteria. To illustrate this, without repeating the process describing the tracing matrices, the results of two further threshold values can be shown for the 6 bus system. Consider a threshold value of 0.1 p.u. which is lower than seen in the previous example, and hence will consider smaller contributions as strong connections. The results island is shown in Figure 6-6.

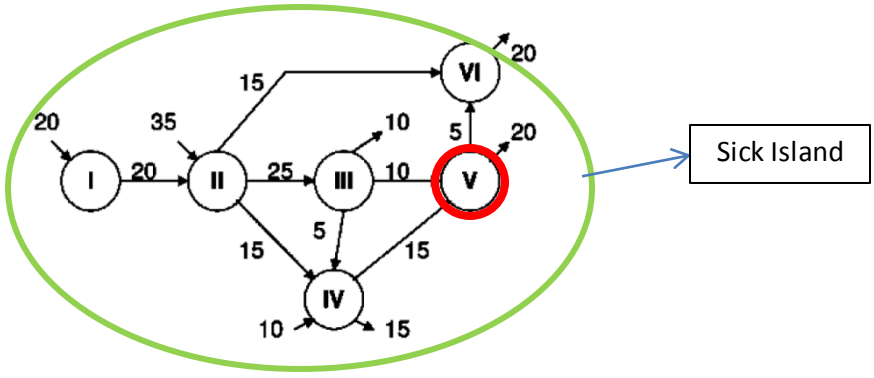

Figure 6-6 Threshold value of 0.1

Considering a larger threshold value will then require larger contributions to make strong connections, and considering a threshold value of 0.25 p.u. for the same system, the solution is shown in Figure 6-7. It can be seen that smaller threshold values increase the size of the sick island, while larger threshold values decrease the size of the sick island.

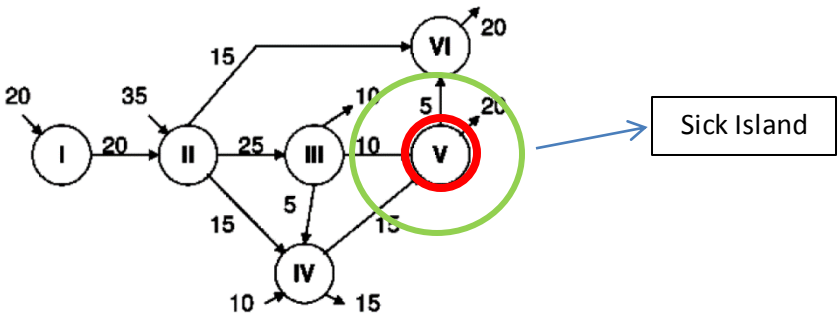

Figure 6-7 Threshold value of 0.25

The basic principle has been shown on the 6 bus system, but it is better to visualise on a larger system with more generators. Following on from the toy examples described by the 6 bus system, the 39 bus system will be looked at to show ICI.

6.5.1 39 Bus System

While the previous examples illustrate the steps in the tracing algorithm, they do not provide much insight into forming useful islands. Using the 39 bus system, which contains 10 generators, offers more flexibility for ICI. Taking a seed node at bus 19 and choosing a threshold value of 1.0 p.u., the resulting islands are shown but as the matrices are quite large, they are not shown. The primary island is shown by the green nodes in Figure 6-8. These are the nodes that exceed the threshold value along row and column 19 of the tracing matrix. The next stage is to repeat the tracing for all the newly identified nodes shown in green.

Repeating the tracing for the secondary island the blue nodes are found where all infected nodes were found within the two levels. Hence the results from the secondary island form the ICI solution shown in Figure 6-8 and Table 6-4. It should also be noted that there is a small island cut out within the sick island consisting of nodes [36 23 24]. The reason for this small island being disconnected is due to the reliance on tracing. The connection between these islands is below the threshold and is disconnected. The tracing algorithm does not consider the sizes of the islands etc., only the contributions between nodes. Such islands should be avoided but will be dealt with in more detail in subsequent chapters.

Table 6-4 Island Imbalance Information

Island	**Imbalance (p.u.)**
Island 2 (+ & -)	0.07263-0.3719-0.3649 = -0.66417
Island 3 (+ & -)	0.4194-0.42=-0.0006
+ = in	- = out
Total Absolute power (p.u.)	1.6475

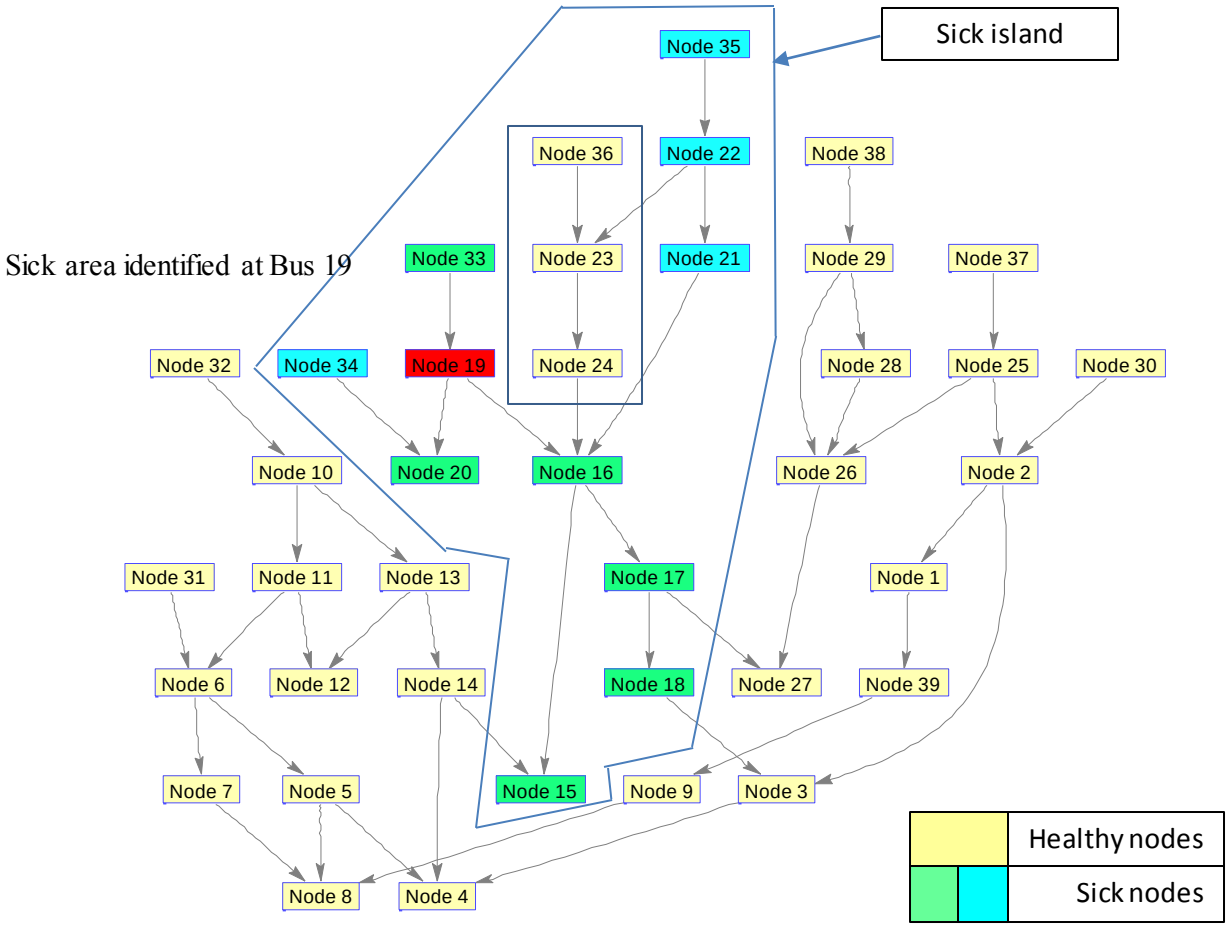

Figure 6-8 39 bus system - Final ICI solution

6.6 Effects on power flows

Chapter 5 emphasised the necessity to find solutions which would minimise the changes in the system due to ICI. The tracing method aims to find the weak solutions in the system and as such prevent cutting through any heavily loaded lines. Cutting through high power flows could cause redistribution of large power flows and cause lines to reach their limits and trip hence worsening the situation. Therefore, tracing should minimise the overall redistribution of power flows by only cutting weak links. To verify this, the pre ICI and post ICI flows for each line in the system of Figure 6-8 are compared and shown in Figure 6-9. It can be seen there is very little change in the line flows as observed by the green difference plot. This verifies that tracing does minimise the redistribution of real power in the system by cutting only weak links.

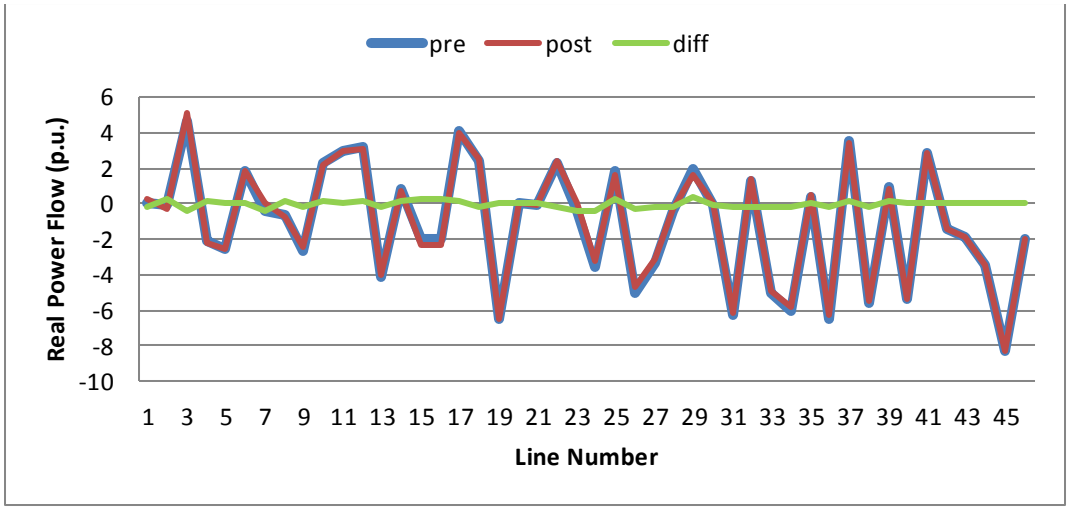

Figure 6-9 Line flow comparison

6.7 Threshold Value

The examples shown above show how the tracing algorithm works for arbitrarily selected threshold values, however, in the real ICI solutions, the threshold value cannot be chosen in such a fashion. As it is ultimately the choice of threshold value that determines the strong and weak contributions between buses, the threshold value will have a major effect on the ICI solution that is created. However, the power flow tracing algorithm does not decide the ICI solution alone, and it is later supplemented with further criteria. Therefore, the tracing algorithm only needs to provide a series of possible ICI candidates which will be evaluated and compared in order to find the best islanding solution. For this reason, it is better to use the tracing to provide a number of ICI solutions which means that the choice of threshold value is less critical.

Instead of using one threshold value, a range of threshold values are used, where the range is large enough to cover all solutions. I.e. the lowest threshold value will result in the entire system being strongly connected and the highest threshold value showing only one node, not strongly connected to anything else. Therefore, there will be a range of ICI solutions such as in Table 6-5. This table is created for the larger 39 bus system. It can be seen that for a particular seed node, there were four possible ICI solutions. Each threshold value does not guarantee a unique island, a contribution between two nodes of 0.9 p.u will be strong for all threshold values up to 0.9 p.u., and only once passed that will it become a weak contribution. Hence, some islands will be the same as in the first solution, for a range of 0.4 to 0.9 p.u.. The % Sick Column shows the size of the sick island as a percentage of the full network before islanding while the imbalance column shows the imbalance of real power in p.u. within the sick island, where negative values imply surplus generation (negative imbalance of generation). It can be seen from the % Sick column

that as the threshold value increases, the size of the sick island decreases, as proven earlier in the 6 bus example. For the threshold ranges, increments of 0.1 p.u. were used.

Table 6-5 Results from range of threshold values

Threshold (p.u.)	% Sick (%)	Imbalance (p.u.)
0.4-0.9	52.95	-0.12
1	14.7	-0.611
1.1-1.3	10.3	0.13
1.4-2.0	7.35	-2.25

NOTE: There is an important note to be made about minimal imbalance. Tracing does inherently minimise imbalance by cutting through the weakly connected lines. However, that is the minimal imbalance island for a specific threshold value only. For a seed node there will be a number of solutions as in Table 6-5, each with their own imbalance values. Here the first island has minimal imbalance of the 4. This quantity will be used to evaluate the best islands. Simplify selecting any tracing solution does not mean it is the best balanced island; rather it is one of the possible solutions to be formally minimised.

6.8 Unique Solutions

The previous section describes how each threshold value does not lead to a unique solution. Indeed for the 20 tested threshold values (0.1 -2.0 p.u.) there were only 4 unique islands. It should also be considered that each seed node in the system does not have to have a unique solution. This will be shown later in Chapter 10. If seeds nodes are located quite close together then they can result in the same islands. For example the seed node used here was bus 19. However if bus 20 or 16 were evaluated, they may provide the same islands as seen in Table 6-5. Therefore, if there are 39 nodes in a system, it is unlikely to get a unique set of solutions for each seed node and therefore, the final number of islands may actually be quite small.

6.9 Power flow tracing example on the UCTE System

This section describes tracing applied to the UCTE system to show how tracing could find an island around the disturbance of 2006 described in Chapter 2. This disturbance led to the disconnection of 15 million customers from unintentional islanding and islands being formed with major imbalances. The data was recreated approximately to the conditions of that day. A number of tracing solutions were then obtained. The available data was only for a DC load flow, there was no reactive power information, or dynamic information and so voltage and dynamics could not be tested to verify the split. It was aimed only to show how the tracing could work to

contain a disturbance within a smaller region and avoid the large imbalances that were seen from unintentional islanding shown in Figure 2-4.

The unintentional islanding led to three areas that had large imbalances which is what led to the large number of customer being affected. For a disturbance that originated in northern Germany, it can be seen how the effect can propagate to affect such a large area. When one consider how a single '*planned'* line outage affected 15 million people, it is possible to see why new techniques are required.

6.9.1 Tracing

The data for the UCTE system was taken from a 2009 powerworld model and converted to a Matlab format. However, as the 2009 system was different to the system of 2006, the dataset was changed slightly. Also In order to illustrate the results for the system of 2006, it would be best to replicate the 2006 system, but also the operating conditions for this particular day. This involved adjusting the loads, generation and finding all lines that were out for maintenance. The data file available was a DC load flow model, and hence only real power flows are considered. Therefore, only the power flow tracing is applied and it can be shown to visually isolate the fault into smaller regions. The test system created was an approximation of the system conditions for the day and based on the following sources:

1. UCTE Nov 4th 2006 disturbance report **[3]**
2. ENTSOE monthly Statistics **[134]**
3. ENTSOE network maps for 2003 and 2012

The data for loads is taken from the UCTE monthly statistics for each country, and based on the flows in and out of each country, the generation can be found. The model that was available was based on a 2009 model, and some differences are expected to the system in 2006, but also, in the model available, not all lines are included. Therefore, in order to make the best approximation for the conditions on the day of the disturbance, it was hoped to remove all lines that were out for maintenance on the day. However, it was not possible to include all line outages as they were not available in the model.

6.9.2 Results

The results are based on using a seed node at bus 795 which is the bus on one end of the conneford-diele line, which was where the event started as the planned outage. Threshold values are varied from 1 to 10 p.u. and all the unique islands are shown here. The information on each solution is summarised in Table 6-6 where the threshold corresponds to the threshold

value used in the tracing method, the sick island power corresponds to the total generation in the sick island for that solution, the sick island size is the % of the total network which is sick. The results are shown in p.u. on a 100 MVA base. Imbalance is the imbalance of real power in the sick island while total power cut is the sum off all power on the lines being cut, which is being linked to the total shock that a generator will experience and hence affect rotor angle stability. The sick islands corresponding to each solution can be seen by the red area in Figure 6-10 to Figure 6-17. It can be seen that within the sick islands shown in red that there are a number of nodes not included in the sick islands. These are primarily due to the different voltage levels within this system. Some of the lower voltage levels will be carrying lower power flows and hence deemed to have small contributions to the sick island shown in red. This is why they appear inside the sick islands, as they simply have a low contribution to the higher networks. It can be seen that these nodes are typically clustered together indicating the lower voltage networks.

Table 6-6 UCTE Island results

Threshold (p.u.)	Sick Island Power (p.u.)	Sick Island Size (%)	Imbalance (p.u.)	Total Power Cut (p.u.)
1	2698	77.376	0.0047443	0.12316
1.4	2485.9	67.671	0.0091346	0.24638
2.2	2129.9	50.268	0.049378	0.51727
2.6	1626.3	37.952	0.085555	0.7044
2.8	1534.1	34.94	0.087075	0.80254
3.6	703.5499	16.6	0.1409	2.4702
4.2	348.6455	5.2209	0.0399	2.3833
7	214.9599	2.1419	0.0264	1.7887

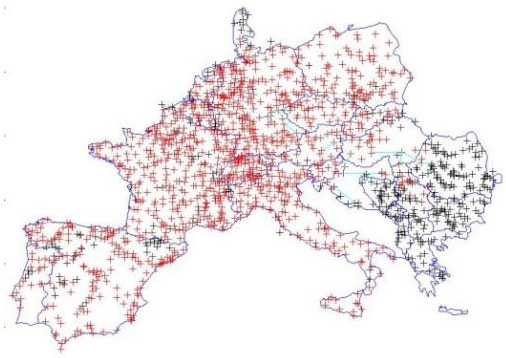

Figure 6-10 Threshold value = 1

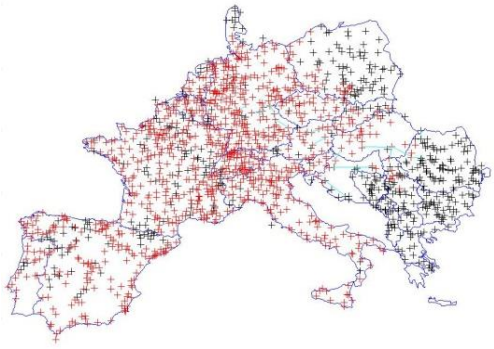

Figure 6-11 Threshold value = 1.4

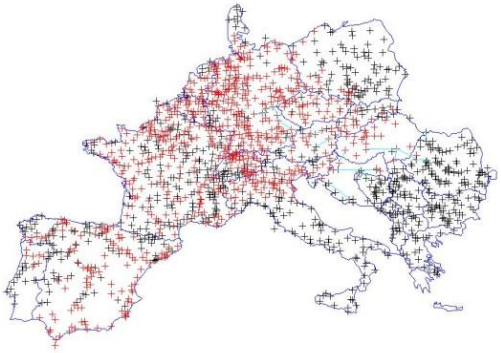

Figure 6-12 Threshold value = 2.2

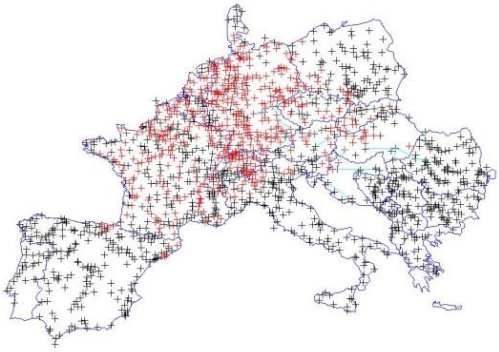

Figure 6-13 Threshold value = 2.6

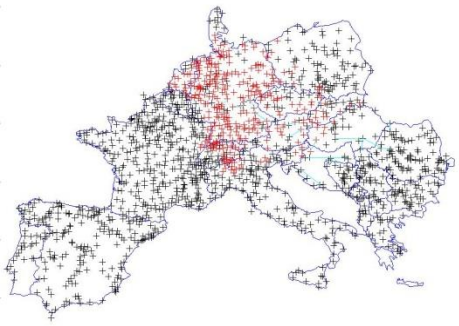

Figure 6-14 Threshold value = Threshold value = 2.8

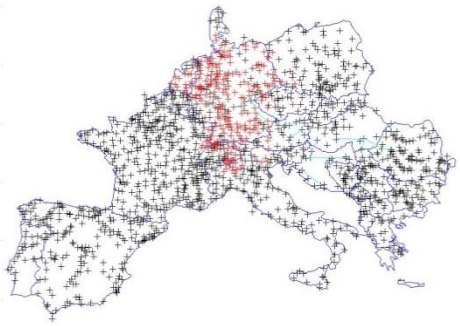

Figure 6-15 Threshold value = 3.6

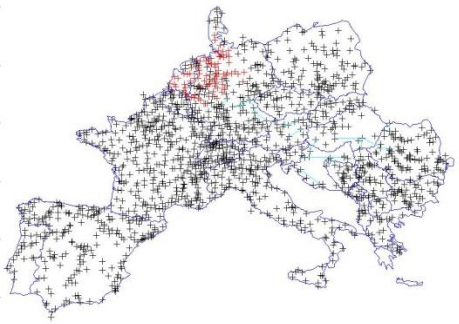

Figure 6-16 Threshold value = 4.2

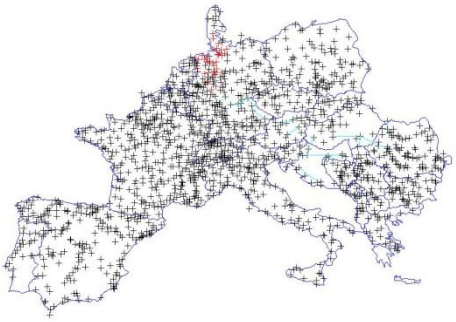

Figure 6-17 Threshold value = 7

6.9.3 Choosing a Solution

The best solution can be chosen visually for this example as there are a limited number of solutions. Therefore, the solution should be chosen on the minimal effects for frequency and total power cut. It can be seen visually that as the threshold values are increased, the island size gets smaller as shown from Figure 6-10 to Figure 6-17. However, looking at the results from Table 6-6, it can be seen that many of these solutions have large affected powers. For example, the smallest sick island solution corresponds to a very small island, about 2%, and would be ideal to contain a disturbance to such a small region, however, looking at the total power cut, the total power being cut is 1.8 times the total power within the sick island. This would be seen as a massive shock to the generators in this island and could be detrimental. Therefore, it appears that from inspection that the island for the threshold value of 2.8p.u. offers a good solution. It has much lower effects on power and hence should be seen as a much smaller shock to the system, and have less of an impact on the frequency changes, and hence load shedding. Such an ICI scheme would be preferential to the three islands formed unintentionally which had large imbalances and shed many customers.

It should be noted that the unintentional islanding yielded very different islands to the tracing solutions. This is because the tracing aims to find the lines carrying the minimal power, while the unintentional islanding is formed by successive line trips, which would have been the lines carrying the most power, and more than the limits. Cutting through the lines carrying larger power will results in larger imbalances and hence the unintentional islanding is not a good solution. By finding the lines carrying less power, the inherent weak connections are being found in the network and it is along these boundaries where the system is islanded, and hence the imbalance in minimised.

This example also shows that ICI can be applied to real systems to contain disturbances, and it can find an effective area of influence around a disturbance. This is an ideal representation of using the seed node to find an island where this island is formed around the line in question, and as the threshold values increase, the size of that containment region can be reduced. Therefore, customers further away from the disturbance will be saved from any potential blackouts.

6.10 Summary

This chapter has introduced the concept of power flow tracing and has shown how the principle was developed as an economic tool. However, following on from the methodology chapter, a method to form an area of influence surrounding a node was required. It was shown that the power flow tracing tool could be expanded into a useful methodology for finding this area of influence. By forming a matrix showing the possible MW contributions between each bus in a system, it is possible to see how strongly certain buses are connected in terms of the real power flow. As it was fundamental in the design to minimise the effect on power flows, the tracing method is used to trace the flows from a seed node to find the weakly connected buses. The weak connections can then be found which create a border for the sick island.

Therefore, two islands are typically formed, one which contains the disturbance and a second which is the remaining network. However, it was described that the weak connections are defined using a threshold value, which is not a unique value. Instead, a range of threshold values will be used which will provide a series of islands based on differing levels of weakness. From the range of ICI solutions, the best one will then be chosen as the final ICI solution. It will be subject to further analysis in following chapters. The methodology was then presented on a simple test system and a larger 39 bus system to show the principle and how tracing could be used to find an island solution.

Finally a brief summary of the UCTE ICI demonstration is given which is detailed in the Appendices. As it only contained DC power flows, it was not possible to test voltage or dynamic stability and so is not discussed further in this thesis. It does show how increasing the threshold value can tighten the area to contain a disturbance and an attempt is made at selecting the best island on minimal balance information.

7 Voltage Stability Techniques

7.1 Introduction

Chapter 6 described a novel method for finding an area of influence around a seed node and finding a suitable island. However, it stated that the islands created were based on real power flows only, and there was no consideration of reactive power, or voltage. A time domain simulation was run for the example in Figure 6-8 and it was seen that the formation of this island resulted in a voltage collapse as shown in Figure 7-1.

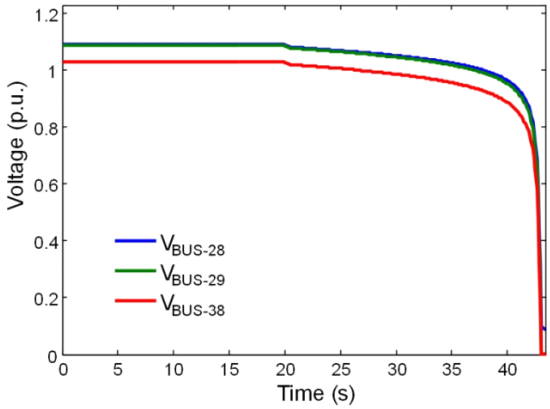

Figure 7-1 Voltage collapse observed from example in chapter 6

Table 6-4 summarised the imbalances for the islands from this example, and these imbalances were considered quite small as they are less than the selected threshold value. Despite this, a voltage collapse occurred showing that minimising imbalance does not guarantee voltage stability. There was no way to evaluate this from the tracing method without running the time domain simulation. There is a need to use other methods to consider voltage stability, or at least the effects on voltage that islanding actions can incur. It is also important to note that a large imbalance of, or total cut, real power can have significant impacts on the voltage; however these would be addressed by minimising the imbalances. It is the instances where a large impact is observed on system voltages despite the low imbalances of real power or total power cut that are of interest.

7.2 Assessing the voltage stability

In keeping with the real time nature of this methodology, a fast method for voltage assessment is required. Recall a number of voltage stability assessment tools were discussed in Chapter 4. Due to the time restrictions, dynamic methods must be ruled out in favour of the speed offered

through static analysis. There are a number of methods described in chapter 4 which will be tested. Islanding can be considered as a contingency where a number of lines are opened at once.

7.3 PV Curves

PV and QV curves are standard tools in the evaluation of voltage stability. It is possible to determine how close you are to instability in terms of a change in the loading. However, they cannot be used for ICI. A PV and QV curve is created for each bus in a system, and is based on a particular operating point. Consider the 14 bus test system which will be islanded as shown in appendix 1. The following PV and QV curves are created for a particular bus in the system. The method for creating these curves is well understood and can be found in most textbooks.

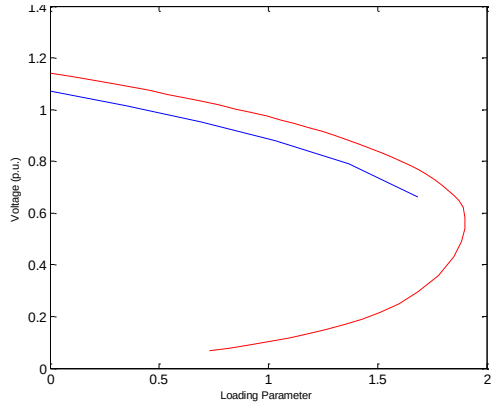

Figure 7-2 PV Curve

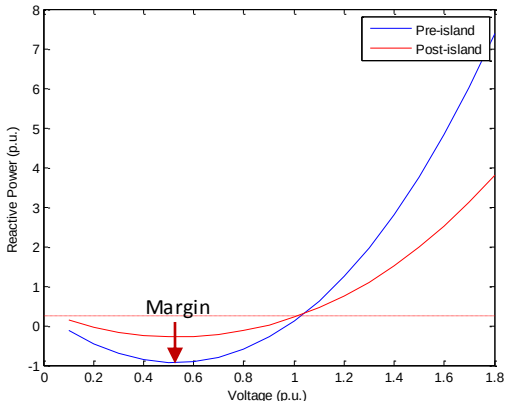

Figure 7-3 QV Curve

Figure 7-2 and Figure 7-3 show the curves for the pre- and post-islanding networks. As the network changes topology, a new curve must be created for each bus. The reason it is important to create the new curve can be seen in Figure 7-3. The margin before collapse between the pre- and post-islanding curves is significantly reduced, therefore without creating the new curve it is not possible to know how far you are form instability. If there are a number of different ICI solutions, then a new curve will need to be created for each bus for each ICI solution. Therefore, the computation required quickly increases making it unsuitable for fast assessment.

7.4 Modal Analysis

The modal analysis appears an ideal candidate as it can determine the system stability along with the cause of any instability. The fact that it can highlight the areas and which components are connected to instability is useful. Knowing that a particular line is important to maintain stability will dictate whether it is to be tripped. The theory behind modal analysis and V-Q

sensitivity analysis is well established, and is therefore not discussed here. However, the full derivation behind the technique can be found in Appendix 2. It is the branch participation information that is to be utilised here. To avoid a situation such as Figure 7-1, it is necessary to evaluate the voltage conditions of any ICI solution. It is proposed to use the branch participation factors to find if any of the lines in the cutset are particularly sensitive to collapse. By looking closer at the branch participation factors, it can also add extra understanding to prevent voltage collapse problems and add an element which will evaluate the voltage and reactive power conditions.

7.4.1 Application to the 39 bus system

The ICI solution which resulted in the collapse in Figure 7-1 is shown again in Figure 7-4, this time with lines in the cutset shown in red. The modal analysis is now applied to the system to investigate the cause of the voltage instability. The reduced Jacobian J_R is formed (see Appendix 2), which was a 39x39 matrix for the 39 bus system. The buses shown in Figure 7-1 are of interest to determine whether instability can be detected without having to run a full time domain simulation. Not only can the modal analysis be used as an indication of proximity to voltage instability, but it is also useful for identifying which areas will benefit more from corrective actions, so will be useful for any control stages of the islanding scheme.

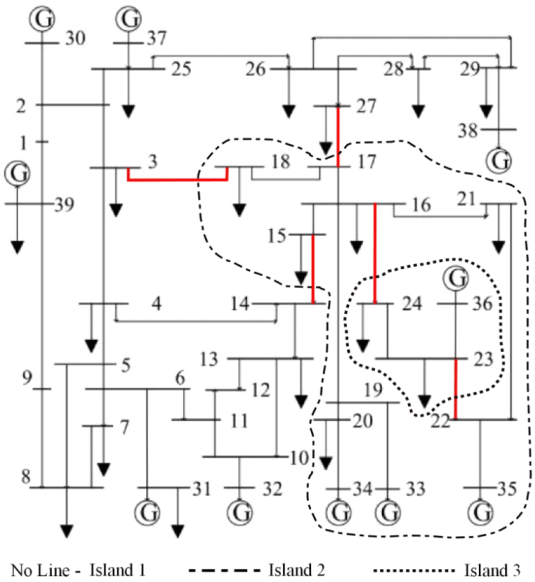

Figure 7-4 Result from the power flow tracing

Table 7-1 Results of modal analysis

Mode	Λ	B	L
24	9.6286	29 39 38 28 1	29-38 10-32 19-33 23-36 26-37
28	21.911	38 29 28 26 27	17-27 26-28 26-29 26-27 16-17
27	35.011	36 39 9 34 1	15-16 16-19 1-2 16-21 23-24

For all the modes found in this example, the smallest three were chosen based on the knowledge attained from the time domain simulation. The actual number of eigenvalues required is yet to be determined. It was clear that the three smallest eigenvalues were linked to the area of collapse, observed from the time domain simulations. The results from the modal analysis can be seen in Table 7-1 for the three smallest modes (most sensitive) and corresponding participation factors, Column B corresponding to the five highest participating buses, and column L corresponding to the five highest participating lines. λ is the value of the eigenvalue.

For this study, the five largest participating elements (most sensitive) were selected based on the knowledge gained from the time domain simulations. The bus participation factors indicate how prone a bus is to voltage instability for each mode. From the same table, it can be seen that the buses shown in Figure 7-1 have some of the highest participations to the most sensitive modes. This shows that there is an evident relationship between the voltage collapse and the modal analysis that was observed as a result of the split. It can also be seen that the same buses are associated with the second mode, and when looking at the highest participating lines, the first line for the second mode (line 17-27) is an element of the cutset. Therefore, the buses where the collapse was observed have been found using the two smallest eigenvalues, and there is a line both common to the cutset and the set of sensitive branches from Table 7-1.

7.4.2 Using modal analysis information to prevent collapse

In order to use modal analysis as a preventive tool rather than just a post-collapse analysis tool, the branch participation factors will be used to assess a lines contribution to instability. If a line in the ICI cutset has a high participation factor to a sensitive mode, this needs to be considered as it could contribute to a voltage collapse. ICI solutions with high participation lines should be avoided in favour of solution with lower participation factors to minimise voltage collapse. For the second most sensitive mode from Table 7-1, line 17-27 has the highest branch participation factor, therefore this line should be selected as 'not available for splitting' and an alternative split should be found.

Chapter 6 has shown that there are a number of different ICI solutions for each seed node. Therefore, an alternative solution is selected and evaluated. This new ICI solution is based on a different threshold value, in this case a smaller threshold value. This new ICI solution is shown in Figure 7-5. Instead of cutting through line 17-27, an alternative cutset with line 25-26 is found. It can be seen that this line is not one of the largest contributing branches to the senistive modes of Table 7-1.

While the size of the 'sick' area increases, using a cutset with lower participating branches should ensure a more stable performance in the voltage conditions. This is verified by time domain simulations in Figure 7-6. It can now be seen that the voltage remains stable. By selecting a line with a lower participation factor, the buses that experienced a voltage collapse are now in a stable condition, but there is also much smaller deviation overall in the system voltages.

7.4.1 Discussion of using modal analysis

It was shown in Figure 7-6 that selecting a lower participating line resulted in a more stable outcome. However, looking at the mode information from Table 7-1, it was seen that this line contributed to the 2nd most sensitive mode. This eigenvalue is very large, and should initially appear to be very stable. Therefore, it becomes very difficult to quantify what a stable eigenvalue is. This method cannot be considered robust enough to make an accurate decision. An eigenvalue close to 0 and positive is close to being unstable, however, there is no method to assess how close to zero you need to be for instability. It would be expected that the λ=21 would be considered stable. Yet, it was shown that the highest participating line for this mode was in the cutset. When removed from the cutset, a much smaller effect on the voltage was seen. Without the insight gained from time domain simulation, this would be considered stable. Clearly the ICI action itself is enough to cause such a stable eigenvalue to go unstable therefore showing the modal analysis pre-islanding cannot asses stability post-islanding. The reason behind this will be discussed later.

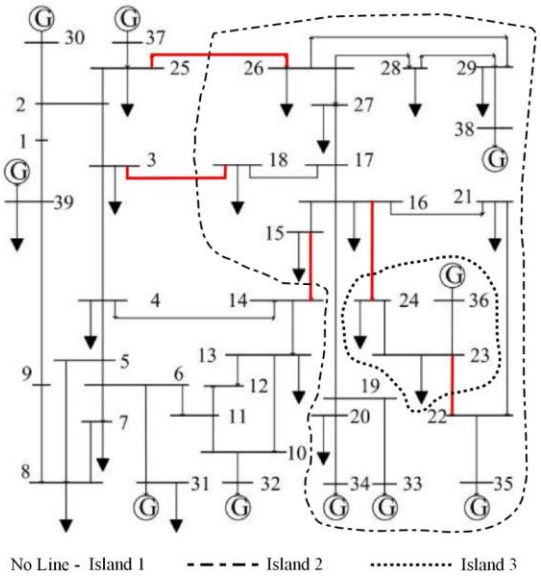

Figure 7-5 New ICI solution

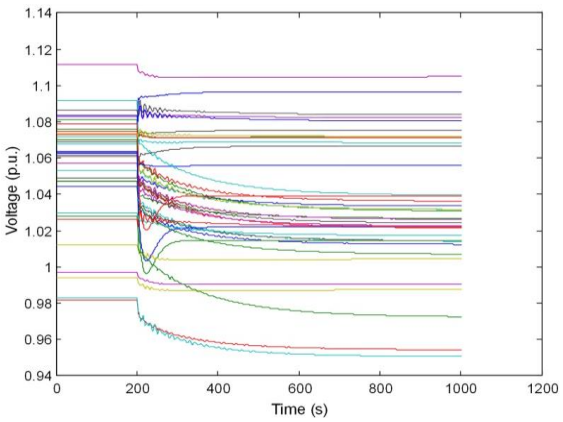

Figure 7-6 New cutset bus voltages

7.5 Voltage Analysis by Distribution factors

Reactive power distribution factors could address the concerns with modal analysis by quantifying the effects of line outages. Where modal analysis finds the most sensitive modes and the related branches, the distribution factors could provide a quantifiable change in voltage as a result of a line outage. The method again relies on information from the Jacobian to create a sensitivity matrix. Using injections of real and reactive power through a sensitivity matrix, the corresponding changes in voltage and angle across a system can be found. This would be useful for ICI where the lines being cut are known and the resultant voltage changes could be computed. The details of the method can be found in Appendix 2. Reactive power distribution factors are well established, especially in the area of contingency analysis. It is typically used to investigate the effects of a line trip.

7.5.1 Single Outages

In order to test the method, it was first tested for single line outages on the 39 bus network where all lines were tested. The voltage changes were then found using the distribution factor method and compared to the voltage changes measured using a time domain simulation. As the method is based on the linearized power flow equations, it aims to approximate the effects on voltage while time domain simulations would be much more accurate. The results were then compared and the errors are summarised in Table 7-2. The largest observed error for the system was 7.77% with the average being relatively small as seen in Figure 7-7 showing all possible line outages with different lines on the x-axis. This shows that it is a good approximate for evaluating line outages without running time domain simulations.

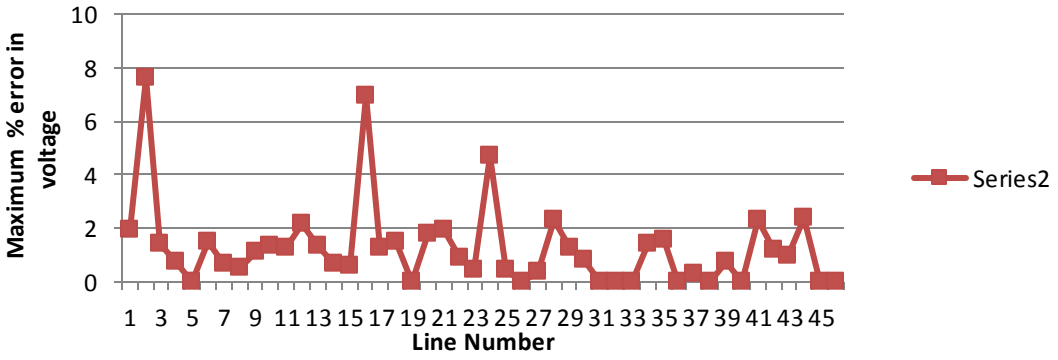

Figure 7-7 % Errors for 39 bus system

Table 7-2 Summary of Errors

Error type	% error V
Largest	7.77467
Average % error	0.29308

7.5.2 Multiple Outage Cases

While the method has been shown to approximate the effects of single line outages, ICI actions typically involve more than one line. Hence, any method will need to be tested for multiple line outages. Multiple outages are handled by extension of the previous method where instead of one line being replaced with injections, multiple lines are replaced with corresponding injections. E.g. for two line outages, there will be four injections to represent each end of the two lines. The 14 bus system is used to investigate the double outages. In this study all combinations of double outages are considered, first taking Line 1 and tripping each remaining line in turn, then moving onto line 2 and tripping all remaining lines in turn until all lines have been modelled in this way. For the 14 bus system, with 20 lines, the results are shown in a 20x20 matrix in Table 7-3, showing the maximum error for each double outage case. All diagonals are

0 as it corresponds to the same line being outaged twice, which is not possible. NaN represent a solution that is not feasible, i.e. power flow failed to converge. The maximum errors from each row are shown in the last column and the errors here are much larger than in the previous cases. This suggests that the linearization techniques do not hold for multiple outages. The largest error being close to 110% is much higher than that seen in the single outage case, which suggests that this method does not work for double, or multiple outages.

7.6 Reactive Power Flows

It may seem obvious that the simplest way to assess the voltage conditions as a result of ICI would be to consider the reactive power flows on the lines being cut. This was initially carried out empirically using time domain simulation. In order to assess a larger number of lines, the 68 bus system was used where Figure 7-8 shows the reactive power flows on the y-axis for each of the lines on the x-axis. Each line was tripped as a single line outage and the resultant maximum measured voltage changes were then found using time domain simulations.

These voltage changes are shown in Figure 7-9. It can be seen that there is no correlation between the maximum flows and the largest changes in voltage. It can therefore be concluded that cutting through the line with the largest reactive power flow does not necessarily have the largest impact the system voltage. Cutting through a line which affects the redistribution of reactive power flows has much more of an effect and therefore it would not be sufficient to consider only the reactive power flows as an indicator to the effects on voltage. From these findings, it can also be stated that reactive power tracing, while possible, would also not be sufficient as it too relies on the reactive power flows.

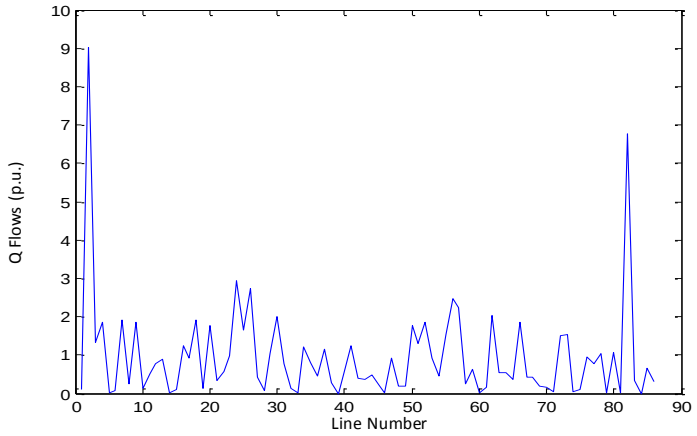

Figure 7-8 Line reactive power flows (68 bus)

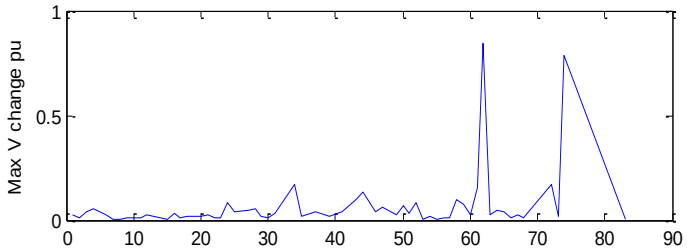

Figure 7-9 Voltage changes for each line outage from Time domain

7.7 Discussion of these findings

The investigation has been extremely useful as it introduced a number of different problems associated with voltage stability and static methods. Firstly, the modal analysis results appeared to show why the voltage collapse occurred. However, the question of why such a stable eigenvalue was connected remains an issue. It is not possible to know if an eigenvalue is close to instability, or indeed how many eigenvalues should be considered. As the eigenvalues will be different for every system, and each operating point, they will always change and hence cannot be tuned ideally to find what an unstable eigenvalue would be. Therefore, it was not an ideal method as it was not able to show what a bad island solution would be, or even if it was stable.

The distribution factors method could not be applied for multiple outages. It was shown that when considering even double outages that errors of 110% were seen. However, further exploration into this brought up a key issue with both the distribution factors method and the modal analysis method. The distribution factors method worked well for single line outages with max errors of 7%. The reason for this is that a single line outage can be considered as a small perturbation. Both methods rely on linearization of the power flows which only holds for small perturbations. This was proven using the multiple outages. These were a significant perturbation and as a result, the error observed was very large. The linearization methods could not compute good approximations which highlighted an important flaw. If the double outages are shown to be large perturbations, then ICI actions must be considered very large, as there are more lines being cut. More importantly, independent systems (each island) are being created which will create their own independent operating points. For ICI, methods based on linearization cannot be used as they offer no useful information for the large perturbations.

Table 7-3 Double outage Errors

8	1	2	3	4	5	6	7	8	9	10	11	12	13	14	15	16	17	18	19	20	Max Error
1	0	NaN	NaN	NaN	NaN	NaN	NaN	NaN	NaN	NaN	NaN	NaN	NaN	NaN	NaN	NaN	NaN	NaN	NaN	NaN	**0**
2	NaN	0	4.52	4.223	3.501	1.741	3.046	2.744	2.184	4.227	15.775	8.856	18.937	NaN	16.156	1.732	5.868	6.906	1.636	11.073	**18.937**
3	NaN	4.52	0	6.723	4.242	NaN	7.596	2.639	2.215	4.193	16.408	8.944	19.326	NaN	16.351	1.692	5.868	7.239	1.671	11.663	**19.326**
4	NaN	4.223	6.723	0	3.977	2.33	5.575	3.404	2.702	5.04	16.658	8.988	19.525	NaN	16.901	2.01	5.868	7.569	1.972	11.9	**19.525**
5	NaN	3.501	4.242	3.977	0	1.184	2.749	2.488	1.944	3.949	15.68	8.837	18.881	NaN	16.004	1.476	5.868	6.763	1.387	10.977	**18.881**
6	NaN	1.593	NaN	2.33	1.252	0	3.725	1.535	1.147	1.944	15.07	8.749	18.647	NaN	15.237	0.762	5.868	6.043	0.745	10.386	**18.647**
7	NaN	4.114	8.554	5.531	2.469	3.725	0	4.354	3.51	6.099	18.512	9.209	20.943	NaN	18.221	3.152	5.868	8.982	7.739	13.273	**20.943**
8	NaN	2.744	2.639	3.404	2.488	1.3	4.656	0	4.034	NaN	16.516	8.933	20.104	NaN	0	1.867	5.868	9.041	1.462	11.381	**20.104**
9	NaN	2.184	2.215	2.702	1.944	0.816	4.069	4.034	0	3.087	18.138	9.078	20.22	NaN	39.267	1.22	5.868	10.288	1.46	12.909	**39.267**
10	NaN	4.227	4.193	5.04	3.949	1.641	7.277	NaN	3.087	0	19.544	8.988	17.71	NaN	NaN	NaN	5.868	NaN	1.69	11.143	**19.544**
11	NaN	15.775	16.408	16.658	15.68	8.599	19.278	16.516	18.138	19.544	0	15.576	22.628	NaN	68.523	0	15.707	NaN	15.285	20.241	**68.523**
12	NaN	8.856	8.944	8.988	8.837	10.057	24.943	8.933	9.078	8.988	15.576	0	NaN	NaN	16.409	8.761	11.262	10.095	NaN	10.44	**24.943**
13	NaN	18.937	19.326	19.525	18.881	13.063	25.294	20.104	20.22	17.71	22.628	NaN	0	NaN	31.917	19.006	109.523	17.146	65.055	33.118	**109.523**
14	NaN	NaN	NaN	NaN	NaN	NaN	NaN	NaN	NaN	NaN	NaN	NaN	NaN	0	NaN	NaN	NaN	NaN	NaN	NaN	**0**
15	NaN	16.156	16.351	16.901	16.004	9.038	15.119	0	39.267	NaN	68.523	16.409	31.917	NaN	0	27.031	20.553	40.415	15.851	45.491	**68.523**
16	NaN	1.732	1.692	2.01	1.476	2.039	12.484	1.867	1.22	NaN	1.00E+08	8.761	19.006	NaN	27.031	0	5.868	NaN	0.744	11.186	**1.00E+08**
17	NaN	5.868	5.868	5.868	5.868	6.637	21.268	5.868	5.868	5.868	15.707	11.262	109.523	NaN	20.553	5.868	0	10.128	7.284	NaN	**109.523**
18	NaN	10.96	10.999	8.447	6.329	6.043	8.982	3.811	7.188	NaN	NaN	9.382	22.483	NaN	59.835	NaN	5.868	0	3.937	15.971	**59.835**
19	NaN	1.636	1.671	1.972	1.387	1.07	4.576	1.462	1.46	1.69	15.285	NaN	65.055	NaN	15.851	0.744	7.284	6.519	0	10.441	**65.055**
20	NaN	11.073	11.663	11.9	10.977	7.359	20.953	11.381	12.909	11.143	20.241	10.44	33.118	NaN	45.491	11.186	NaN	17.503	10.441	0	**45.491**

As the modal analysis is also based on the linearization methods, it means that it too cannot be used. The modal information will change once the lines are tripped as it will have a new operating point. Therefore, these values tell us nothing about the post-split systems. While the results did show that eigenvalues could be used to minimise the effect on the voltages, this was more about finding weak areas in the systems rather than actually finding the effects of cutting lines. The modal analysis is useful for finding weak areas in a system, but the proximity to instability for these weak areas will only hold for small perturbations. It could be considered that while and eigenvalue of 21 would typically be considered stable, the ICI actions may have been significant enough to drive it unstable. One of the fundamental assumptions in reducing the Jacobian for eigenanalysis is that $\Delta P = 0$. However, if an island is created, there will be an imbalance in the systems. There is a change in real power, and so the method cannot be linearized around this point. The ICI will immediately move it to a new operating point for which all the eigenvalues and sensitivities will change and provide no useful information.

7.8 Summary

This chapter gives a comprehensive study on the use of static voltage stability techniques for ICI methods. Modal analysis was tested due to its ability to provide information on proximity and the mechanisms behind voltage instability. The method is based on linearization of the power flow equations to create the sensitivity matrix. Further Eigen analysis can provide information on which buses and lines are participating towards instability. The method was then used to understand the voltage collapse from an ICI solution. It was shown that using modal analysis could prevent the collapse but there were a number of issues. The results from the modal analysis would not necessarily identify the example case as being close to unstable. Indeed an eigenvalue of 21 is very far away from 0, but a line seemed to be sensitive to this mode. Without the time domain simulation, it would not be possible to draw any conclusions from the modal analysis information alone.

Further analysis was done to quantify the effects of a line outage using reactive power distribution factors which would be ideal in quantifying a voltage change as a result of a line outage. The method is again based on linearized power flow equations and worked well for single line outages. However, when tested on multiple outages, major problems were identified. The voltage changes from the distribution factors did not correspond well to the time domain simulations. This meant that there was a fundamental issue which was traced down to the original assumptions to linearized methods. Linearization works well for small perturbations about the operating point. However as these perturbations become larger, a new operating

point is formed. This was an important finding as it meant that modal analysis was also flawed for ICI purposes as it relied on the same assumptions. Indeed, in forming the reduced Jacobian, it was required to assume that there was no change in real power. However, in ICI, there would indeed be a change in power. Therefore, these methods could not be used.

Considering reactive flows would be a simple method to reduce reactive power imbalance. However, it was shown that tripping a line with the largest reactive power flow did not correspond to large changes in voltage. This is because voltage and reactive power are local phenomena. They cannot be made global by considering an overall imbalance for the purposes of voltage changes. The same could be applied to reactive power tracing, where it too is based on the reactive power flows. Therefore, this chapter has shown that there is a need to develop a new methodology for analysing voltage and reactive power for the purposes of ICI in particular for multiple outages.

8 Voltage Stress indicator for ICI

8.1 Introduction

Islanding actions cannot be considered a small perturbation due to the multiple outages shown in the previous chapter. A method is needed to assess the impacts of multiple outages to give an indication on the systems voltage stability. Voltage behaviour is highly non-linear and it has been shown that methods to linearize it cannot be applied to large perturbations. To fully evaluate voltage stability, taking all the non-linearity into account would require time-domain simulations due to the number of control systems, dynamic loads and devices in the system. Therefore, the thesis will move away from the hard definition of voltage stability, and will instead investigate the effects splitting actions could incur on the reactive power changes. It is ultimately these changes that will affect the voltage behaviour in the system.

The relationship between reactive power and voltage is complex. However voltage is also related to real power through the power flow Jacobian from Appendix 2. The changes in real power are considered in the tracing solution where selecting an ICI solution with minimal real power imbalance and power cut should also minimise the effects that real power will have on voltage directly. It is the effects that reactive power will have on voltage that are important to identify as such aspects are not found through tracing. It will be through the combination of real power and reactive power analysis that the effects on voltage are to be minimised. Therefore, the aim of this section is to introduce a method to quantify the effects on voltage due to reactive power which is currently missing from the methodology.

Full analysis of voltage stability requires time domain simulations, or at the very least, multi-time scale simulations in order to catch all the dynamics. Therefore, the problem must be simplified in order to provide a fast solution while sacrificing the accuracy of full simulation. As with active power, reactive power must be balanced in a system but in a localised way. The voltage profile is mainly dependent upon the balances of reactive power. Voltage controllers such as AVRs and reactive power sources (SVCs, statcoms etc.) are linked to this imbalance. These will respond to a voltage change resulting from an imbalance in reactive power. By injecting more reactive power into the system, the voltage profile can be restored. Therefore, the reactive power imbalance is fundamental to the voltage conditions.

In order to make this method general, AVR models, SVCS etc. will not be considered directly, but rather the fundamental principle on which they rely. All these devices will respond to a change

in voltage which is caused by the changes in real and reactive power. By analysing the potential changes in real and reactive power, the inherent change in voltage can be found and hence the signal by which any reactive power sources will act. If more information is available on the system, the method could be further enhanced with knowledge of AVRs, SVCs etc. The aim is to find the local imbalances within the system as a result of ICI. These imbalances will lead to voltage excursions which controllers respond to.

8.2 Voltage Excursions & Power imbalance

Voltage changes are linked to both changes in real and reactive power. The important distinction between real and reactive power is that an imbalance of real power between generators and loads is covered by the kinetic energy of all the generators and can be interpreted as a global imbalance. Reactive power however does not have a global imbalance as is has no net energy transfer. Reactive power is required to maintain high voltage levels around the system which is important for active power transmission. Reactive power cannot be transmitted over long distances as it will result in a voltage drop according to $\Delta v = \frac{PR+QX}{V}$. Therefore, if there is insufficient reactive power available in an area, low voltage levels will exist, hence limiting the ability to transmit active power. It is important to keep voltage levels high, therefore localised reactive power imbalances can be defined as follows:

Definition: Local reactive power imbalance: The amount if extra reactive power required to maintain nominal voltages at a bus.

Reactive power can be produced by generators, SVCs etc. but also from the lines themselves. Therefore, every line in the network has the potential to behave as a reactive power source or sink and should be modelled as such. This means that reactive power should be evaluated in a localised manner.

Changes in real power will also affect voltage. However, the imbalance in real power can be quantified from the tracing solutions as in Table 6-5. By choosing the solution with minimal imbalance, the effects on voltage due to real power imbalance would also be minimised. However, the tracing solution does not provide any information on the reactive power changes, which as stated must be considered locally. Therefore, it would be blind to the effects of voltage from reactive power changes. This chapter will propose a method by which to observe the potential impact of reactive power on voltage. The best voltage solution should minimise both real and reactive power changes.

Consider the 14 bus system, from Appendix 1, operating in steady state where the generator is supplying exactly the electrical load at its terminals. When the system experiences a sudden change in topology, there will be a shift in the reactive power flows around the system. This corresponds to a sudden change on the generator loading. This can be seen in time domain simulations in Figure 8-1 and Figure 8-2. In this example, the q_{syn} shows the reactive power loading of the generator. When there is a sudden change in the loading, there is a corresponding voltage change at the generator. In Figure 8-1 the reactive power loading on the generator increases. This corresponds to a change in the voltage due to the insufficient reserve of reactive power. The opposite effect is observed in Figure 8-2 where the generator loading is decreased. There is then a settling time associated with the various controllers. It is clear that this transient change in reactive power has a direct effect on the voltage. However as these were obtained using time domain simulations it is infeasible for fast assessment. Therefore, the aim is to asses this type of change in Q using static methods. It will be a static approximation of the dynamic increases or decreases in reactive loading. This change will be thought of as the instantaneous imbalance in reactive power at that node.

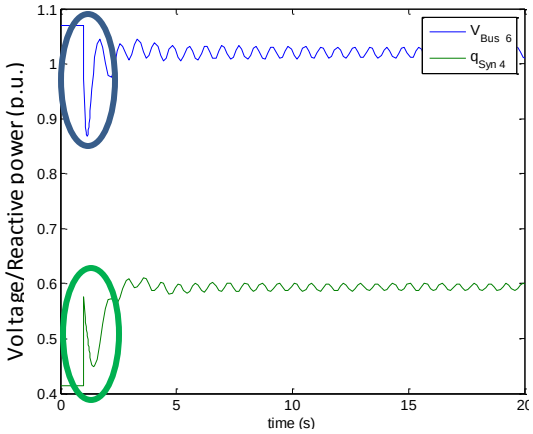

Figure 8-1 Voltage drop

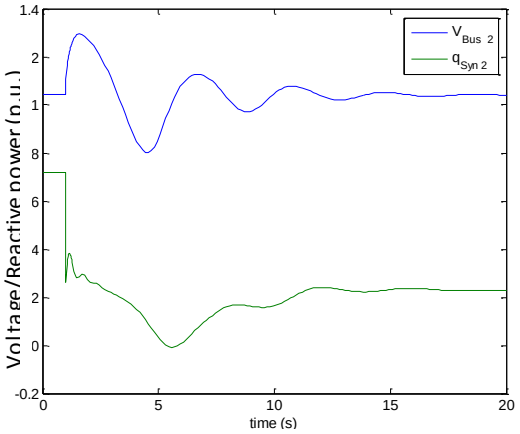

Figure 8-2 Voltage rise

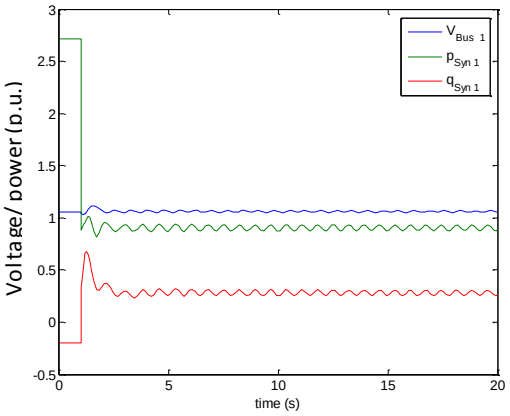

Figure 8-3 Voltage change (P and Q)

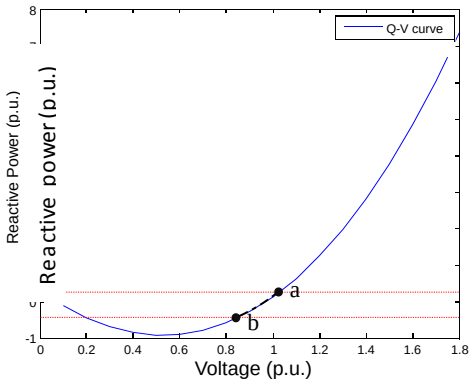

Figure 8-4 PV curve load bus

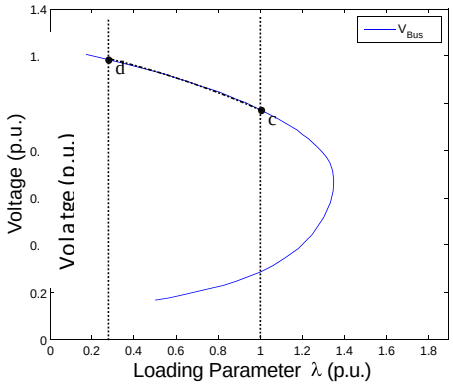

Figure 8-5 QV curve load bus

It is important to note that the voltage changes are not purely dependent upon the reactive power changes as in Figure 8-1. Figure 8-1 and Figure 8-2 correspond to examples with small changes in real power. However, consider the example in Figure 8-3 where the deficit in Q results in a very small increase in voltage. These results can be easily visualised with the PV and QV curves.

In Figure 8-4 and Figure 8-5, points *a* and *c* refer to the steady state (before contingency) operating points. Looking at Figure 8-4, an imbalance (increase in loading) would result in a voltage drop down to point *b*. However, from Figure 8-3, it can be seen that the real power load actually decreases corresponding to point *d* in Figure 8-5. Therefore, the actual voltage drop will be made up of the changes in P and Q where in this example, the effects of P outweigh the effects of Q and lead to a voltage increase due to the lower real power loading. This is a simplified example showing how the real and reactive power imbalances will affect voltage. Using PV and QV curves for the actual ICI solutions would be infeasible as described in chapter 7. The pre and post islanding curves would be different and it would take too long to generator new curves for all buses for each ICI solution. The following approach is therefore adopted.

8.3 Voltage Stress due to reactive power changes

It has been shown that the reactive power changes do not always result in a direct change in voltage and that the effects of real power must be considered. However, the tracing solutions will evaluate any imbalance in the real power. The missing component is the ability to assess the reactive power imbalances. If the imbalances in real power are minimised, then the effects such as those in Figure 8-3 will be avoided and the relationship will be much closer to that in Figure 8-1 and Figure 8-2. A large imbalance in real power should be avoided anyway due to its effects on frequency and transient stability, but now also for its effects on voltage stability.

Therefore, this methodology will develop a static method by which to account for changes in reactive power due to ICI. The short (transient) voltage change (Figure 8-1 and Figure 8-2) before the controllers operate can be used to portray how much stress is being placed on the system. Voltage stress is therefore defined as a large transient change in bus voltages due to a large imbalance of reactive power. If any actions cause a substantial change in bus voltage, it is said to increase the voltage stress. It is based on this principle that a voltage stress predictor is developed for large transient voltage changes caused by ICI. It is the short term transient voltage changes that are of interest here as they may lead to severe long-term voltage problems and they also reduce transient synchronous torque.

The approach is justified the following way. Power on the lines will redistribute itself instantaneously after ICI but it will take some time for Automatic Voltage Regulators to respond to maintain set voltages. According to [135] a typical value for an AVR on a 50MW machine can be between 0.4s and 1.2s which is the main time constant for the exciter. There are a number of times associated with an exciter as in Figure 8-6. According to [108] it is usually assumed that with an accuracy of regulation $\varepsilon \leq 0.5\%$ and with a 10% step change of the voltage reference value, the settling time is $t_\varepsilon \leq 0.3s$ for static exciters and is $t_\varepsilon \leq 1.0s$ for rotating exciters. While the rise time t_r is much shorter than this, typically in the order of ms which varies between manufacturers and is dictated by limits, ceilings etc. One such static device from Siemens has the ability to reach its ceiling voltage in under 100 ms for a terminal voltage drop of 0.15 p.u. [136]

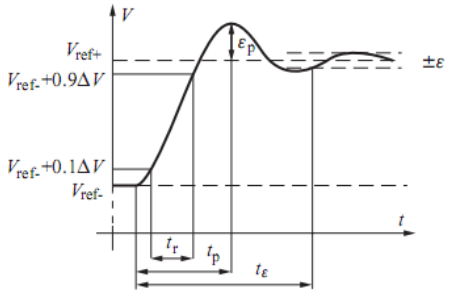

Figure 8-6 Dynamic voltage response to a step change in reference voltage [108]

It is this transient period between the cutting of the lines and the adjustment of AVRs that is of interest as voltage can change significantly during that period due to local reactive power imbalances. Hence a large pre- and post-islanding difference between nodal reactive power flows, i.e. reactive power flows through a node, may serve as a predictor of a transient voltage

problem as it indicates a large local transient reactive power imbalance before AVRs attempt to restore the voltages to their set values.

Longer timeframes would require more detailed analysis of the control mechanisms and hence will take longer to compute. However, the approach is very much simplified where minimising the amount the voltage changes in the transient period will also reduce the amount of post-split control required and hence can be approximated quite well by this initial voltage change. The importance of Over Excitation Limiters (OXLs) was identified in [137] where their activation can push a system further into instability. If creating an island requires AVRs to further increase their output the limits of OXLs may have severe impacts. Therefore, the imbalance is used as a proxy for the voltage change that will initiate all controllers around the system and minimise this change.

The assumption is made that by minimising the voltage stress, the effects leading to voltage instability are inherently minimised. While it cannot be stated categorically that voltage stability is guaranteed, it will be said that this solution will aim to minimise the effects on voltage stress. A voltage collapse is typically observed after a large change in voltages, or a progressive series of voltage changes. It is therefore the aim to minimise the voltage changes and therefore minimise the chances of collapse. Long term voltage stability can be in the order of minutes. Therefore, it will be assumed that should voltage conditions deteriorate over longer periods, corrective actions can be taken within that period, such as load shedding. Hence, it is not an immediate concern for the voltage stress.

8.4 Voltage Changes due to ΔQ

8.4.1 The concept

In order to evaluate the voltage stress on a system, the method will rely on how much the reactive power will change as a result of ICI. It is not possible to measure the voltage changes as a result of line cuts without running dynamic simulations. However, running a series of power flows, it is possible to find where the reactive power changes and by how much. It is well known that voltage is tightly linked to reactive power, and where there is a deficit of reactive power, there will be lower voltage levels and vice-versa. Therefore, the method aims to exploit this principle during the transition between the normal state to the islanded state in order to predict what the voltage changes as a result of the ICI could be. When a system is islanded, lines are cut and independent networks are created. In the moments before the split, there will have been areas that were being fed, or feeding, reactive power via the lines being cut. When these lines

are cut, these areas will not have the reactive power supplies from the lines, and the reactive power is redistributed. This is where the generators will change their production to produce/absorb more reactive power to stabilize the system, if they can and there will be an overall redistribution of the reactive power. Therefore, it is this period that will be captured, where these areas of deficit/surplus reactive power are, which generators need to change their outputs and by how much.

When a line is cut, power is distributed almost instantaneously among other parallel lines. Inertia causes power angles to change slowly as generation cannot change quickly as valves cannot move quickly enough in thermal stations. Therefore, as soon as lines are cut, the flows on the remaining lines change. It is assumed that the reactive power produced can change quickly also. The only component that does not change instantaneously is the real power production. However, it is assumed that there is enough inertia in the system so that an instantaneous frequency change is not possible. Therefore, this state, just after splitting will be replicated using a power flow solution.

This power flow solution is obtained for each island and the purpose of the power flow is to rebalance each island. While the focus is on the reactive power imbalances, by running a power flow, the real power will also be balanced. However, the tracing algorithm aims to find a solution with minimal real power imbalance. If this imbalance can be minimized, then the system will not change significantly for real power. However, the governor action will balance the system eventually, running the power flow will essentially be finding the balanced state when all governor action is complete. It is the fact that the real power imbalance is being minimized that it can be assumed that this method can be applied. The real power production changes are essentially being neglected from this study as it is assumed there is inertia in the system, that the tracing will minimize the effects on real power flows and that it is of a longer timescale than the reactive power.

For an already stressed system, it is beneficial to take actions which reduce any additional stress on voltage. Instead of considering individual line outages and adding their effects cumulatively, a new method is devised which will consider the voltage effects from all the line outages together as one trip.

8.4.2 Drawback

The drawback to this method lies in the real power – voltage relationship. No matter how weak the relationship, it is evident and it will affect the results. However, by understanding these effects, it is possible to go a long way to minimising their influence. These are now explained but the argument for overcoming them is also shown:

A change in real power will have an effect on voltage

Voltage is dependent upon real and reactive power, however the tracing takes the real power into account, i.e. by minimising the amount of real power being cut and hence the corresponding effects on voltage. As there was no method to assess the relation between reactive power and voltage, the main purpose of this methodology is to study this relationship while taking the effects of real power into account indirectly. If a large change in real power is observed, this will be detected from the tracing method.

Running the power flow will balance reactive power but also real power

As it is the voltage change at the moment of splitting that is of interest, load flows are used to find the imbalance. However, the power flow solution will automatically balance the real power also, which will not happen in this short transient period. However, the real power flows on the lines will redistribute within that period, it is this effect which need to be caught. It is not possible to separate the two from each other. It must be assumed that the effects of the real power balancing will be minimal. As voltage is more tightly linked to reactive power, this relationship will be the priority. As the changes in real power are minimised, the effects on voltage due to that real power will also be small.

Another method to reduce the effects of the real power rebalancing is through the slack bus. If there are a number of generators in an island, all other generators will remain at their fixed real power value, which reflects their actions during the transition period. Only one generator will change its output. Therefore, the power flow can better model this period, if one slack generator is used compared to a distributed slack where all generators would change. By applying this method to islands with minimal imbalance, then only a small change in the slack generator will be observed and hence have only a small impact on the result.

In order to obtain a fast solution, using static methods, there has to be some trade-off with accuracy. However, it will now be demonstrated that this method works quite will for detecting large changes in voltage. In fact, when considering large voltage changes which is defined as greater than 10%, the drawbacks mentioned above are negligible.

8.4.3 Observing Bus throughput

For real power, losses are incurred along a length of line. However, for reactive power, depending on the capacitive or inductive nature of the line, reactive power can be either produced or consumed by the line. Therefore, the lines themselves can appear as reactive power

sources. There is a relation between the real power and the reactive power, and when the lines in the system are cut the real power will be redistributed. This can affect the reactive power flows where in an extreme case could change from a consumer to a producer.

Hence all nodes are investigated, not only the PV nodes where AVRs are installed, in order to take into account changed reactive power generation/consumption by transmission lines. Indeed it is a similar approach to that of [127] where all lines can be considered as reactive power generators. The reactive power throughput through every bus is therefore used. The bus throughput will be the sum of all the reactive power at that bus, i.e. the sum of all incoming reactive power from lines or generators, or the sum of all outgoing reactive flows such as lines or loads. Any changes in the reactive power production from lines can be detected through this quantity.

It is essentially a method of incorporating the effects of real power indirectly into the reactive power solution. Looking at generators only would give general information about how much added injection a system required. However, this method will measure the same quantity but on a local scale, at every bus. Therefore, it can be used to predict which buses in the system will see voltage drops/increased and based on the injection of reactive power, and can make a prediction about the size of that voltage change.

8.5 Algorithm

The intention is to define a index for each of the outage/ICI scenarios based on the observed changes of reactive power. The purpose of this analysis is to minimise voltage stress which has already been defined as the maximum change in voltages or reactive power injections. Therefore, in order to assign a single index to each scenario, the index will be set according to the largest change in the reactive power. It is being proposed that the largest changes in reactive power at a bus, will result in the largest changes in voltages. Therefore, the maximum change in reactive power will be used as the index.

The algorithm is as follows

1. **Run base case power flow**

   This is to get the values of all reactive power bus throughputs. In the real system, this could be taken from WAMS in real time. Load flow solution is used here to simulate the pre-islanding values.

2. **Record all bus throughput values**

   All bus throughput values are recorded as a vector $\boldsymbol{T}_q^0$

$$\boldsymbol{T}_q^0 = [Q_1, Q_2, Q_3 \dots Q_n] \tag{8.1}$$

Where Q is the bus throughput and n is the number of buses.

3. **Trip line/cutset**

   The line(s) is removed from the model. If such removal splits a network into islands, the model must be modified to change one of the PV nodes in each island into a slack node, as this is a requirement for the load flow.

4. **Run a power flow for each island**

   This step will balance the islands and change the powers and bus values accordingly

5. **Record all the new bus throughput values**

   The new throughput values for reactive power are recorded at each bus in the system in vector $\boldsymbol{T}_q^+$, to indicate the time just after splitting.

$$\boldsymbol{T}_q^+ = [Q_1^+, Q_2^+, Q_3^+ \dots Q_n^+] \tag{8.2}$$

   Where Q^+ is the bus throughput recorded from the new power flows, or the time just after splitting.

6. **Calculate the index**

   The index is based on the maximum change in reactive power, it can be done on an island by island basis, or on a system wide basis. Here, it is on a system wide basis where it is said that the location is less important, only the magnitude of the change is being looked at. This index is then assigned to that line/cutset

$$\Delta \boldsymbol{T}_q = \boldsymbol{T}_q^+ - \boldsymbol{T}_q^0 \tag{8.3}$$

$$W_V = \max(\Delta \boldsymbol{T}_q) \tag{8.4}$$

   Where ΔT_q is the vector of all changes in reactive power bus throughput and W_Q is the index assigned to that line/cutset. All values of T are in p.u. of reactive power.

7. **For the purposes of validation ONLY, a time domain simulation is run**

   The time domain simulation is carried out to accurately measure the voltage change to compare with the changes in reactive power. This would not be done in the final ICI solution, but only here to validate the method.

8.5.1 Positive and Negative changes

A further simplification is added in order to minimise the data and analysis required in the later stages. Consider again Figure 8-1 and Figure 8-2 where the dynamic change in reactive power

and voltages were shown. It is clear from these figures that a large deficit of reactive power leads to a voltage drop while a large surplus of reactive power leads to a voltage rise. Figure 8-7 shows the real changes in bus voltage and the changes in generator loading (purple) for the five generators in the 14 bus system when islanded. These were created using dynamic simulations. Recall, it is these dynamic changes in reactive power that is being approximated using static methods. Applying this static methodology, the changes of reactive power at each generator using equation 8.3 are shown in red in Figure 8-7.

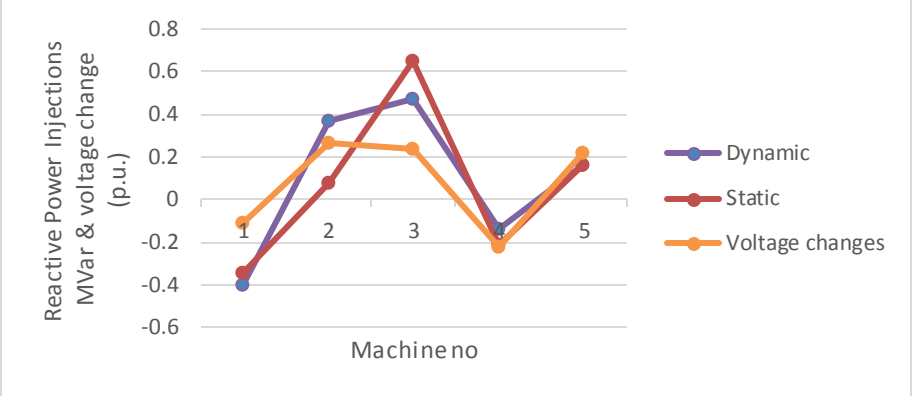

Figure 8-7 comparison of dynamic and static results

It is clear that there is a strong relation between the static and dynamic changes of reactive power. Both the static increases and decreases in reactive power follow the actual increases and decreases of reactive power as calculated using time domain simulations. The voltages will also change accordingly. Therefore the proposed algorithm serves as a good approximation for the reactive power changes. While the effects of sustained undervoltages are already well understood, a major overvoltage can also be dangerous for the system. Taking the same 14 bus example as described in Appendix 1**,** with a slight change increase in one load, an overvoltage situation can be created. Upon islanding this system, the overvoltage area leads to collapse as seen in Figure 8-8.

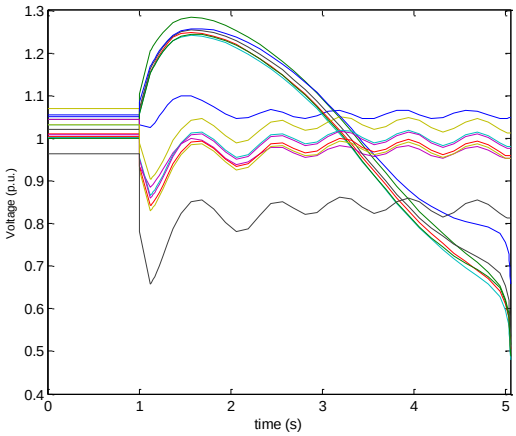

Figure 8-8 Overvoltage Collapse

Therefore both under and over voltage scenarios should be equally avoided as they pose severe risk to the system. Therefore, it is not necessary to distinguish between positive and negative changes in reactive power, but only the largest absolute changes. This means that equation 8.4 becomes:

$$W_V = \max(\text{abs}(\Delta \boldsymbol{T}_q)) \tag{8.5}$$

The main advantage to this simplification is for easier visualisation of the results as now only the absolute changes in reactive power and corresponding changes in voltage need be assessed and it allows the minimisation in the optimization to be simplified. Therefore, all subsequent results will refer to absolute voltage and reactive power changes from nominal.

8.6 Validating the concept

8.6.1 Single Outages

The concept needs to be validated in order to verify the assumptions that have been made. It must also be verified that it can provide a prediction, or an indication into what will happen with the voltages. The first validation was using single line outages to ensure that the method holds and to determine if a clear relationship existed between the changes in reactive power and bus voltages.

The method is evaluated using a comparison to time domain simulations. For this study, the 68-bus 16 machine system was used as it provided a larger number of lines for assessment. For each line outage, the outlined methodology is used to look at the change in reactive power outputs, and only the maximum absolute values are shown here. To compare, a time domain simulation

is used to evaluate the actual change in voltages as a result of the line outage around the moments of splitting, not considering longer times where control actions could take effect. The largest absolute change in bus voltages is used for comparison.

The results for this test are shown in Figure 8-9. The top plot shows the maximum absolute change in bus voltage in p.u. for each line outage in the system from the time domain. The bottom plot shows the maximum absolute changes in reactive power bus throughput, or the index defined in equation (8.5) using this methodology. The lines which are tripped are shown along the x-axis.

It is the peaks of the graphs which are the most important as these outline the lines that cause the largest changes, and the peaks on both graphs align quite well.

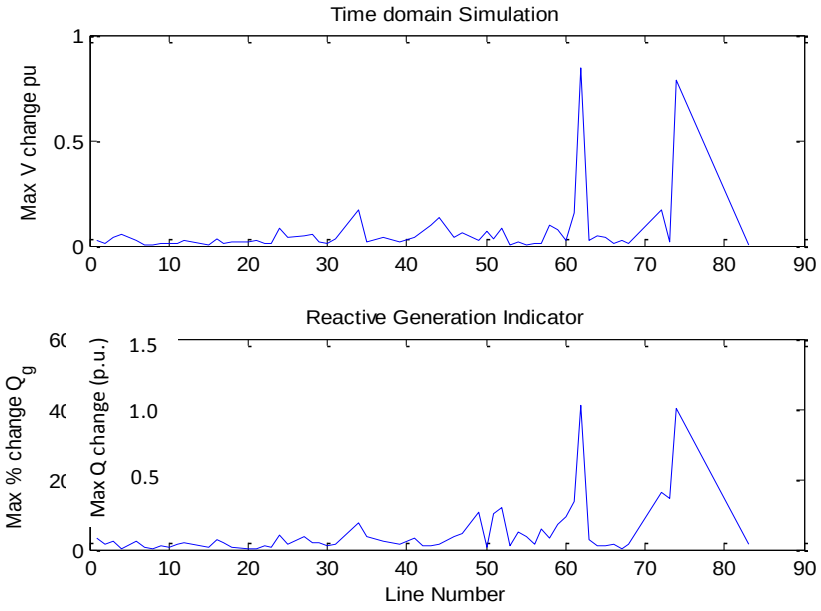

Figure 8-9 Time domain Vs % Q change for 68 bus system

It can be seen that the lines corresponding to large changes in voltage correspond to the largest changes of reactive power. This indicates that large voltage changes, which are more likely to increase system stress, can be clearly seen from changes in the reactive power throughput. It can be concluded that the voltage index, W_Q could give a good estimation into changes in voltage for a system, especially for large voltage changes.

8.6.2 Smaller voltage changes

It should be noted here that for the smaller peaks and smaller voltage changes there is reduced accuracy and there are a number of reasons for this.

Relationship is non-linear

The voltage and reactive power changes will follow each other but not linearly, and this can cause issues for the smaller voltage changes where much higher accuracy is needed.

Effects of real power having an effect

As described earlier, the effects of rebalancing the real power affect the voltage. As this is a relatively weak relationship, it will have small changes on voltage. However, this means that at these small voltage changes the relation may not be purely reactive power based.

However, the method was designed as an approximation for large voltage changes where speed was more important than accuracy. As it is large voltage changes that are of interest, the accuracy for smaller voltage changes is being sacrifices as they will have little effect on the ICI decisions. Also, if more accuracy is required for small changes, the linearization methods can be adopted as it has been shown that these work quite well for small perturbations.

8.7 Multiple Outages - ICI

The method is now applied to ICI. For these studies, the tracing is used to provide the ICI solutions which are then assessed using this methodology for voltage. For completeness, all seed nodes are considered using all possible threshold values to give a range of solutions. From the tracing results on the 68 bus system, there are a number of islands which could significantly increase voltage stress as shown in Figure 8-10.

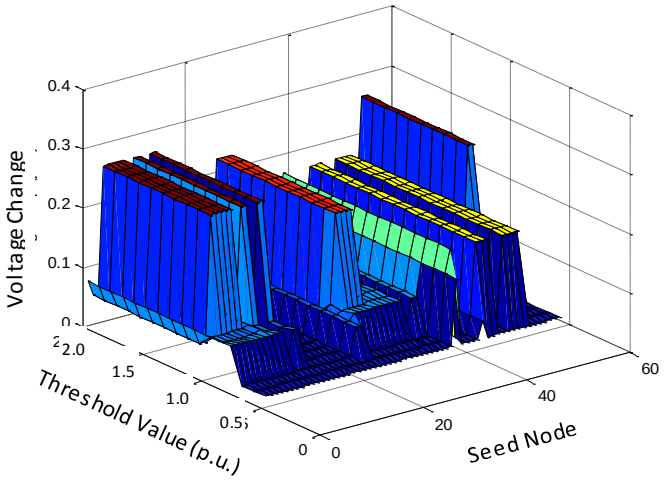

Figure 8-10 Voltage Changes for all possible islands in the 68 bus system

For all seed nodes evaluated over a range of threshold values from tracing, the corresponding voltage changes are shown. It is the peaks of this graph which should be avoided as these result

in the largest voltage changes. As mentioned in Chapter 6, the ICI solutions are not unique for all seed nodes, with many seed nodes and threshold values sharing the same solution as indicated by the flat sections.

Figure 8-11 shows the correlation between the peaks of Figure 8-10 (in blue), i.e. the maximum voltage drops for each seed node, with the maximum changes in nodal reactive power (in red) calculated by the proposed voltage change prediction algorithm. The graph is not continuous due to certain seed nodes having no feasible solution, i.e. when power flow fails to converge (discussed later).

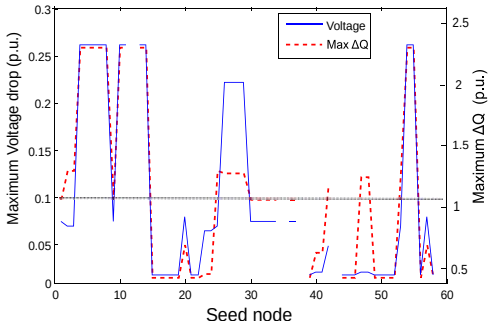

Figure 8-11 Correlation of maximum possible voltage changes with changes in nodal reactive power flows for each seed node

There is an excellent correlation between the large voltage changes (defined as larger than 0.1 p.u.) and the changes in nodal reactive power flows. Admittedly the correlation is less strong for smaller voltage changes but it is only the large voltage changes, which threaten voltage stability, which is of interest. It can be therefore concluded that while the relationship is non-linear, there is a strong correlation between large voltage changes and large reactive power changes that provides a good predictor to the size of transient voltage changes without doing time-domain simulations.

8.7.1 Screening

An important step required to illustrate the effectiveness of this method is screening. It has been shown that the large voltage changes are of interest and therefore being able to penalise islands which may result in large voltage changes. There is little interest in small voltage changes, or indeed the accuracy of the method for small voltage changes. Due to the non-linear nature, it is difficult to guarantee accuracy for small voltage changes. Indeed, methods such as modal analysis have been demonstrated to work well for small changes.

Therefore, the usefulness of the method is quantified by its ability to detect large voltage changes. Large voltage change are defined as greater than 10%, or 0.1 p.u. as anything under

10% is within normal operation. The results presented will be screened to focus on the voltage changes of interest.

8.8 Detecting large voltage changes

For each seed node in a system, the tracing method will provide a range of solutions for different threshold values. Therefore, taking one seed node, there can be a number of possible ICI solutions. As each independent solution will have a voltage index assigned to it, there will be a number of indices for each seed node which can be used to assess the voltage stress of a certain solution. For each seed node, all possible island solutions can be presented using two plots, one showing the indices and one showing the maximum measured voltage changes at a bus as in Figure 8-12 and Figure 8-13.

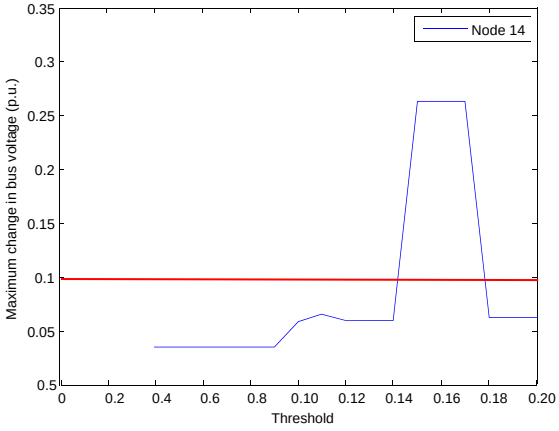

Figure 8-12 Max bus voltage change

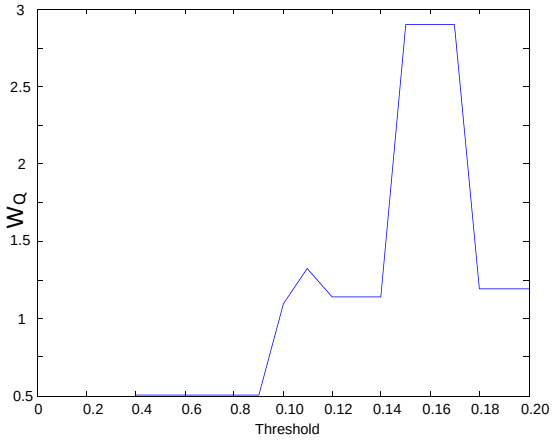

Figure 8-13 Voltage index

The threshold values from tracing are shown along the x-axis, which are the different ICI solutions from chapter 6, recall each threshold value does not provide a unique island. Figure 8-12 shows the maximum change in bus voltage for different threshold values. This is calculated from running a time domain simulation, measuring the change in bus voltages at the moment of splitting. (+/- 1 time step at 0.1s). This is in line with the time period before AVRs acts. The largest changes in voltage are then recorded. A red line indicates the 10% voltage change that is used for screening. For each seed node in the system, if an ICI solution exists, there will be a pair of figures like these. It is clear from this example that using screening, the peaks of Figure 8-12 can be identified from Figure 8-13.

8.8.1 Results for 39 bus system (TS-I)

The results from Figure 8-12 showed the voltage changes for a number of different ICI solutions for only one seed node.

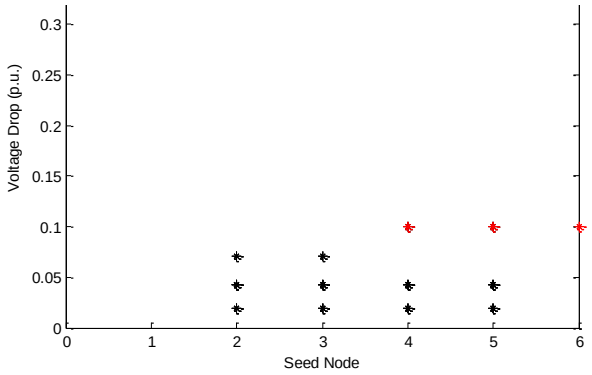

Figure 8-14 Voltage changes for different seed nodes

Figure 8-14 shows the same type of results for 5 seed nodes from the 39 bus system. Each point refers to a different ICI solution. i.e. for seed node 2, there are three ICI solutions and the corresponding voltage change from each island can be seen from the y-axis. Points shown in red are classed as large voltage changes. The voltage changes for all seed nodes are shown in Figure 8-15. The corresponding changes in reactive power are shown in Figure 8-16. In this figure, the voltage index assigned to each of the ICI solutions are shown, with the points marked in blue representing those with voltage changes larger than 10%. If a threshold value shown by the green line was used in this system, any voltage index under this would ensure an island with low voltage stress. However, defining such a threshold value would be extremely difficult as it is system specific and would need extensive analysis to determine. It could also be said that avoiding the largest voltage indices will ensure lower voltage stress.

It is clear from comparing Figure 8-15 and Figure 8-16 that the largest voltage indices do correspond to the largest voltage changes. However there is a single false positive point shown by the purple circle. This will be explained in section 8.9.

8.8.1 Results for 68 bus system (TS-I)

Applying the methodology to the 68 bus system the same relationship can be found. In general the large voltage indices, or changes in reactive power result in the largest voltage changes. It can be seen from Figure 8-17 that some islands would result in very large voltage changes, however these are also seen by the blue points from Figure 8-18. In this system, any voltage index over 2.0 would result in a large voltage change.

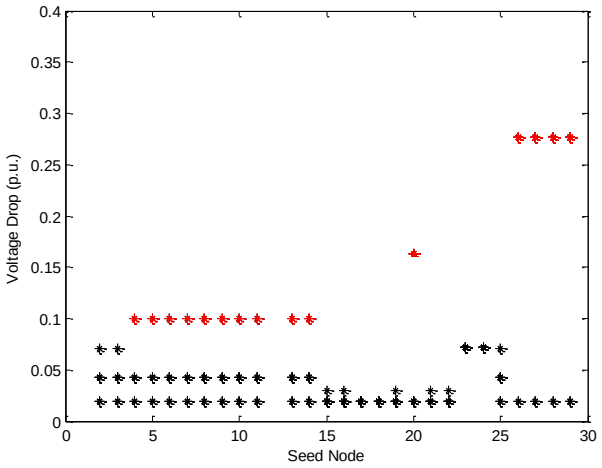

Figure 8-15 Voltage changes for 39 bus system

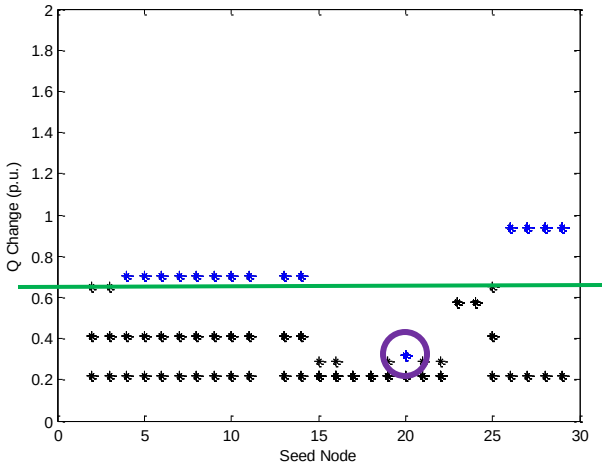

Figure 8-16 Corresponding Voltage indices for 39 bus system

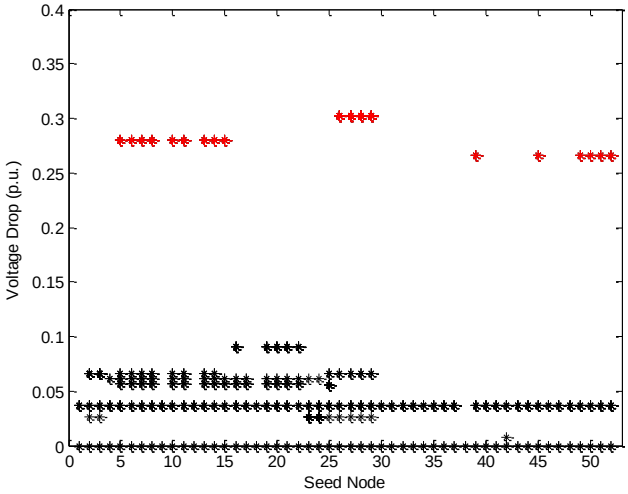

Figure 8-17 Voltage changes for 68 bus system

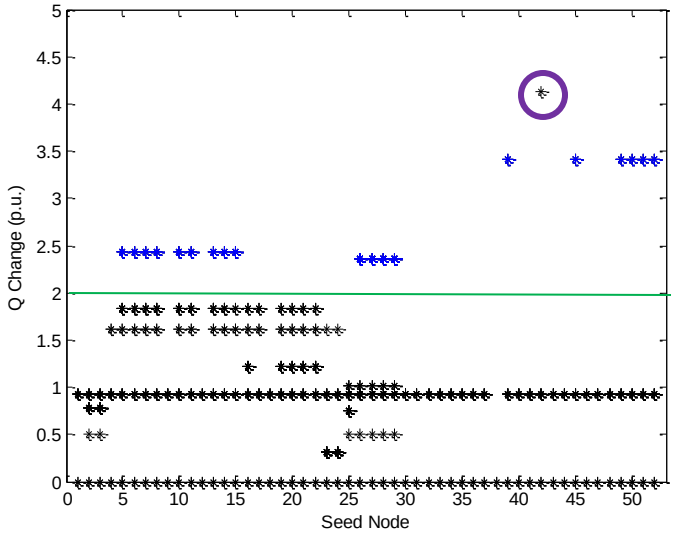

Figure 8-18 Corresponding Voltage indices for 68 bus system

It should be noted that the point shown in the purple circle in Figure 8-18 has a large voltage index but does not correspond to a large voltage change. These points are discussed in the next section.

Therefore, in general from these two systems, the large voltage changes are tightly linked to the changes in reactive power. It shows that this method could be used with ICI to penalize potential voltage stressed islands and hence ensure lower risk of voltage instability.

8.9 Handling False Positive and False Negative Values

In order for the method to be robust, it must be able to deal with false positives and false negatives. A false positive value is one which incorrectly predicts a large voltage change due to the large reactive power change. This is seen in Figure 8-18 indicated by the purple circle. It should be noted that false positives pose very little risk to the final solution. If a large reactive power change is predicted, this solution will be avoided in favour of a lower power change. Hence, it does not add any extra risk to the system. A false negative does however add risk to the system as in Figure 8-16 where a small voltage index fails to find the large voltage change of 0.16 p.u..

In this chapter, only the changes of reactive power are being considered while the final solution should minimise real and reactive power imbalance. Therefore looking at reactive power on its own does not provide the full picture for voltage. Indeed this is the cause behind both the false positive and negative values.

Consider the false positive value first in Figure 8-18. The detailed solution for this seed node is shown in Figure 8-19 but with real power imbalance also. All the posible solutions for this seed node are shown. It can be seen that the island corresponding to a threshold value greater than 1.8 p.u. has a high voltage index. However there is no large voltage change. This is due to the surplus of real power acting against the reactive power as described in section 8.2. This island has a high real power imbalance which in this case acts to support voltage. However it would also result in over frequency in this area. Due to the large real power imbalance, this would not be selected as the optimal island where an island with lower imbalance would be selected instead.

Indeed, the same effect leads to the false negative value from Figure 8-16 which is detailed in Figure 8-20. The island solutions corresponding to a tracing threshold value greater than 1.3 p.u. have a relatively low voltage index but a large voltage change. This is due to the very large real power change affecting the voltage as also described in section 8.2. As with the previous case, such islands would not be selected in the final optimization due to the large real power imbalance.

Therefore, when using voltage indices on their own, it is possible to obtain false positive and negative values. However, the voltage indices are created to account for voltage changes due to the reactive power. They do correctly identify voltage changes from reactive power. It is when the voltage changes are caused from changes in real power that false values emerge. However, the changes in real power will be minimised in a final solution thus minimising the chance of false values.

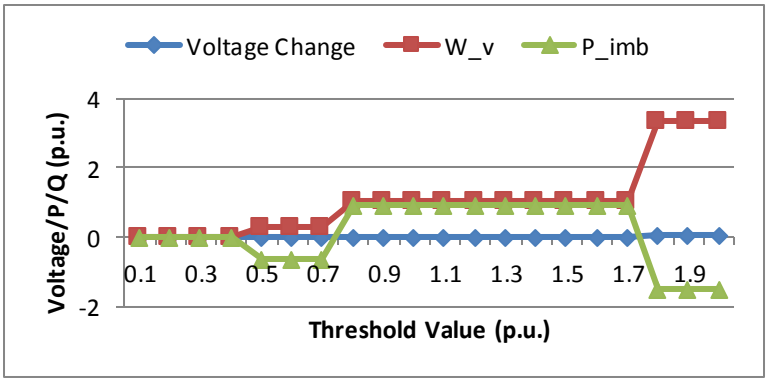

Figure 8-19 False Positive

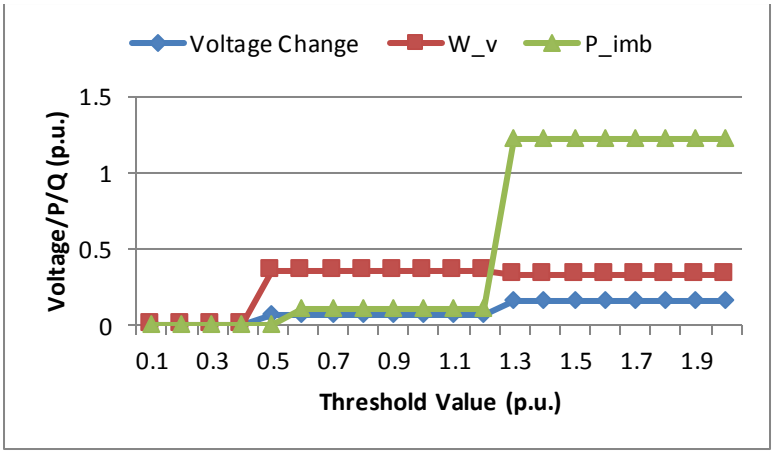

Figure 8-20 False Negative

8.10 Normalising the voltage index

When considering the voltage indices for the best solution, it is useful to normalise the values for a particular system. A high voltage index for the 39 bus system in Figure 8-16 is significantly different from that of the 68 bus system in Figure 8-18. By normalising the values, a large index for a particular system should be easily identifiable. In order to normalise the values, the maximum change in reactive power must first be established. Without prior knowledge of where this lies it is necessary to carry out a full island solution for all seed nodes. This can be done offline in order to characterise a large reactive power change. When all possible islands for a system are found, the voltage indices are normalised against the largest value observed here. This still does not provide any relative information on the size of the voltage changes. It only indicates that a certain solution has a large voltage index. This information by itself can be used to minimise the voltage stress by choosing the solution with the lowest voltage index. Larger indices have larger voltage changes as observed. However, if knowledge was known about what size voltage change could be expected from a particular voltage index, it would allow better operator decisions. For this step calibration is required.

8.10.1 Calibration

The focus of this method has been on quick assessment of the islands without having to rely on time domain simulations. It is possible to calibrate the results using time domain simulations if there is sufficient time available or if carried out offline. The developed method aims to minimise the effects on the reactive power and hence the related effects on voltage. However, without knowing the physical changes in voltage, the decision is based on minimising effects on reactive power only.

For calibration, time domain simulations are unavoidable. However, it is only the largest changes that are being looked at from the complete solution it means that a time domain simulation is not needed for every island solution. Also, as it is short term voltage changes that are of interest, a long time domain simulation is not necessary, in fact, there is only the need to calculate the change in voltage immediately after splitting so simulation periods of less than 0.1 seconds can be used. The basic principle is that the highest voltage index is selected for time domain valuation where this then allows the voltage index to be directly related to a physical change in voltage. It is useful to check at least two of the largest voltage indices to ensure that the decreasing voltage indices do correspond to decreasing voltage changes.

Using this method it would be possible to set the levels (green lines) from Figure 8-16 and Figure 8-18 to indicate what size voltage index would cause a large voltage change. This may be simplified with operator experience however if it is known how sensitive parts of a system are to changes in reactive power.

8.11 Summary

This chapter has developed a new methodology for finding the local imbalance of reactive power at each bus around a system. It was shown that in a dynamic simulation there is a dynamic change in reactive power loading corresponding to a voltage change. The method developed aims to approximate these dynamic changes in reactive power using static methods.

The method was developed using a series of power flows to find how the reactive power changes during the transition between the pre and post islanding states. It was shown that even though the relationship was non-linear, there was an evident relationship there for both positive and negative changes in power. These were first illustrated using simple examples on the 14 bus system.

The effects of real power on the voltage were then discussed where a change in voltage would be the result of both real and reactive power. However, as there is already a method for finding the real power imbalances with tracing, it is the effects of reactive power that were of interest. Voltage stress was then defined as a large transient change in voltage as a result of a reactive power imbalance. The algorithm was then described which created a voltage index which would be used to determine the best islands in terms of voltage stress.

The voltage index was then simplified further to consider only absolute changes in voltage and reactive power. It was shown that the effect of an overvoltage could be just as severe as an

undervoltage and therefore both should be considered dangerous. This method would therefore not bias towards under or over voltages. The concept was then validated using single line outages before moving onto multiple line outages with ICI. It was shown that the method worked well for identifying large voltage changes which was the objective. There was less accuracy for smaller voltage changes due to the non-linearity and also the fact that real power was not being considered. However, small voltage changes pose little risk to the system.

The issue of false positive and false negative values arose which could add extra risk to the system. However, it was shown that these arise when a large imbalance of real power affects the results, as was described in an earlier section. The results of the tracing will provide a set of islands for a particular seed node. The best solution from these must then be evaluated. Minimising the real power imbalance would be one of these objectives. These false readings could be easily eliminated by minimising the imbalance of real power which is also a requirement for frequency stability. Therefore a final solution for voltage would be based on minimal real and reactive power evaluation and this methodology allows visualisation of the reactive power effects of islanding on the system. When combined with the tracing solution it allows a complete picture of the real and reactive power situation in the system to allow a more informed decision to be made.

Finally, a section on the calibration is added which is a further step which can be carried out if time allows. This step allows the changes in reactive power to be tuned with offline simulations to the actual voltage changes to give a quantifiable measure of a large reactive power change, or voltage index.

It is aimed that minimising the stress on the system will minimise the chances of voltage collapse. It was found through testing that most of the collapses that resulted from ICI where due to significant voltage changes. However, as the method is fundamentally a static method, full dynamic assessment of all control aspects would not be considered. The focus is on speed and fast assessment. For the purposes of this methodology, an effective indicator into voltage stress has been developed, where the aim will be to minimise stress in the hope that further negative effects on voltage can be avoided.

9 The Recommended Solution

9.1 Introduction

A method to find island boundaries along with a methodology to assess voltage stress have been developed thus far. These methods must now be combined to create a feasible ICI solution. For any particular seed node, there can exist a range of ICI solutions from the tracing method depending on the threshold value. The aim is now to recommend or prioritise the islanding solutions. This chapter combines the work developed in previous chapters. Ideally, the best island would be one that considers all aspects of stability as described in chapter 4. However, it may not always be the case that the ICI solution is the best solution for all three. A visualisation tool is therefore introduced allowed an ICI solution to be considered with respect to the different forms of stability.

There have been a number of factors that have been created to assess the quality of an island. These include, voltage indices, total cut power, island imbalance and sick island size. Using this information, the islands for each seed node can be prioritised according to the indices. Due to the on-going development of a dynamic stability assessment tool, it is difficult to get an optimal solution for all stability. The factors that will affect the optimal solution are summarised in Figure 9-1 where all factors are essentially independent, making it a very difficult problem to find the best solution.

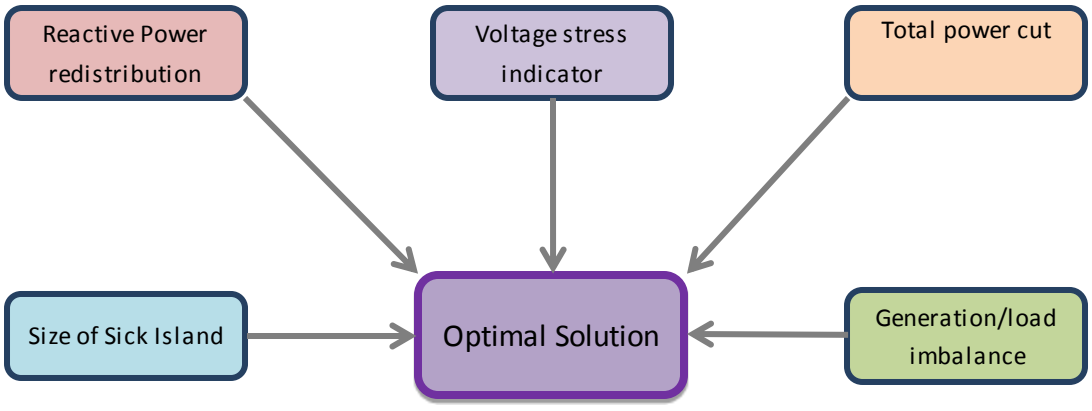

Figure 9-1 Optimal Islanding decision

9.2 Node Merging

The tracing method will only find weak connections between nodes and does not really consider topology. It cannot determine what it is cutting, or if certain nodes are weakly connected but still within a sick island. Such a case is shown in Figure 9-2 where an island is formed within the

sick island consisting of three nodes. This is correct under the criteria to minimise the sick area. However, it is clear from inspection that merging these two islands would have greater benefits to both islands. Forming small islands other than the sick island should be avoided, where a small island will be considered a single generator island.

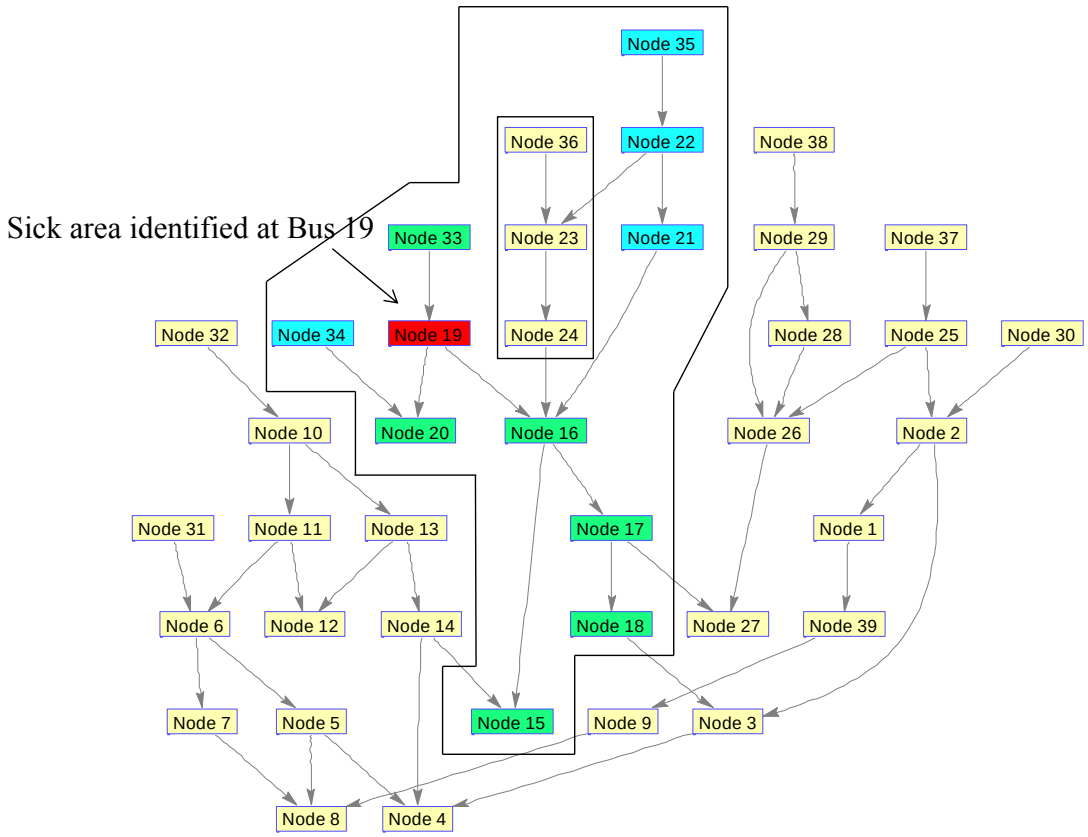

Figure 9-2 Tracing example on 39 bus system

The tracing has identified weak connections between the sick island and the island with node [23, 24 36] and does not consider the implications of cutting these connections. Therefore, there is additional complexity where all island solutions must be evaluated for single generator islands outside of the sick area. Due to the fact that all island solutions could possibly suffer from this problem, it is not beneficial to simply penalise these solutions as it will limit the number of solutions available. Visually, from Figure 9-2, there is an easy method to overcome the problem which is to leave the sick island, and the smaller 3 node island connected together. The small island on its own will be difficult to control and maintain. However when combined with the sick island, it has better chance of survival and can also be used to help the sick island to survive. While it does increase the number of customers at risk, it is deemed an acceptable risk as it benefits both islands. Therefore, there is an additional step to island formation which is node merging. This node merging step is performed after the power flow tracing solution to eliminate

these types of island. However it is not always possible to merge nodes as the following algorithm shows in Figure 9-3.

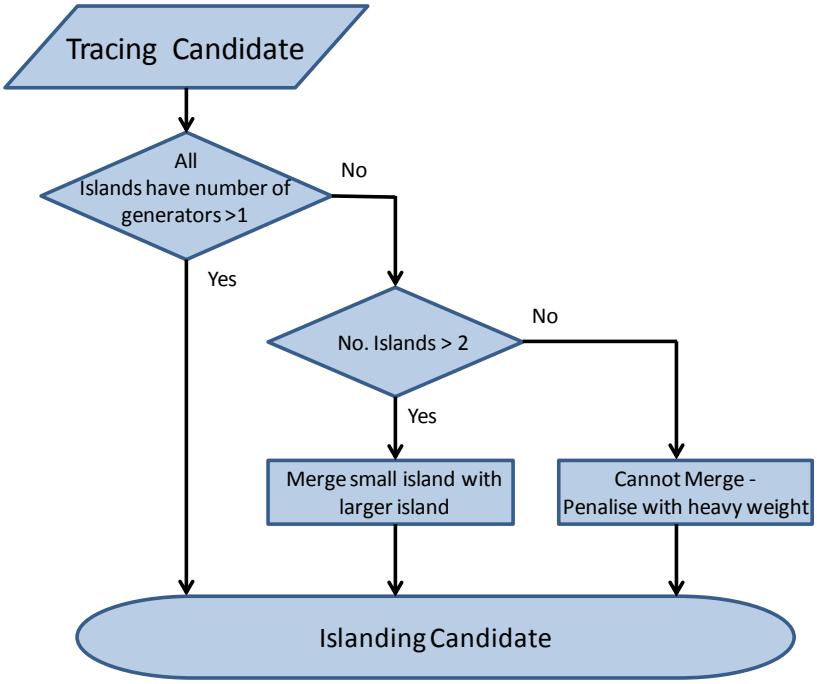

Figure 9-3 Merging Algorithm

The solution from tracing will provide a cutset of the weak connections between islands, however, it does not become an ICI candidate until it passes through this algorithm. There are three possible scenarios that need to be evaluated from the tracing solutions. If the tracing solution provides islands where the number of generators in each island is greater than 1, then that forms an acceptable ICI candidate and will move onto the next stage of evaluation. This can result in more than 2 islands in some cases. If a large healthy island is formed within a sick island, then it will be separated resulting in two healthy islands. If the tracing solution forms a sick island, a healthy island and another small island then further action is required. The best solution would be to merge the small island into either the sick or healthy island. The decision on which one would be based on minimal effects on power. This only applies when there are three islands or more formed. If only 2 islands are formed, one of which is small then this is a successful ICI solution provided the sick island is the smaller island. From this point on, it is taken that all islands have gone through this step of node merging.

9.3 Ideal Solution

The ideal ICI solution would be based on inputs from both the real power flow tracing and the voltage stress predictor to create the best possible island. The main objectives are as follows:

1. Minimise the power imbalance of the islands
2. Minimise the total power cut
3. Minimise voltage stress
4. Minimise the size of sick island

Minimising the power imbalance is important in order to reduce the impacts on post-split frequency and therefore load shedding, but also the post-split power redistribution and it will be quantified by

$$P_{imbalance} = \sum_{m=1}^{m} L_m \tag{10.1}$$

where L_m is the real power flowing in line m, and m is the number of lines in the ICI cutset. The total power cut is important for the consideration of transient stability as it reduces the shock to the generators when the lines are cut and it can be quantified by

$$P_{cut} = \sum_{m=1}^{m} |L_m| \tag{10.2}$$

By minimising the voltage stress, cutsets that could lead to large voltage changes are penalised. In a stressed system, large voltage changes could negatively affect voltage stability and further increase the stress on the islands leading to a collapse.

Minimising the island size will reduce the number of customers at risk and a simple limit can be added where islands over say 50% size of the whole system (or any other user-defined value) will be penalised. A size limit for the sick island is therefore added but it is not added as an index, but rather as a yes/no indicator of exceeding the size limit.

The influence of those different factors on the quality of an ICI solution will be quantified by using three different indices. The voltage index W_v is derived from the maximum nodal reactive power imbalance which is normalised to the largest observed change in reactive power, as discussed in the previous chapter and shown in equation 9.6. The power imbalance will have an effect on the frequency stability (and load shedding) and hence will be dealt with using a frequency index W_f, equation 9.5. The total power cut is related to rotor angle (transient) stability so a transient index is defined as W_t in equation 9.4. As the real power does not share the localised nature of reactive power, these two indices will be relative to the total power P^{total} in each island to better indicate the size of the disruption:

$$P_{sick}^{total} = \sum_{n=1}^{n} P_n^G \tag{10.3}$$

where $P_n{}^G$ is the power output of the n^{th} generator, n is the number of generators in the sick island. The transient and frequency indices are therefore defined as:

$$W_t = P_{cut}/P_{sick}^{total} \tag{10.4}$$

$$W_f = P_{imbalance}/P_{sick}^{total} \tag{10.5}$$

$$W_V = \max(\text{abs}(\Delta \boldsymbol{T}_q)) \tag{10.6}$$

9.4 Representing the solutions – Solution Space

The full solution for a system, or for a particular seed node can be represented in a multidimensional space. There are three indices, however, which represented on a 3-dimensional space while exceeding the size limit is shown using colour as the 4th dimension. In this case, solutions which exceed the size limit will be represented by a different colour allowing the solution to be shown on a three dimensional space. An example of the solution space is shown in Figure 9-4. There is one solution which exceeds the limit in this case and is shown using the red marker close to the origin. Ignore the blue markers at this point.

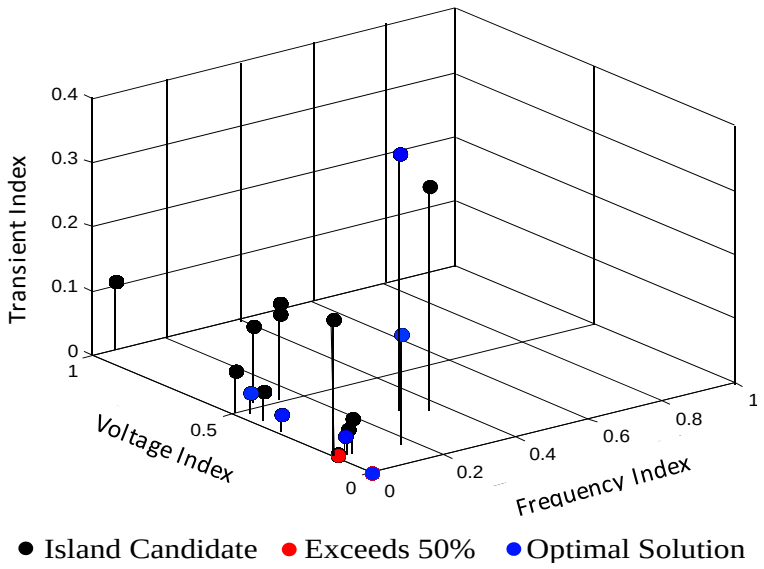

Figure 9-4 3D solution space for 39 bus system

Figure 9-4 corresponds to a solution set for the 68-node system. There are $(s \times t)$ solutions tested where s and t are the number of seed nodes and threshold values respectively, (68×20) in this example. Of these, there are only 19 unique islands shown by the black, blue and red

points. Each seed node and threshold value does not correspond to a unique solution as there may be one solution shared by a range of threshold values. Different seed nodes can also share the same solutions, e.g. two adjacent nodes. There will also be a number of infeasible islands where a solution is not possible. This was discussed in chapter 6.

Solutions near the origin have smaller indices and are hence better solutions. As you move away from the origin, the risk of instability increases, dependent on the axis. For example moving along the Voltage Index axis will increase risk of voltage instability while moving along the Transient Index axis will increase the risk of transient instability. Analysing spatial position of different ICI solutions allows one to take a choice favouring one criterion over another, depending on what is considered more important for a particular system. All points in this plot are possible candidates but the red points show island solutions that exceed the 50% limit, i.e. the sick island is large and will therefore put a large number of customers at risk.

Therefore, the indices can be used to recommend a certain solution, or to prioritise a certain form of stability. The best or optimal solution is not currently considered as it may not be the best for all indices. It is possible to use the solution space to find the recommended solution for a particular seed node, i.e. the solution with the lowest stability index which may of concern.

Table 9-1 shows how the indices would be used. A large index suggests the greatest risk corresponding to that index, i.e. a high value of W_f and a low value of remaining indices implies a greater risk of frequency instability. Therefore, the indices allow the operator to make an informed decision on which solution to choose. If the system is particularly prone to voltage collapse, then solutions with a greater risk of voltage instability must be avoided. By providing the operator with the indices, it is providing the necessary information to perform open-loop control actions on the system.

Table 9-1 Using Solution Indices

W_f	W_T	W_V	Greatest Risk
1	0	0	Frequency Instability
0	1	0	Rotor angle instability
0	0	1	Voltage instability

9.5 Solution Prioritised for voltage

A brief example will now be shown on how this tool is used. It will prioritise an ICI solution based on minimising the voltage index W_v. Obviously the best island should also consider both the W_f

and W_t in order to provide a truly optimal island but this simple example concentrates on the effects on voltage.

Minimising W_v in the solution space of Figure 9-4, the prioritised voltage solutions are shown in blue. Hence, from the 19 possible solutions, seven of these can be used to form islands for any seed node with minimal effects on voltage. Clearly, many seed nodes will share the same solution. In order to verify the optimal points correspond to minimal voltage changes, Figure 9-5 shows the voltage changes from the optimal solution for each seed node as calculated by time domain simulations. The maximum voltage change is just over 0.07 p.u., significantly less than the maximum of 0.25 p.u. that is possible without using this tool shown in Figure 8-17. This is a brief illustration for using the tool, further detail will be given in the next chapter.

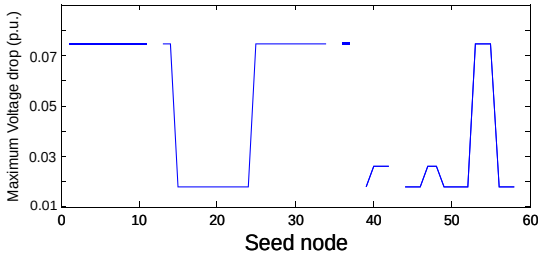

Figure 9-5 Maximum Voltage changes for optimal solution

9.6 Summary

This chapter combines the discussions and developments described in previous chapters. It aims to use all the developed methodologies to be used together to recommend and prioritise certain solutions. For each seed node, a single optimal island does not exist, as the best solution for one index may not be the best for other indices. This chapter has shown how the indices are developed and how they related to the various types of stability. For each of the three types of stability, an index is defined which will consider the stability as a value between 0 and 1. This normalisation allows the indices to be graphically shown on a 3D plot as a visualisation tool for stability.

Having the solutions shown on a solution space will still not provide the optimal results. It does however show where a solution lies in terms of a particular stability, or indeed all forms of stability. It is difficult to define a perfect optimal function as the three types of stability are not directly comparable. One may wish to prioritise voltage stability over frequency etc. There may

also be other issues such as requirement for a full dynamic stability assessment tool. Therefore, it can be used to visualise where an ICI solution lies in terms of stability, but can also be used to find the optimal solution for one type of stability. A simple example showed how it could be used to show how minimising voltage indices could result in minimal voltage changes and it was shown on the solution space. Further details and results will be shown and discussed in the next chapter.

10 Results

This chapter will discuss the results obtained for a number of test systems based on the developed methodology. It will show the use of the indices in deciding the best islands and also prioritising certain indices described in chapter 9 to form islands which create the least stress on voltage. The details on the test systems can be found in the Appendix 1.

The ICI methodology has been developed using a number of different building blocks throughout this these. The first stage is to apply a tracing algorithm to find the area of influence which uses information from the real power flows in the system. It is important to consider the impacts that forming an island will have on the system as islanding itself is a significant disturbance. Therefore, this chapter will show that the effect of the islanding action itself through the developed methodology can be minimised. The three main forms of stability, transient, frequency and voltage, are used to assess the quality of an island where three indices were created. These indices were defined as:

$$W_t = P_{cut}/P_{sick}^{total} \tag{10.1}$$

$$W_f = P_{imbalance}/P_{sick}^{total} \tag{10.2}$$

$$W_V = \max(\text{abs}(\Delta \boldsymbol{T}_q)) \tag{10.3}$$

Each islanding solution will have three indices normalised between 0 and 1 by which to evaluate the risk that such a solution would pose on a particular stability. I.e. if an island had a high voltage index W_v then there is a greater risk posed the voltage stability, or, using that solution will be a significant disturbance to the voltage conditions of the system.

The aim of this chapter is to show how these indices can be used to evaluate a particular islanding solution, show how to prioritise certain solutions but also evaluate the performance of the voltage indices that are a novel contribution of this thesis. There is less focus on the frequency and transient indices as these have been well documented in previous research found in chapter 3.

The results are split into two main sections, the first section will illustrate in detail how the voltage indices are used to select the solutions with minimal effects on reactive power. It serves to show that the developed methodology will correctly identify increased voltage instability risk using the voltage indices. This will be demonstrated using detailed time domain simulations of

particular seed nodes to illustrate the effects on voltage which islanding can have. It will prove that using the voltage index can minimise the risk of voltage collapse.

The second section is less detailed where it builds upon the proof developed in the first section. This section will instead show how prioritising the solutions for minimal changes in voltage can be used for the overall system. I.e. taking the solution with the lowest voltage index for each seed node and evaluated the results on a system wide basis. It will not look at each of the solutions individually for every seed now, but only select the recommended one. This section will also illustrate the importance of the other indices and the effects on voltage.

10.1 Simulation Tool

The software that was used for this thesis was the Power Systems Analysis Toolbox (PSAT) for Matlab which is an open source freeware toolbox created by Frederico Milano [138]. The advantage of using open source software is full access to the operations within the toolbox, for example the power flow Jacobians can be easily obtained. Also, it can be easily modified by the user to be tailored to the specific requirements. In this thesis, it was useful for the tracing in order to alter the power flow matrices to modify the systems for bus reordering, and also for islanding actions where systems could be split and studied individually. In most commercial software, access to the internal operations would be more difficult and hence, PSAT became an appropriate platform for the studies. PSAT also has a number of load models which can be used along with example system data and component data ideal for creating a variety of different test systems. In the dynamic simulations in the remainder of this chapter, ICI occurs at 0.1s unless stated otherwise, i.e. all line breakers for ICI will open at t=0.1s.

10.2 Detailed Index Studies

This section aims to show the detailed results from the derived methodology and to verify the performance of the voltage indices. The following tests will show how the indices will be used by considering a number of seed nodes and examining the solutions fully. The problem with using a tracing solution and indices based on real power only is that there is no knowledge gained about the voltage conditions. The results in this section will show how the voltage index provides this information and that it correctly identifies the level of risk of a voltage instability.

As the methodology is developed to create a disturbance dependent solution, there will be an island solution based on each node in the system. It would not be feasible to show all these results, therefore, selected nodes for each system will be shown.

Test Details
Two Test systems will be used, and 2 different seed nodes will be tested. All the possible islanding solutions for the selected seed nodes will be summarised in a table using the following key information: • Threshold Value • Island Size • Frequency index • Transient Index • Voltage Index • Within Size Limit This information will be used to evaluate each of the available islanding solutions for the selected Seed node. No disturbance is applied at the seed node, only the effects of the islanding action itself is being quantified. As the islanding action itself may cause instability, this will show that by minimising the indices, the risk that the islanding actions itself of causing collapse is also minimised.
Purpose
The purpose of this test is to show the relationship between the developed voltage index and voltage collapse. The 68 bus test system was originally designed to naturally oscillate, and therefore is very easy to drive into instability. As the method does not use corrective control, once the system starts to oscillate, there is no control to damp these out. It will be shown that the smaller voltage index will have the largest voltage stability margin, i.e. longest time before voltage collapse. This will verify the necessity of the voltage index for the later studies. It will verify if the voltage weight derived using static analyses holds for dynamic analysis.
Test
The test will be carried out using time domain simulations for the various islanding solutions. The voltages will be plotted from the time domain results and the results from a full time domain simulation will be evaluated against the voltage indices that were computed based on the purely static analyses.

10.2.1 Test 1: 68 Bus TS I, Frequency and Voltage Dependent loads

Seed node: Bus 5

From the tracing methodology, there are 5 different islanding solutions found for this seed node. These are shown as solutions 1-5 in Table 10-1 along with the corresponding threshold values. It can be seen that the sick island size decreases as the threshold increases. The size limit which is set at 50% is used to penalise the large islands. Island solutions 1 and 2 both exceed the size limit and are therefore ruled out. The stability indices are shown with the corresponding values for each of the different islanding solutions. For this test, the voltage indices are of interest and are hence shown in bold.

Table 10-1 Results for an island around Bus 5

Island Solution	1	2	3	4	5
Threshold (p.u.)	0.5-0.7	0.8	0.9	1.0	1.1-2.0
% sick (%)	79.4	51.5	32.4	25	17.64
W_f	-0.0038	0.016	0.014	0.08	-0.06
W_t	0.0062	0.028	0.12	0.0646	0.108
W_v	**0.006**	**0.05**	**0.1**	**0.12**	**0.41**
Within Size Limit	**no**	**no**	**yes**	**yes**	**yes**

The island solution should be selected from solutions 3-5 as they are within the size limits. These island solutions are shown in Figure 10-1 with the key shown at the bottom.

Investigating the voltage indices, it can be seen that solution 5 is the smallest island but has a much larger voltage index in comparison to the other solutions. Therefore, there is a higher risk of having a large voltage change with this solution which is verified from a time domain simulation in Figure 10-2. In fact, it is large enough to cause a voltage collapse in this island. Recall, there is no disturbance applied prior to islanding, so in case, it is the islanding action itself which causes the collapse. This is clearly a poor solution.

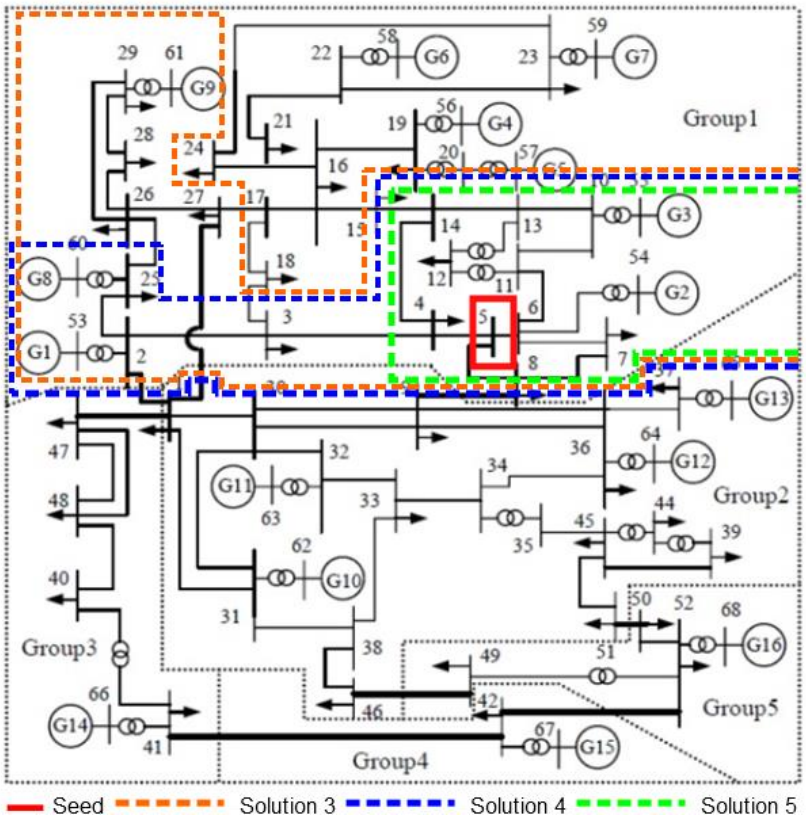

Figure 10-1 68 Bus System showing Solutions 3-5 for seed node 5

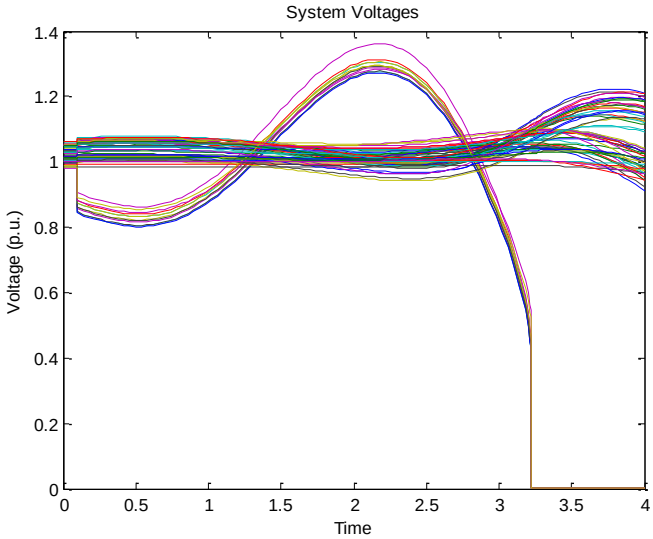

Figure 10-2 Bus Voltages from solution 5, showing early collapse with large voltage index, W_v = 0.41

This leaves two possible candidates for ICI which are solutions 3 and 4. Solution 3 has the lowest voltage index out of the two, and is therefore selected as the optimal solution. Solution 3 is also the solution with the lowest imbalance. To verify as the best solution, time domain simulation results for voltage are shown in Figure 10-4.

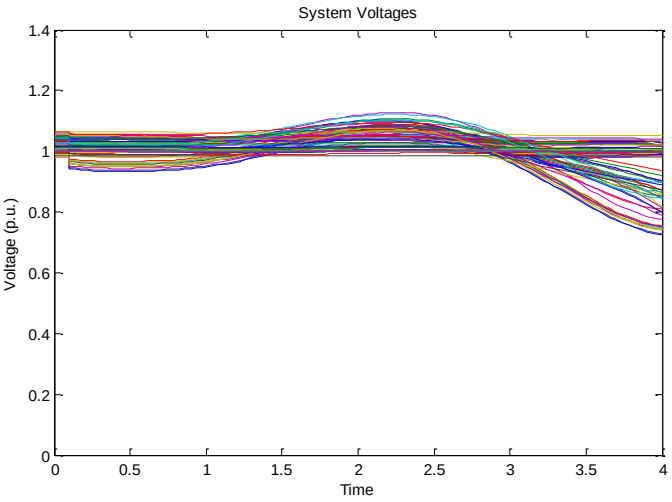

Figure 10-3 Bus Voltages for Solution 4, voltage weight W_v = 0.12, no voltage collapse

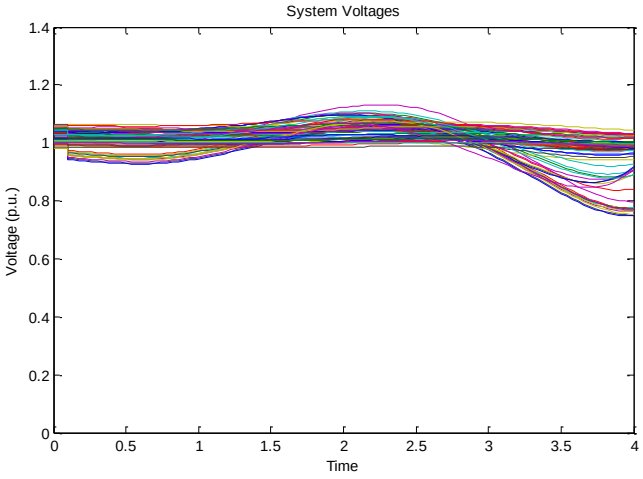

Figure 10-4 Bus Voltages for Solution 3, voltage weight W_v = 0.1, no voltage collapse

Both the bus voltages for solutions 3 and 4 are very similar, as seen by the very close voltage weights. While the bus voltages do oscillate and grow, this is due to the system being oscillatory. As this system can experience major voltage oscillations, a better measure of the stability margin would be the time before collapse. The times before collapse obtained from a time domain simulation are summarised in Table 10-2. It is clear from this table that a relationship exists between the time before collapse and the voltage index. It can be seen that there is a margin of about 2.3 seconds for solution 3 over the next most stable solution, and that the voltage index indicator correctly identified the largest index with the solution that collapses first, I.e. least stable.

Table 10-2 Summary of time to collapse

Island Solution	Time to collapse (s)
3	14
4	11.7
5	2.4

Conclusion of test

Therefore, this test verifies that the voltage indices do align quite well with the dynamic voltage tests seen from using time domain simulations. This test shows that there is a clear relationship between the derived voltage index and the voltage stability margin, therefore, it serves as a useful approximate for voltage stability which is much faster than running full time domain simulations.

10.2.2 68 bus system: TS II – Voltage dependent loads

Seed node: Bus 26

From the tracing methodology, there are 4 different islanding solutions found for this seed node. These are shown as solutions 1-4 in Table 10-3 along with the corresponding threshold values. It can be seen that the sick island size decreases as the threshold increases. The size limit which is set at 50% is used to penalise the large islands. Island solution 1 exceeds the size limit and is therefore ruled out. The stability indices are shown with the corresponding values for each of the different islanding solutions. For this test, the voltage indices are of interest and are hence shown in bold.

Table 10-3 Results for an island around Bus 26

Island Solution	**1**	**2**	**3**	**4**
Threshold (p.u.)	0.4-0.9	1	1.1-1.3	1.4-2.0
% sick (%)	52.95	14.7	10.3	7.35
W_f	0.0025	0.039	0.01	0.28
W_t	0.017	0.198	0.14	0.28
W_v	**0.05**	**0.0148**	**0.06**	**0.33**
Within Size Limit	**no**	**yes**	**yes**	**yes**

Solution 4 has a relatively large voltage index, and hence should be avoided due to risk of collapse which, when simulated can be verified as in Figure 10-5, It collapses very early. Solution 3 has a small voltage index and the smallest frequency index and it provides a sick island of about 10% which is ideal. According to these values, it has the lowest risk where its stability is verified from Figure 10-6.

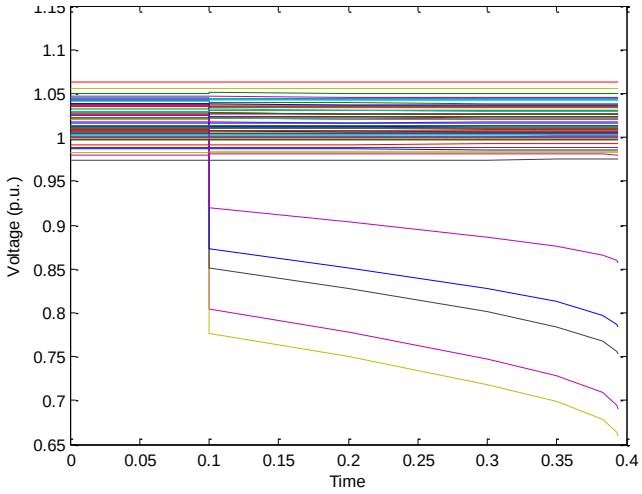

Figure 10-5 Bus Voltages for Solution 4, voltage weight W_v = 0.33, with voltage collapse

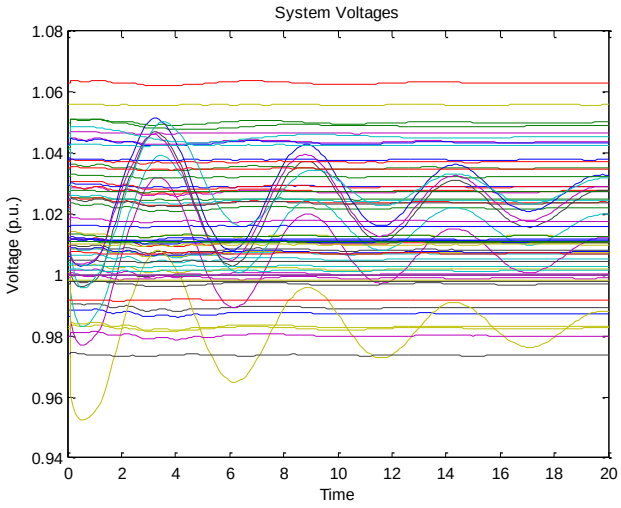

Figure 10-6 Bus Voltages for Solution 3, voltage weight W_v = 0.06, no voltage collapse

10.2.3 68 bus system: TS II – Voltage dependent loads

Seed Node: Bus 5

From the tracing methodology, there are 5 different islanding solutions found for this seed node. These are shown as solutions 1-4 in Table 10-4 along with the corresponding threshold values. There are four possible solutions where the size limit is not exceeded, which are all possible candidates.

Table 10-4 Results for an island around Bus 5

Island Solution	1	2	3	4	5
Threshold (p.u.)	0.4-0.9	1.0-1.1	1.2-1.4	1.5-1.7	1.8-2.0
% sick (%)	52.94	36.76	35.29	17.65	16.18
W_f	0.0025	0.0682	0.0849	0.02	0.24
W_t	0.0217	0.09	0.11	0.28	0.31
W_v	**0.05**	**0.153**	**0.196**	**0.35**	**0.196**
Within Size Limit	**no**	**yes**	**yes**	**yes**	**yes**

Solution 4 has a much higher voltage weight compared with those of solution 2, 3 and 5. It is therefore indicated that there is likely to be voltage problems from this solution. When the time domain simulation is carried out, it can be seen that there is a significant voltage drop which leads to a large swing before the collapse. It is seen to have a large voltage index when compared to the rest of the solutions which is reflected in the time domain simulation of the bus voltages shown in Figure 10-7. When compared with a solution with a lower voltage index such as solution 2, 3 or 4 a smaller effect on voltage is expected which is verified from the time domain simulations in Figure 10-8, Figure 10-9 and Figure 10-10 respectively.

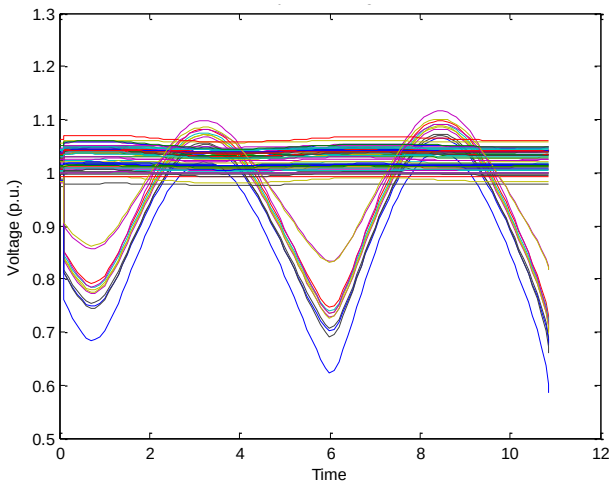

Figure 10-7 Bus Voltages for Solution 4, voltage weight W_v = 0.35, voltage collapse

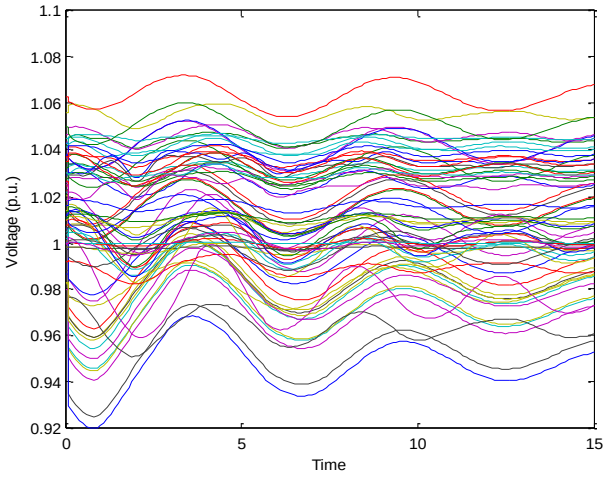

Figure 10-8 Bus Voltages for Solution 2, voltage weight W_v = 0.196, no voltage collapse

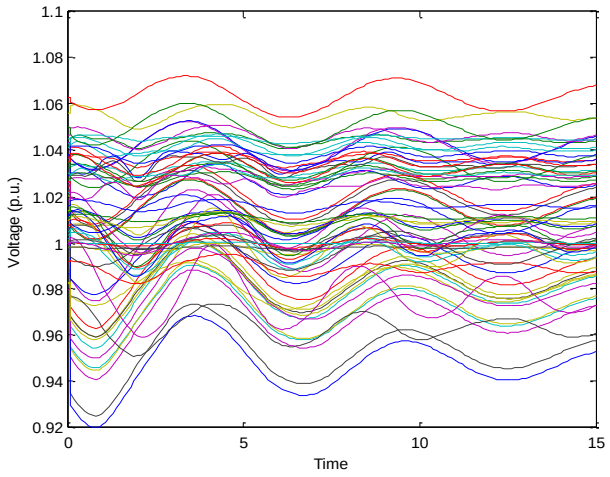

Figure 10-9 Bus Voltages for Solution 3, voltage weight W_V = 0.153, no voltage collapse

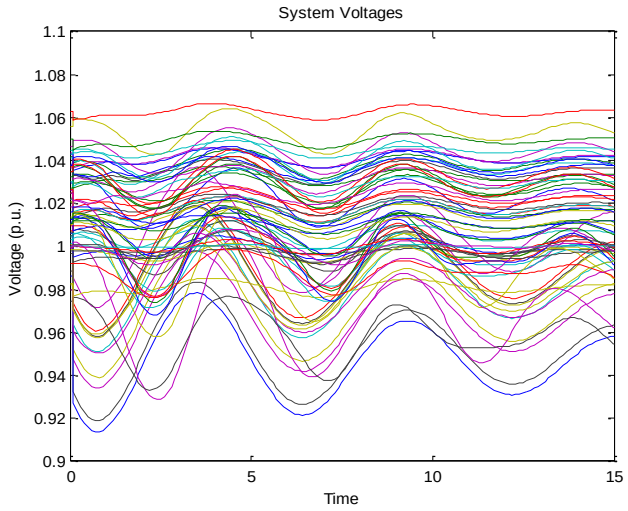

Figure 10-10 Bus Voltages for Solution 5, voltage weight W_v = 0.196, no voltage collapse

10.2.4 Conclusion to Detailed Tests

The voltage induces are effective in identifying voltage stability issues. For two different test systems, using 2 different seed nodes, it has been shown that the solutions with largest voltage indices have poor voltage conditions when the system is islanding. This shows that despite the voltage indices being developed using static means, they have strong correlations to the full dynamic models which are utilised in the time domain simulations. These detailed examples show that for each seed node, the best solution is the one which minimised the indices and was verified using the time domain simulations.

10.3 Prioritising Voltage Weight

The detailed studies for each solution of a seed node was evaluated in the previous section. This test will now focus on the complete system considering all seed nodes in a system. As there are a number of seed nodes, it is not possible to consider each of the possible island solutions for every seed node in the system, therefore, the system will be evaluated based on the solutions which are prioritised for voltage stability only. i.e. each seed node will have one solution based on the minimal voltage index.

This prioritised islands which are based on minimal voltage changes are described here. The maximum voltage changes from the prioritised solution will be used as a measure of the voltage stress as it has been shown in the previous section that larger voltage changes put added stress on the system which can lead to collapse.

Test Details
Five Test systems will be used, considering all seed nodes. How the solutions for each seed node fit in the larger context of a system is important to understand why there are limited solutions, but also the interaction between the different indices. For each test system, all the possible ICI solutions, i.e. each column of Table 10-1 for all seed nodes will be shown using the 3D solution space as it allows more solutions to be compared and prioritising certain solutions. The information which is shown on these solutions spaces are: • Frequency index • Voltage index • Transient index • Within Size limit All solutions are first shown, then the solutions which prioritise voltage are shown. This is carried out by selecting solutions which minimise the voltage indices for each seed node. The prioritised solutions are then shown according to the following key.

Colour	Key
	Non optimal points (i.e. not voltage prioritised)
	Solution which Exceeds size limit
	Prioritised solution
	Prioritised solutions which exceeds limit

All points on the graph are possible solutions where the optimal solutions are selected based on the chosen criteria, in this case minimal voltage index. There will be cases where the optimal island also exceeds the size limit due to the fact that there is no other solution available. The best island for a particular seed node will then be taken from these optimal islands. Recall that there is not an optimal solution for each seed node as many will share the same solutions. Also, there is not a new island for each threshold value. It can occur that one island may be feasible over the entire threshold value range if it is strongly connected. Therefore, there is often very few unique solutions, and normally, very few optimal solutions.

Purpose

The purpose of this test is to show how using the voltage indices only can be used to minimise the effects on voltage stability that would occur from reactive power. It will be shown that using just the voltage indices information, that an island can be created with minimal impact on the voltage. It will also show the interaction between the weights and voltage and how the real power affects can impact the voltage. Recall, the voltage index is designed to account for the reactive power behaviour, however the real power behaviour should not be neglected for voltage. The system wide results are focused on here rather than the single buses in the previous tests. Each seed node will have a prioritised solution where these tests will show the effects of these prioritised solutions. In some cases, the prioritised solutions so exceed the size limit, where these tests will illustrate why this happens. This section should provide an in-depth review of how the method works, cover any anomalies of the method and highlight any important factors which must be considered when using this method.

Test

The test will use the results obtained from the tracing and voltage indices and plot the results in 3D space. The prioritised solutions will be studied in more detail to verify the performance and will be evaluated using the results from time domain simulations. For each seed node, the maximum voltage drop is measured from a time domain simulation. In some cases, the more detailed time domain simulations are required. For the static quantities, the information will be shown for each seed node corresponding to the prioritised solution. Where further description is required to verify certain aspects, more detailed analysis of the interesting seed nodes will be done. In these tests – the 'optimal' results are those which minimise W_V

10.3.1 Test 1: 39 bus system TSI

Problem:

This test will show why there are limited unique solutions for a complete test system. For a 39 bus system with 39 possible seed nodes, there are usually very few unique recommended solutions which will be explained here.

Results

First, the full solution space, as described in chapter 9 is shown in Figure 10-11. Ignoring the colours, each point represents an ICI solution and shows how they relate to the indices and are shown for all seed nodes.

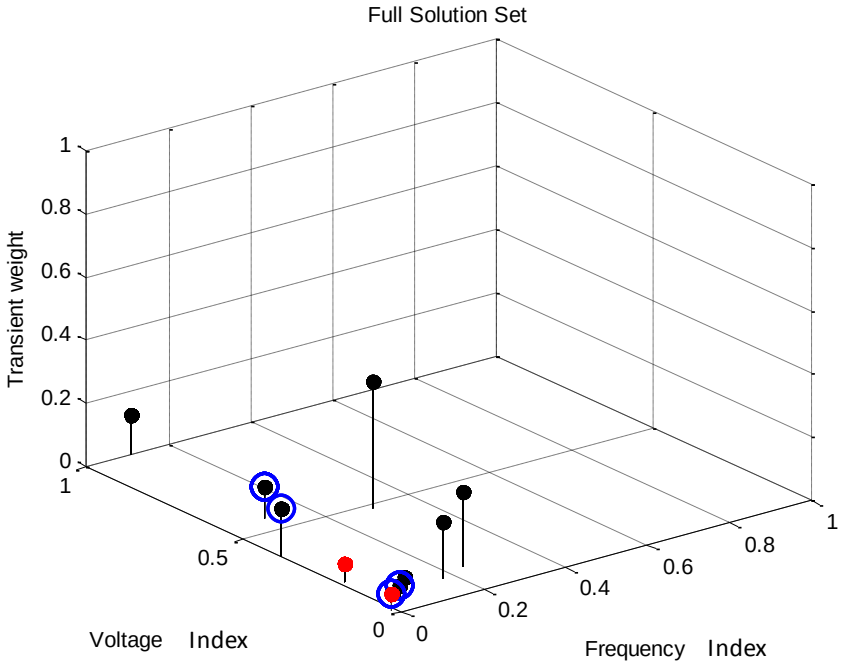

Figure 10-11 39 Bus System TS1 - full solution

From these solutions, the solutions with minimal voltage indices are selected and are shown using the blue rings. The size limit is also considered where a solution that does not exceed the size limit should be selected first. It can be seen that there are only four points on this plot which means there are only four unique solutions from all the possible seed nodes. To understand this, it is useful to look at the actual solutions for each individual seed node. The imbalance plot shown in Figure 10-12 can be used for this where it shows the imbalance for the optimal solutions for each seed node. Looking at the values of the imbalance, it can be seen that for a number of seed nodes, the optimal imbalance is the same, which indicates that the same ICI solution has been chosen for each of these seed nodes. I.e. seed nodes 5-10 will have the same solution. Generally this means that these nodes are quite close together and the area of

influence around these nodes is the same. Therefore, it can be seen that there are 4 different levels, or values of imbalance. Node 25 too shares the same solution as node 3. Therefore, the optimal solutions from Figure 10-11 is correctly identifying the four unique islands that have been found. Even though it is evaluated for 29 seed nodes, there are only four unique optimal solutions.

The maximum voltage changes for each of the optimal solutions are shown in Figure 10-13, however it can be seen that the nodes from 4-14 are on the limit of the 0.1 p.u. definition of a large voltage change. This can also be seen from Figure 10-11 where some of the optimal solutions are quite high along the voltage index axis. There are three solutions for seed node 5 which are summarised in Table 10-5. There is only one solution here which does not exceed the size limit, hence it is chosen first. It is solution with the minimal voltage indices that do not exceed the size limits that are being shown here.

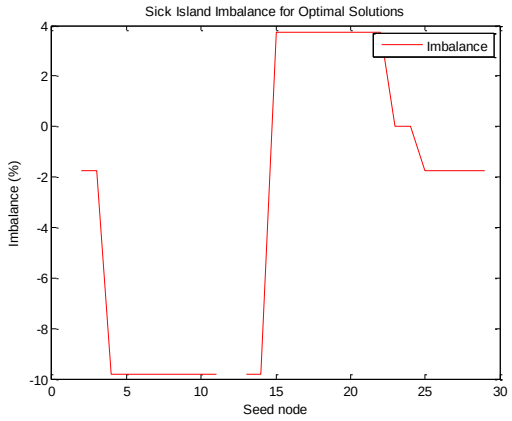

Figure 10-12 39 bus system TSI - Optimal Imbalance

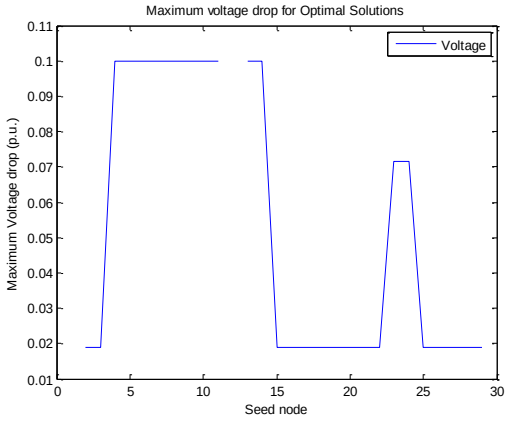

Figure 10-13 39 bus system TSI - Optimal Solutions - Maximum Voltage change

Table 10-5 Seed node 5 Indices

W_v	W_t	W_f	Within Size Limit	% Sick
0.0556	0.0214	0.0176	No	64.1026
0.1911	0.0579	0.008	No	51.2821
0.5644	0.1022	0.0984	Yes	35.8974

The higher voltage index is chosen as it is deemed a better solution overall. If the size limit was relaxed, a solution with a lower voltage index could be found. However, the sick island is then putting more customers at risk. With this solution, the voltage stress is higher, but for fewer customers.

10.3.2 Relaxing the size limit constraint

Problem

The previous example showed that a large voltage index may be recommended due to the size limit being a constraint. The effects of relaxing this constraint will be tested here to evaluate of better voltage conditions can be created.

Results

If the size limit was increased to 52%, then the second island solution in Table 10-5 would not exceed the limit and this would be the optimal voltage index. The resulting voltage changes are shown in Figure 10-14 where it can be seen to reduce the voltage changes from 0.1 p.u. to 0.045 p.u. for seed node 5. This is an example of using the visualisation tool and that a solution could be selected lower on the voltage index axis. The sizes of the optimal islands are shown in Figure 10-15.

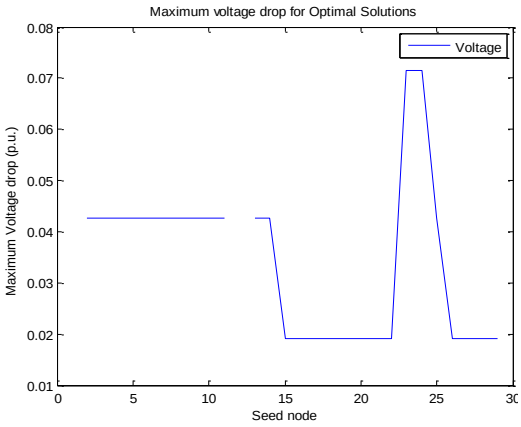

Figure 10-14 Increasing the size limit to 52%

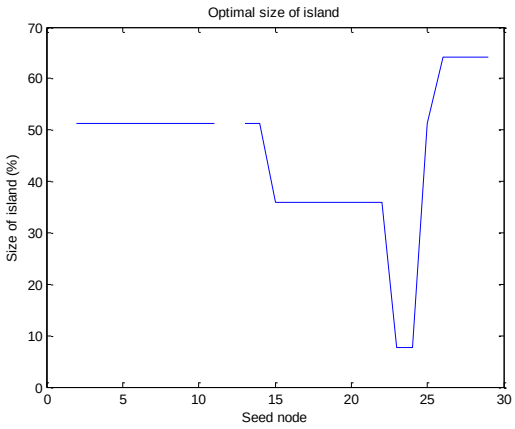

Figure 10-15 Corresponding island size

Table 10-6 Detailed results for seed node 26

W_v	W_t	W_f	Within limit	% Sick
0.0556	0.0214	0.0176	No	64.1026
1	0.1257	0.1082	yes	12.8205

10.3.3 Recommended solutions exceeding the size limit

Problem

In some cases the optimal solution will exceed the size limit. Even when the size limit was increased in the previous example, the seed nodes around 26 exceeded this value, yet they were the recommended solutions. This test will show why a larger island is sometimes recommended when minimising voltage indices.

Results

For seed node 26 from Table 10-6, it can be seen that the smaller island has a voltage index W_v at a maximum value of 1. This is predicting a very severe voltage change. Such a high voltage index should be avoided and therefore it would be more acceptable to increase the island size rather than risk such a large voltage change. This is the way the method is currently designed where a maximum value of an index is always rejected. Running a time domain simulation to verify this, the large voltage change can be seen in Figure 10-17 where the voltage change in the sick island is almost 0.33 p.u. This solution should almost certainly be avoided in favour of the significantly smaller indexed larger island. Plotting the voltages for the larger optimal island in Figure 10-16, it can be seen that there is no significant voltage changes and hence very little added stress to the system.

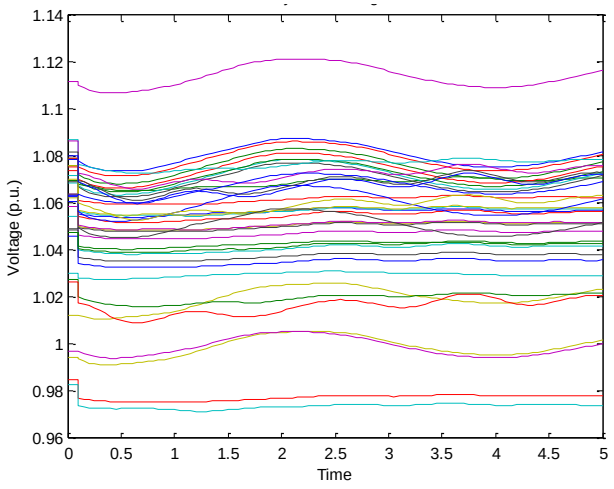

Figure 10-16 Voltage changes for larger island

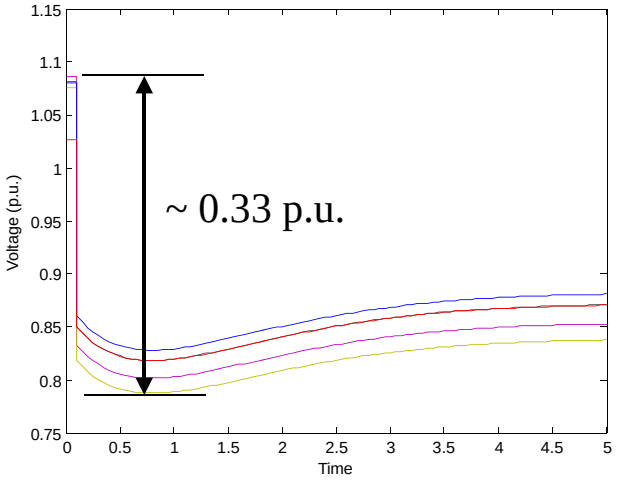

Figure 10-17 Sick Island voltage changes

Even with the increased size limit of 52%, optimal islands for seed nodes around 26 exceed this value.

10.3.4 Infeasible results

Problem

In some cases, there are no islanding solutions available. This can be due to no power flow solution being available, or due to no solution possible from the tracing. The following test shows how infeasible results can be formed. It was stated in previous chapters that it is not always possible to find an ICI solution for a particular seed node. This is indeed confirmed by the gaps in the data for sick nodes 12 and 13 in Figure 10-12 for example.

Results

In a network, it is possible for the situation to arise where a bus has little or no load, and also has very little throughput, which is what is occurring at these buses. Consider Figure 10-18 where a threshold value of 0.1 p.u. in the tracing algorithm will identify the full system as connected to the seed node 12. This means that the contribution between node 12 and all other buses exceeds 0.1 p.u.. This is not a feasible ICI solution as it would be the original network, no ICI actions.

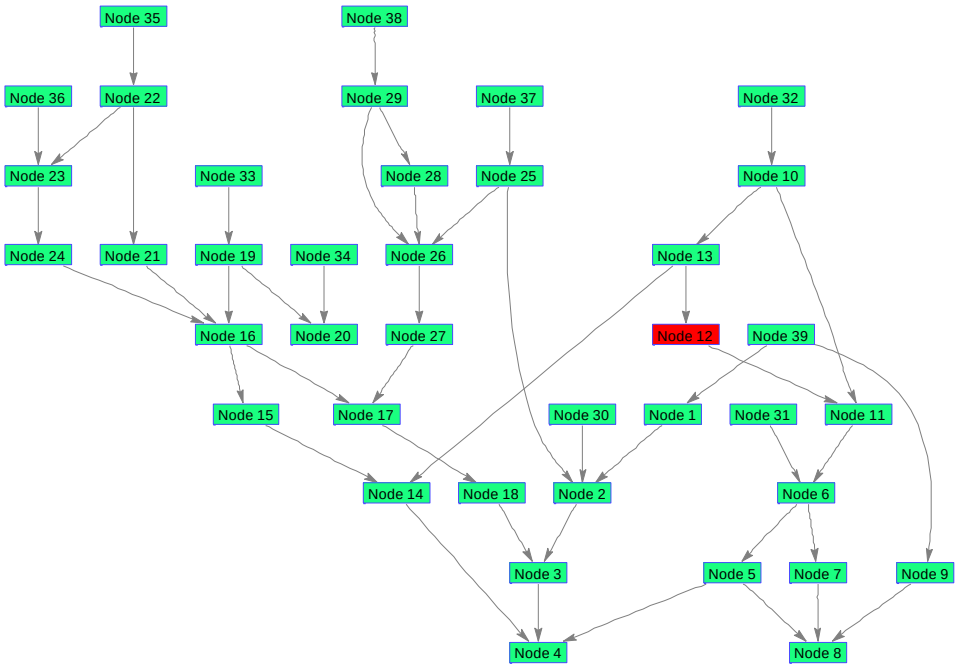

Figure 10-18 Seed node 12 with threshold value of 0.1 p.u.

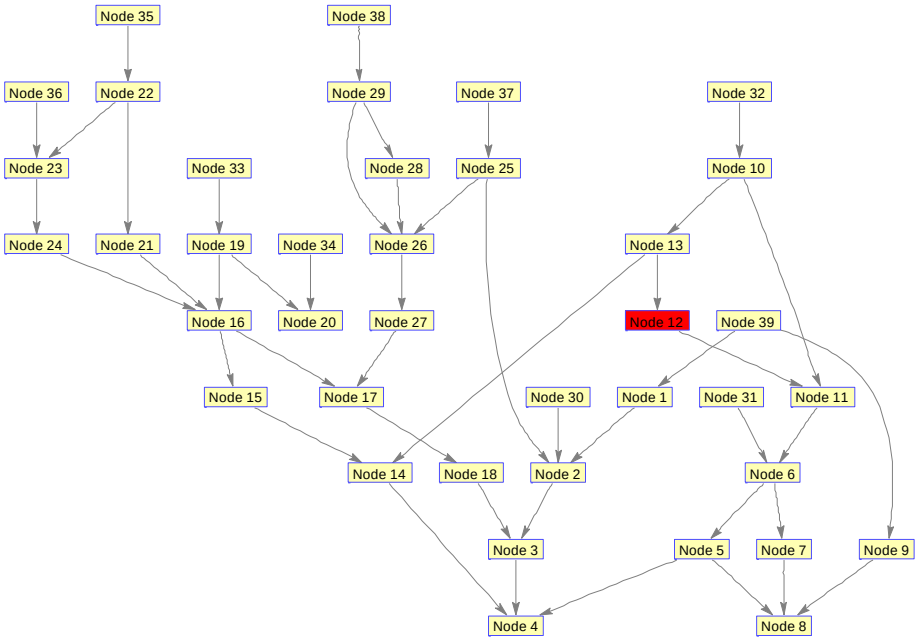

Figure 10-19 Seed node 12 with threshold value of 0.2 p.u.

By increasing the threshold value, the island size should decrease, however, using a threshold value of 0.2 p.u., the result shown in Figure 10-19 is achieved, where now node 12 is islanded on its own and will collapse as there is no generation. Therefore, this is deemed an unsatisfactory result as it means that an island is created with one load and no generators and cannot survive, and it is also disconnecting a path for power to flow which can reduce the system security. The load at node 12 is 0.085 p.u., hence there is a small amount of power flowing through this bus, less than 0.2 p.u. that provides these results. As there are only two possible islands, the full network, and the seed node alone, both are deemed unsatisfactory as they do not meet the required criteria for ICI conditions and hence no solution is available for this seed node.

In these instances the node should be merged to the nearest node with a satisfactory ICI solution. In this way it will be included in another island and hence can be disconnected from the healthy network still. In this example it would be merged with bus 13 or bus 11. Therefore if there is a fault at bus 12, the optimal solution from either 11 or 13 is selected.

This highlights that there are areas where the methodology does not perform as desired and could benefit from additional work.

10.3.5 Test 2: 39 bus system – TS- II – New Operating Points

Problem

This test will show the effects of a changing operating point and how using situational awareness can provide better solutions that using pre-planned approaches. The only different between this test case and the previous case is that one line is removed. However, it has a different operating point and a new solution set of islands are formed.

Results

Line 3-4 is carrying approx. 1.8 p.u. of real power through it and the outage of this line changes the power flows enough to provide a different set of ICI solutions. This is useful to show the advantage of having a disturbance dependent methodology for ICI. Where previous methods such as slow coherency are not disturbance dependent, this example shows that the same system with only one line out can result in different ICI solutions.

The full solution set is shown in Figure 10-20 where it can be seen that there are some solutions that have very high indices. But the optimal solutions are shown in blue. It can be seen that the optimal solutions from this test system are different to those in Figure 10-11, therefore verifying that even after a line outage, a new set of solutions should be found specific for that operating point.

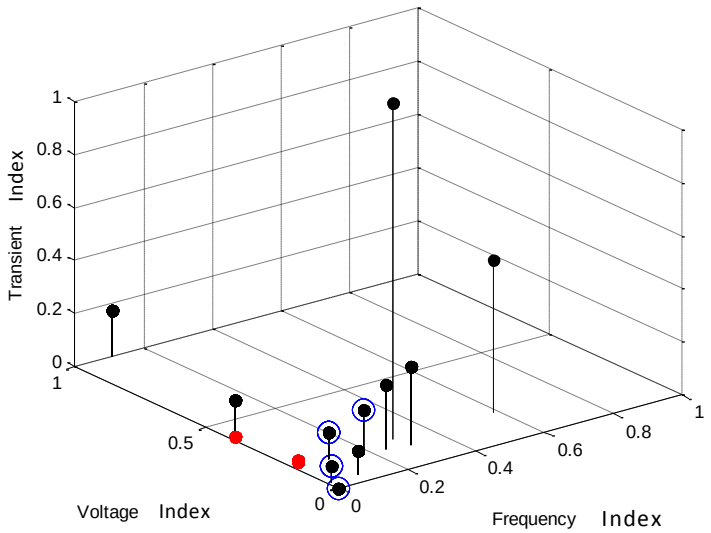

Figure 10-20 39 bus system TSII - full solution set

10.3.6 Test 3: 39 bus system – TS- II –Effects of real Power

Problem

The details for each seed node for the optimal solutions are shown in Figure 10-21, Figure 10-22 and Figure 10-23. Again, it can be seen that there is no solution around nodes 12 for the same reasons as previously described. From Figure 10-22 it can be seen that there is a relatively large voltage change for the solution at node 20. However, this was identified as the optimal solution from the data for seed node 20 in Table 10-7. The voltage index does appear to be relatively low therefore, there must be another cause for the large voltage drop seen in this example.

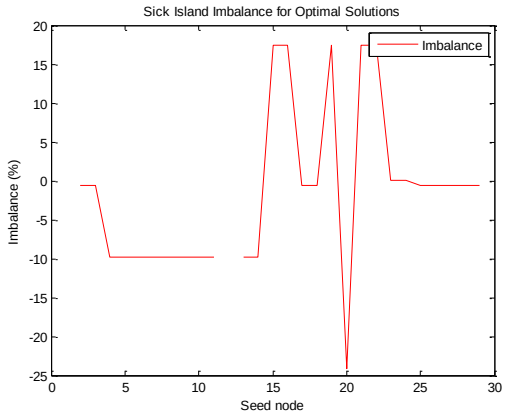

Figure 10-21 39 bus system TSII - Optimal Imbalance

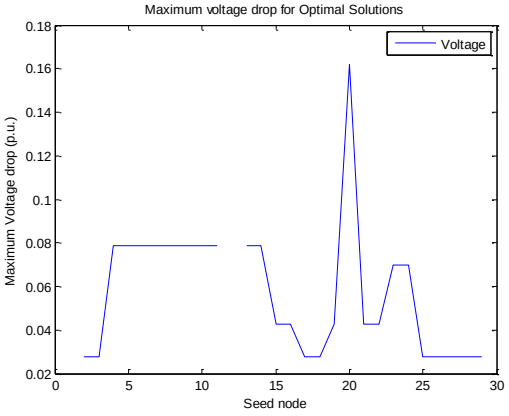

Figure 10-22 39 bus system TSII - Optimal Solutions maximum voltage change

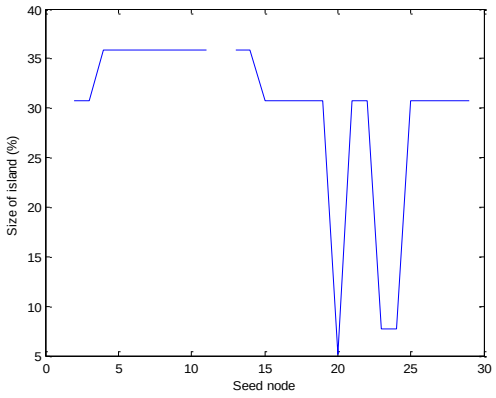

Figure 10-23 39 bus system TSII - Optimal Size

Table 10-7 Detailed results for seed node 20

W_v	W_t	W_f	Within limit	% Sick
0.3903	0.0151	0	No	92.3077
0.1585	0.0262	0.0028	No	66.6667
0.1337	0.2416	0.2414	yes	5.1282

Result

It can be seen that the prioritised solution in Table 10-7 does not have a very high W_v, yet there is a larger value of W_t and W_f, where almost 25% of the power in the sick island is being disturbed. This was also described in chapter 8 as being the cause for the large voltage change. Therefore, the voltage change here is not due to the changes in reactive power, but due to the larger values of W_f, which can affect voltage as previously described. It is the recommended solution due to the minimal W_V. Creating an island which contains a disturbance to within a 5% region is preferable to having a 67% region to contain the disturbance. In fact, looking at a graph of the optimal solution, Figure 10-24 , it can be seen that there are only 2 nodes in the island, with the corresponding voltage changes shown in Figure 10-25. Despite the large change in voltage, having a large voltage change in 2 buses may be more beneficial than exposing a significantly larger area to the disturbance.

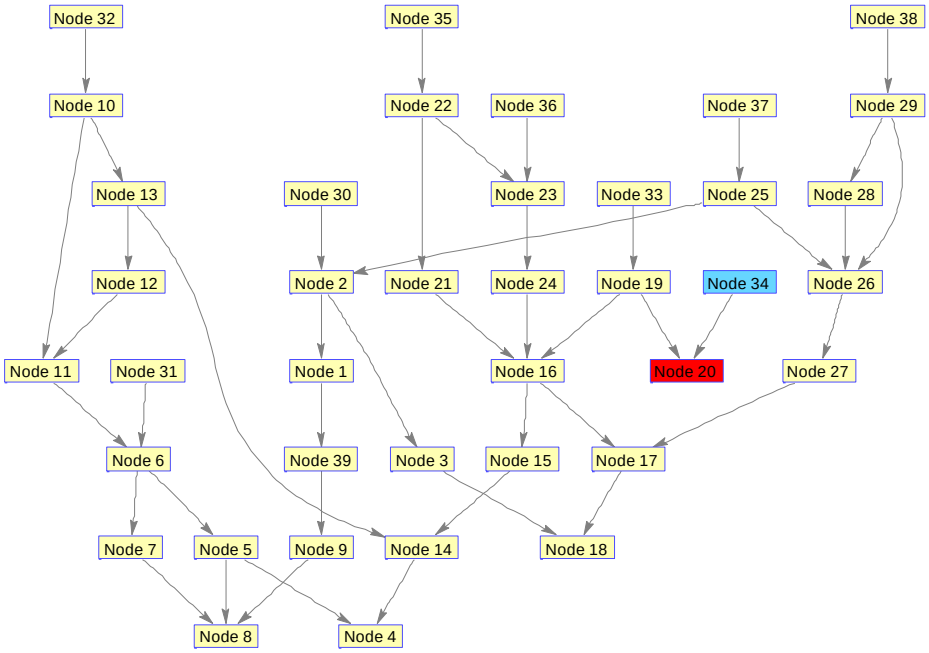

Figure 10-24 Optimal solution - seed node 20

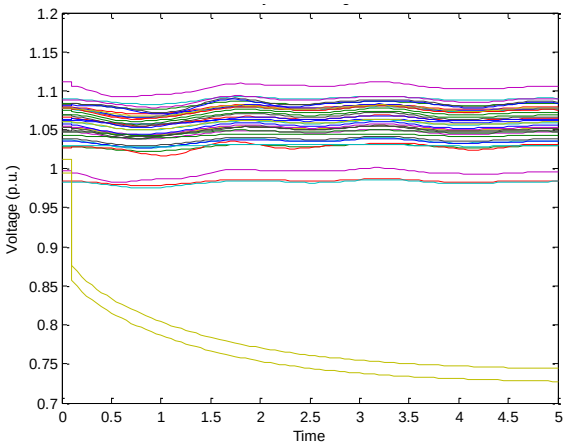

Figure 10-25 Bus voltages for optimal solution for seed node 20

In order to prove that this is the best island, despite the voltage change, it is useful to compare it to another available solution, solution 2, for seed node 20 from Table 10-7. This solution was originally penalised due to it exceeding the 50% sick island design criteria. Having a sick island of 67% puts a greater area at risk but it has much lower values of W_f and therefore the impact on voltage from the real power will be minimised. This island solution is shown in Figure 10-27 where it can be seen that the sick island does cover a very large area, however, as a result, the impact on the voltages is significantly reduced, as seen in Figure 10-26

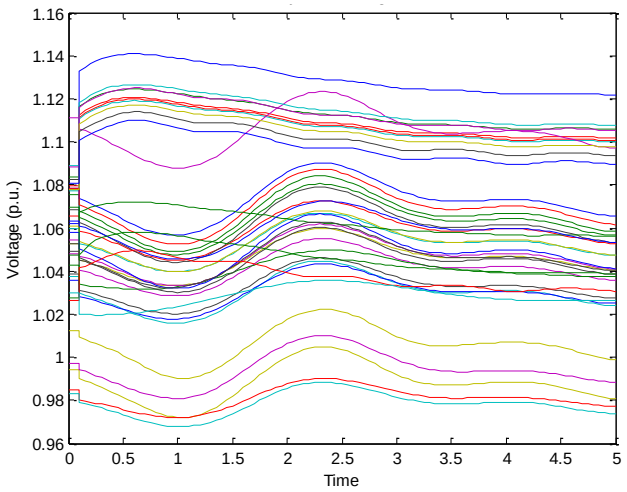

Figure 10-26 39 Bus system voltages for non-optimal solution

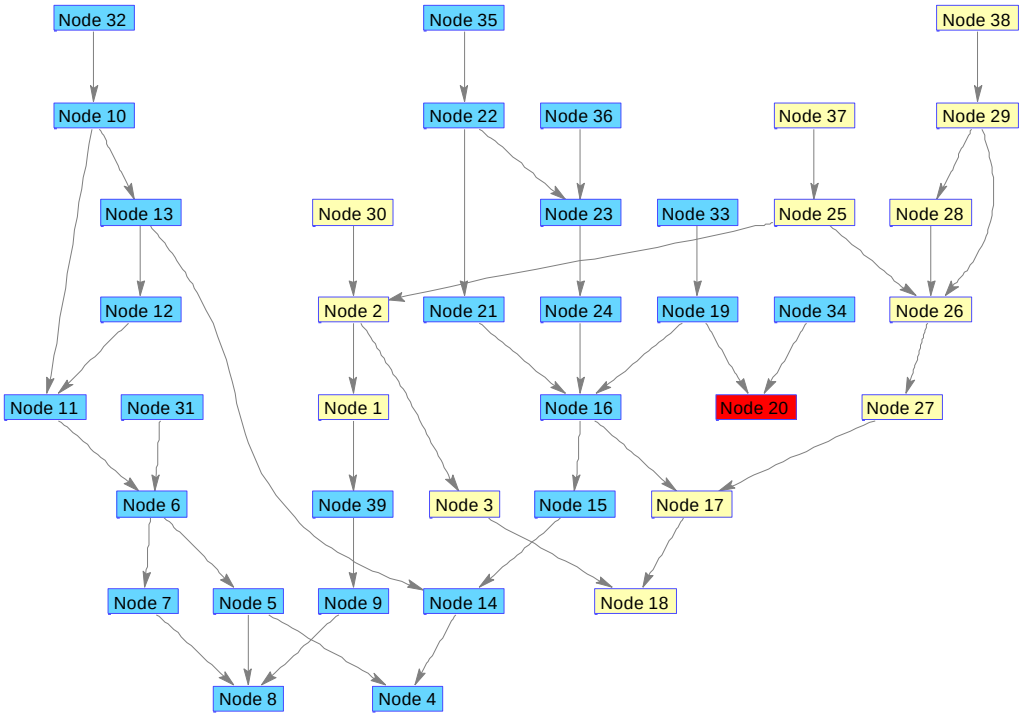

Figure 10-27 Non-optimal solution for seed node 20

While based on the voltage stability it would appear a better split, it is useful to consider the purpose of the ICI. The main purpose is to contain a disturbance to a region which has the risk of cascading across a network causing a blackout. It is also about minimising the number of affected customers. Based on this, having a sick island of 67% to contain a disturbance would mean there is a large area for a disturbance to propagate within, and hence puts many more customers at risk. Should this island blackout, it is a significant loss. However, if the smaller island of 5% was to collapse, there is a smaller area for which a disturbance can propagate, and the number of customers that would be affected is significantly reduced. While the purpose of the ICI is not to sacrifice an island intentionally, it should always try to first find islands which can survive on their own, if no such island exists, or meets the criteria, then a small island which may be sacrificed would be the favourable option. It is for these reasons that the 5% size island is the optimal solution from this test case.

10.3.7 Test 4: 68 bus TS II

Three test systems based on the 68 bus system were created using a number of different load models and loading levels. However, only one of these test systems is detailed here..

Problem

When using larger system, it is expected that the number of unique islands will increase significantly hence making the decision on which solution to use more difficult. However, despite the larger system there are still very few unique solutions and this test will prove that for a new test system that the static voltage indices are still useful indicators for minimising the dynamic impacts on voltage which splitting has. This test system has also added in voltage dependent models which would be expected to increase the complexity. Therefore, the ability of the static indices to perform properly with the presence of dynamic load models must be verified.

Results

The following system was tested for all seed nodes and the full solution space is shown in Figure 10-28. It is interesting to note that despite the solution being disturbance dependent, for the many seed nodes tested, there are only five unique optimal ICI solutions. The detailed optimal results are shown in Figure 10-29, Figure 10-30 and Figure 10-31, where it can be seen the optimal solutions have very small voltage changes. For the majority of cases the sick island size is less than 50% and therefore would be seen as ideal results. The islands which exceed the 50% limits have already been covered in section 10.3.3.

The results prove that wit the inclusion of dynamic load models, the static index is able to minimise the dynamic voltage changes and for larger systems the index works well as an approximation tool to recommend an islanding solution which will minimise the voltage shock to the system.

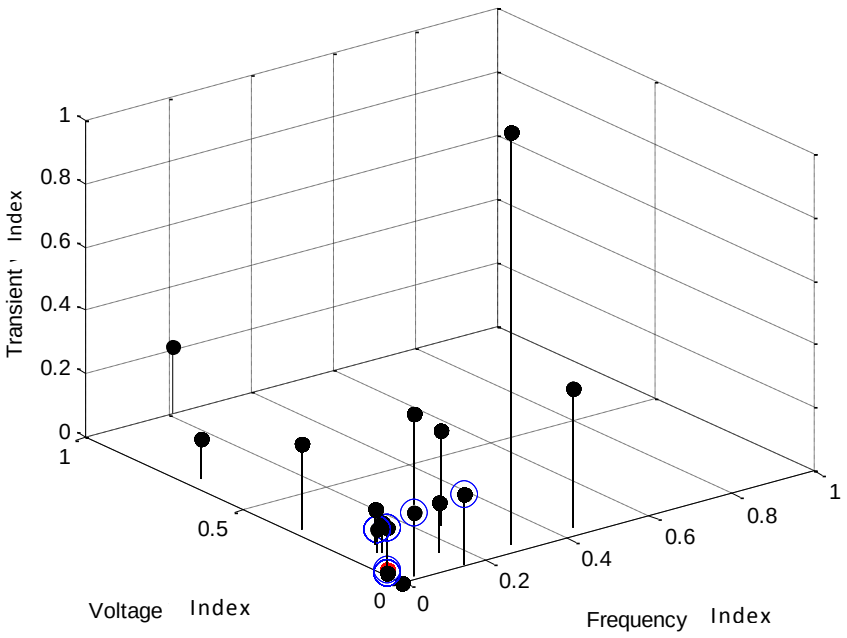

Figure 10-28 68 bus Voltage dependent load - full solution

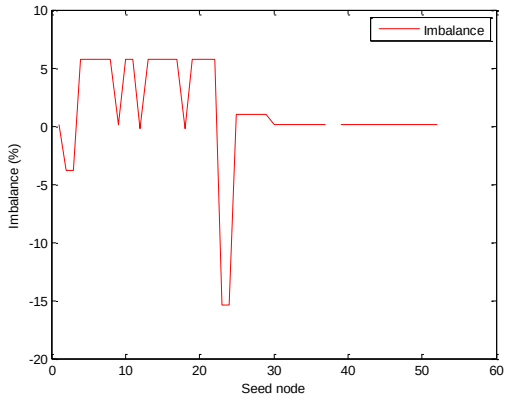

Figure 10-29 68 Bus system - TSI - Optimal imbalance

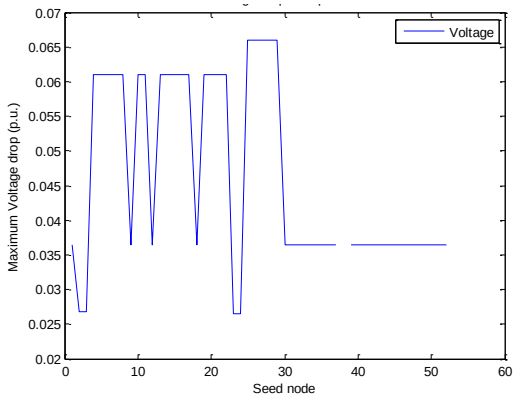

Figure 10-30 68 bus System - Maximum voltage changes

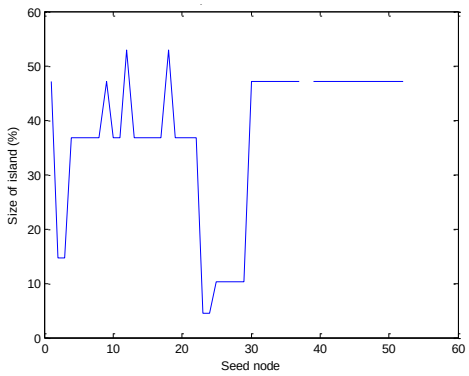

Figure 10-31 68 Bus system TSI - Optimal Island size

10.3.8 Test 5: 68 Bus TS I

Problem

This test is similar to the previous test however is applied using different load models. It is necessary to test the methodology for a variety of different test systems with different conditions to truly evaluate the performance. This test system adds another dynamic component using frequency and voltage dependent loads which the static voltage indices must be evaluated for.

Results

The full solutions for this system are shown in Figure 10-32 while the optimal results shown in blue. Here there are 5 unique optimal solutions. It can be seen that some of the optimal solutions are red and have exceeded the maximum limit and have been penalised for this. This is verified by the result in Figure 10-35 where some optimal islands have been found to be almost 80%.

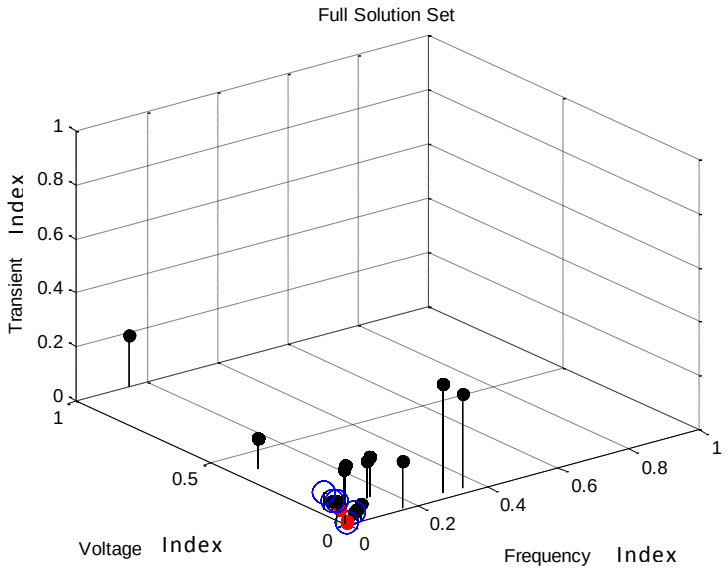

Figure 10-32 68 bus TSII full solution

Figure 10-33 Figure 10-34 and Figure 10-35 show the detailed results where it can be seen that there is a solution for the majority of the islands, but also, a number of nodes for which no solution can be found. Looking at Figure 10-34, it can be seen that the maximum voltage changes are minimised, all well below a 0.1 p.u. voltage change, however, from Figure 10-35, it can be seen that there are a number of solutions that have sick islands in excess of 80%.

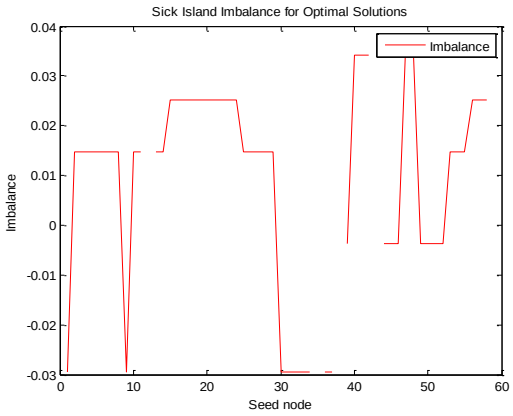

Figure 10-33 68 Bus system TSII - optimal imbalance

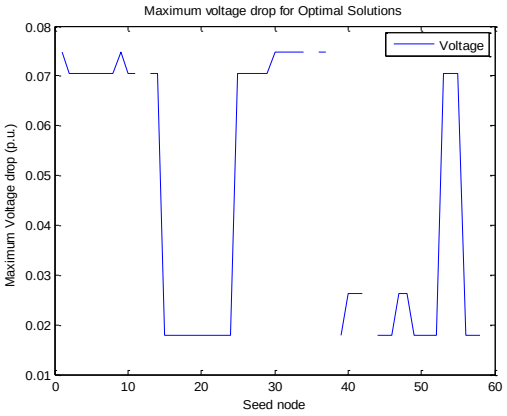

Figure 10-34 68 Bus system TSII - Maximum voltage changes

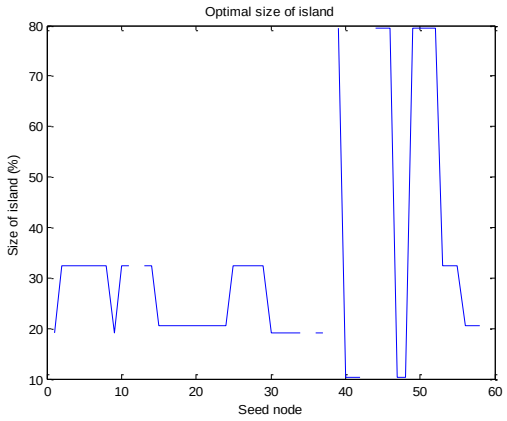

Figure 10-35 68 Bus system TSII - optimal sick island size

Table 10-8 Details for node 52 - 80% sick

W_v	W_t	W_f	Within Limit	% Sick
NaN	NaN	NaN	No	1.4706
0.0067	0.0046	0.0038	No	79.4118
NaN	NaN	NaN	No	1.4706

The reason for the large islands can be seen in Table 10-8. Looking at the indices, there is only one real value representing only one feasible solution for this seed node. All other solutions have been found to be infeasible. Typically the reason for not finding a solution for a particular island stems from the reliance of the method on power flows. One of the requirements inherent in the solutions is that a power flow solution must be solved for an island solution to be considered a candidate. Should a power flow fail to converge, it suggests that there will be problems with that islands operation but would require deeper simulation analysis. In this case it was found to be congestion in part of the sick island but it can be a number of reasons such as insufficient resources. It has been found that where a power flow fails to converge, it typically results in a time domain simulation to also fail, and therefore such solutions are avoided.

10.3.9 Test 6: 68 Bus TS III

Problem

This test will evaluate the performance of the methodology to find solutions when a system is stressed, i.e. higher flows and closer to instability. If no solutions are found when a system is under severe pressure the effectiveness of such a safety net would be significantly reduced.

Results

In this test system, the voltage dependent loads are used, but the system is stressed further by modifying the line susceptance values. It was found that this significantly decreased the stability margin of the system in order to validate the performance of a stressed system. While increasing

load values only would decrease the stability margin, it was decided that by changing the line susceptance, the system could be stressed more in terms of its voltage conditions, making the system more susceptible to voltage collapse. This was to show that when a system is stressed, especially in terms of voltage that the method could still find the optimal solution and minimise the voltage changes. The full solutions of this system are shown in Figure 10-36 while the optimal solutions are shown in blue. In this example, there are 3 unique solutions, one red which exceed limit.

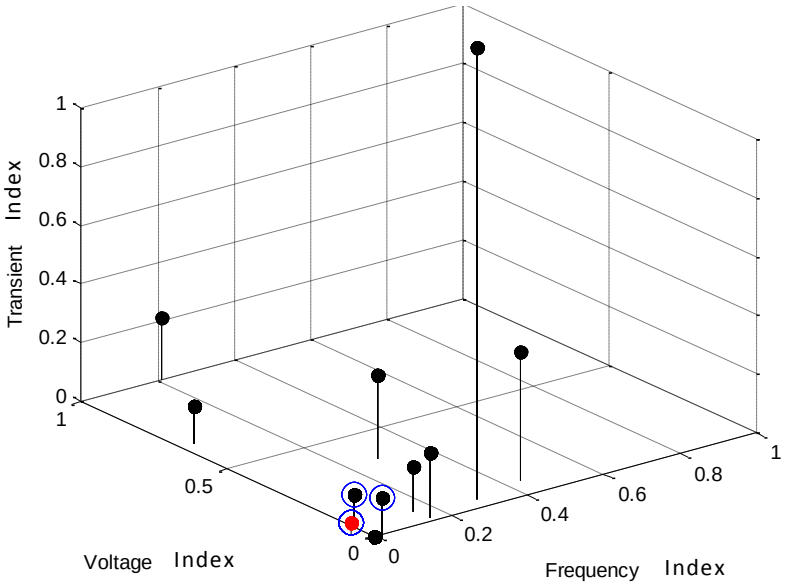

Figure 10-36 68 bus TSIII full solution

It can be seen that optimal solutions can be achieved with relatively small imbalances as in Figure 10-37 and small voltage changes as seen in Figure 10-38. However, as Figure 10-39 shows, some of the optimal islands are extremely large, over 90%, and the benefit of islanding these has to be questioned. However, this was found to be the optimal solution, but in the majority of cases the only solution.

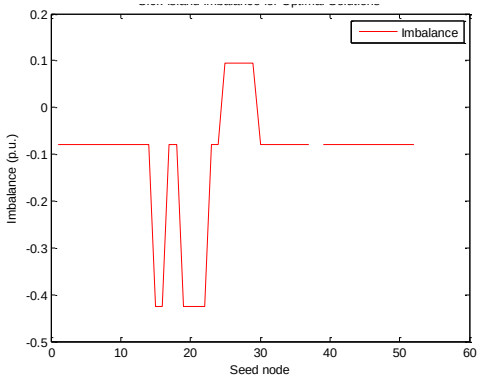

Figure 10-37 68 bus system TSIII - Optimal Imbalance

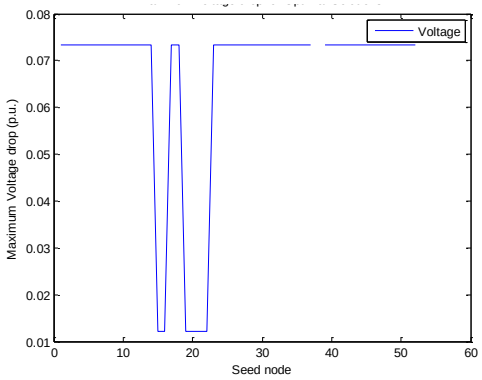

Figure 10-38 68 bus system TSIII - Maximum voltage changes

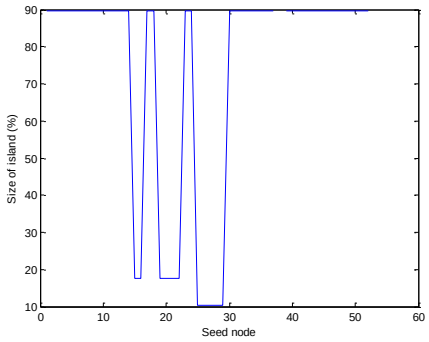

Figure 10-39 68 bus system TSIII - Optimal Sick Island Size

It is possible to penalise the larger islands further by increasing their penalty value, however, this adds little benefit as seen in Figure 10-40. Here, and island greater than 50% is given a heavier penalty and so for seed nodes 2 and 3, a different solution is chosen, where the island size is reduced to under 5%. However, there is an increased imbalance value now, as seen in Figure 10-41. While this does give a reasonable solution, it can be seen that it is only an advantage to these two buses, and the rest of the island solutions that are close to 90% remain unchanged. In this stressed system, very large power flows exist between the nodes and therefore due to the high connectivity and flows, tracing will only find large islands as it deems such a large area to be infected.

Indeed, this is not a drawback to the method, but a reflection of how heavily the nodes in a system depend on the power flows for connectivity and as the loading is increased, the number of available islands decreases.

It shows that despite the system being severely loaded, that ICI solutions can still be obtained and can be priorities, though to a lesser extent. It proves that the methodology is a useful tool to apply as an emergency safety net to the system.

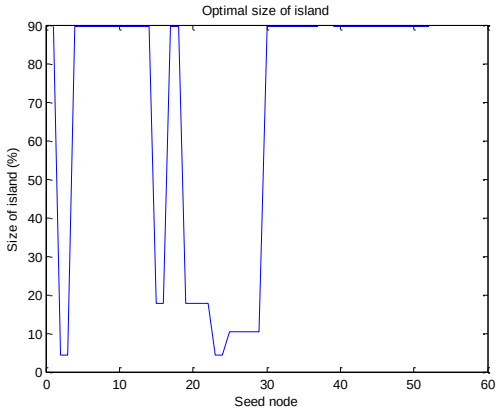

Figure 10-40 increased penalty – island size

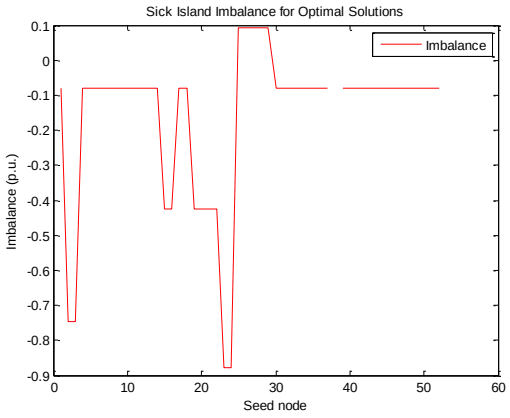

Figure 10-41 Increased penalty - imbalance

10.4 All systems

This section shows a summary of the key information from the previous test cases. The aim was to minimise the voltage changes that would occur as a result of the islanding action itself using knowledge only from the voltage indices. This summary will show that the method can be used to minimise the effects on voltage. In order to show how important this developed methodology is. The possible changes in voltage which could occur with the voltage index knowledge should be considered. This can be shown in Figure 10-42. This figure shows the results for all five test systems. It shows the maximum possible voltage change for each seed node in that system. Without knowledge of the voltage index, it would be difficult to select a solution which would reduce the risk of voltage instability.

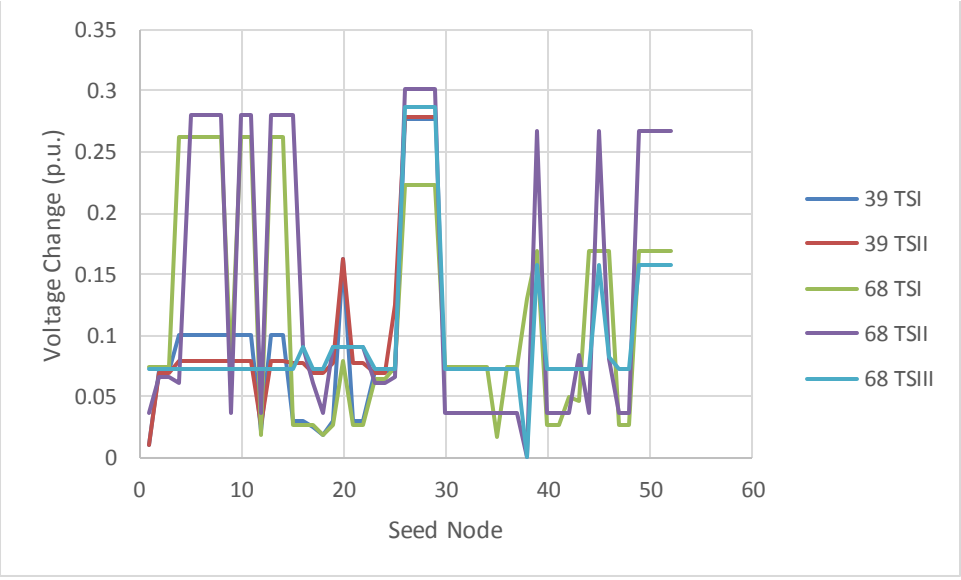

Figure 10-42 Worst Case Scenarios Summary

However, if the voltage index is considered, then it is possible to avoid such scenarios and minimise the voltage changes due to the splitting actions. While the results here focus on minimising the voltage indices, these could lead to larger values in real powers and may not be ideal. However, for the purposes of demonstrating minimal voltage changes it can be seen that it works very efficiently. Using the visualisation tool, the operator could choose a different metric by which to choose the best island. The results for minimising the voltage indices are shown in Figure 10-43. It can be seen that the voltage changes can be significantly minimised. The methodology has achieved a change of less than 0.1 p.u. for the majority of cases.

There is a spike in the graph corresponding to the 39 bus test system II. This has been covered in section 10.3.6 where an addition to the objective function for real power would eliminate this. These results only minimise the voltage indices or the reactive power imbalance. A full ICI optimization was not carried out as a tool for transient stability assessment was still being designed at the time of this thesis. When this tool is completed the results from this thesis would be combined with the transient stability tool to provide a proper optimization tool. Therefore, this section only shows how the voltage changes resulting from reactive power imbalances are minimised.

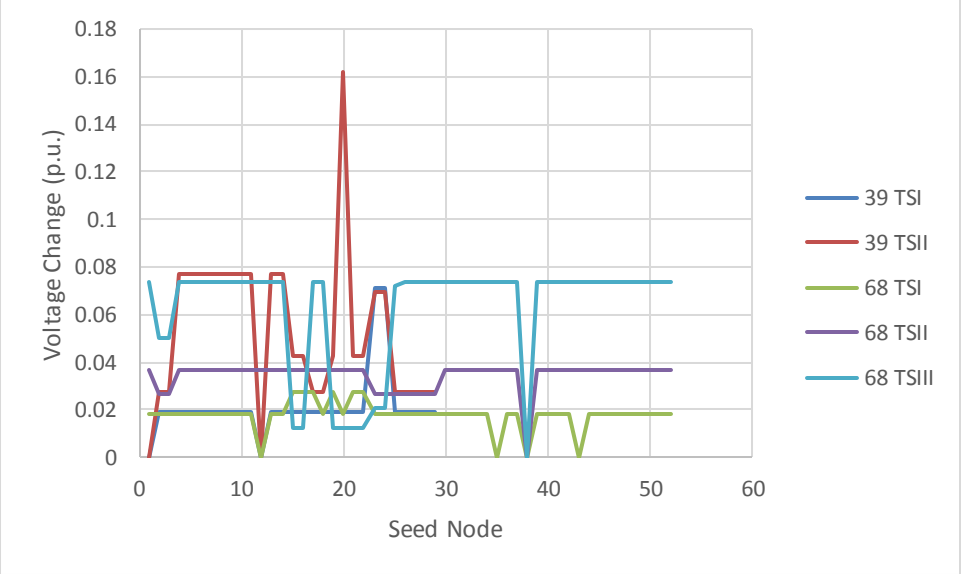

Figure 10-43 Summary of results minimising voltage index

10.5 Solution Times

The solution times are a critical component of the methodology. The purpose of the entire method is to compute an islanding solution using real time information which therefore must be extremely fast to prove a just-in-time solution. The solutions times for the tracing method

and the voltage assessment methods are given individually to allow for comparison between methods and test systems. It is important to note that the algorithm used were not optimised and times are based the following specification machine:

Processor: Intel Core i5-3337U CPE @1.80 GHz

Ram: 4.00 GB

Operating System: Windows 8.1, 64 bit, x65-based processor

These times could be significantly reduced using a more powerful computer and also with much better optimization of the algorithms. The results are shown in Figure 10-44.

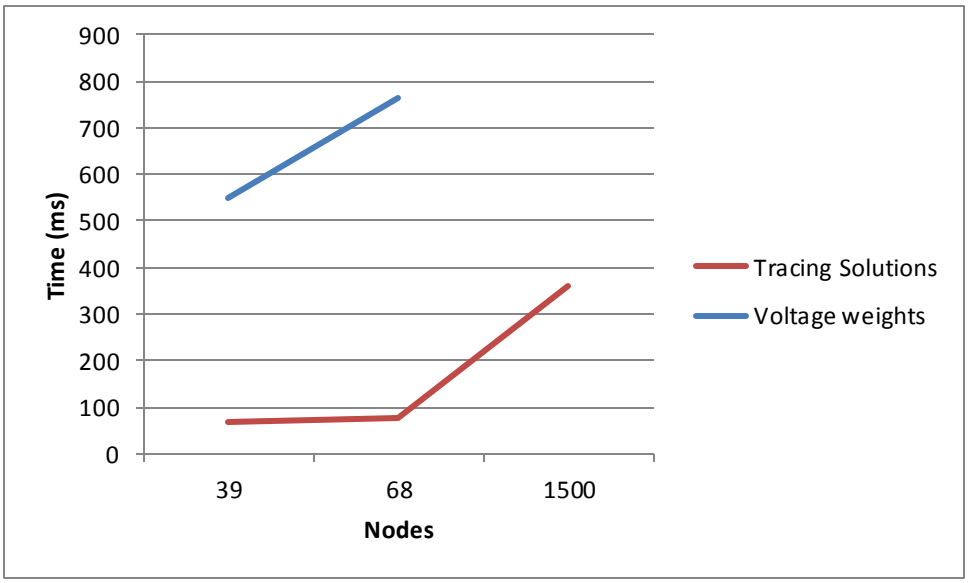

Figure 10-44 Solution Times

It can be seen that the tracing solutions are very fast, for the 39 and 68 bus system they are under 100ms. These times are the average times from a number of runs. When the system was tested for the EU case which consists of over 1500 nodes, the solution time increases to 360ms however, given the size of the system, this is still a very fast solution.

Indeed, for the voltage calculations, the solution times are longer, but this is due to a number of power flow solutions being required. However, given that time domain simulations will take a much longer time in comparison, a number of seconds for even small systems, the times are deemed satisfactory given the level of information that can be provided. The EU case did not have voltage information, hence no solution time was available for this system. The main

component in this analysis is the running of power flow solutions. If faster methods are available for this, then the method can be significantly enhanced.

Therefore, this proves that the methodology is an extremely fast tool and that it could be readily employed as an ideal solution method using real time information. Solution times well under a second, even for 1500 nodes show that the tracing tool is very effective in finding islanding solutions very quickly.

10.6 Summary

The results from this chapter show that the methodology is able to find the optimal solutions for a range of disturbance locations. One of the interesting findings shown in the optimal solution space as that there are not always a large number of unique islands. Typically there are 4-5 islands which are unique, and all the seed nodes will fit into one of these islands. Therefore, this knowledge could be used to determine if having a unique disturbance dependent solution is required seeing as many seed nodes share a common optimal island.

Detailed results were presented first which showed that the indices designed for voltage could identify the solutions which would lead to an increase in voltage stress. This proved that the derived methodology could be effective for reducing risk of voltage collapse. The optimal solutions were then presented where it was shown that it can find solutions which will minimise the voltage changes as long as other criteria are satisfied. One example showed that it may be more beneficial to have a larger voltage change on 5% of the network rather than forming an island of 67%. This holds with the ICI approach of reducing the number of customers being affected in order to get the maximum gain from ICI.

Finally, a summary of all results was given where the maximum voltage changes from all the test systems were shown without voltage indices and then could be compared to the optimised solutions. It was shown that using the optimal functions that the majority of seed n odes could create islands with voltage changes less than 10% which was the objective of the methodology.

Therefore, despite the simplistic minimisation, it has provided a set of results which show voltage changes can be minimised. It could still benefit from further work such as a full optimisation considering all indices and the incorporation of a full dynamic assessment tool. However, it has shown to serve as a good approximation to provide promising initial results for future development and serves as an excellent fast predictor into voltage stress on the system.

Using the tracing method combined with the voltage indices, it is possible to create an island around a disturbed node, minimise the effects on all forms of stability and successfully island the system. This is a significant contribution as it has shown that two novel methodologies could be put forward and combined to produce a feasible solution into prevention of wide area blackouts, especially those linked to cascades.

Finally, the solution times are given for both the tracing and the voltage index methodologies. It was seen that both these methods are extremely fast and even when very large systems are tested, solution times are still under a second.

11 Comparison with Other ICI Schemes

Chapter 3 described many other ICI methods, but to show that the ICI principle developed in this thesis offers an approach that is not just novel, but also feasible, it should be compared to these methods. The two main methods in ICI are spectral clustering techniques and slow coherency methods. It has already been described that this methodology has an advantage over slow coherency as it produces fewer islands, and therefore puts fewer customers at risk. However, the main aim is to keep the system stable by keeping coherent groups together. It will be shown in this chapter that while this approach is effective, it can be conservative as stable islands can still be created by separating up the slowly coherent groups.

Spectral clustering methods, are usually based on either the admittance matrix or the power flows. While tracing used contributions between buses rather than the physical flows it is expected to provide slightly different results and they will be compared here.

The tests being carried out here differ from those in the results chapter. Voltage stability is not considered in the spectral clustering techniques or in the slow coherency techniques. This means that this methodology cannot be compared directly with these techniques. Therefore, solutions will instead be prioritised according to the related stability indices for each technique, namely frequency stability for clustering and transient stability for coherency. Each of the techniques has a particular strength with a slightly different focus. However, the methodology from this thesis has added flexibility in that different stability criteria can be prioritised. This is how this method can be compared to different techniques, neglecting the voltage indices.

11.1 Spectral Clustering techniques

The spectral clustering method has been developed in parallel with the tracing method, and the details can be found in [139]. These results were produced using this reference which was conducted in parallel to this project to investigate graph theory techniques for ICI. The spectral clustering is not the focus of this thesis, only the results will be discussed and described here. The edges are weighted according to the power flows and the system is split with the aim of minimising power imbalance. The spectral clustering method typically divides a system into a number of parts, but the work mentioned has allowed an island of any size to be chosen. The results from clustering can be found in Appendix 4.

The methods are not directly comparable, therefore the size is used to compare different islanding solutions. A tracing solution is selected which will have a certain amount of nodes. Then a clustering solution is chosen which is the same size and then compared to the tracing solution. It allows comparison of the same size islands for minimal imbalance to determine the best solution.

The developed methods are based on real power flows, and do not consider voltage or dynamics. Therefore, it is the results from tracing only that will be compared without voltage indices. The 39 bus system is used for a variety of different thresholds. It is the tracing without node merging which is used as the clustering method would not merge islands either.

11.2 Pure Power Flow Tracing

The spectral clustering methods have been based on DC power flows, so tracing must use the same for comparison. Voltage is not considered in clustering, therefore the voltage indices are not considered in this comparison. Three seed nodes are selected from the 39 bus system, each with a number of solutions. The spectral clustering method does not find a specific solution like the tracing method does but finds a large number of solutions for any island size and gives values such as the total power cut and imbalance for an island of that size. Taking the size of the islands from the tracing, an equivalent sized island is then found from clustering and compared. The results are shown in Table 11-1

Table 11-1 Tracing and Clustering results

Seed node	No. Nodes	Imbalance (MW)		Total power cut (MW)		Difference	
		Tracing	Clustering	Tracing	Clustering	Imbalance	Total power
19	11	29	29	191.59	191.59	0	0
19	9	201	187	363.59	347.39	14	16.2
19	7	359	189	521.59	640.94	170	-119.35
2	25	-32.9	-32.9	104.87	104.87	0	0
2	7	42.4	42.4	177.99	177.99	0	0
2	5	244	393.6	332.12	771.77	-149.6	-439.65
14	25	-32.9	-32.9	104.87	104.87	0	0
14	12	10.7	10.7	121.73	121.73	0	0

The islands are being compared using size, so looking at the first example for seed node 19, for an island with 11 nodes, both the tracing and clustering methods agree. However, it can be seen

that for an island of size 9 and 7, the tracing and clustering form different islands. The differences are shown as the tracing results minus clustering results, where a positive value implies the clustering solution is better. Therefore, it would appear here that for these 2 nodes, the spectral clustering forms better islands in terms of imbalance. However, the total power cut is larger for the island of size 7. This would appear to show that tracing may not provide the best solutions, but further analysis can uncover some problems with the clustering method.

The tracing method examines all connections between buses, if a line has a high power flow, or a strong contribution, the line is not cut through. Therefore it is lines with lower flows/contributions that are selected instead. The aim is to minimise the imbalance indirectly through cutting lower line flows. Table 11-1 shows clustering can find better islands in terms of imbalance directly, showing that the tracing method does not guarantee minimal imbalance. While it may be possible to find a better imbalance globally by cutting through larger lines, the impacts of cutting through such lines can also be more severe. The cutsets and corresponding line flows are shown in Table 11-2 and Table 11-3 for tracing and clustering respectively. It can now be seen that the clustering does in fact cut through higher power flow lines, with the largest power flow being 3.35 p.u. compared to 2.27 p.u. from tracing. It is necessary to consider what impacts cutting through large power flows actually has, is there an advantage to using tracing?

Table 11-2 Tracing cutset

From	To	Flow (p.u.)
14	15	0.3599
16	17	**2.2689**
16	24	-0.4531
19	20	1.7200
22	23	0.4141

Table 11-3 Clustering Cutset

From	To	Flow (p.u.)
14	15	0.3599
16	21	**-3.3459**
16	24	-0.4531
17	18	2.0206
17	27	0.2482

The two different ICI solutions, for the same size are shown in Figure 11-3 and Figure 11-4. In order to fully evaluate these islands, time domain simulations are used. It will investigate if there is added risk in cutting through larger power flows even if it minimises the imbalance. The bus voltages are shown in Figure 11-1 and Figure 11-2, and it can be seen, that although the tracing solution reaches a lower voltage, only 2 buses fall under 0.9 p.u. voltage compared with six buses in the clustering. Therefore, the clustering result is putting a much larger area at risk due to under voltage. It has been said throughout this thesis that the transient rotor angle stability is

strongly connected to the size of the power being cut. It would therefore be expected that a bigger effect would be seen by generators as the clustering method cuts through higher power lines. The rotor angle plots for each island (with more than 1 generator) are shown from Figure 11-5 to Figure 11-9. While there are four islands in tracing, two have single generators, therefore the generators cannot swing against any other machines. It is only the islands with more than one generators where these swings are possible are described. The rotor angle plots are all shown with the rotor angles being relative to one set generator in the system. From Figure 11-5 Figure 11-6, the results for the tracing are shown, and it can be seen that the healthy island experiences little deviation and all generators swing together. However, for the sick island, there is less inertia and a larger oscillation is seen. However, it does stabilise, i.e. does accelerate or decelerate away from the other generator. The clustering results are then compared, and again the healthy island from Figure 11-8 is the larger island, and does not experience much oscillation. However, for both the sick island, and the other healthy island, the angles are accelerating away and are going unstable. If this acceleration continued, the generators would trip causing a large imbalance in the islands and could lead to a blackout. Therefore, it can be seen that the clustering method is at a disadvantage in considering only the total power cut and imbalance values, as it is shown that the individual values are very important. While many of the results between tracing and clustering are the same, it was shown here that where the clustering appears to give a better solution, it can in fact be slightly worse.

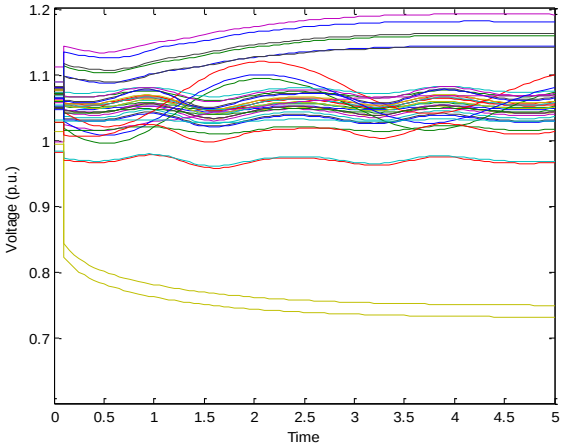

Figure 11-1 Bus Voltages – Tracing

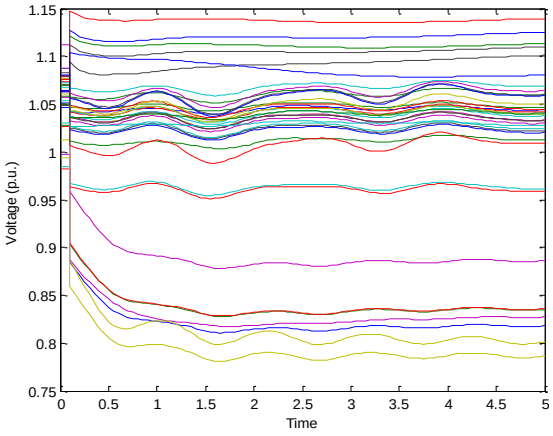

Figure 11-2 Bus Voltages - Clustering

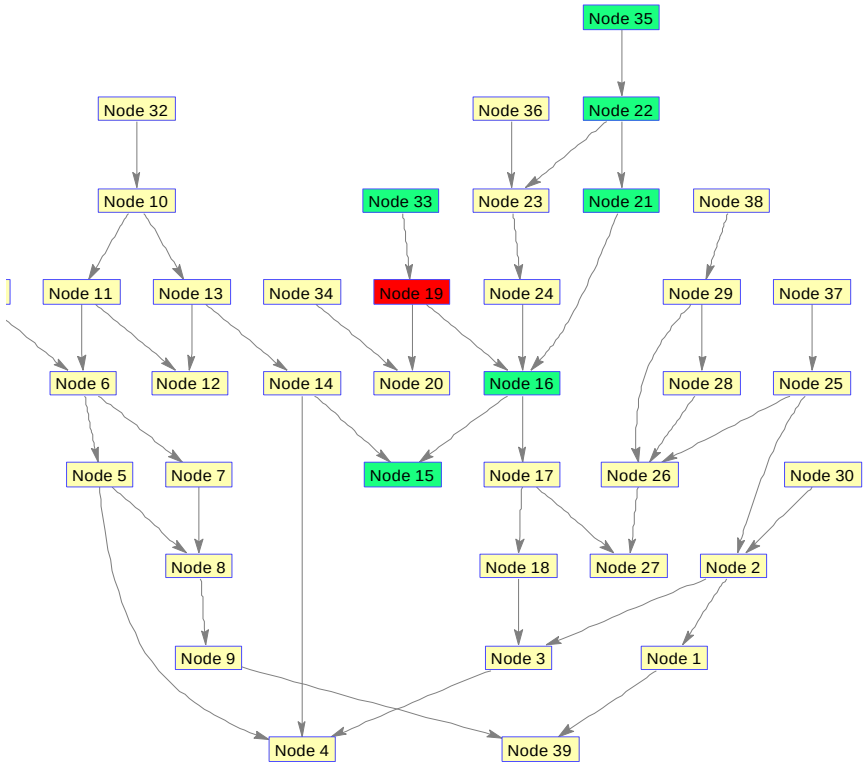

Figure 11-3 Tracing Solution Size =7

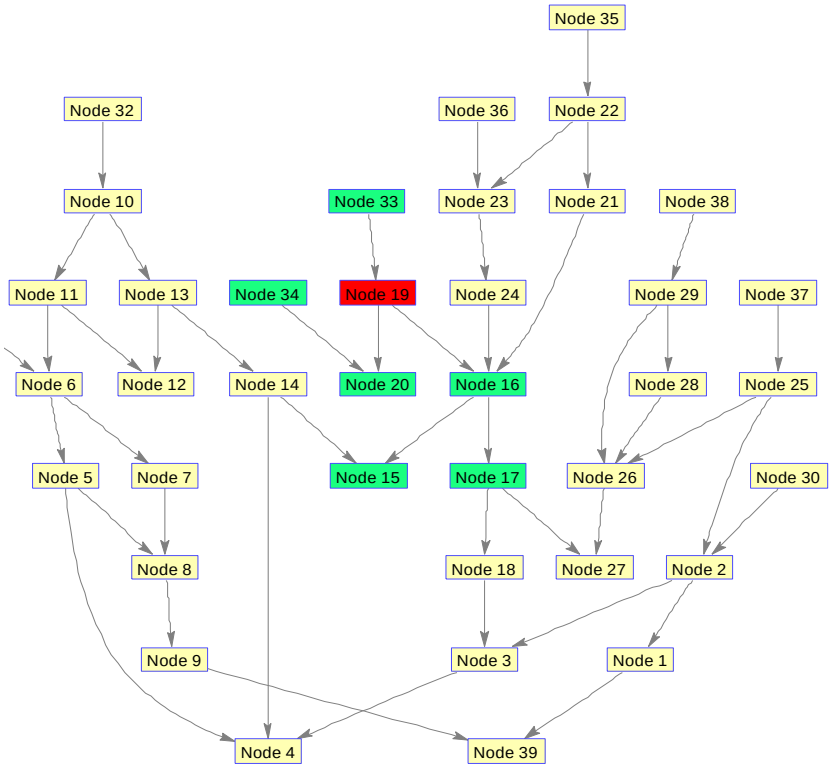

Figure 11-4 Clustering Solution Size = 7

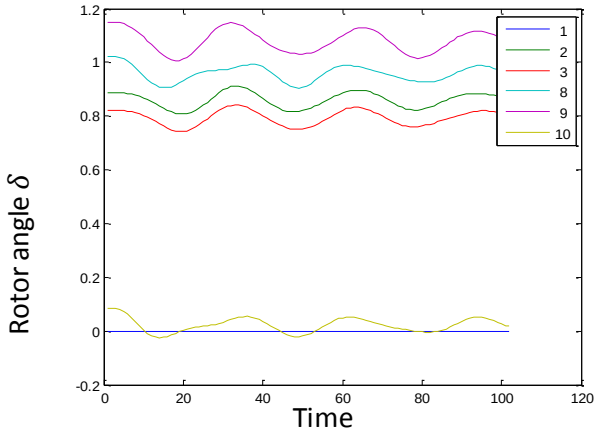

Figure 11-5 Tracing Healthy Island

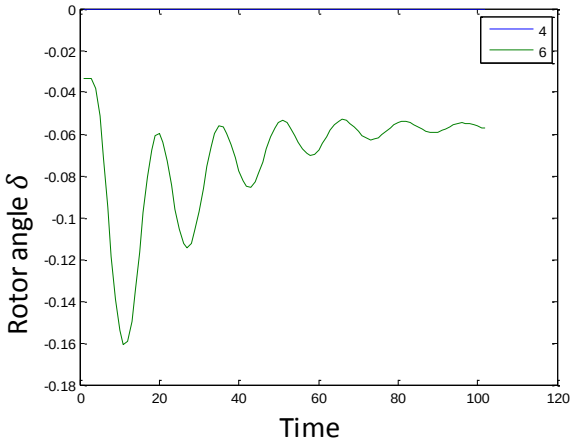

Figure 11-6 Tracing Sick Island

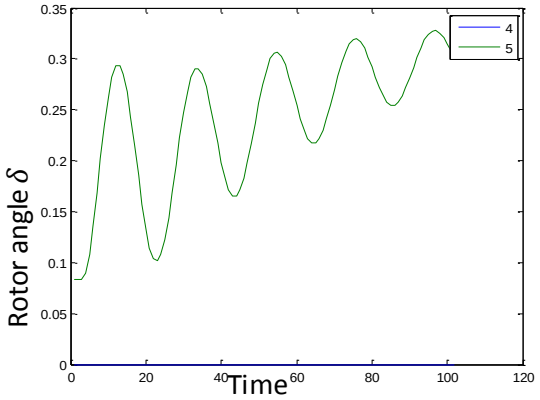

Figure 11-7 Clustering Sick Island

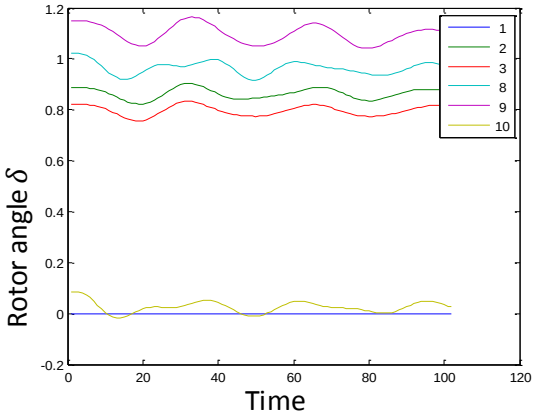

Figure 11-8 Clustering Healthy Island 1

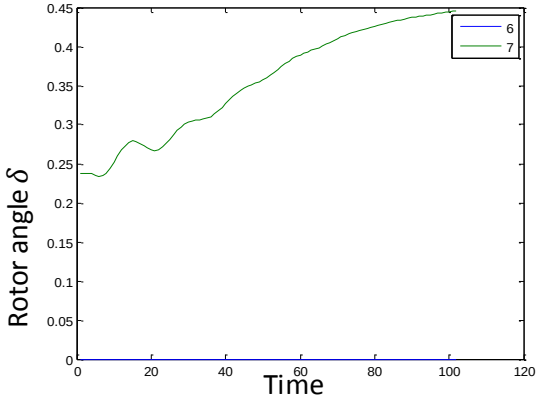

Figure 11-9 Clustering Healthy Island 2

11.3 Slow Coherency

The slow coherency method is the most widely published ICI scheme which splits a system into its coherent generator groups in order to maintain generator stability. Work done in [140] parallel to this project provided a comparison between slow coherency and tracing for ICI. The work from that paper is now presented here. The Slow Coherency method did not consider voltage stability either in its formulation, therefore it in not directly comparable to the full methodology derived in this thesis. Instead, the coherency is based on dynamic stability, where the closest comparable index for dynamic stability from this thesis would be W_T. Therefore, the slow coherency method is compared to solutions from this thesis which are prioritised for W_T.

11.3.1 Slow Coherency based Controlled ICI

In large-scale power systems, interactions between the rotating machinery cause oscillations throughout the system. These oscillations can be classified as local modes and inter-area modes depending on their frequency. When the faster local dynamics have decayed, generators in the same area swing together with a slow oscillation. They can be thought of as 'coherent' with respect to these slow modes. Using eigenvalue analysis, it is possible to group generators together based on their participation to selected modes of oscillation. The groups are referred to as slow coherency groups.

Slow coherency ICI is based on two inherent assumptions; coherent groups of generators are almost independent on the location and severity of the disturbance allowing the linearized model to be used; coherent groups of generators are independent of the level of detail used in modelling the generating units so that a classical generator model can be considered. Therefore, the dynamics of power systems for different fault locations may not be completely considered. The coherency between machines is developed through threshold levels, where generators are said to be coherent if the connection between them is above a defined threshold value. This is covered in more detail in the Appendix 5.

After the coherent groups of generators have been determined, the next step is to search for optimum cut sets to split the power systems into several islands. Chapter 3 covered a wide range of techniques available to find the optimal islands. In this work, the minimal cutset method is used in which minimal power flow disruption is taken as the objective function, considering the coherency groups obtained in the first step.

11.3.2 Evaluation of the ICI strategies

Along with the mentioned ways to evaluate an island, power imbalance and power cut, a new index is used to quantify the stability margin. It is called the Critical Islanding Time (CIT) which is the maximum time for ICI actions to save the system. It is similar to the critical clearing time typically used in transient stability analysis. Critical Clearing Time (CCT) is defined as maximal fault duration for which the power system remains stable after fault clearing. To test the islands, faults are applied greater than the CCT to induce instability where ICI must then prevent the instability. As a progression of CCT, CIT can be defined as maximum duration before implementing the ICI strategy for which all the split islands remain transiently stable. If the ICI strategy is implemented beyond the CIT, the power system which has been split into the islands will be unstable.

The larger the CIT, the more time for implementing the ICI strategy which translates into a larger stability margin for the ICI strategy. Therefore, the CIT is an appropriate index for evaluating ICI strategies and can be used for determining the best ICI strategy.

The ICI strategies are evaluated using a step-by-step time-domain simulation method and trial-and-error to check the transient stability after ICI. In practice, one of the fast direct methods for transient stability assessment would be used such as E-SIME which is the work of a parallel project.

11.3.3 Results of evaluation

Two test systems are evaluated in this study and the result from these systems will be shown here. The methods described earlier are used to find the coherent groups and an example for the 39 bus test system can be found in Appendix 5.

39 bus system

The 39 bus system contains 10 generators which can be broken up into four slowly coherent groups, i.e. [G1, G8, G9], [G2, G3], [G4, G5, G6, G7] and [G10]. Then the power system can be easily split into four islands by using minimal cutset of power flow cut/disruption. The optimal ICI strategy, denoted as S1 and shown by short dashed line, is shown in Figure 11-10.

With slow-coherency, the system is split into the same islands independent of fault location. In contrast, the tracing method may produce different islands depending on the disturbance location. It was shown in chapter 9 that there is not a unique island for each seed node, but often a small number of optimal islands. In this study, transient stability was being addressed. Therefore islands were optimised based on the power flow being cut, or the transient stability

index. In this system two unique optimal ICI strategies have been identified shown as T1 (the long dashed line) for seed nodes 1-8, 10-11, 13-22 and 25-29 and T2 (the dot dashed line) for seed nodes 23 and 24 in Figure 11-10. For seed nodes 9 and 12, no ICI strategies can be found by using the proposed tracing based ICI method. It can be seen that different coherent groups of generators, such as [G1, G8, G9] and [G2, G3], are merged into one island in ICI strategy obtained by the tracing method.

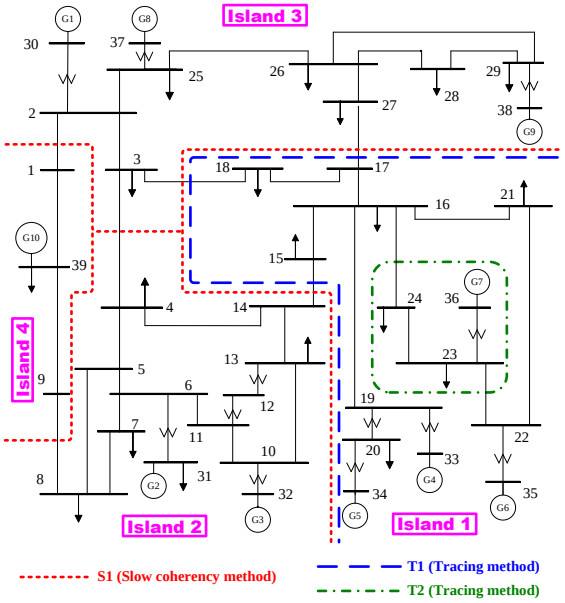

Figure 11-10 Optimal cutsets of New England power system for slow coherency and power flow tracing based ICI methods

An important result here is that one of the islands identified by tracing (T1) is identical to one of the coherency-based islands. This confirms that tracing does take transient stability implicitly into account by minimizing the shock to the system caused by ICI.

Table 11-4 shows the power flow cut and power imbalance of the two ICI methods. It is clear that tracing performs significantly better as it results in smaller power flow cut and more balanced islands.

Table 11-4 Comparison of Power flow disruption and imbalance for different ICI strategies

Methods	ICI Strategy No.	Power Flow cut (p.u.)	Power Imbalance (%) (W_f)
Power Flow Tracing	T1	2.139	2.834 %
	T2	2.245	2.278%
Slow Coherency	S1	3.082	10.430 %

Table 11-5 Critical islanding times for ICI strategies

Bus No	CCT (s)	CIT (s)			
		Slow coherency	Power Flow Tracing		Difference
1	0.276	0	0		0
2	0.201	3.059	2.946		0.113
3	0.208	0.368	0.394		-0.026
4	0.215	0	0		0
5	0.226	0.126	0.312		-0.186
6	0.222	0.117	0.308		-0.191
7	0.243	0	0		0
8	0.239	0	0		0
9	0.297	0	0		0
10	0.224	0.139	0.354		-0.215
11	0.233	0.128	0.333		-0.205
12	0.314	0	0		0
13	0.236	0.156	0.341		-0.185
14	0.221	0	0		0
15	0.202	0.404	0.424		-0.02
16	0.154	0.28	0.28		0
17	0.174	0.427	0.451		-0.024
18	0.205	0.392	0.417		-0.025
19	0.156	2.255	2.255		0
20	0.163	1.355	1.355		0
21	0.205	0.209	0.209		0
22	0.205	0.195	0.195		0
23	0.2	0.218	0.029		0.189
24	0.187	0.25	0.505		-0.255
25	0.184	3.566	3.093		0.473
26	0.149	0.636	0.506		0.13
27	0.19	3.01	2.976		0.034
28	0.147	0.589	0.575		0.014
29	0.124	0.601	0.583		0.018

Table 11-5 shows the results of transient stability simulations by showing the CCT of faults for each bus and CIT of ICI strategies obtained by power flow tracing and slow coherency methods. The final column shows the difference between the CITs of the slow coherency and the tracing method. If that difference is negative, the tracing outperforms slow coherency from the transient stability point of view and vice-versa.

For ten buses, the tracing methodology outperforms slow coherency. For seven buses the opposite is true while for remaining buses the methods behave similarly. This in itself is an important result as it shows that the tracing alone can provide results similar to coherency and hence can be seen as a fast assessment tool avoiding complex eigenvalue analysis. Therefore, the tracing method appears to outperform slightly (on average) the slow coherency method from the transient stability point of view while it behaves significantly better from the static point of view (power flow cut and power balance of the islands). There are cases where neither slow coherency nor tracing based ICI can prevent stability. In these cases other corrective control measures (such as generation tripping and/or load shedding) would be required.

68-bus System

Using the slow coherency, the 16 generators have been divided into five coherent groups, i.e. [G1-G9], [G10-G13], [G14], [G15] and [G16]. The optimal ICI strategy is shown as S1 in Figure 11-11. From power flow tracing, the optimal ICI strategy is shown as T1 for all of seed nodes excluding seed node 38. Again, the tracing-based island is identical to one of the coherency-based islands confirming that tracing does take transient stability inherently into account by minimizing the shock to the system caused by ICI. For seed node 38, no tracing-based ICI strategies can be found.

Table 11-6 shows the power flow cut and power imbalance from the tracing and coherency strategies. Tracing outperformed slow coherency from the static point of view where it resulted in much smaller power flow interruption and in better balanced islands.

Table 11-7 shows the results associated with CCT of the faults in each bus and CIT of ICI strategies. In 22 cases the tracing-based ICI resulted in significantly higher CIT than the slow coherency-based ICI suggesting better performance from the transient stability point of view. It was only outperformed by coherency in two cases.

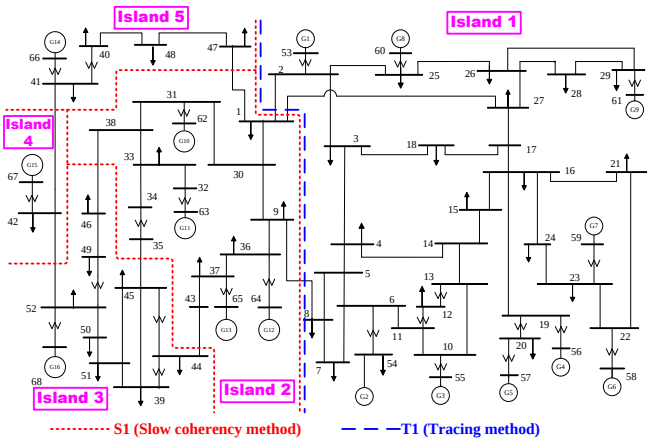

Figure 11-11 Optimal cutsets of the 16 for slow coherency and power flow tracing islands

Table 11-6 Comparison of power flow cut and power imbalance

Methods	ICI Strategy No.	Power Flow Cut (p.u.)	Maximum Power Imbalance (%)
Power Flow Tracing	T1	0.889	0.249%
Slow Coherency	S1	6.926	20.980%

Table 11-7 CCT and CIT of ICI strategies

Bus No	CCT (s)	CIT (s)		
		Slow coherency	Power Flow Tracing	Difference
1	0.529	0	0	0
2	0.452	2.162	3.244	-1.082
3	0.415	2.208	3.354	-1.146
4	0.411	2.229	3.352	-1.123
5	0.385	2.274	3.352	-1.078
6	0.369	2.294	3.394	-1.1
7	0.456	0	0	0
8	0.448	0	0	0
9	0.444	2.061	3.061	-1
10	0.386	2.315	3.394	-1.079
11	0.41	2.283	3.371	-1.088
12	>20	------	------	------
13	0.425	2.271	3.366	-1.095
14	0.416	2.235	3.374	-1.139
15	0.398	2.238	3.366	-1.128
16	0.277	2.317	3.55	-1.233
17	0.337	2.259	3.443	-1.184
18	0.415	2.214	3.403	-1.189
19	0.332	2.378	3.609	-1.231
20	0.363	0	0	0
21	0.379	2.32	3.475	-1.155
22	0.335	2.404	3.629	-1.225
23	0.357	2.395	3.575	-1.18
24	0.351	2.296	3.549	-1.253
25	0.362	0	0	0
26	0.372	0	0	0
27	0.425	0	0	0
28	0.391	0	0	0
29	0.337	2.649	3.568	-0.919
30	0.415	0	0	0
31	0.452	0	0	0
32	0.289	0	0	0
33	0.355	0	0	0
34	0.436	0	0	0
35	0.66	0	0	0
36	0.277	2.248	0	2.248
37	0.235	2.371	0	2.371

38	0.79	0	------	------
39	1.192	0	0	0
40	1.641	0	0	0
41	0.538	0.19	0	0.19
42	0.711	1.804	5.103	-3.299
43	0.799	0	0	0
44	2.905	0	0	0
45	0.765	0	0	0
46	>20	------	------	------
47	>20	------	------	------
48	>20	------	------	------
49	>20	------	------	------
50	0.658	0	0	0
51	0.739	0	0	0
52	0.226	0.248	1.21	-0.962

For the faults in buses 1, 7, 8, 20, 25-28, 30-37, 39-41, 43-45 and 50-51, neither ICI strategy (i.e. T1 and S1) could maintain stability of the islands. For the faults in buses 36, 37 and 41, the ICI strategies obtained by tracing method could not maintain stability of the islands, but the ICI strategy based on slow coherency method could maintain stability stable. For the faults in the buses 12 and 46-49, CCTs were more than 20 s, which means that the faults in these buses would not lead to transient instability of power system.

11.4 Summary

The tracing method has been compared to two methods in this chapter and it has shown that it can offer better results in certain cases than clustering and coherency methods. The clustering methods are more closely related as they can find the island around a disturbance. It was found when compared with pure power flow tracing, the clustering method can find solutions with lower imbalances and in some cases the total power cut. Further investigation was carried out into how these imbalances were being achieved. The tracing aims to minimise the imbalance indirectly by cutting through the lines with minimal power flow. However, the clustering does not rank lines according to the power flow and aims just to find the minimal imbalance. It is possible to minimise the imbalance by cutting through much larger power flows. However, cutting through lines with large power flows can have effects elsewhere.

There will be large redistributions of power which can have effects on both the voltage and rotor angle stability in the system. Running time domain simulations it was possible to show that there was a larger low voltage area and that generators were accelerating away for the clustering

islands. This was despite the minimal imbalance. Therefore, the way the imbalance is made up is vitally important and it is not sufficient to form the best balanced island, but to consider the actual power flows being cut in doing so. The tracing has shown that even with a larger imbalance, there is better stability for voltage and rotor angles.

It was also shown that for the majority of the islands, the same result is found. This is also a promising result. The clustering method can take time due to the necessity of Eigen analysis, indeed the same for slow coherency. The tracing method can be considered a much faster approximation which avoids this timely step. For the majority of islands, the same solutions are found and when the different islands are found, the tracing ones are shown to be more stable.

For the analysis between the slow coherency and tracing based ICI there are some interesting conclusions. In the test systems used, some of the islands from both tracing and coherency were the same which indicated that the tracing does consider transient stability from the same perspective as coherency. As the tracing method is fast and does not require complex eigenanalysis to compute modes it shows that it serves as a good proxy for coherency, or indeed finding the weak connections in a system.

Slow-coherency based ICI seems to be overly conservative on average from both static and dynamic point of view as tracing-based ICI results in better-balanced islands which are also transiently more stable (on average). However tracing-based ICI does not always maintain transient stability when slow-coherency based ICI does. A hybrid approach may be appropriate whereby an ICI strategy is usually based on tracing however for disturbances originating at certain locations slow coherency-based ICI would be used. However, this would require extensive offline studies to determine which to use. As slow coherency is more conservative it will find more solutions. However for the majority of cases, tracing can provide better results despite it being less conservative.

The tracing being and entirely static method has the advantage of speed. Its ability to find islands that are similar to coherency show that it provides an excellent fast proxy for coherent islands. It also shows that coherency can be overly conservative and that there are other methods by which to find dynamically stable islands. This does mean that tracing can find unstable islands at times due to it being less conservative however this is currently being investigated.

12 Conclusions

This thesis set out to develop a disturbance dependent approach to ICI where the advancement of real time measurements allows new ways to be developed and new approaches to be devised for emergency control. The key original contribution that this thesis would address was devising a new fast method which could use real time information to deliver a 'just-in-time' solution for emergency control. Section 5.2.3 outlined number of design criteria which any new method would need to adhere to.

The thesis was divided into a number of development stages by which to address the design criteria. The first of these was to find the island boundaries, answering where to island question. This was typically carried out using offline approaches which were not disturbance dependent and also did not allow for adjustment due to changes in the operating points. This methodology would use real time information and hence would properly address the current state of the system, but computing a solution quickly puts a severe constraint on what can be done. Therefore, a methodology based on real time power flow information was devised to find an island boundary. Using power flow tracing, a set of nodes which are strongly connected to the original disturbance node can be found, where this set forms the island that will be disconnected. This technique therefore addressed the first design criteria of finding a disturbance dependent solution. The second design criteria was to minimise the number of islands as excessive islanding was deemed to be a shortfall with previous techniques. The tracing methodology would also address this directly by only finding strongly connected elements to a disturbance node and not performing any unnecessary islanding. This approach will also ensure greater network security.

One of the fundamental tasks in forming islands is to avoid cutting through highly loaded lines. Such actions could in themselves start a cascading situation when the power is redistributed. The tracing methodology directly addresses this issue based on the contributions between buses. If two buses share a high power flow between them, they are said to be strongly connected and are therefore not split. This then avoids any issues with cutting through heavily loaded lines. Lower power flows will always be explored first. This also indirectly minimised the total power that is being affected as the minimum number of islands are being formed through cutting through the lower power flows. Indeed in other methods more islands are formed and higher power flows may be cut. This highlights the importance of creating the minimum number

of islands which is a major contribution of this these as it has a number of potential benefits. Table 6-4 showed how an island could be created which would:

a. Minimise the number of island
b. Demonstrate a disturbance dependent solution
c. Minimise the imbalance and total power disruption

Therefore, the tracing methodology was shown to be an effective tool address the disturbance dependent nature that the thesis was offering. The performance of the algorithm in real systems and real events was tested where it was applied to the EU 2006 disturbance event. While the example was based on DC power flows only, it was useful to demonstrate how a solution could be selected for a particular disturbance location. When the methodology was applied, it provided a range of solutions where the best solution could then be selected. However, a key emphasis of the methodology was on speed. A solution using the tracing algorithm only on this system, which consisted of over 1500 nodes, was complete in 390ms. There was about 13s in the real event before the cascade began, therefore leaving plenty time to implement this methodology and it proves that not only is this contribution novel, but also extremely fast when used on real system. For the smaller test system of the 39 bus and 68 bus, the solution times were between 55ms and 77ms for a large number of runs.

It was then discovered that islanding itself being a severe disturbance could negatively impact upon the voltage conditions of the system. The tracing methodology relied on real power flow information and therefore provided no information on the voltage conditions of the system. Also, it was found that there were no readily available methods to use to predict the effect on voltage that a severe disturbance may have. Therefore, another original contribution was developed in the form of a voltage stress index. For a severe disturbance, islanding in this case, the voltage stress index would be calculated and assigned to that islanding solution. The purpose of this index was to gather information that a particular islanding solution would have on the system. As voltage stability is an extremely complex problem, it usually required time domain simulations to consider all aspects of controllers and loads etc. However, there was a constraint on time with the islanding solutions. Therefore, this novel methodology relied on power flow information only and it was shown through a series of tests that the indices obtained from statically derived methods had excellent correlation to the dynamic behaviour. This was verified in Figure 8-7. The method relies on running a series of power flows to measure the effects on reactive power across a system that a particular outage, or set of outages will have. As it relies

only on a series of power flows instead of the detailed time domain simulation it is quite fast. For the 39 bus system, the solution times were 550ms on average and 760ms for the 68 bus system. It is also important to realise that all these solution times could be significantly improved if the coding was optimised and better computers were used.

These two contributions needed to be combined and properly evaluated on a number of study systems. There are three main areas of stability in power systems, and it was in the islanding design criteria that the methodology must be able to address all of these. A parallel project was developing a complete transient stability assessment tool, therefore full consideration of transient stability was not addressed. Instead a proxy would be used for transient stability which was based on the total power disruption which resulted from islanding. This was a common method of considering transient stability, though it is only an approximate. Frequency stability could be considered through imbalance of power within each island. The two values could be easily computed from the power flows of the lines in the cutsets. A stability index was then created for each form of stability, for frequency, transient and voltage. Therefore each islanding solution could be evaluated based on these indices.

For a particular seed node, a number of islanding solutions would be available. These indices were then used to display the solution set on a 3D solution space. This information would be available to the operator as a form of open loop control and would allow certain forms of stability to be prioritised. As one of the key novelties in this thesis was on a measure of voltage stability, the methodology was evaluated where voltage was prioritised. Finding islands which minimised frequency imbalance and total power disruption was already well documented.

The results then verified that there was a strong link between the voltage indices and a voltage stability margin in Table 10-2. It showed for a particular seed node that choosing the solution with the smallest voltage index had the longest time before the system experienced voltage collapse. Indeed it also verified that choosing higher voltage indices had a much greater risk of voltage collapse as seen from a very fast collapse after splitting.

The results then went on to show how the operator could prioritise voltage stability in the selection for solutions for ICI. The results for minimising voltage indices were shown in Figure 10-43. From the five test systems, an island could be found for the majority of the seed nodes with voltage changes of less than 10%. There was only one seed node from these which resulted in a 16% change in bus voltage. However this was due to the binding size constraint and effects of real power. If this constraint was lifted, and island could be found with a maximum change of

5% however with a very large sick island of 67%. The decision would need to be taken on whether it is better to have a smaller area at risk with lower voltages than to have a much larger area at risk. The fundamental function of ICI is to contain a disturbance, where the economic advantage would be much greater if the area at risk can be reduced.

It was shown that without the knowledge of the voltage indices, very large voltage drops could be caused from the islanding action itself and therefore a high risk of collapse. This was shown in Figure 10-42 where voltage drops as high as 0.3 p.u. were observed. Without the developed methodology, there was no insight available into the possible effects islanding could have on voltage. Indeed, voltage is not considered in any of the popular methods of islanding. Using the voltage indices, these major voltage drops could be significantly reduced to below 0.1 p.u. therefore proving the usefulness of the methodology.

The results showed that it was possible to develop a fast, disturbance dependent solution that would allow an operator to prioritise a certain stability of concern and a set of solutions would then be recommended. A new methodology was created which uncovered the voltage aspects of splitting and derived an appropriate index which would be computed quite quickly in comparison to time domain methods, while still offering an effective tool to minimise the risk of voltage instability in a system. The results were shown for a number of test system, using different load models and it was shown that the indices performed well in each case.

An important contribution of this thesis was that the solution would be based on real time information. Typical methods were carried out offline and hence did not consider changes in the operating conditions. The results shown in section 10.3.5 showed how even the removal of a line from the system would provide a new set of solutions. This also verified how this methodology could adapt to new operating conditions, and given its fast solve time, could be easily integrated with real time information to provide just in time solutions. This is identified as a key advantage over existing methods.

12.1 **Comparison**

The developed methodology was then compared with two of the most popular ICI techniques clustering and slow coherency methods. Both these methods do not include voltage stability, therefore this methodology was not directly comparable using the voltage indices. However the remaining indices for frequency and transient stability would be more directly comparable and were instead used. This demonstrated the flexibility of the methodology to be applied with different stability priorities.

The clustering comparison concluded that clustering did find islands which have a better imbalance, and therefore seemed like the better solutions. However, under further scrutiny it was found that the formation of the imbalance is crucial. The tracing does not consider the imbalance directly, but implicitly by cutting the minimal power flows. It is possible to minimise the overall imbalance by cutting through high power flows. As the clustering minimises imbalance it was found to cut through larger power flows in order to achieve minimal imbalance. For one seed node it was found that the largest flow being cut using tracing was 220 MWs, compared to 380 MWs in clustering. The results from Figure 11-7 showed that when tested for stability, one generator accelerates away slowly and would trip compared to the solution from tracing which reached a steady state much earlier. Therefore proving that cutting through lower power flows would minimise risk if instability. Therefore, it was shown that despite finding lower imbalances, the clustering method does not provide the best results for overall stability.

Slow coherency aims to minimise dynamic instability, the ICI solutions from tracing are minimised based on the transient stability index as this was a proxy for rotor angle stability. This comparison concluded that the slow coherency will find a greater number of islands than the tracing method which is a disadvantage. As the tracing method does not consider rotor angle stability directly this may be seen as a disadvantage. However, the comparison between the coherency and tracing showed that in both test systems some of the tracing islands were the same as the coherent islands. Therefore minimising the tracing solutions according to total power cut is an excellent proxy for the rotor angle stability. Therefore it is not necessary to run the time consuming eigenvalue analysis to find coherent boundaries.

However, the tracing does merge non-coherent groups elsewhere in the islands as by definition of the problem it aims to find only two islands. It was shown for the two test systems, in terms of total power cut and power imbalance, tracing outperforms slow coherency. A new method for assessing the transient stability margin was then introduced called the Critical ICI Time (CIT). This is the final time by which ICI must be carried out to prevent instability. It was found that, on average, the tracing solutions would find islands with longer CITs hence allowing more time for action, which can be translated into bigger stability margin. It was therefore concluded that while there were cases where slow coherency was better than tracing, on average tracing performed better and proves that there is still scope for new methods of for ICI.

12.2 Novelty

A novel methodology is presented for ICI based on the location of a disturbance. While there will only be a small number of unique islands, the operator would be able to prioritise an island based on which form of stability is most at risk. It was found that many nodes in the system will share the same optimal islands and hence it makes selection of the best island simpler. When compared with existing methods it was shown that this new methodology can outperform in the majority of the cases, but can also find the same islands in some cases. It proves that the total power cut serves as a good proxy for rotor angle stability and the development of the voltage stress indicator has been shown to be able to find islands which can minimise the voltage excursions after ICI. Therefore the key novelties from this thesis can be summarised as follows:

1. Disturbance dependent solution based on real time information
2. Considers current operating point
3. Minimises the number of islands formed
4. Develops a method to incorporate voltage stability
5. Produces a method by which to prioritise certain stabilities
6. Produced a fast method by which to apply islanding solutions

These novelties are important as they expand what was previously available in this area. Much if the focus was on generalised solutions which were offline. However these would not adjust readily to changes in operating conditions. Using the real time information to create solutions allows solutions to be created which are tailored for the specific operating conditions. Being able to compute the results very quickly then allows a 'just-in-time' approach to be taken which could not previously be done in this field.

The addition of the voltage stability indices brings forward what is currently available with islanding. As islanding itself is a severe disturbance, it is important that the emergency actions being applied to not cause catastrophic failure. There was previously no way to evaluate the effects that the islanding would have on the voltage conditions. This methodology adds that component and provides a complete tool which will allow an operator to choose an ICI solution with minimal impact on the system.

12.3 Future Work

The aim of this thesis was to develop a fast ICI searching method. Selecting a disturbance dependent island boundary close to real time was the focus and as such the modelling had to be significantly simplified. Dynamics have been purposely neglected for two reasons. It was the subject of a parallel project and was not considered fast enough for search space reduction. Instead, fast methods would reduce the search space where then dynamics would then be tested. The tracing accompanied with the voltage stress predictor will quickly identify the best islands in terms of real and reactive power imbalance. The total power cut was used as a proxy for dynamic stability and indeed was shown to work quite well.

It does not take away from the necessity to consider dynamic behaviour, such as that of synchronous machines. For any seed node in a system, there are a number of islands available. Testing each of those islands for dynamic stability would be time consuming. Therefore, the best island would be selected from ICI and then tested for dynamic stability, or indeed the best few. This significantly minimises the number of islands that need to undergo dynamic assessment hence offering a faster solution. The thesis does not propose ICI based on the tracing results alone, but proposes the best islands for which to test for dynamic stability. A parallel project is currently being completed which uses Single Machine Equivalent (SIME) methods to quickly assess the dynamic stability of any potential island. When this work is completed, the results from the tracing would be combined with this fast assessment tool to provide islands which are dynamically stable.

Another important area which should be assessed in future work is the detailed effects of AVRs and OXLs. These can have significant effects during system emergencies and should be considered. In this thesis by minimising the imbalances, and hence resultant voltage changes everywhere in an island the effects on AVRs would be reduced. This may be an unnecessary limitation as an AVR may be capable of significant increases of reactive power and hence avoiding instability. The next stage would be to begin modelling of the AVRs and OXLs in conjunction with the voltage changes from the predictor method. Knowing if an AVR is near its limit would dictate how serious an imbalance is. If the AVRs are near the limit, then imbalances must be minimised due to the high risk of instability. However, if there is a significant margin, larger imbalances would be allowed. This would require a fast approximation method to assess how the local imbalances would push an AVR and would be a useful addition to this study.

13 Appendices

13.1 Appendix 1 – Test Systems

Chapter 5 introduced the test systems that would be used in this thesis. Due to the limited availability of dynamic test systems, there are three common systems. The 14 bus, 39 bus and 68 bus systems. However the 14 bus has limited islanding capabilities due to its size and is hence only reserved for simplified examples. The two larger systems were used for full ICI solutions. In order to create more scenarios by which to validate the methodology, these tests systems were modified to create different scenarios.

13.1.1 14 bus test system

The 14 bus test system is shown below and the details can be found in [141]. It consists of two real power sources and three additional reactive power sources. The blue division marks the islands used in the illustrations for chapter 5 and 8.

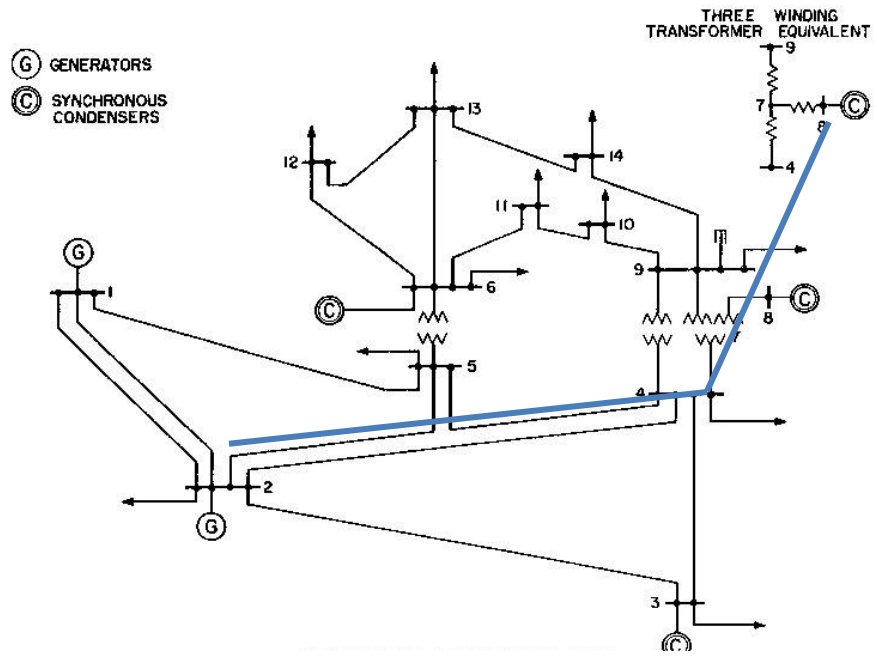

Figure 13-1 14 bus test system [141]

13.1.2 39 bus system

The 39 bus system consists of 10 generators, 46 lines and is based on the New-England system in the US. It contains dynamic information for the generators along with exciter models and it is regularly used as a test system. There were two cases created, the first was the standard system with the slack bus moved to the interconnector. A second case was created using the same system but with the removal of one heavily loaded line, line 3-4. This allowed sufficient changes

in the power flows to create a different islanding scenario. The 39 bus system is shown in Figure 13-2 along with the line out for TS II.

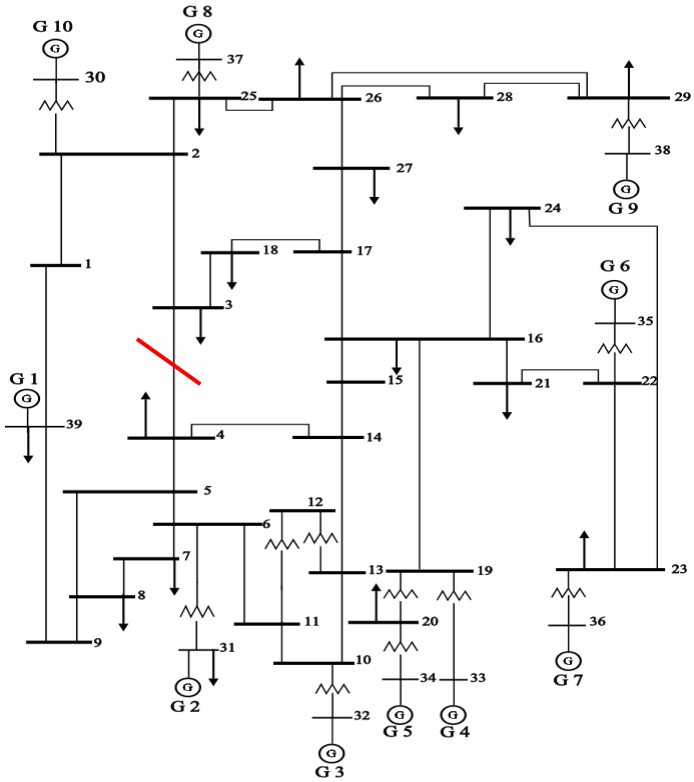

Figure 13-2 39-bus system TS1 (TS2 with red line cut)

13.1.3 68-bus system

The 68 bus system is again based on the New-England system, but it incorporates a much larger area. It contains dynamic generator data and exciter information. It consists of 16 generators and 86 lines and is shown in Figure 13-3. For this test system, 3 scenarios were created to explore more islanding options. One case was created with higher loading in order to push the system harder, while two further test cases were created using different load models. The first load model was a voltage dependent load model while the second was a full frequency and voltage dependent load. It is important to note that this test system was designed for the purposes of transient stability oscillations, and therefore is an inherently oscillatory system. Therefore, it is quite easy to make the system unstable but must be used as the number of dynamic test systems is limited. The details of the load models are given next.

- 68-bus TS-I
  - Frequency and voltage dependent load
- 68-bus TS-II
  - Voltage dependent load

- 68-bus TS-III
    - Stressed system for voltage

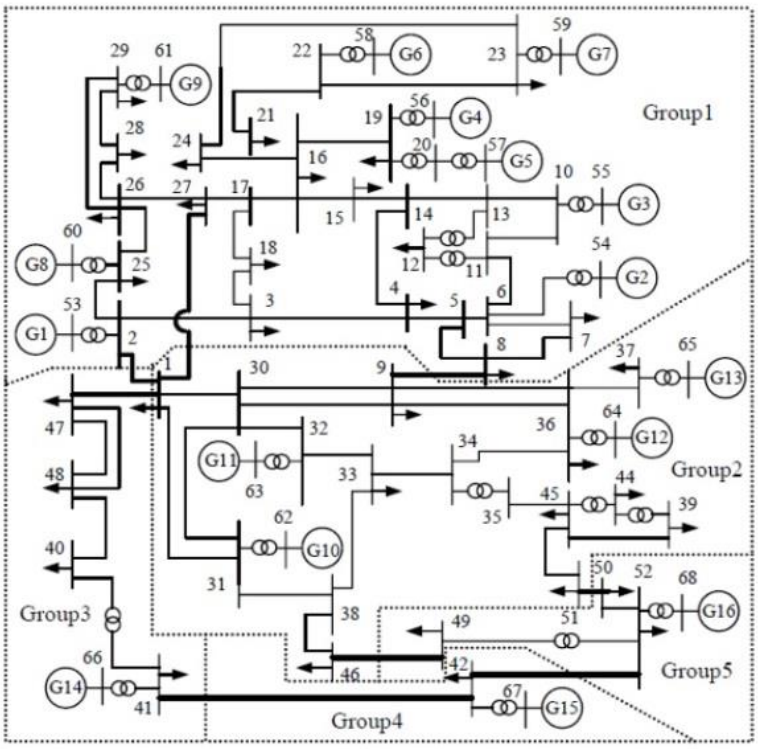

Figure 13-3 68 bus system

13.1.4 Load Modelling data

The section describes the different load models that were used in the 68 bus test systems in order to create a more realistic voltage scenario.

Voltage dependent model

PSAT contains a number of load models which can be used. For the voltage dependent load, data is not readily available, and therefore, the test case was developed using generic data from PSATs example models. For this case, half of the loads from the 68 bus system were taken and converted into voltage dependent loads based on this example data.

The voltage dependent loads were added to the 68 bus PSAT system in order to add a dynamic voltage condition. While the actual voltage collapse is not being considered here outside of the usual static limitations, the inclusion of this load was to allow for increased voltage stress on the system at the point splitting. If as a result of the switching actions, bus voltages reach significant under and over, such situations are created in order to be able to verify they can be detected.

This means that a voltage dependent load (VDL) is added to the system. VDLs are loads whose power are monomial functions of the bus voltage, where V_0 is the initial voltage at the load bus defined by the power flow solution:

$$P = P_0 \left(\frac{V}{V_0}\right)^{\alpha P} \tag{13.1.1}$$

$$Q = Q_0 \left(\frac{V}{V_0}\right)^{\alpha Q} \tag{13.1.2}$$

Frequency dependent model

A generalised exponential voltage frequency dependent load is modelled as follows [Hirsch 1994]: [142]

$$P = \frac{k_P}{100} \left(\frac{V}{V_0}\right)^{\alpha_P} (1 + \Delta w)^{B_p}$$

$$Q = \frac{k_Q}{100} \left(\frac{V}{V_0}\right)^{\alpha_Q} (1 + \Delta w)^{B_Q}$$

Where Δw represents the frequency deviation at the load bus, determined by filtering and differentiating the bus voltage phase angle θ as follows:

$$\dot{x} = -\frac{1}{T_F}\left(\frac{1}{2\pi f_0}\frac{1}{T_F}(\theta - \theta_0) + x\right)$$

$$\Delta w = x + \frac{1}{2\pi f_0}\frac{1}{T_F}(\theta - \theta_0)$$

And V_0 and θ_0 are the voltage magnitude and phase angle determined in the power flow solution. This component is initialized after power flow computations. A PQ load must be connected to the same bus, and its power and voltage ratings will be inherited by the frequency dependent load. The following table shows some typical coefficients for characteristic loads [143] [Berg 1973].

Table 13-1 Typical Load Coefficients

Load	$\boldsymbol{\alpha_P}$	$\boldsymbol{\alpha_Q}$	$\boldsymbol{\beta_P}$	$\boldsymbol{\beta_Q}$
Filament Lamp	1.6	0	0	0
Fluorescent Lamp	1.2	3.0	-0.1	2.8
Heater	2.0	0	0	0

Induction motor (half load)	0.2	1.6	1.5	-0.3
Induction Motor (Full load)	0.1	0.6	2.8	1.8
Reduction Furnace	1.9	2.1	-0.5	0
Aluminium Plant	1.8	2.2	-0.3	0.6

As the load models can't be created arbitrarily, the aim of this section is to define a benchmark to model system loads. Modelling purely voltage dependent, constant PQ or constant Z is unrealistic.

13.1.5 Developing the loads

In order to create a realistic load model, it was necessary to create loads which would represent a real system, and therefore information from [144] is used. The loads for typical days can be shown in Figure 13-4. These can then be broken down into types of industry according to Table 13-2 where the main loads in these industries are:

Industry 3 – 56% (Induction Motors, heaters, lighting)

Industry 4 - 7.5% (Induction Motors, heaters, furnaces,)

Industry 8 – 5.3% (heaters, lights)

Industry 11 – 13% (heaters, lights)

Leave the rest as PQ standard

The individual loads are broken down according to Table 13-3. This is based on an estimate of typical load.

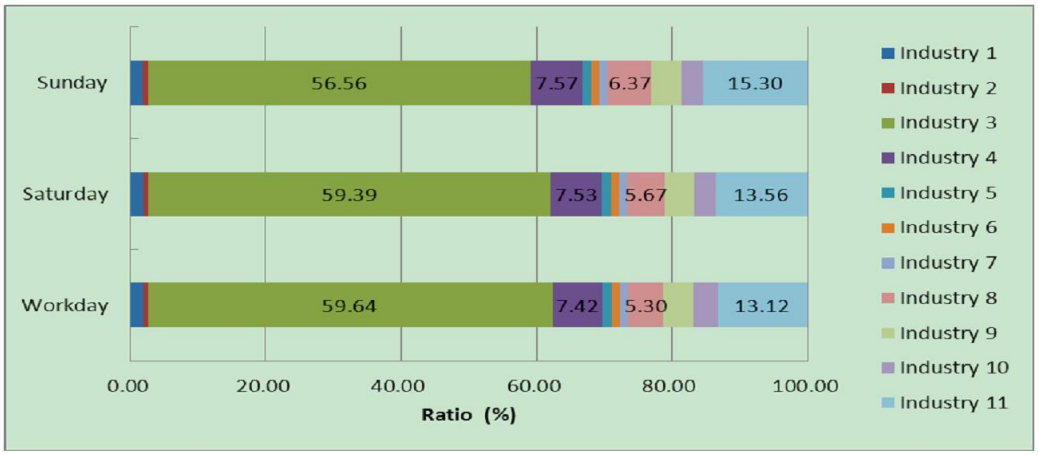

Figure 13-4 Typical load breakdown

Table 13-2 Types of industry

Industry	**Type**
Industry 1	Agricultural herd fishery industry
Industry 2	Mining
Industry 3	Manufacturing
Industry 4	Electricity, Gas and water production and supply
Industry 5	Construction
Industry 6	Transport
Industry 7	Information transmission, computer services
Industry 8	Commerce, hotels and catering industry
Industry 9	Finance, real estate business and residential services
Industry 10	Public utilities and management organizations
Industry 11	Residential electricity consumption

Table 13-3 Estimate of load breakdown

Industry	Induction motors	Furnaces	Heaters	Fluorescent lighting	Incandescent lighting
Industry 3	50	10	20	20	0
Industry 4	70	10	20	0	0
Industry 8	0	0	50	40	10
Industry 11	0	0	50	0	50

13.2 Appendix 2: Modal analysis

13.2.1 Background to the techniques [121]

7.1.1.1 V-Q Sensitivity analysis

The load-flow Jacobian can be created using equations 13.4.1 to 13.4.6 from [108].

$$\begin{bmatrix} \Delta P_1 \\ \vdots \\ \Delta P_N \\ \Delta Q_1 \\ \vdots \\ \Delta Q_N \end{bmatrix} = \begin{bmatrix} \frac{\partial P_1}{\partial \theta_1} & \cdots & \frac{\partial P_1}{\partial \theta_N} & \frac{\partial P_1}{\partial V_1} & \cdots & \frac{\partial P_1}{\partial V_N} \\ \vdots & \ddots & \vdots & \vdots & \ddots & \vdots \\ \frac{\partial P_N}{\partial \theta_1} & \cdots & \frac{\partial P_N}{\partial \theta_N} & \frac{\partial P_N}{\partial V_1} & \cdots & \frac{\partial P_N}{\partial V_N} \\ \frac{\partial Q_1}{\partial \theta_1} & \cdots & \frac{\partial Q_1}{\partial \theta_N} & \frac{\partial Q_1}{\partial V_1} & \cdots & \frac{\partial Q_1}{\partial V_N} \\ \vdots & \ddots & \vdots & \vdots & \ddots & \vdots \\ \frac{\partial Q_N}{\partial \theta_1} & \cdots & \frac{\partial Q_N}{\partial \theta_N} & \frac{\partial Q_N}{\partial V_1} & \cdots & \frac{\partial Q_N}{\partial V_N} \end{bmatrix} \begin{bmatrix} \Delta \theta \\ \vdots \\ \Delta \theta_N \\ \Delta V_1 \\ \vdots \\ \Delta V_N \end{bmatrix} \tag{13.2.1}$$

Or

$$\begin{bmatrix} \Delta P \\ \Delta Q \end{bmatrix} = \begin{bmatrix} J_{P\theta} & J_{PV} \\ J_{Q\theta} & J_{QV} \end{bmatrix} \begin{bmatrix} \Delta \theta \\ \Delta V \end{bmatrix} \tag{13.2.2}$$

Where the elements of the Jacobian are:

$$\frac{\partial P_i}{\partial \theta_j} = -V_i V_j \left[B_{ij} \cos(\theta_i - \theta_j) - G_{ij} \sin(\theta_i - \theta_j) \right] \quad \text{for } i \neq j \tag{13.2.3}$$

$$\frac{\partial P_i}{\partial \theta_i} = \sum_{\substack{j=1 \\ j \neq i}}^{N} V_i V_j \left[B_{ij} \cos(\theta_i - \theta_j) - G_{ij} \sin(\theta_i - \theta_j) \right]$$

$$\frac{\partial Q_i}{\partial \theta_j} = -V_i V_j \left[G_{ij} \cos(\theta_i - \theta_j) + B_{ij} \sin(\theta_i - \theta_j) \right] \quad \text{for } i \neq j \tag{13.2.4}$$

$$\frac{\partial Q_i}{\partial \theta_i} = \sum_{\substack{j=1 \\ j \neq i}}^{N} V_i V_j \left[G_{ij} \cos(\theta_i - \theta_j) + B_{ij} \sin(\theta_i - \theta_j) \right]$$

$$\frac{\partial P_i}{\partial V_j} = V_i \left[G_{ij} \cos(\theta_i - \theta_j) + B_{ij} \sin(\theta_i - \theta_j) \right] \quad \text{for } i \neq j \tag{13.2.5}$$

$$\frac{\partial P_i}{\partial V_i} = 2V_i G_{ii} + \sum_{\substack{j=1 \\ j\neq i}}^{N} V_j \left[G_{ij}\cos(\theta_i - \theta_j) + B_{ij}\sin(\theta_i - \theta_j)\right]$$

$$\frac{\partial Q_i}{\partial V_j} = V_i\left[G_{ij}\sin(\theta_i - \theta_j) - B_{ij}\cos(\theta_i - \theta_j)\right] \quad \text{for } i \neq j \tag{13.2.6}$$

$$\frac{\partial P_i}{\partial V_i} = -2V_i G_{ii} + \sum_{\substack{j=1 \\ j\neq i}}^{N} V_j \left[G_{ij}\sin(\theta_i - \theta_j) - B_{ij}\cos(\theta_i - \theta_j)\right]$$

$$J = \begin{bmatrix} J_{P\theta} & J_{PV} \\ J_{Q\theta} & J_{QV} \end{bmatrix} \tag{13.2.7}$$

The elements of the Jacobian matrix, J, give the sensitivity between the power flow and the bus voltage changes. If the conventional power flow model is used for voltage stability analysis, this Jacobian matrix is the same as the Jacobian matrix used when the power flow equations are solved using the Newton-Raphson technique [145]. The system voltage is affected by both P and Q, but P is kept constant at each operating point in order to evaluate voltage stability by looking at the incremental relationship between Q and V, comparable to the Q-V curve approach. Changes in P can be taken into account by studying Q-V at different operating points. Based on this, the following relation can be derived, with $\Delta P = 0$.

$$\Delta Q = J_R \Delta V \tag{13.2.8}$$

Where

$$J_R = \left[J_{QV} - J_{Q\theta} {J_{P\theta}}^{-1} J_{PV}\right] \tag{13.2.9}$$

J_R is the reduced Jacobian matrix of the system. For the change in voltage:

$$\Delta V = {J_R}^{-1} \Delta Q \tag{13.2.10}$$

The matrix ${J_R}^{-1}$ is the reduced V-Q Jacobian. Its i^{th} diagonal element is the V-Q sensitivity at bus *i*. A positive V-Q sensitivity suggests stable operation while the smaller the sensitivity, the more stable the system. On the other hand, a negative sensitivity suggests unstable operation with a small value being very unstable. The elements will indicate which way voltage will tend for a change in reactive power, so if the reactive power injection is increased and the corresponding voltage also increases, this will be observed by a positive sensitivity, and stable operation.

7.1.1.2 Q- V Modal analysis

Stability characteristics can be identified by performing Eigen-analysis on the reduced Jacobian matrix, J_R which was developed in [145]:

$$J_R = \xi \Lambda \eta \tag{13.2.11}$$

Where:

ξ = right eigenvector matrix of J_R
η = left eigenvector matrix of J_R
Λ = diagonal eigenvalue matrix of J_R

From the above equation:

$$J_R{}^{-1} = \xi \Lambda^{-1} \eta \tag{13.2.12}$$

And

$$\Delta V = \xi \Lambda^{-1} \eta \Delta Q \tag{13.2.13}$$

Or

$$\Delta V = \sum_i \frac{\xi_i \eta_i}{\lambda_i} \Delta Q \tag{13.2.14}$$

Where ξ_i is the i[th] column right eigenvector and η_i the i[th] row left eigenvector of J_R. Each eigenvalue λ_i and the corresponding right and left eigenvectors ξ_i and η_i define the i[th] mode of the Q-V response.

Since $\xi^{-1} = \eta$, it can be said:

$$\eta \Delta V = \Lambda^{-1} \eta \Delta Q \tag{13.2.15}$$

Or

$$v = \Lambda^{-1} q \tag{13.2.16}$$

where $v = \eta \Delta V$ is the vector of modal voltage variations and $q = \eta \Delta Q$ is the vector of modal reactive power variations. The above equation represents uncoupled first order equations, so, for the i[th] mode:

$$v_i = \frac{1}{\lambda_i} q_i \tag{13.2.17}$$

If $\lambda_i > 0$, the i[th] modal voltage and the i[th] modal reactive power variations are along the same direction which indicates that the system is voltage stable. If $\lambda_i < 0$, they are along opposite directions and this indicates the system is voltage unstable. The magnitude of each voltage variation is the inverse of λ_i times the magnitude of the modal reactive power variation. The smaller the value of λ_i, the closer the i[th] modal voltage is to being unstable. When $\lambda_i = 0$, the i[th]

modal voltage collapses because any change in the modal reactive power causes infinite change to the modal voltage.

7.1.1.3 Relationship between bus V-Q sensitivities and eigenvalues of J_R

From the equation seen earlier:

$$\Delta V = \sum_i \frac{\xi_i \eta_i}{\lambda_i} \Delta Q \tag{13.2.18}$$

Let $\Delta Q = e_k$ where e_k has all zero elements except for the kth element which is equal 1. So:

$$\Delta V = \sum_i \frac{\eta_{ik} \xi_i}{\lambda_i} \tag{13.2.19}$$

Where η_{ik} is the kth element of η_i. Then the V-Q sensitivity at bus *k* is given by:

$$\frac{\partial V_k}{\partial Q_k} = \sum_i \frac{\xi_{ki} \eta_{ik}}{\lambda_i} \tag{13.2.20}$$

The V-Q sensitivities cannot identify individual voltage collapse modes, instead they provide information regarding the combined effects of all modes of the voltage-reactive power variations. However, it is in getting more detailed information on voltage stability where the modal analysis becomes more useful, such as finding areas in the network which are weak, or finding certain lines that could be sensitive to changes of reactive power.

13.2.2 Participation factors

Participation factors are used to extract more detail on the voltage conditions of the system. There are three aspects which can be looked at which are bus, branch and generator participation factors. The factors are used to find if a component (bus, line or generator) has a high participation to a mode which may cause voltage instability. If there is a mode identified as being unstable, or close to unstable, the components which participate highly to these modes are of interest.

13.2.3 Bus Participation factors

The relative bus participation of bus k in mode i is given by the bus participation factor

$$B_{ki} = \xi_{ki} \eta_{ik} \tag{13.2.21}$$

From this, B_{ki} determines the contribution of λ_i to the V-Q sensitivity at bus *k*. The bus participation factors determine the areas associated with each mode. The size of the bus participation in a given mode indicates the effectiveness of remedial actions applied at that bus in stabilising the mode. Generally two types of modes summarised in Table 13-4:

Table 13-4 Description of Modes

Mode	Description	Typical occurrence
Localised	Few buses with large participations, all other buses close to zero participations	Single load connected to strong transmission system through long transmission line.
Non-localised	Many buses with small but similar degrees of participation, remaining buses close to zero.	When a region within a large system is loaded up and the main reactive power support in that region is exhausted

It may not always be practicable to find all eigenvalues of J_R, it is also not sufficient to only find the minimum as there is usually more than one weak mode associated with different parts of a system, the minimum node may not be the most troublesome. In practice, 5-10 of the smallest eigenvalues is usually sufficient to identify all the critical modes [145].

Branch Participation factors

In the same way that bus participation factors can be helpful in finding weak areas in a system, knowing which lines in a system are prone to affecting voltage stability, or indeed are better for remedial actions would be useful. For the purposes of ICI, it would be helpful to know if any of the lines in a cutset could affect stability if cut.

To compute the branch participation factors associated with mode i, assume that the vector of modal reactive power variations q has all elements equal to zero except for the i^{th} which equals 1. From equation (13.4.10), the corresponding vector of bus reactive power variations becomes

$$\Delta Q^i = \eta^{-1} q = \xi q = \xi_i \tag{13.2.22}$$

Where ξ_i us the i^{th} right eigenvector of J_r. If all the right eigenvectors are normalized so that

$$\sum \xi_{ji}^2 = 1 \tag{13.2.23}$$

With the vector of bus reactive power variations equal to ΔQ^i, the vector of bus voltage variations ΔV^i is

$$\Delta V^i = \frac{1}{\lambda_i} \Delta Q^i \tag{13.2.24}$$

While the corresponding vector of bus angle variation is

$$\Delta\theta^i = -J_{P\theta}^{-1} J_{PV} \Delta V^i \qquad (13.2.25)$$

With the angle and voltage variations for both the sending end and the receiving end known, the linearized change in branch reactive power loss can be calculated. Therefore, the branch participation is evaluated on the changes in the losses on the lines due to the modal angle and voltage changes. The relative participation of branch j in mode i is given by the participation factor:

$$L_{ji} = \frac{\Delta Q_{loss} \text{ for branch } j}{\text{maximum } \Delta Q_{loss} \text{ for all branches}} \qquad (13.2.26)$$

Branch participation factors indicate, for each mode, which branches consume the most reactive power in response to an incremental change in reactive load. They are useful for identifying remedial measures to alleviate voltage stability problems and for contingency selection.

13.2.4 Reactive power distribution factors

Single Line outage case

The purpose of the method is to quantify the voltage changes due to the outage of a line. This is done using a distribution factor method. In the basic case, it is assumed that all PV generators (including the slack bus) are not at their limits, so they can maintain constant power output and voltage level. The Jacobian matrix from a power-flow is used. Each PV node and slack bus is then removed from the Jacobian assuming they have not reached their limits. If they have not reached their limits, they can be assumed to keep constant Voltage and power, if they have reached their limits, then they will be treated as PQ nodes. This new Jacobian J* is made up of the nodes where voltages are not fixed.

The power flow equations are then formed as follows:

$$\begin{bmatrix}\Delta P \\ \Delta Q\end{bmatrix} = J^* \begin{bmatrix}\Delta\theta \\ \Delta V\end{bmatrix} \qquad (13.2.27)$$

The aim is to find the changes in voltages and angles due to a line outage, therefore, a line outage is modelled as injections of P and Q. The 2 bus example shown in Figure 13-5 shows power flow from bus i to bus j.

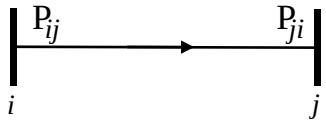

Figure 13-5 Original Line flow

If this was to be modelled as a line outage, the admittance Y_{ij} would need to be changed to zero and all diagonals associated with the line would need to be adjusted. This requires re-computation of the admittance matrix which is computationally expensive. A method developed in [146] proposes modelling the line as a series of injections instead of modifying the admittance matrix. Redrawing Figure 13-5 as a series of power injections is shown in Figure 13-6.

Figure 13-6 Line flow as power injections

This will provide the same result as in Figure 13-5 with small errors due to the addition of low admittance lines to connect the new generators/loads for the injections. The new injections are modelled as PQ loads and generators as they have a set PQ injection based on P_{ij} and P_{ji}. By running a new power flow with the modified network, there are 2 added buses for the outaged line, one at each end, which will form a new Jacobian of the size $(2n + 2l) \times (2n + 2l)$ where n is the original number of buses and l is the number of added buses. The Jacobian was modified to remove the slack node and PV nodes to form J^* which is $(2n + 2l - 2n_{PV} - 1) \times (2n + 2l - 2n_{PV} - 1)$ where n_{PV} is the total number of PV nodes (not at their limits).

To find the voltages and the angles as a result of the line outage, the following is used

$$\begin{bmatrix}\Delta\theta \\ \Delta V\end{bmatrix} = S \begin{bmatrix}\Delta P \\ \Delta Q\end{bmatrix} \tag{13.2.28}$$

Where $S = J^{*^{-1}}$

In order to model the line outage, the powers in the above equation are the negative of P_{ij} and P_{ji}, to simulate the outage of that line by the negative injection of their powers. Therefore, ΔP will have two non-zero terms corresponding to P_{ij} and P_{ji} where $\Delta P_i = P_{ij}$ and $\Delta P_j = P_{ji}$. The same applies for the injections of Q. Two terms are then formed for the real and reactive powers where the changes in voltage and angle are found for each of the real and reactive power injections.

$$\begin{bmatrix}\Delta\theta_P\\ \Delta V_P\end{bmatrix} = S\begin{bmatrix}\Delta P\\ 0\end{bmatrix} \quad (13.2.29)$$

$$\begin{bmatrix}\Delta\theta_Q\\ \Delta V_Q\end{bmatrix} = S\begin{bmatrix}0\\ \Delta Q\end{bmatrix} \quad (13.2.30)$$

Then, the combined effect of the real and reactive injections are found using:

$$\Delta V = \Delta V_P + \Delta V_Q \quad (13.2.31)$$

$$\Delta\theta = \Delta\theta_P + \Delta\theta_Q \quad (13.2.32)$$

The changes in voltages and angles are found due to the outage of a line using this method.

13.3 **Appendix 3: Generator models**

In order to model the dynamic behaviour of generators, dynamic models are required for the machines. As the ICI actions will introduce a number of line trips into the system, the dynamic assessment using time domain simulations must be done. As full dynamic assessment is not being carried out in this thesis, the full detailed models are not required, however a model sufficient to detail the voltage behaviour is required. The full theory behind the models outside the scope of this work and is not detailed here but full details and derivations can be found in [108] but the main equations governing each of the models are summarised here.

A generator model is detailed through different periods and the behaviour of the emfs in these periods. These are the subtransient and transient emfs. These emfs are modelled behind the appropriate reactance. The way the armature flux gradually moves through the rotor during a fault affects the nature of these emfs. This behaviour can be shown as follows:

$$T''_{d0}\dot{E}''_q = E'_q - E''_q + I_d(X'_d - X''_d) \tag{13.3.1}$$

$$T''_{q0}\dot{E}''_d = E'_d - E''_d - I_q(X'_q - X''_q) \tag{13.3.2}$$

$$T'_{d0}\dot{E}'_q = E_f - E'_q + I_d(X_d - X'_d) \tag{13.3.3}$$

$$T'_{q0}\dot{E}'_d = -E'_d - I_q(X_q - X'_q) \tag{13.3.4}$$

T''_{d0} T'_{d0}	Open circuit d-axis transient and subtransient time constants
T'_{q0} T''_{q0}	Open circuit q-axis transient and subtransient time constants
E''_q	q-axis component of the Sub-transient internal EMF proportional to the total flux linkages in the d axis damper winding and the field winding
E''_d	d axis component of the sub transient internal EMF proportional to the total flux linkages in the q-axis damper winding
E'_q	q-axis component of the transient internal emf proportional to the field winding flux linkage

E'_d	d-axis component of the transient internal emf proportional to the flux linkages in the q-axis solid steel rotor body
$I_d \ I_q$	D and q-axis component of the Armature current
$X_d \ X'_d \ X''_d$	d-axis synchronous, transient and subtransient reactance
$X_q \ X'_q \ X''_q$	q-axis synchronous, transient and subtransient reactance

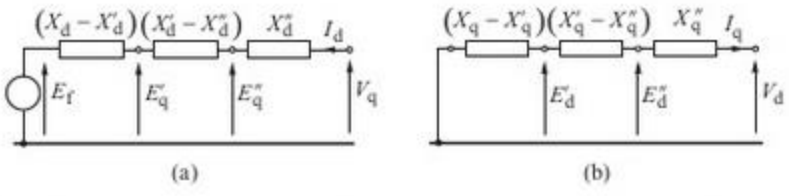

Figure 13-7 Generator equivalent circuits with resistances neglected (a) d-axis; (b) q-axis [108]

These equations all share a similar structure. The left hand side shows the time derivative of the emfs multiplied by the appropriate time constant.

The right hand side of the equation is linked to Figure 13-7 which shows the armature circuits for the d- and q- axes. The first component is the driving voltage while the final component relates to the voltage change in the relevant reactance. The right hand side of equation 13.3.1 constitutes Kirchhoff's voltage law for the middle part of the circuit shown in Figure 13-7a. This is the driving voltage E'_q, the voltage change $I_d(X'_d - X''_d)$ and the emf E''_q. Similarly equation 13.3.2 refers to the middle part of Figure 13-7b for the q-axis. In equation 13.5.3, the left part of the Figure 13-7a is derived with the driving voltage E_f, the voltage change $I_d(X_d - X'_d)$ and the emf E'_q. Finally equation 13.3.4 corresponds to the left hand part of Figure 13-7b but here there is no driving voltage due to the lack of excitation in the q-axis.

From Equations 13.3.1-13.3.4, different generator models of decreasing complexity and accuracy can be developed. The model number indicates the number of differential equations required. The larger the number, the greater the model complexity and solution time.

Sixth Order model

The sixth order model is the most detailed model where the generator is represented by the subtransient emfs E_q'' and E_d'' behind the subtransient reactances X_q'' and X_d''. It is defined by the modified armature voltage equations in 13.3.5. The differential equations 13.5.1-13.5.4 describe how the emfs change as the flux linking the rotor circuit decays. The speed deviation and angle change of the rotor must be also be included as in 13.3.6

$$\begin{bmatrix} V_d \\ V_q \end{bmatrix} = \begin{bmatrix} E_d'' \\ E_q'' \end{bmatrix} - \begin{bmatrix} R & X_q'' \\ -X_d'' & R \end{bmatrix} \begin{bmatrix} I_d \\ I_q \end{bmatrix} \tag{13.3.5}$$

$$\frac{d\Delta\omega}{dt} = \frac{1}{M}(P_m - P_e - D\Delta\omega), \qquad \Delta\omega = \omega - \omega_s = \frac{d\delta}{dt} \tag{13.3.6}$$

Where P_e is the air-gap electrical power, P_m is the mechanical turbine power, D is the damping power co-efficient, ω is the generator rotational speed, ω_s is the synchronous speed and $\Delta\omega$ is the speed deviation.

Equations 13.3.1 and 13.3.2 include the influence of the damper windings, therefore the damping co-efficient in the swing equation need only quantify the mechanical damping due to the windage and friction. This is usually small and so can be neglected and $D \approx 0$. For the sixth order model, the full set of differential equations describing the generator are:

$$M\Delta\dot{\omega} = P_m - P_e \tag{13.3.7}$$

$$\dot{\delta} = \Delta\omega \tag{13.3.8}$$

$$T_{d0}'\dot{E'}_q = E_f - E_q' + I_d(X_d - X_d') \tag{13.3.9}$$

$$T_{q0}'\dot{E}_d' = -E_d' - I_q(X_q - X_q') \tag{13.3.10}$$

$$T_{d0}''\dot{E''}_q = E'_q - E_q'' + I_d(X'_d - X_d'') \tag{13.3.11}$$

$$T_{q0}''\dot{E}_d'' = E_d' - E''_d - I_q(X'_q - X_q'') \tag{13.3.12}$$

The changes in mechanical power P_m in 13.3.7 should be calculated using the models of turbines and their governing systems. Accordingly, changes in emf E_f in the 13.3.9 should be calculated using the models of excitation systems. The air gap power of the generator can be calculated from 13.3.13.

$$P_e = \left(E_d'' I_d + E_q'' I_q\right) + \left(X_d'' - X_q''\right) I_d I_q \tag{13.3.13}$$

Fifth order model

In this model the screening effect of the rotor body eddy currents in the q-axis is neglected so that $X'_q = X_q$ and $E'_d = 0$. Equation 13.3.4 from the equation set of the sixth order model is eliminated to give a set of five differential equations:

$$M\Delta\dot{\omega} = P_m - P_e \tag{13.3.14}$$

$$\dot{\delta} = \Delta\omega \tag{13.3.15}$$

$$T'_{d0}\dot{E'}_q = E_f - E'_q + I_d(X_d - X'_d) \tag{13.3.16}$$

$$T''_{d0}\dot{E''}_q = E'_q - E''_q + I_d(X'_d - X''_d) \tag{13.3.17}$$

$$T''_{q0}\dot{E''}_d = E'_d - E''_d - I_q(X'_q - X''_q) \tag{13.3.18}$$

Fourth Order model

The fourth order model is used predominantly in this thesis. The full sixth order model is not required where the effect of damper windings in the sixth order model can be neglected. The generator can be represented by the transient emfs E'_q and E'_d behind the transient reactances. It is defined by:

$$\begin{bmatrix} V_d \\ V_q \end{bmatrix} = \begin{bmatrix} E'_d \\ E'_q \end{bmatrix} - \begin{bmatrix} R & X'_q \\ -X'_d & R \end{bmatrix} \begin{bmatrix} I_d \\ I_q \end{bmatrix} \tag{13.3.19}$$

The changes in the emfs E'_q and E'_d are determined from 13.5.20 and 13.5.21.

$$T'_{d0}\dot{E'_q} = E_f - E'_q + I_d(X_d - X'_d) \tag{13.3.20}$$

$$T'_{q0}\dot{E'_d} = -E'_d + I_d(X_q - X'_q) \tag{13.3.21}$$

$$P_e = E'_q I_q + E'_d I_d + (X'_d - X'_q) I_d I_q \tag{13.3.22}$$

As the damper windings are ignored, the air gap power is calculated by 13.3.22. This equation neglects the synchronous torque produced by the damper windings. Consequently the damping co-efficient in the swing equation should be increased by an amount corresponding to the average asynchronous torque, or power, calculated using 13.3.23.

$$P_D = \left[D_d \sin^2 \delta + D_q \cos^2 \delta\right]\Delta\omega = D(\delta)\Delta\omega \tag{13.3.23}$$

Where D_d, D_q are the damping co-efficient of both axis. Under these assumptions, the model is described by the following four differential equations

$$M\dot{\Delta\omega} = P_m - P_e - \Delta D\omega \tag{13.3.24}$$

$$\dot{\delta} = \Delta\omega \tag{13.3.25}$$

$$T'_{d0}\dot{E'_q} = E_f - E'_q + I_d(X_d - X'_d) \tag{13.3.26}$$

$$T'_{q0}\dot{E'_d} = -E'_d + I_d(X_q - X'_q) \tag{13.3.27}$$

Changes in mechanical power P_m and emf E_f should be calculated as in the sixth order model. This simplified model of the synchronous generator is widely considered to be sufficiently accurate to analyse electromechancial dynamics. The main disadvantage of this model is that the equivalent damping co-efficient appearing in the swing equation can only be calculated approximately.

The third order model is similar to the fourth order model except the d-axis transient emf E'_d is assumed to remain constant.

Classical Model/2nd Order

The classical model is widely accepted for use in simplified dynamic stability analyses. This model assumes that the d-axis armature current I_d or the internal emf E_f representing the excitation voltage will not change much in the transient period. The classical model is represented by a constant emf E' behind a transient reactiance X'_d and the swing equation:

$$M\dot{\Delta\omega} = P_m - P_e - D\Delta\omega \tag{13.3.28}$$

$$\dot{\delta} = \Delta\omega \tag{13.3.29}$$

The justification of the classical model is that the time constant T'_{d0} is relatively long, the order of a few seconds. Therefore, E'_q does not change much providing that changes to E_f and I_d are small. This means that $E'_q \approx$ constant and, because it has already been assumed that E'_d= constant in the 3rd order model, both the magnitude of the transient emf E' and its position α with respect to the rotor are assumed constant.

13.4 Appendix 4: Clustering Results

An example of the clustering results is shown below. These results were produced by **Dr. Ruben Garcia-Sanchez** who was working in parallel with this project to investigate graph theory techniques for ICI. These results are for the 39 bus system with a seed node 19. The results show the results of the minimal energy imbalance spectral clustering which can be selected for any island size. It has been greatly enhanced compared to the simple options of splitting a system in two halves. This method allows the operator to choose the island size (no. of nodes) and the results show the best island for that size. The size column is the second column. If an operator wants an island of 5 nodes, they will select all nodes until they reach the row corresponding to size 5. I.e. nodes [19 33 16 15 17]. These are the 5 most highly connected nodes and will be grouped together to form the island of 5 nodes. The related total power cut (Boundary (MW)) and power imbalance (energy (MW)) are shown in columns 4 and 5.

Node				
19	BEST ISLANDS AROUND 19 SORTED BY SIZE:			
33	Size = 1	Ratio = 100.00%	(boundary = 1264.00,	energy = -0.00)
16	Size = 2	Ratio = 33.33%	(boundary = 632.00,	energy = -632.00)
15	Size = 3	Ratio = 32.73%	(boundary = 1062.80,	energy = -303.00)
17	Size = 4	Ratio = 14.92%	(boundary = 460.00,	energy = -460.00)
18	Size = 5	Ratio = 20.09%	(boundary = 890.80,	energy = -131.00)
20	Size = 6	Ratio = 13.48%	(boundary = 640.94,	energy = 189.00)
34	Size = 7	Ratio = 12.31%	(boundary = 640.94,	energy = 189.00)
21	Size = 8	Ratio = 8.15%	(boundary = 597.25,	energy = -507.00)
22	Size = 9	Ratio = 4.54%	(boundary = 347.39,	energy = -187.00)
14	Size = 10	Ratio = 4.29%	(boundary = 347.39,	energy = -187.00)
24	Size = 11	Ratio = 2.27%	(boundary = 189.39,	energy = -29.00)
35	Size = 12	Ratio = 2.73%	(boundary = 261.04,	energy = -190.90)
23	Size = 13	Ratio = 2.61%	(boundary = 261.04,	energy = -190.90)
36	Size = 14	Ratio = 1.00%	(boundary = 103.04,	energy = -32.90)
13	Size = 15	Ratio = 3.16%	(boundary = 333.47,	energy = 248.10)
27	Size = 16	Ratio = 4.22%	(boundary = 472.47,	energy = 387.10)
3	Size = 17	Ratio = 5.13%	(boundary = 614.69,	energy = 467.10)
12	Size = 18	Ratio = 6.86%	(boundary = 851.32,	energy = 789.10)
10	Size = 19	Ratio = 1.04%	(boundary = 131.97,	energy = 46.60)
26	Size = 20	Ratio = 7.42%	(boundary = 958.03,	energy = 539.10)
32	Size = 21	Ratio = 3.00%	(boundary = 339.54,	energy = -269.40)
2	Size = 22	Ratio = 6.29%	(boundary = 684.40,	energy = 52.60)
30	Size = 23	Ratio = 5.25%	(boundary = 517.54,	energy = 52.60)
1	Size = 24	Ratio = 2.78%	(boundary = 267.54,	energy = -197.40)
28	Size = 25	Ratio = 1.82%	(boundary = 169.94,	energy = -99.80)

29	Size = 26	Ratio = 1.22%	(boundary = 112.43,	energy = 4.20)
4	Size = 27	Ratio = 7.51%	(boundary = 648.83,	energy = 4.20)
38	Size = 28	Ratio = 6.20%	(boundary = 504.20,	energy = 504.20)
25	Size = 29	Ratio = 6.86%	(boundary = 515.86,	energy = 504.20)
39	Size = 30	Ratio = 7.00%	(boundary = 522.36,	energy = 510.70)
37	Size = 31	Ratio = 6.96%	(boundary = 519.23,	energy = 519.23)
11	Size = 32	Ratio = 9.79%	(boundary = 544.54,	energy = -137.27)
9	Size = 33	Ratio = 11.05%	(boundary = 539.13,	energy = -137.27)
5	Size = 34	Ratio = 11.31%	(boundary = 545.63,	energy = -130.77)
6	Size = 35	Ratio = 14.28%	(boundary = 393.49,	energy = 334.00)
8	Size = 36	Ratio = 26.53%	(boundary = 599.49,	energy = 540.00)
31	Size = 37	Ratio = 70.39%	(boundary = 110.50,	energy = -110.50)

13.5 Appendix 5: Slow Coherency

The following section has been created from a report on slow coherency from ***Dr. Zhenzhi Lin*** *describing slow coherency and finding the coherent groups on the 39 bus system:*

There are generally three main methods by which to identify coherent groups of generators such as observation of the generator angle or speed, eigenvalue analysis of the state matrices or from phasor angle measurements. Methods using eigenvalue analysis are suitable for small disturbances and would need to be recalculated for any change in the state matrix. Slow coherency based controlled islanding is based on the eigenvalue analysis, so the various disturbances and/or different power system conditions are not considered, and the threshold for slow modes will impact the number of coherent generator groups.

For ICI, once coherent groups of generators are determined, the optimum cut sets are found to split the systems into several islands based on the coherent generator groups. There are two objectives for determining optimum cut sets, minimal generation-load imbalance and minimal generation-load disruption. There are a number of methods by which to use coherency to form islands, however these have been covered in Chapter 3. The definition of coherency and slow coherency based on modal analysis is as follows [147]:

The states x_i and x_j of a system $\dot{x} = Ax$ are slowly coherent if and only if they are coherent with respect to a set of *r* slowest modes σ_a of the system.

In [148], a generator coherency index is defined as follows.

$$I_{ij} = \frac{w_i w_j^T}{|w_i||w_j|}$$

where w_i and w_j are respectively the *i*-th and *j*-th row vectors of slow right eigenvector transfer matrix *V*. If I_{ij} is larger than ε_2, it can be concluded that the *i*-th generator is coherent with the *j*-th generator.

Slow coherency is based on the observation of oscillations of large-scale power systems. Oscillations in power systems can be classified into two types of modes, local modes (1-3Hz) and inter-area modes (<1Hz). After the decay of the fast local dynamics, generators in the same area

will swing together and are termed 'coherent' as they oscillate with these slow modes. Generators can then be grouped together based on their participation to the selected inter-area modes. Coherent groups of generators are independent of the location and severity of the disturbance allowing a linearized model to be used to determine coherency. The 39-bus power system shown in Figure 13-2 is used to compare coherency and tracing based ICI. The fifth-order generator model is used for all the generators in the test system. The detailed data associated with this power system can be found in [149].

13.5.1 Slow coherency based ICI

The methods described here are used to perform eigenvalue analysis on the 39-bus power system. The inter-area modes less than 1 Hz are selected for determining slow coherency, and the threshold ε_2 for generator coherency is chosen as 0.6. The results from the eigenvalue analysis and coherency indices of generators with the detailed model can be found in Table 13-5 to Table 13-6.

Table 13-5 Coherency Results

Generator model	Slowest modes	Coherent groups of generators
5th Order	*f*=0.1Hz, 0.606Hz, 0.873Hz, 0.931Hz	[G1, G8, G9], [G2, G3], [G4-G7], [G10]

It can be seen from Table 13-5 that there are four slow modes, i.e. 0.1Hz, 0.606 Hz, 0.873 Hz and 0.931 Hz. The coherency indexes of generators can then be obtained based on these modes. It can be seen from Table 13-6 that ten generators can be divided into four coherent groups, i.e. [G1, G8, G9], [G2, G3], [G4, G5, G6, G7] and [G10].

Using these coherent groups of generators, the power system can be split into four controlled islands by using minimal cutset of power flow disruption. It is these islands which are used in Chapter 11.

Table 13-6 Coherency indexes of generators with detailed model

	G1	**G2**	**G3**	**G4**	**G5**	**G6**	**G7**	**G8**	**G9**	**G10**
G1	1	0.2003	0.4698	0.036	-0.3468	0.3373	0.3545	0.9892	0.7953	-0.4656
G2	0.2003	1	0.902	-0.1064	-0.3287	0.1241	0.1181	0.0721	-0.2741	-0.2248
G3	0.4698	0.902	1	0.2331	-0.0982	0.4986	0.4916	0.3433	-0.121	-0.4106
G4	0.036	-0.1064	0.2331	1	0.9114	0.9354	0.9211	-0.0016	-0.3246	-0.3205

G5	-0.3468	-0.3287	-0.0982	0.9114	1	0.7101	0.6914	-0.3557	-0.5261	-0.0848
G6	0.3373	0.1241	0.4986	0.9354	0.7101	1	0.9961	0.2737	-0.1336	-0.5243
G7	0.3545	0.1181	0.4916	0.9211	0.6914	0.9961	1	0.2887	-0.1027	-0.5945
G8	0.9892	0.0721	0.3433	-0.0016	-0.3557	0.2737	0.2887	1	0.8614	-0.3876
G9	0.7953	-0.2741	-0.121	-0.3246	-0.5261	-0.1336	-0.1027	0.8614	1	-0.2414
G10	-0.4656	-0.2248	-0.4106	-0.3205	-0.0848	-0.5243	-0.5945	-0.3876	-0.2414	1

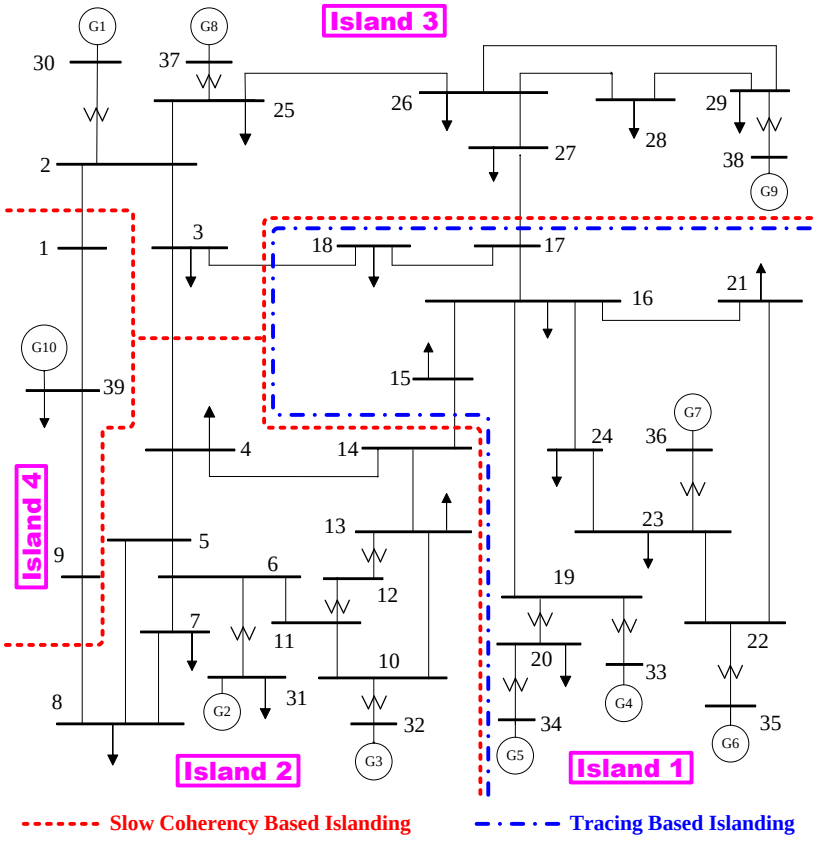

Figure 13-8 Coherent groups

Bibliography

1. Bialek, J.W., *Why has it happened again? Comparison between the UCTE blackout in 2006 and the blackouts of 2003.* 2007 IEEE Lausanne Powertech, Vols 1-5, 2007: p. 51-56.
2. Ministry of power, G.o.I., *Report of the Enquiry Committee on Grid Disturbance in Northern Region on 30th July 2012 and in Northern, Eastern & North-Eastern Region on 31st July 2012*, 2012.
3. Federal Energy Regulatory Commission, N.A.E.R.C., *Arizona-Southern California Outages on September 8, 2011 – Causes and Recommendations*, 2012.
4. National Grid, *Updates from the November 2009 Brazilian Blackout - A simplified account based on public documents*, 2010.
5. U.S. Canada Power System Outage Task force, *Final Report on the August 14, 2003 Blackout in the United States and Canada: Causes and Recommendations*, 2004.
6. Elkraft System, *Power failure in Eastern Denmark and Southern Sweden on 23 September 2003 - Final Report on the course of events*, 2003.
7. UCTE, *FINAL REPORT of the Investigation Committee on the 28 September 2003 Blackout in Italy*, 2004.
8. Bialek, J.W., *Recent Blackouts in US and Continental Europe: Is Liberalisation to Blame?* Cambridge Working Papers in Economics, 2004(CMI Working Paper 34).
9. Union for the co-ordination of transmission of electricity, *Final Report, System Disturbance on 4 November 2006*, 2007.
10. Task Force on Understanding Prediction Mitigation and Restoration of Cascading Failures of the IEEE Computing & Analytical Methods (CAMS) Subcommittee, *Mitigation and Prevention of Cascading Outages: Methodologies and Practical Applications*, in *IEEE Power and Energy Society General Meeting* 2013: Vancouver.
11. Knight, U.G., *Power systems in emergencies : from contingency planning to crisis management* 2001, Chichester: John Wiley & Sons.
12. Madani, V., M. Adamiak, and M. Thakur, *Design and implementation of wide area special protection schemes.* 2004 57th Annual Conference for Protective Relay Engineers, 2004: p. 392-402.
13. Anderson, P.M., *Power system protection* 1999, New York ; London: McGraw-Hill.
14. Heniche, A., Kamwa, I., Dobrescu, M.,. *Hydro-Quebec's defense plan: Present and future*. in *Power and Energy Society General Meeting (PES), 2013 IEEE*. 2013.
15. Moshref, A., et al., *Design of a special protection system to maintain system security at high import.* 2003 IEEE Power Engineering Society General Meeting, Vols 1-4, Conference Proceedings, 2003: p. 311-319.
16. Pimjaipong, W., T. Junrussameevilai, and N. Maneerat. *Blackout Prevention Plan; The Stability, Reliability and Security Enhancement in Thailand Power Grid*. in *Transmission and Distribution Conference and Exhibition: Asia and Pacific, 2005 IEEE/PES*. 2005.
17. Gomes, P., et al. *An innovative special protection system involving long distance actions*. in *Bulk Power System Dynamics and Control (iREP) - VIII (iREP), 2010 iREP Symposium*. 2010.
18. De La Quintana, A. and R. Palma-Behnke. *Challenges for special protection systems in the Chilean electricity market*. in *Power and Energy Society General Meeting (PES), 2013 IEEE*. 2013.
19. Fu, W.H., et al., *Risk assessment for special protection systems.* IEEE Transactions on Power Systems, 2002. **17**(1): p. 63-72.

20. Wang, L., F. Howell, and K. Morison, *A Framework For Special Protection System Modeling For Dynamic Security Assessment of Power Systems.* 2008 Joint International Conference on Power System Technology (Powercon) and Ieee Power India Conference, Vols 1 and 2, 2008: p. 588-593.
21. Zhu, J., *Optimization of power system operation* 2009, Piscataway, N.J.: Wiley-IEEE ; Chichester : John Wiley [distributor].
22. H. Seyedi, M.S.-P., *Design of New Load Shedding Special Protection Schemes for a Double Area Power System.* American Journal of Applied Sciences, 2009. **6**(2): p. 317-327.
23. Michel, A.N., D. Liu, and P.J. Antsaklis, *Stability and control of dynamical systems with applications : a tribute to Anthony N. Michel,* 2003, Boston ; Basel.
24. Terzija, V.V., *Adaptive underfrequency load shedding based on the magnitude of the disturbance estimation.* Power Systems, IEEE Transactions on, 2006. **21**(3): p. 1260-1266.
25. McCalley, J.D., *Frequency control (MW-Hz) with wind*, in *PSERC Seminar* 2010.
26. Horowitz, S.H. and A.G. Phadke, *Power system relaying* 1992: Research Studies Press.
27. Horowitz, S.H., A.G. Phadke, and J.S. Thorp, *Adaptive transmission system relaying.* Power Delivery, IEEE Transactions on, 1988. **3**(4): p. 1436-1445.
28. Jongepier, A.G. and L. Van der Sluis, *Adaptive distance protection of a double-circuit line.* Power Delivery, IEEE Transactions on, 1994. **9**(3): p. 1289-1297.
29. Sidhu, T.D., D. Sebastian Baltazar, and M.S. Sachdev, *A New Method for Determining Settings of Zone-2 Distance Relays.* Electric Power Components and Systems, 2004. **32**(3): p. 275-293.
30. Yi, H., et al., *An adaptive scheme for parallel-line distance protection.* Power Delivery, IEEE Transactions on, 2002. **17**(1): p. 105-110.
31. Zhu, Y., S. Song, and D. Wang, *Multiagents-based wide area protection with best-effort adaptive strategy.* International Journal of Electrical Power & Energy Systems, 2009. **31**(2–3): p. 94-99.
32. Ojaghi, M., M. Azari, and K. Mazlumi. *New adaptive scheme for calculating zone-3 setting of distance relay*. in *Industrial Technology (ICIT), 2013 IEEE International Conference on*. 2013.
33. Seong-Il, L., et al., *Blocking of Zone 3 Relays to Prevent Cascaded Events.* Power Systems, IEEE Transactions on, 2008. **23**(2): p. 747-754.
34. El-Hadidy, A. and C. Rehtanz. *A new algorithm to improve the operation of distance relays zone 3 by using Synchronized Phasor Measurements*. in *Modern Electric Power Systems (MEPS), 2010 Proceedings of the International Symposium*. 2010.
35. Nan, Z. and M. Kezunovic. *A study of synchronized sampling based fault location algorithm performance under power swing and out-of-step conditions*. in *Power Tech, 2005 IEEE Russia*. 2005.
36. Dean, S.M., *The design and operation of a metropolitan electrical system from the viewpoint of possible major shutsowns (Detroit).* AIEE transactions, 1940. **59**: p. 575-579.
37. Schleif, F.R., *A swing relay for the east-west intertie.* IEEE Transactions on Power Apparatus and Systems, 1969. **88**: p. 821-825.
38. Henner, V.E., *A Network Separation Scheme for Emergency Control.* International Journal of Electrical Power & Energy Systems, 1980. **2**(2): p. 109-114.
39. Persoz, H., *Automatic operation in case of a serious incident*, in *CIGRE SC 32 Report 69-A1-2(0)* 1969.
40. Stepunin S. Ye., S., V. M. , *Divider protection against stable asynchonous conditions in power systems.* Electrical technology (USSR), 1966. **2-3**: p. 202-217.
41. Dicaprio, U., *Emergency Control.* International Journal of Electrical Power & Energy Systems, 1982. **4**(1): p. 19-28.

42. Bertigny, F., Gaborit, S., Guidicelli, M. , *Dispositions de sauvegarde dans les reseaux de transport et de distribution d'energie electrique - limitation des consequences d'un incident grave et acceleration de la reprise de service*, in *Rev. Gen. Electr*1978.
43. Knight, U.G., *Aids for the emergency control of power systems.* Electra. **67**.
44. Quintana, V.H. and N. Muller, *Partitioning of Power Networks and Applications to Security Control.* IEE Proceedings-C Generation Transmission and Distribution, 1991. **138**(6): p. 535-545.
45. Muller, N. and V.H. Quintana, *A Sparse Eigenvalue-Based Approach for Partitioning Power Networks.* IEEE Transactions on Power Systems, 1992. **7**(2): p. 520-527.
46. Ross, H.B., et al., *An Agc Implementation for System Islanding and Restoration Conditions.* IEEE Transactions on Power Systems, 1994. **9**(3): p. 1399-1410.
47. Jyrinsalo, J.L., E. O., *Planning the Islanding Scheme of a Regional Power Producer*, in *Electricity Distribution, 1993. CIRED. 12th International Conference* 1993: Birmingham.
48. You, H.B., V. Vittal, and X.M. Wang, *Slow coherency-based islanding.* IEEE Transactions on Power Systems, 2004. **19**(1): p. 483-491.
49. Yusof, S.B., G.J. Rogers, and R.T.H. Alden, *Slow Coherency Based Network Partitioning Including Load Buses.* IEEE Transactions on Power Systems, 1993. **8**(3): p. 1375-1382.
50. Gallai, A.M. and R.J. Thomas, *Coherency Identification for Large Electric-Power Systems.* IEEE Transactions on Circuits and Systems, 1982. **29**(11): p. 777-782.
51. Ni, Y., V. Vittal, and W. Kliemann, *System separation mechanism in the neighbourhood of a relevant type-n UEP using the normal form of vector fields.* IEE Proceedings-Generation Transmission and Distribution, 1998. **145**(2): p. 139-144.
52. Thapar, J., et al., *Application of the normal form of vector fields to predict interarea separation in power systems.* IEEE Transactions on Power Systems, 1997. **12**(2): p. 844-850.
53. Vittal, V., et al., *Determination of generator groupings for an islanding scheme in the Manitoba Hydro system using the method of normal forms.* IEEE Transactions on Power Systems, 1998. **13**(4): p. 1345-1351.
54. You, H., V. Vittal, and Z. Yang, *Self-healing in power systems: An approach using islanding and rate of frequency decline-based load shedding.* IEEE Transactions on Power Systems, 2003. **18**(1): p. 174-181.
55. Wang, X.V., V.;, *System islanding using minimal cutsets with minimum net flow*, in *Power Systems Conference and Exposition, 2004. IEEE PES*2004. p. 379 - 384.
56. Yang, B.V., V; Heydt, G. T.;, *Slow-Coherency-Based Controlled Islanding—A Demonstration of the Approach on the August 14, 2003 Blackout Scenario.* IEEE Transactions on Power Systems, 2006. **21**(4): p. 1840-1847.
57. Kamwa, I., A.K. Pradhan, and G. Joos, *Automatic segmentation of large power systems into fuzzy coherent areas for dynamic vulnerability assessment.* IEEE Transactions on Power Systems, 2007. **22**(4): p. 1974-1985.
58. Kamwa, I., et al., *Fuzzy Partitioning of a Real Power System for Dynamic Vulnerability Assessment.* IEEE Transactions on Power Systems, 2009. **24**(3): p. 1356-1365.
59. Shuti, F.Z., Xu;, *An Intelligent Approach for System Separation to Prevent a Blackout*, in *Power System Technology (POWERCON), 2010 International Conference on*2010: Hangzhou.
60. Hashiesh, F., Mostafa, H. E., Helal, I., Mansour, M.,, *A wide area synchrophasors based controlled islanding scheme using Bioinformatics toolbox* in *Developments in Power Systems Protection, 2012. DPSP 2012. 11th International Conference on*2012: Birmingham, UK.
61. Honglei, S., Junyong, W., Linfeng, W.;, *Controlled islanding based on slow-coherency and KWP theory*, in *IEEE,Innovative Smart Grid Technologies - Asia (ISGT Asia),* 2012: Tianjin.

62. Irving, M.R. and M.J.H. Sterling, *Optimal Network Tearing Using Simulated Annealing.* IEE Proceedings-C Generation Transmission and Distribution, 1990. **137**(1): p. 69-72.
63. Bout, D.E.V.D., Miller, T. K.,, *Graph partitioning annealed neural networks.* IEEE Transactions on Neural Networks, 1990. **1**(2): p. 192-203.
64. Kai, S., et al., *A two-phase method based on OBDD for searching for splitting strategies of Large-Scale power systems.* Powercon 2002: International Conference on Power System Technology, Vols 1-4, Proceedings, 2002: p. 834-838.
65. Zhao, Q.C., et al., *A study of system splitting strategies for island operation of power system: A two-phase method based on OBDDs.* IEEE Transactions on Power Systems, 2003. **18**(4): p. 1556-1565.
66. Sun, K., D.Z. Zheng, and Q.A. Lu, *Splitting strategies for islanding operation of large-scale power systems using OBDD-based methods.* IEEE Transactions on Power Systems, 2003. **18**(2): p. 912-923.
67. Sun, K., D.Z. Zheng, and Q. Lu, *A simulation study of OBDD-based proper consideration of transient stability splitting strategies for power systems under.* IEEE Transactions on Power Systems, 2005. **20**(1): p. 389-399.
68. Sun, K., D.Z. Zheng, and Q. Lu, *Searching for feasible splitting strategies of controlled system islanding.* IEE Proceedings-Generation Transmission and Distribution, 2006. **153**(1): p. 89-98.
69. Lin, H.Y., S.Y. Kuo, and F.M. Yeh, *Minimal cutset enumeration and network reliability evaluation by recursive merge and BDD.* Eighth IEEE International Symposium on Computers and Communication, Vols I and Ii, Proceedings, 2003: p. 1341-1346.
70. Liu, W.X., D.A. Cartes, and G.K. Venayagamoorthy, *Particle swarm optimization based defensive islanding of large scale power system.* 2006 IEEE International Joint Conference on Neural Network Proceedings, Vols 1-10, 2006: p. 1719-1725.
71. Liu, L., Li L., Cartes, D. A.,, *Slow Coherency and Angle Modulated Particle Swarm OptimizationBased Islanding of Large Scale Power Systems*, in *Neural Networks, 2007. IJCNN 2007. International Joint Conference* 2007: Orlando, FL.
72. Liu, W.X., L. Liu, and D.A. Cartes, *Angle modulated particle swarm optimization based defensive islanding of large scale power systems.* 2007 IEEE Power Engineering Society Conference and Exposition in Africa, Vols 1 and 2, 2007: p. 334-341.
73. Shen, C., et al., *An efficient method of network simplification for islanding control studies of power systems.* 2006 International Conference on Power Systems Technology: POWERCON, Vols 1- 6, 2006: p. 1698-1703.
74. Zhou, Z.G., et al., *A New Islanding Boundary Searching Approach Based on Slow Coherency and Graph Theoretic.* Icnc 2008: Fourth International Conference on Natural Computation, Vol 6, Proceedings, 2008: p. 438-442.
75. Najafi, S., *Evaluation of Interconnected Power Systems Controlled Islanding.* 2009 IEEE Bucharest Powertech, Vols 1-5, 2009: p. 878-885.
76. Wang, C.G., et al., *A Novel Fast Searching Algorithm for Power System Self-adaptive Islanding.* 2009 Asia-Pacific Power and Energy Engineering Conference (Appeec), Vols 1-7, 2009: p. 1503-1508.
77. Wang, C., Zhang, B., Hao Z, Bo Z, Sun Y, , *Study on power system self-adaptive islanding*, in *Advanced Power System Automation and Protection (APAP), 2011 International Conference on* 2011: Beijing.
78. Xu, G.Y. and V. Vittal, *Slow Coherency Based Cutset Determination Algorithm for Large Power Systems.* IEEE Transactions on Power Systems, 2010. **25**(2): p. 877-884.
79. Xu, G.Y., et al., *Controlled Islanding Demonstrations on the WECC System.* IEEE Transactions on Power Systems, 2011. **26**(1): p. 334-343.

80. Mehrjerdi, H., Lefebvre, S., Saad, M., Asber, D., *A Decentralized Control of Partitioned Power Networks for Voltage Regulation and Prevention Against Disturbance Propagation* IEEE Transactions on Power Systems, 2013. **28**(2).
81. Moreno, R. and A. Torres. *Security of the power system based on the separation into islands*. in *Innovative Smart Grid Technologies (ISGT Latin America), 2011 IEEE PES Conference on*. 2011.
82. Cheeger, J., *A Lower Bound for the Smallest Eigenvalue of the Laplacian.* Princeton Univ. Press, Problems in Analysis (R. C Gunning, ed.), 1970: p. 195-199.
83. Moreno, R., Ríos, Mario A., Torres, Á,, *Security schemes of power systems against blackouts*, in *Bulk Power System Dynamics and Control (iREP) - VIII (iREP), 2010 iREP Symposium*2010: Rio de Janeiro.
84. Ding, L., Wall, P., Terzija, V.V.,, *A novel controlled islanding algorithm based on constrained spectral clustering* in *Advanced Power System Automation and Protection (APAP), 2011 International Conference on*2011: Beijing.
85. Ding, L., et al., *Two-Step Spectral Clustering Controlled Islanding Algorithm.* IEEE Transactions on Power Systems, 2013. **28**(1): p. 75-84.
86. Tortos, J.Q. and V. Terzija, *Controlled Islanding Strategy Considering Power System Restoration Constraints.* 2012 IEEE Power and Energy Society General Meeting, 2012.
87. Pradhan, B., Reddy, K. H. K,; Roy, D. S., Mohanta, DS. K.,, *Intentional islanding of electric power systems in a grid computing framework: A graph-theoretic approach*, in *Recent Trends in Information Systems (ReTIS), 2011 International Conference on*2011: Kolkata.
88. Morioka, Y., et al., *System Separation Equipment to Minimize Power-System Instability Using Generators Angular-Velocity Measurements.* IEEE Transactions on Power Delivery, 1993. **8**(3): p. 941-947.
89. Novosel, D., et al., *Practical protection and control strategies during large power-system disturbances.* 1996 IEEE Transmission and Distribution Conference Proceedings, 1996: p. 560-565.
90. Sancha, J.L., et al., *Application of long-term simulation programs for analysis of system islanding.* IEEE Transactions on Power Systems, 1997. **12**(1): p. 189-194.
91. Ahmed, S.S., et al., *A scheme for controlled islanding to prevent, subsequent blackout.* IEEE Transactions on Power Systems, 2003. **18**(1): p. 136-143.
92. Barkans, J.D. and D.A. Zalostiba, *Short-term splitting of a power system with its self-restoration as blackout prevention.* 2007 Conference Proceedings Ipec, Vols 1-3, 2007: p. 413-418.
93. El-Werfelli, M., J. Brooks, and R. Dunn, *An Optimized Defence Plan for a Power System.* 2008 Proceedings of the 43rd International Universities Power Engineering Conference, Vols 1-3, 2008: p. 199-204.
94. Liu, Y.Z., W.; Yu, Z.;, *Measures to Keep Islands Stable after Power Oscillation or Out of Step Islanding*, in *Advances in Power System Control, Operation and Management (APSCOM 2009), 8th International Conference on*2009: Hong Kong, China. p. 1-4.
95. Franco, R., Sena, C., Taranto, G. N., Giusto, A., *Using Synchrophasors for Controlled Islanding—A Prospective Application for the Uruguayan Power System.* IEEE Transactions on Power Systems, 2013. **28**(2).
96. Anuar, M.A.D., U.; Hiyama, T.;, *Principle Areas for Islanding Operation Based on Distribution Factor Matrix*, in *Intelligent System Applications to Power Systems, 2009. ISAP '09. 15th International Conference on*2009: Curitiba. p. 1-6.
97. Sena, C.T., G. N.; Giusto, Á.;, *An investigation of controlled power system separation of the Uruguayan network* in *Bulk Power System Dynamics and Control (iREP) - VIII (iREP), 2010 iREP Symposium*2010: Rio de Janeiro.

98. Ahsan, M.Q., et al., *Technique to Develop Auto Load Shedding and Islanding Scheme to Prevent Power System Blackout.* IEEE Transactions on Power Systems, 2012. **27**(1): p. 198-205.
99. Senroy, N., G.T. Heydt, and V. Vittal, *Decision tree assisted controlled islanding.* IEEE Transactions on Power Systems, 2006. **21**(4): p. 1790-1797.
100. Dola, H.M., Rolla, M.O.,Chowdhury, B. H., , *Intentional islanding and adaptive load shedding to avoid cascading outages*, in *Power Engineering Society General Meeting, 2006. IEEE*2006: Montreal, Que.
101. Chowdhury, B.H. and S. Baravc, *Creating cascading failure scenarios in interconnected power systems.* 2006 Power Engineering Society General Meeting, Vols 1-9, 2006: p. 1892-1899.
102. Vittal, V. and G.T. Heydt, *The Problem of Initiating Controlled Islanding of a Large Interconnected Power System Solved as a Pareto Optimization.* 2009 IEEE /PES Power Systems Conference and Exposition, Vols 1-3, 2009: p. 952-958.
103. Zaag, N., et al., *Analysis of contingencies leading to islanding and cascading outages.* 2007 IEEE Lausanne Powertech, Vols 1-5, 2007: p. 63-67.
104. Diao, R.S., et al., *Decision Tree Assisted Controlled Islanding for Preventing Cascading Events.* 2009 IEEE/PES Power Systems Conference and Exposition, Vols 1-3, 2009: p. 21-28.
105. Senroy, N. and G.T. Heydt, *Timing of a controlled islanding strategy.* 2005/2006 IEEE /PES Transmission & Distribution Conference & Exposition, Vols 1-3, 2006: p. 1460-1466.
106. Ostojic, D.R., *Stabilization of Multimodal Electromechanical Oscillations by Coordinated Application of Power-System Stabilizers.* IEEE Transactions on Power Systems, 1991. **6**(4): p. 1439-1445.
107. Tabandeh, S.M., Aghamohammadi, M. R.;, *A new algorithm for detecting real-time matching for controlled islanding based on correlation characteristics of generator rotor angles* in *Universities Power Engineering Conference (UPEC), 2012 47th International*2012: London.
108. Machowski, J., J.W. Bialek, and J.R. Bumby, *Power system dynamics : stability and control*. 2nd ed. ed2008, Oxford: John Wiley. xxvii, 629 p.
109. Wadhwa, C.L., *Electrical power systems*2009, Kent: New Age Science. xvi, 962 p.
110. Kundur, P., et al., *Definition and classification of power system stability.* IEEE Transactions on Power Systems, 2004. **19**(3): p. 1387-1401.
111. CIGRE Task Force 38.02.14, *Analysis and Modeling Needs of Power Systems Under Major Frequency Disturbances*, 1999.
112. Parker, C.J., I.F. Morrison, and D. Sutanto, *Simulation of load shedding as a corrective action against voltage collapse.* Electric Power Systems Research, 1998. **46**(3): p. 235-241.
113. VanCutsem, T. and R. Mailhot, *Validation of a fast voltage stability analysis method on the Hydro-Quebec system.* IEEE Transactions on Power Systems, 1997. **12**(1): p. 282-288.
114. Taylor, C.W., N.J. Balu, and D. Maratukulam, *Power system voltage stability*1994: McGraw-Hill Ryerson, Limited.
115. Van Cutsem, T., *Voltage instability: phenomena, countermeasures, and analysis methods.* Proceedings of the Ieee, 2000. **88**(2): p. 208-227.
116. Gao, B., G.K. Morison, and P. Kundur, *Towards the development of a systematic approach for voltage stability assessment of large-scale power systems - Response.* IEEE Transactions on Power Systems, 1996. **11**(3): p. 1323-1324.
117. Ajjarapu, V. and C. Christy, *The continuation power flow: a tool for steady state voltage stability analysis.* Power Systems, IEEE Transactions on, 1992. **7**(1): p. 416-423.

118. Lof, P.A., et al., *Fast Calculation of a Voltage Stability Index.* IEEE Transactions on Power Systems, 1992. **7**(1): p. 54-64.
119. Morison, G.K., B. Gao, and P. Kundur, *Voltage stability analysis using static and dynamic approaches.* Power Systems, IEEE Transactions on, 1993. **8**(3): p. 1159-1171.
120. van Cutsem, T. and C. Vournas, *Voltage Stability of Electric Power Systems*1998: Springer.
121. Kundur, P., N.J. Balu, and M.G. Lauby, *Power system stability and control*1994, New York ; London: McGraw-Hill. xxiii,1176p.
122. Kundur, P., N.J. Balu, and M.G. Lauby, *Power system stability and control*. The EPRI power system engineering series.1994, New York: McGraw-Hill. xxiii, 1176 p.
123. Beiraghi, M. and A.M. Ranjbar, *Online Voltage Security Assessment Based on Wide-Area Measurements.* IEEE Transactions on Power Delivery, 2013. **28**(2): p. 989-997.
124. Mathworks. *Transient Stability of a Power System with SVC and PSS*. 2013 [cited 2013 26/06/2013]; Available from: http://www.mathworks.co.uk/help/physmod/powersys/ug/transient-stability-of-a-power-system-with-svc-and-pss.html.
125. Vittal, E., M. O'Malley, and A. Keane, *Rotor Angle Stability With High Penetrations of Wind Generation.* Power Systems, IEEE Transactions on, 2012. **27**(1): p. 353-362.
126. Great Britain Office of Electricity Regulation, *The Transmission Price Control Review of the National Grid Company: Proposals, October* 1996.
127. Bialek, J., *Tracing the flow of electricity.* IEE Proceedings-Generation Transmission and Distribution, 1996. **143**(4): p. 313-320.
128. Bialek, J.W. and P.A. Kattuman, *Proportional sharing assumption in tracing methodology.* IEE Proceedings-Generation Transmission and Distribution, 2004. **151**(4): p. 526-532.
129. Haixia, W., et al. *Power Flow Tracing with Consideration of the Electrical Distance*. in *Power and Energy Engineering Conference, 2009. APPEEC 2009. Asia-Pacific*. 2009.
130. Olmos, L. and I.J. Perez-Arriaga, *Evaluation of Three Methods Proposed for the Computation of Inter-TSO Payments in the Internal Electricity Market of the European Union.* Power Systems, IEEE Transactions on, 2007. **22**(4): p. 1507-1522.
131. Bialek, J.W. and S. Ziemianek. *Tracing based transmission pricing of cross-border trades: fundamentals and circular flows*. in *Power Tech Conference Proceedings, 2003 IEEE Bologna*. 2003.
132. Bialek, J. and S. Ziemianek, *Tracing Based Transmission Pricing of Cross-Border: Fundamentals and Circular Flows*, in *IEEE Bologna Power Tech Conference*2003, IEEE: Bologna, Italy.
133. Bialek, J.W., *Tracing-based unifying framework for transmission pricing of cross-border trades in Europe.* International Conference on Electric Utility Deregulation and Restructuring and Power Technologies, Proceedings, 2000: p. 532-537.
134. ENTSOE, *Monthly Statistics*, 2006.
135. Sheldrake, A., *Handbook of electrical engineering : for practitioners in the oil, gas and petrochemical industry*2002, New York ; Chichester: Wiley.
136. Siemens. 08/03/2014]; Available from: http://pennwell.websds.net/2013/vienna/pge/slideshows/T5S7O5-slides.pdf.
137. Johannsson, H., A.H. Nielsen, and J. Ostergaard, *Wide-Area Assessment of Aperiodic Small Signal Rotor Angle Stability in Real-Time.* IEEE Transactions on Power Systems, 2013. **28**(4): p. 4545-4557.
138. Milano, F., *An open source Power System Analysis Toolbox.* IEEE Transactions on Power Systems, 2005. **20**(3): p. 1199-1206.

139. Sanchez-Garcıa, R., Fennelly, M., Norris, S., Wright, N., Niblo, G., Brodzki, J., Bialek, J.,, *Hierarchical Spectral Clustering of Power Grids.* IEEE Transactions on Power Systems, article accepted for publication, 2014.
140. Lin, Z., Norris, S., Shao, H., Bialek, J.W.,, *Controlled Islanding: Comparison between Power Flow Tracing and Slow Coherency* Awaiting Submission to IEEE Transactions on Power Systems, 2014.
141. Gonzalez-Longatt, D.F.; Available from: http://www.fglongatt.org/Test_Case_IEEE_14.html.
142. Hirsch, P., *Extended Transient-Midterm Stability Program (ETMSP) Ver. 3.1: User's Manual*, 1994.
143. Berg, G.J., *Power System Load Representation.* Proceedings of the Institution of Electrical Engineers-London, 1973. **120**(3): p. 344-348.
144. Liang, C., et al. *Statistical inference and analysis of load composition in power systems*. in *Electric Utility Deregulation and Restructuring and Power Technologies (DRPT), 2011 4th International Conference on*. 2011.
145. Gao, B., G.K. Morison, and P. Kundur, *Voltage Stability Evaluation Using Modal-Analysis.* IEEE Transactions on Power Systems, 1992. **7**(4): p. 1529-1542.
146. Singh, S.N. and S.C. Srivastava, *Improved voltage and reactive power distribution factors for outage studies.* IEEE Transactions on Power Systems, 1997. **12**(3): p. 1093-1093.
147. Chow, J.H., *Time-Scale Modeling of Dynamic Networks with Applications to Power Systems*1982: Springer-Verlag.
148. Chow, J.H., *A nonlinear model reduction formulation for power system slow coherency and aggregation endnote*, in *Proceedings of Workshop on Advances in Control and its Applications: Lecture Notes in Control and Information Sciences*1996. p. 282-298.
149. Pai, A., *Energy Function Analysis for Power System Stability*1989: Springer.

14 Papers Published

Conference papers

1. Guo, S., Norris, S., Wilson, D. and Bialek, J., *"Increasing the available transmission capacity by using a dynamic transient stability limit",* ISGT Europe 2011, Manchester, 5-7th December 2011
2. *Norris, S. ; Guo, S. ; Bialek, J., "Tracing of power flows applied to islanding",* IEEE Power and Energy Society General Meeting, San Diego, California, 2012
3. *Norris, S ; Shao, H ; Bialek, J., "Considering voltage stress in preventive islanding", IEEE* Powertech 2013, Grenoble, 2013
4. *Shao, H; Norris, S; Lin, Z; Bialek, J,. "Determination of when to island by analysing dynamic characteristics in cascading outages",* IEEE Powertech 2013, Grenoble, 2013

Journal Papers

5. *Guo, S., Norris, S., Bialek, J., "Identification of Power System Dynamic Model using Wide Area Measurement Systems", IEEE Transaction on power systems. (Submitted - In Review)*
6. *Sanchez-Garcia, R., Fennelly, M., Norris, S., Niblo, G., Wright, N., Bialek, J. and Brodski, J., "Hierarchical Spectral Clustering of Power Grids", IEEE Transaction on power systems. (Submitted - In Review)*

Working Groups

7. Vaiman, M., Hines, P., Jiang, J., Norris, S., Papic, M., Pitto, A., Wang, Y., Zweigle, G., "*Mitigation and prevention of cascading outages: Methodologies and practical applications*", Prepared by the Task Force on Understanding, Prediction, Mitigation and Restoration of Cascading Failures of the IEEE Computing & Analytical Methods (CAMS) Subcommittee, IEEE Power and Energy Society General Meeting (PES), 2013, 21-25 July 2013